



**Third Workshop on  
Iberian Snakes  
and  
Spin Rotators**

September 12-13, 1994

**Editors:**  
Alfredo Luccio  
Thomas Roser

Brookhaven National Laboratory  
Upton, New York 11973-5000

#### DISCLAIMER

This report was prepared as an account of work sponsored by an agency of the United States Government. Neither the United States Government nor any agency thereof, nor any of their employees, nor any of their contractors, subcontractors, or their employees, makes any warranty, express or implied, or assumes any legal liability or responsibility for the accuracy, completeness, or usefulness of any information, apparatus, product, or process disclosed, or represents that its use would not infringe privately owned rights. Reference herein to any specific commercial product, process, or service by trade name, trademark, manufacturer, or otherwise, does not necessarily constitute or imply its endorsement, recommendation, or favoring by the United States Government or any agency, contractor or subcontractor thereof. The views and opinions of authors expressed herein do not necessarily state or reflect those of the United States Government or any agency, contractor or subcontractor thereof.

Printed in the United States of America  
Available from  
National Technical Information Service  
U.S. Department of Commerce  
5285 Port Royal Road  
Springfield, VA 22161

NTIS price codes:  
Printed Copy: A11; Microfiche Copy: A01

## THIRD WORKSHOP ON SIBERIAN SNAKES and SPIN ROTATORS

Brookhaven National Laboratory  
Upton, Long Island, New York  
September 12-13, 1994

The aim of the Workshop was to provide a forum to discuss new developments in the area of siberian snakes and spin rotators, also in preparation for the "SPIN 94" Conference.

In the Workshop we had presentations followed by in-depth discussions in working groups:

- A Snake/Spin Rotator Design  
Physics and Engineering Aspects
  
- B Spin Dynamics  
Tracking of Polarized Beams, Resonances, Stability
  
- C Accelerator Optics  
Effects of Insertion of Snakes/Rotators in the Lattice

The following Proceedings contain the contributions to the Workshop. They are copies of the transparencies that were presented and discussed.

The Editors



## CONTENTS

H. Sato and T. Toyama Polarized Beam Project at the KEK PS	p. 1
V.I. Ptitsin and Yu. M. Shatunov Helical Spin Rotators and Snakes	p. 15
R. Gupta, G. Morgan and E. Willen Design and Status of Helical Magnets at BNL	p. 25
R. Baiod Siberian Snakes for the Fermilab Main Injector	p. 45
T. Roser Fully Compensated Spin Flipper	p. 73
M. Böge Spin Tracking Calculations for the HERA electron ring	p. 77
T. Roser, K. Brown, G. Bunce, E. Courant, R. Fernow, S. Y. Lee, A. Luccio, Y. Makdisi, S. Mane, L. Ratner, H. Spinka, S. Tepikian, A. G. Ufimtsev and D. Underwood Conceptual Design for the Acceleration of Polarized Protons in RHIC	p. 97
D. P. Barber, K. Heinemann and G. Ripken Spin tune shift due to closed orbit distortion	p. 121
D. P. Barber Longitudinal Polarization at HERA: Rotators + Spin Matching	p. 139
Yu. Shatunov Motivation for high field	p. 145

<b>F. Pilat</b>	
<b>Models for the Helical Snake</b>	p. 171
<b>A. Luccio</b>	
<b>SNIG Formalism</b>	p. 193
<b>S. Tepikian</b>	
<b>Snake Resonances</b>	p. 213
<b>R. A. Phelps</b>	
<b>Spin Flipping a Stored Polarized Proton Beam in the Presence of     Siberian Snakes</b>	p. 225
<b>S. Tepikian</b>	
<b>Polarized Proton Collisions at Brookhaven</b>	p. 235

**H. Sato and T. Toyama**

**KEK**

1-1 Oho: Tsukuba-shi: Ibaraki-ken 305, Japan

**Polarized Beam Project at the KEK PS**

# Polarized beam project at the KEK PS

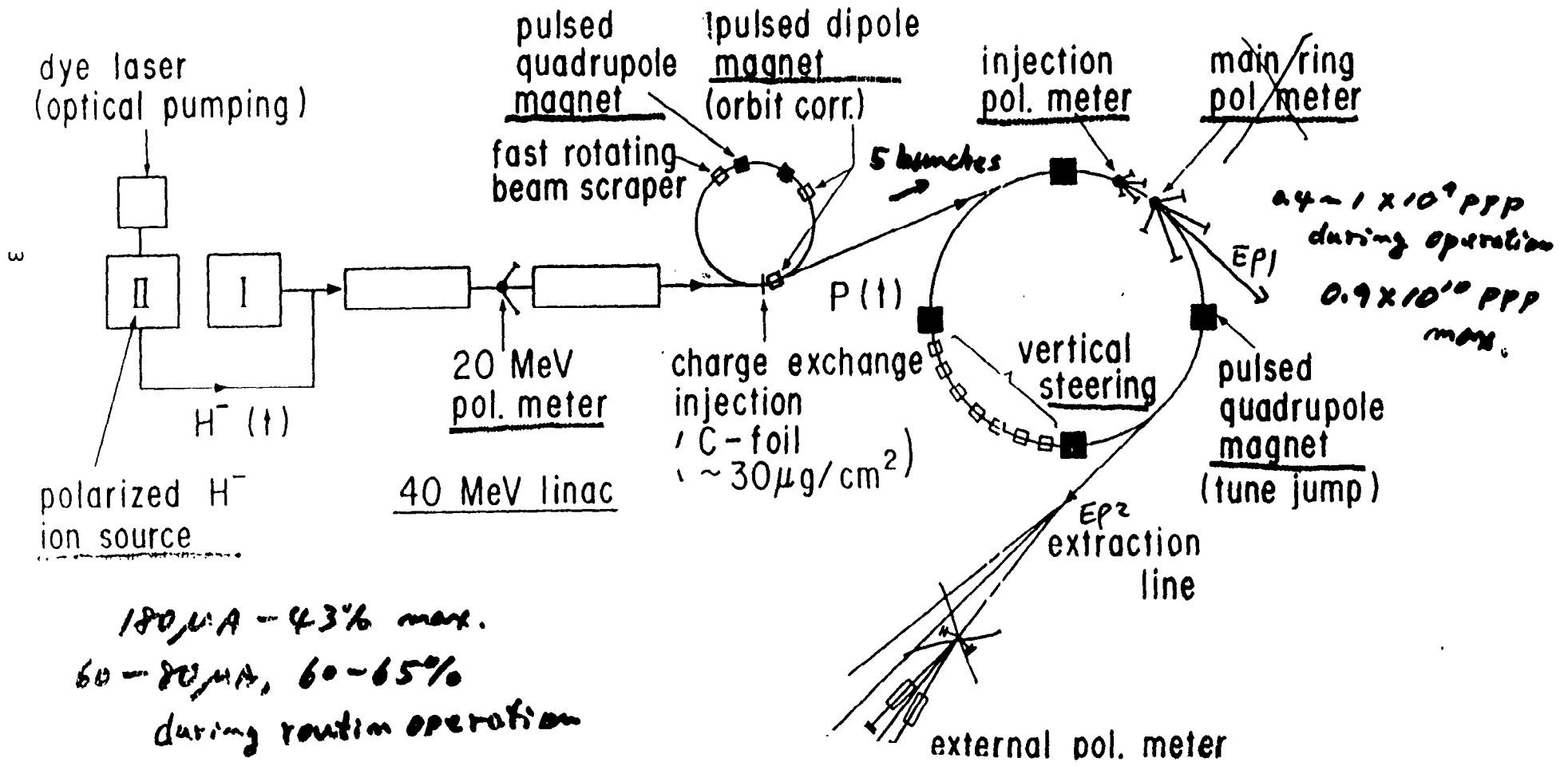
1994 Sep. 12 H. Sato, KEK  
T. Toyama

- Performance of polarized proton beam acceleration until 1988.
- Polarized deuteron acceleration.  
APPROVED by PS-PAC.
- Polarized proton acceleration using partial wake

750 keV preaccelerator

500 MeV booster

12 GeV main ring

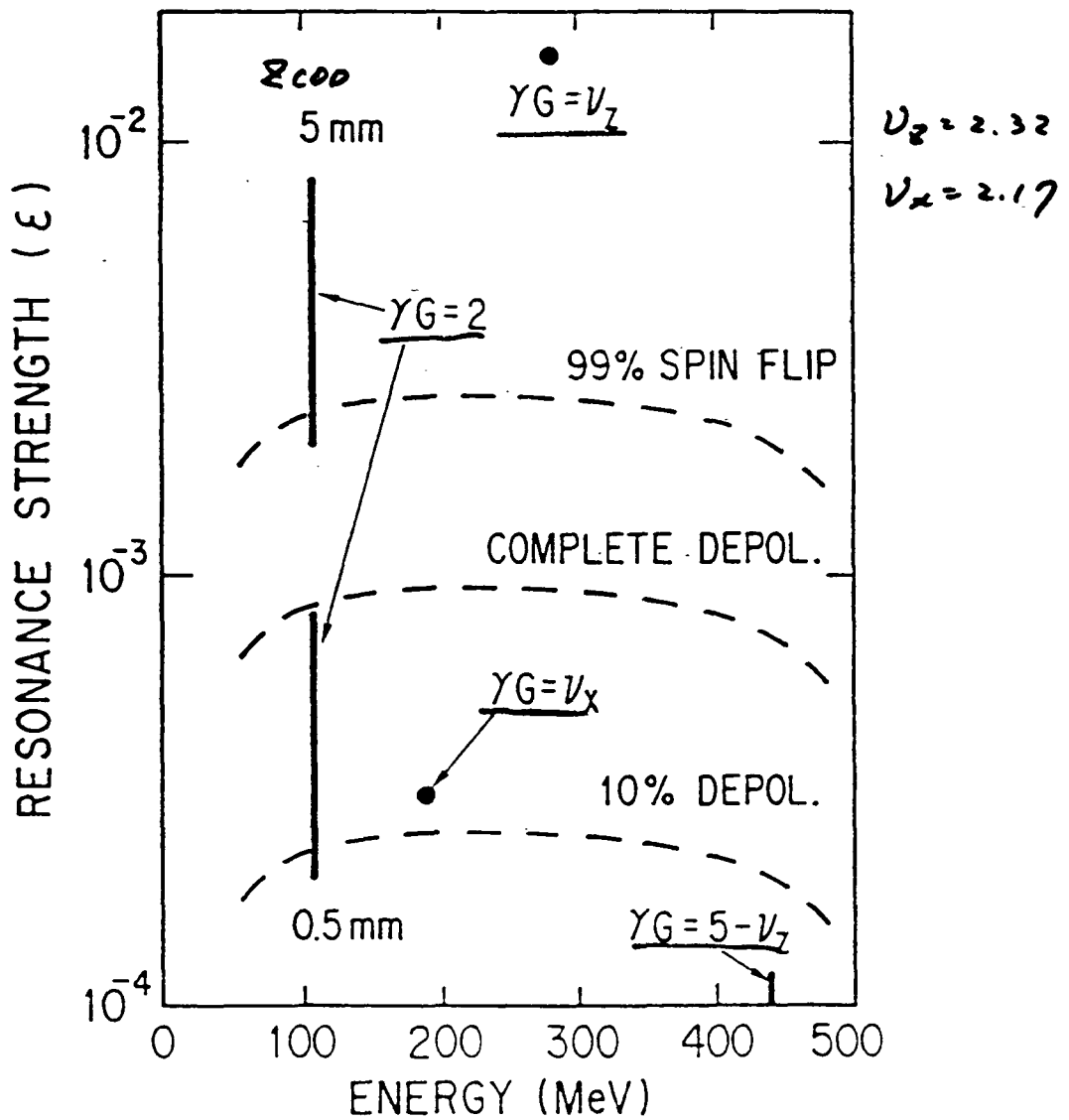


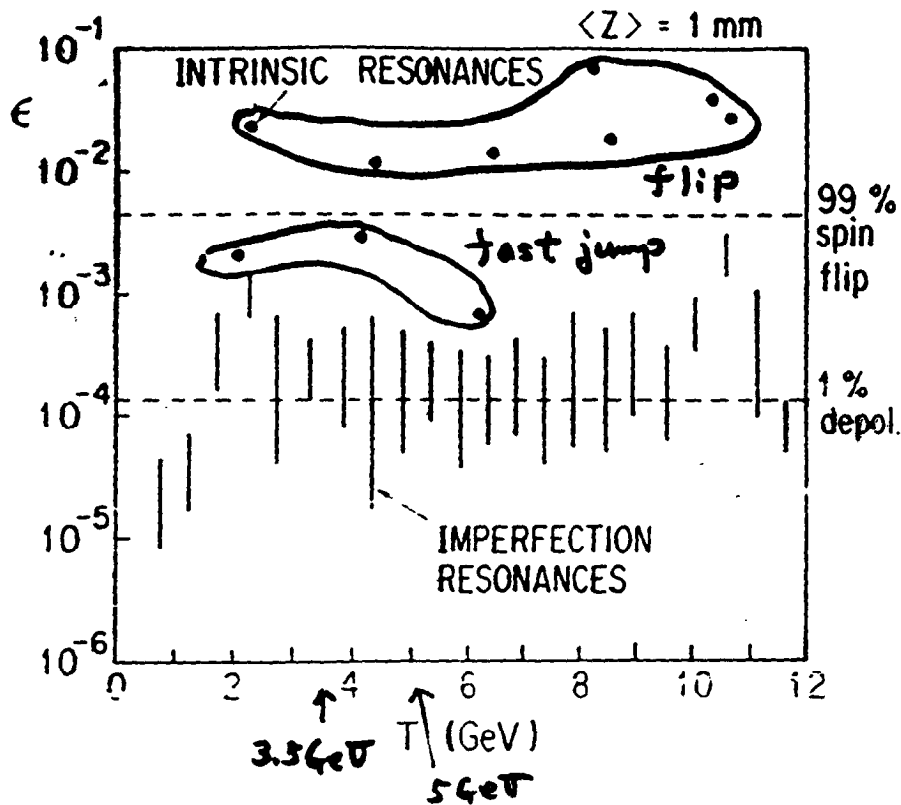
$\gamma G = 2$  flip, correction

$\gamma G = U_z$  flip (synchrotron osc.)

$\gamma G = U_x$  0% p < 4%

$\gamma G = 5 - U_z$  0% p < 2%





Depolarizing resonance  
in the main ring.

$$V_z = 6.25$$

$$V_x = 7.11$$

$$\langle Z_{\text{COD}} \rangle = 1 \text{ mm}$$

$$E_U = 20 \text{ km} \cdot \text{m} \cdot \text{r}$$

at 500 MeV

◦ Intrinsic resonance up to 5 GeV

fast jump

$\delta G$	$T(\text{GeV})$	$\Delta V_z$	$T_r$
$12 - V_z$	2.1	0.15	70 $\mu\text{s}$ ( $\times 50$ )
$16 - V_z$	4.2	0.17	120 $\mu\text{s}$ ( $\times 40$ )

slow passage

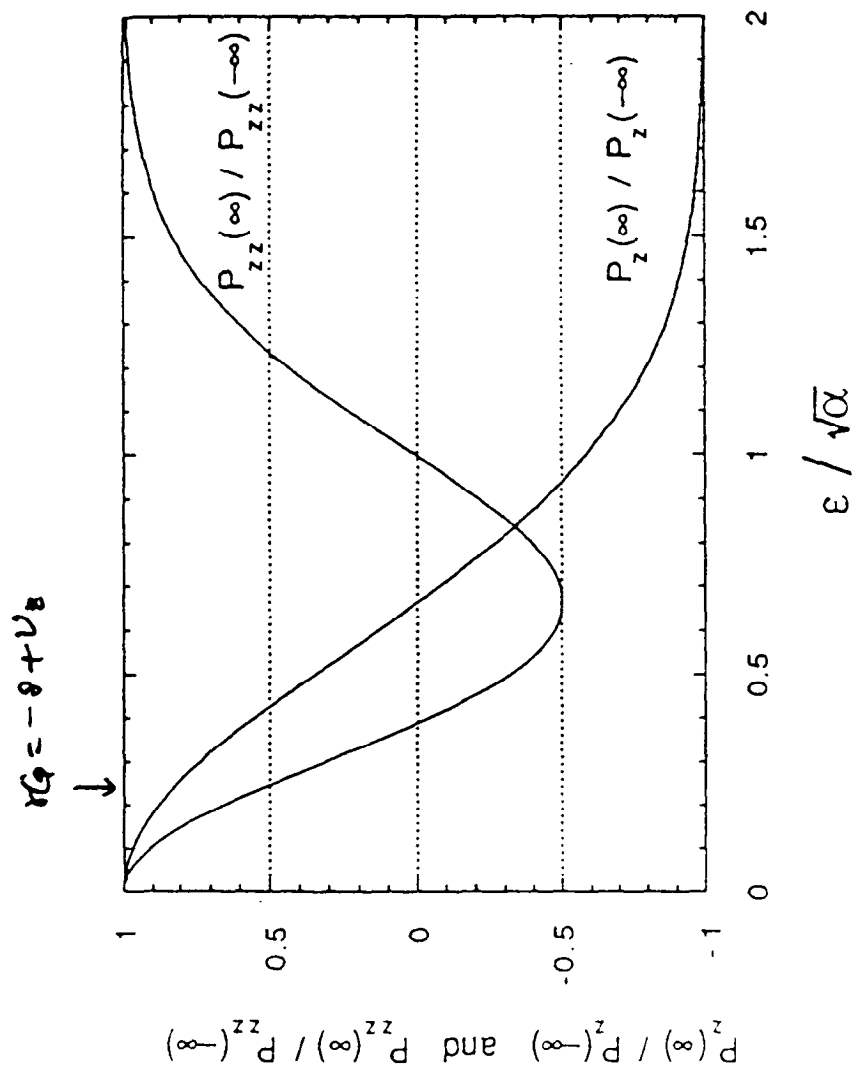
$\delta G$	$T(\text{GeV})$	
$V_z$	2.3	natural spin flip
$4 + V_z$	4.4	artificial spin flip

◦ Imperfection resonance up to 5 GeV

$\delta G = 3, 4, 5$  and  $9$  : very weak ; no depol.

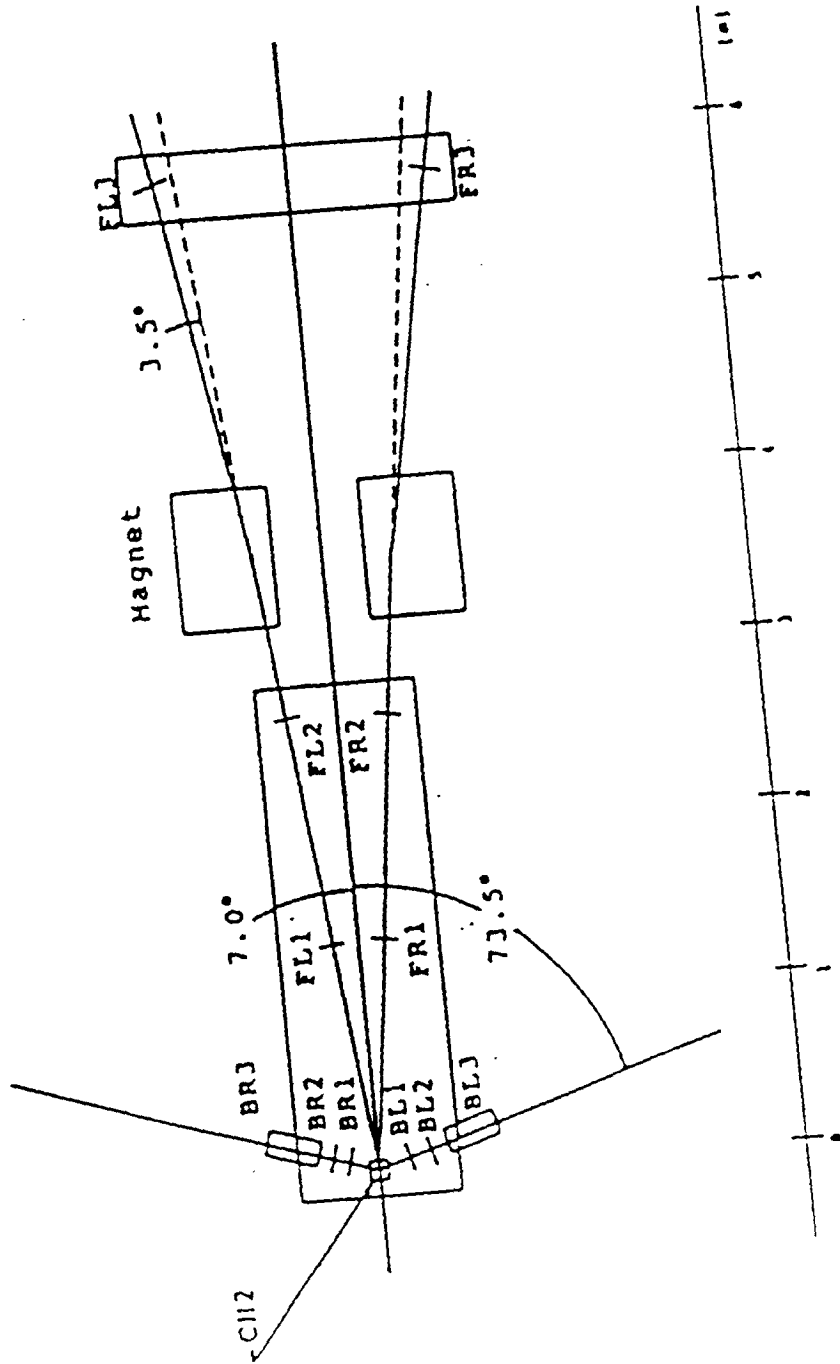
6, 7 and 8 : COD correction or spin flip

10 and 11 : COD correction



## Resonance Crossing





External Polarimeter

# Polarized Proton Acceleration

## Partial Snake for Imperfection Resonances

$\epsilon < 2 \times 10^{-2}$  (Calculated using random field error  $\langle z_{\text{COD}} \rangle = 1 \text{ mm}$ )

Resonance	Strength	(6-th harmonic correction)
$\gamma G = 18$	$\epsilon < 1.8 \times 10^{-2}$	---> $< 0.6 \times 10^{-2}$
19	$1.4 \times 10^{-2}$	...
22	$1.3 \times 10^{-2}$	---> $< 0.6 \times 10^{-2}$
23	$0.94 \times 10^{-2}$	

$\epsilon < 1 \times 10^{-2}$  (Calculated using the field error from measured COD  
COD was corrected  $\langle z_{\text{COD}} \rangle \sim 1 \text{ mm}$ )

$\gamma G = 19$        $\epsilon < 0.97 \times 10^{-2}$

Partial Snake      with 1/2 ramping (  $2.3 \times 0.5 \text{ T/sec}$ ,  $\alpha = 5.8 \times 10^{-6} \times 0.5$ )

Solenoid                      **7** degree      **1.87** Tm @ 12 GeV

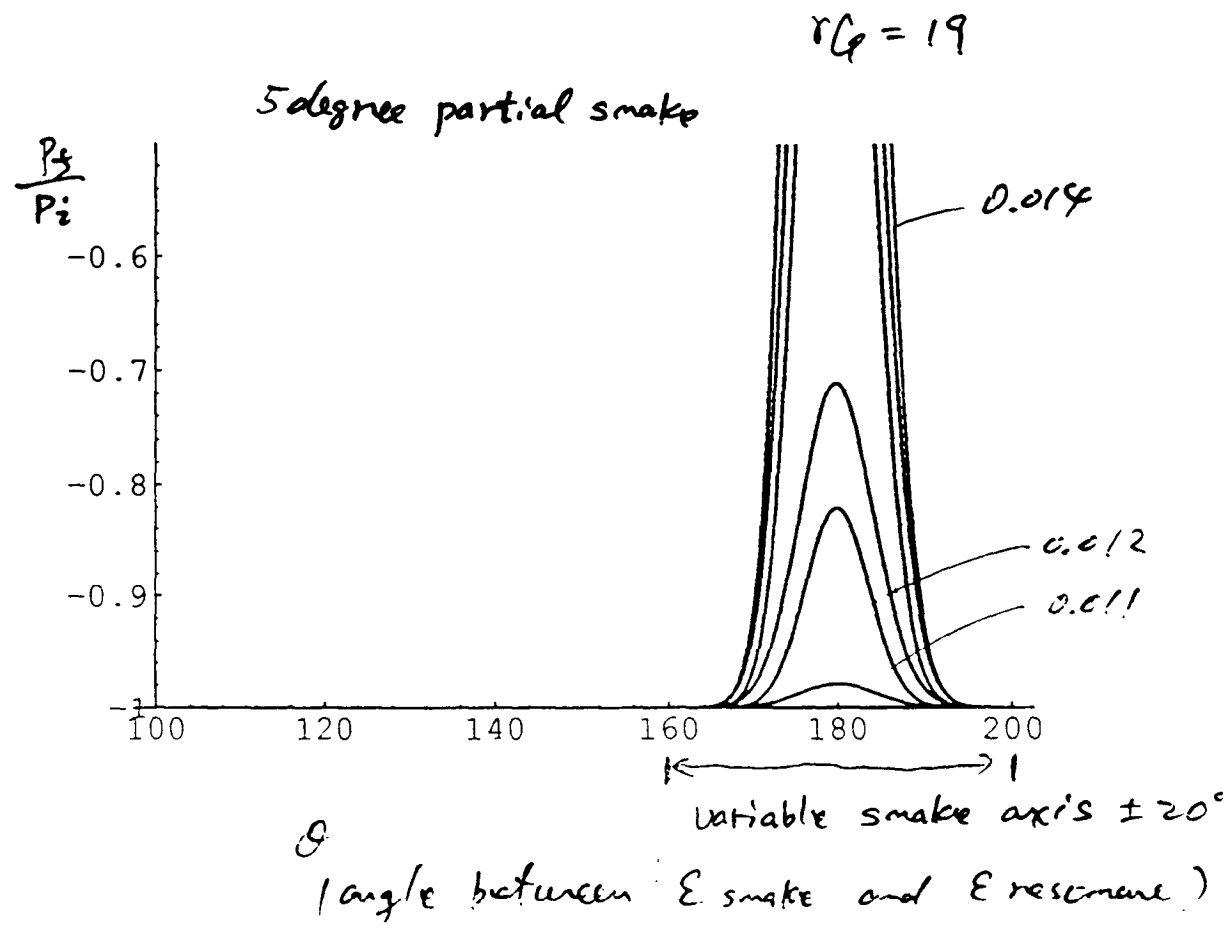
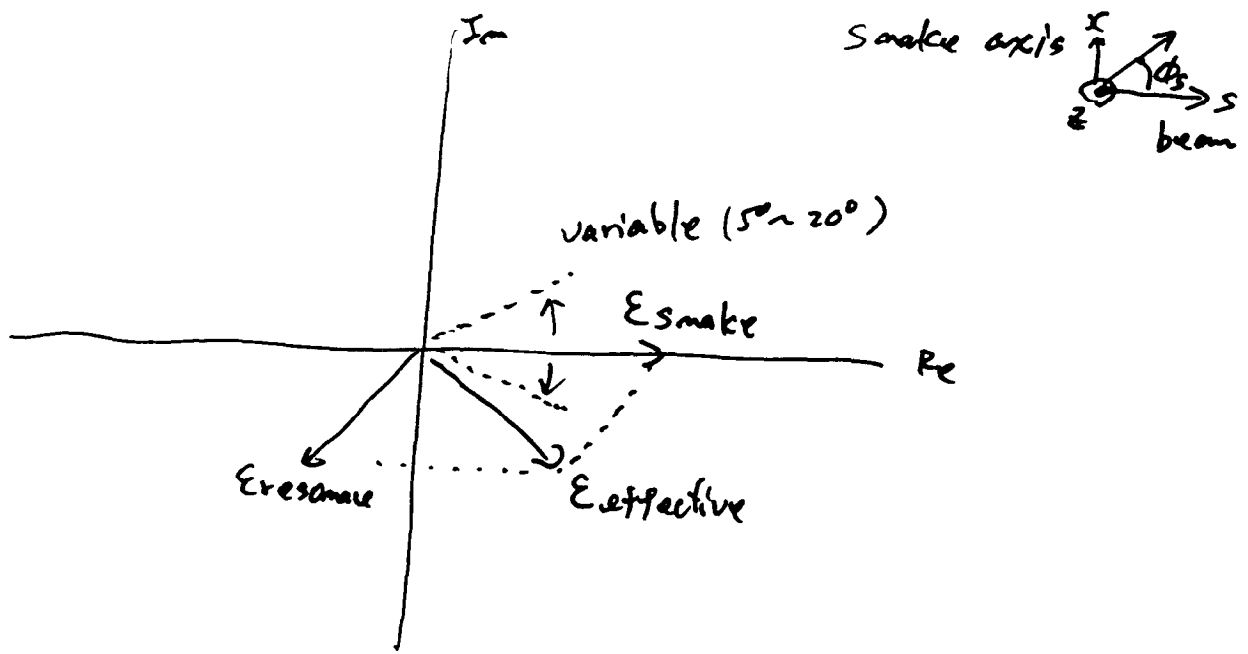
Resonances of  $\epsilon < 1.4 \times 10^{-2}$       O.K.

Helical Dipole                      5 degree      1.83 Tm @ 12 GeV

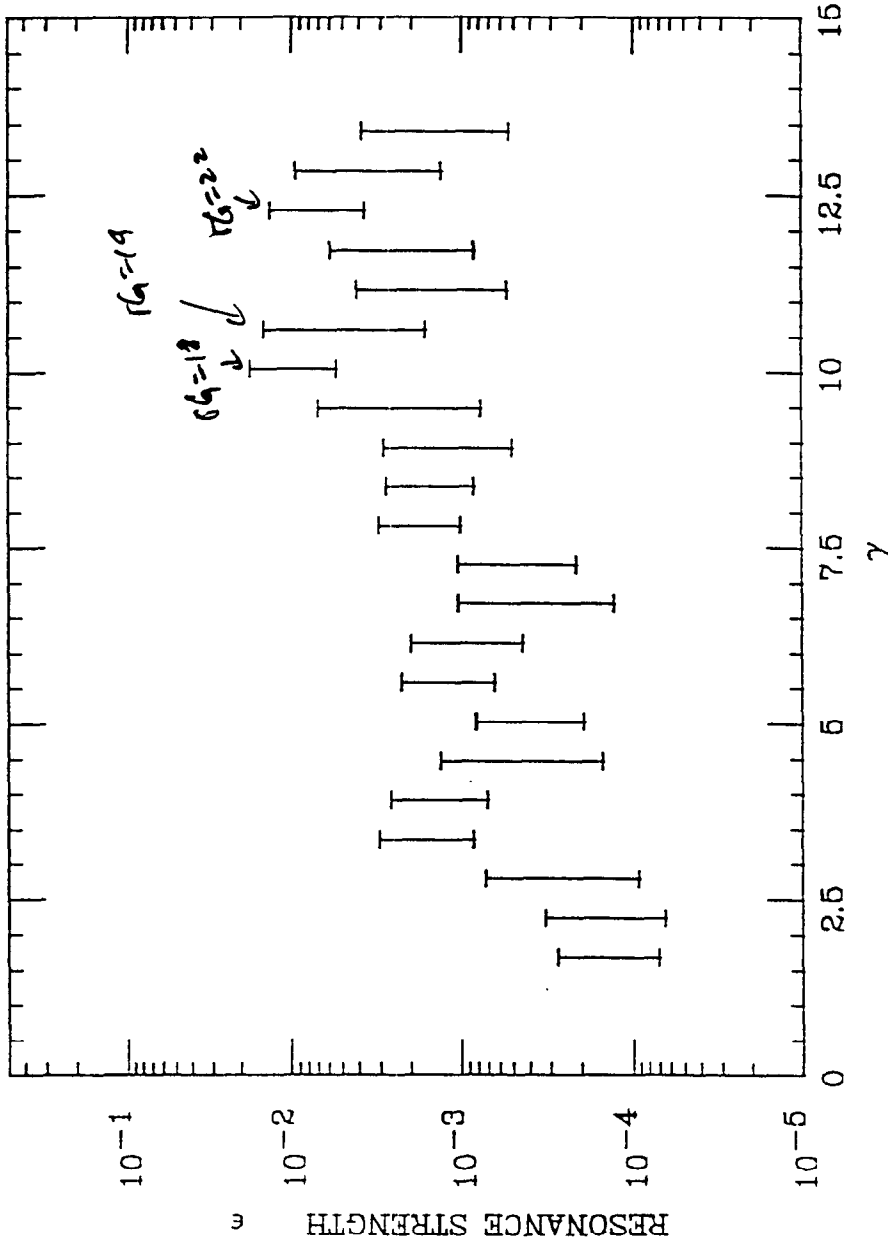
Resonances of  $\epsilon < 1 \times 10^{-2}$       O.K.

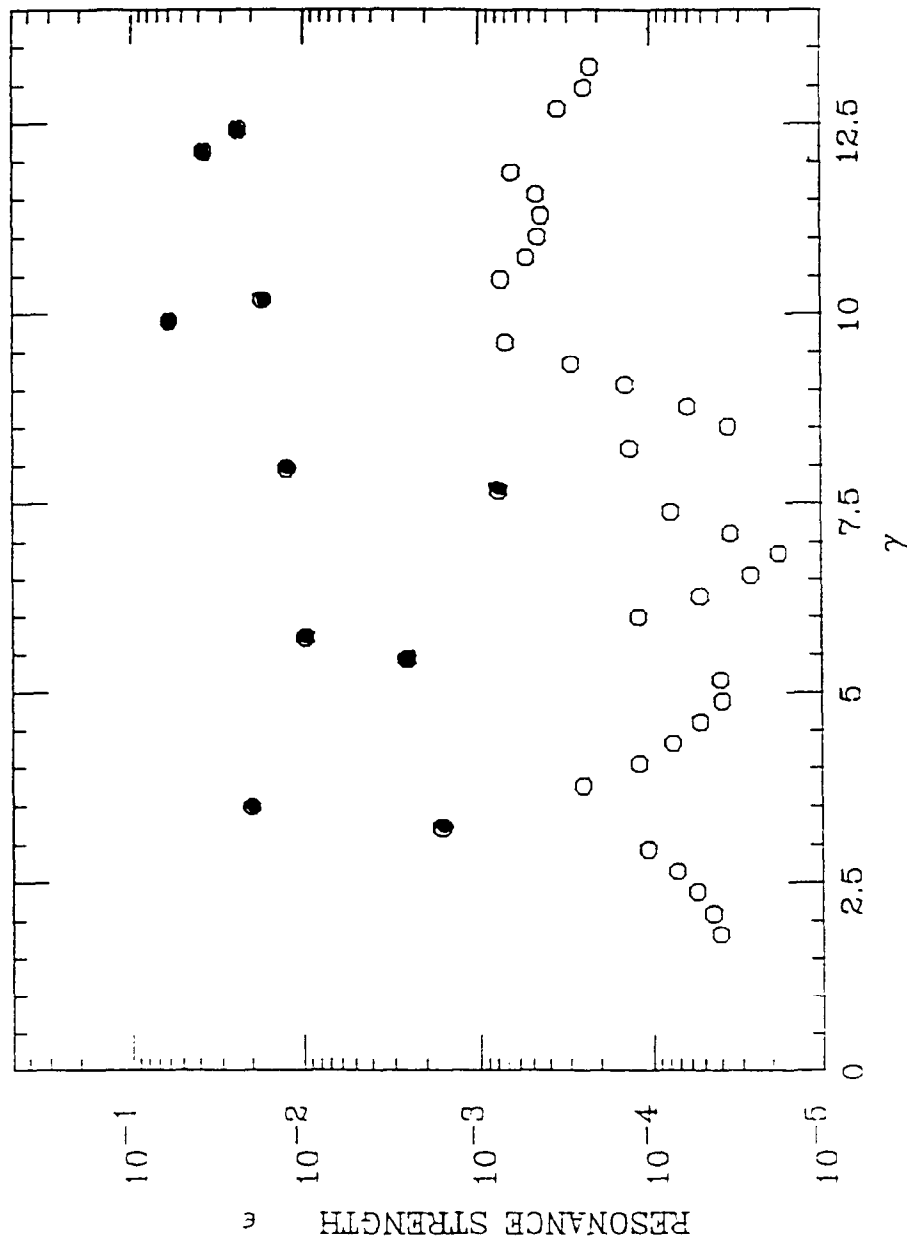
$\gamma G = 19$                        $\epsilon \sim 1.4 \times 10^{-2}$   
variable snake axis  $\pm 20$  degree  
---> escape to safe region (Fig)

Ramping is necessary:  
decrease the focusing of the helical dipole  
due to the resonances  $\gamma G = k \pm \nu_z$



recalculated  
using C and R format

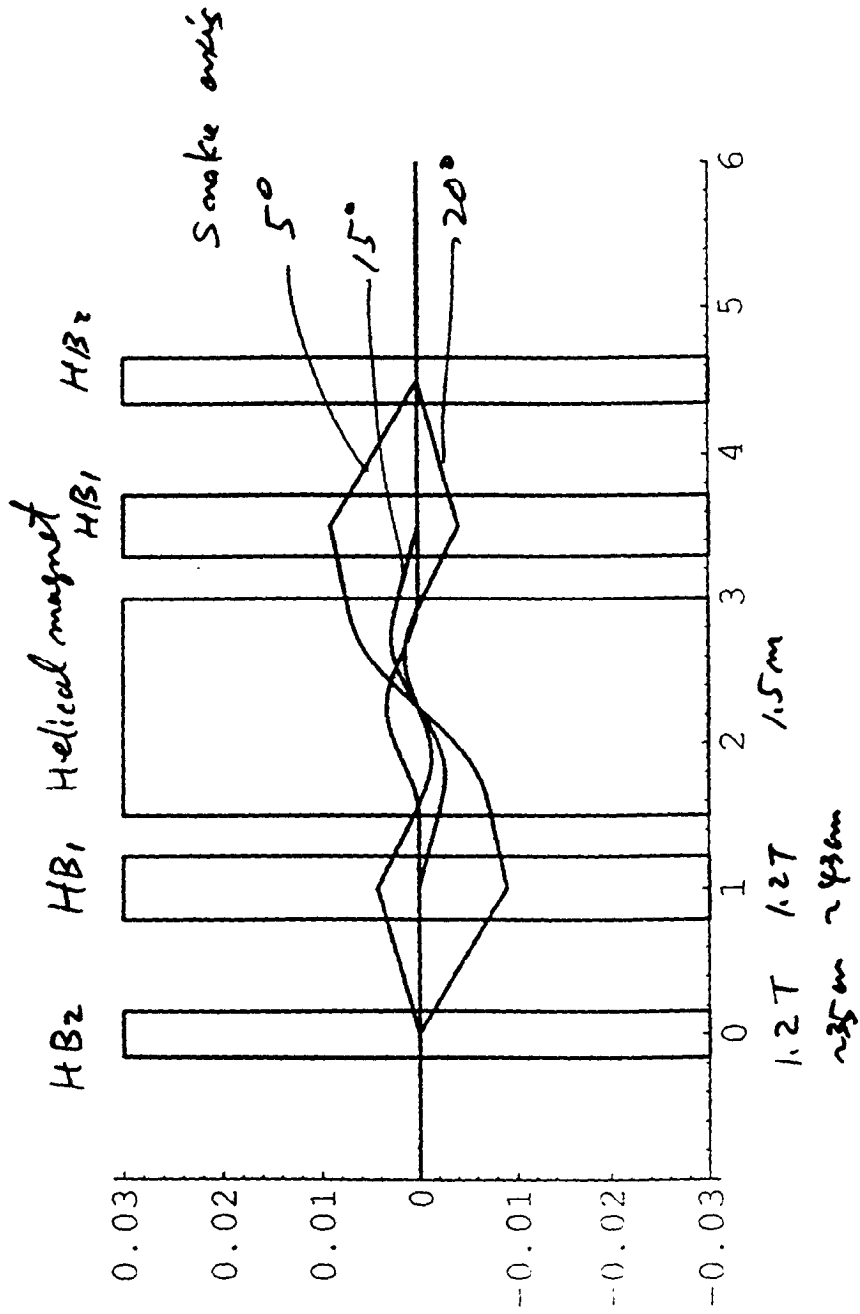




$$\gamma G = mN \pm \nu z$$

(N=1 by snake magnet)

Orbit displacement at  $12600^\circ$   
 (50 snake)



Solenoid is superior on its compactness.  
simple system.

Helical snake needs long straight section.  
can provide a variable snake axis  
will be essential in the spin colliders

V.I. Ptitsin and Yu. M. Shatunov

Budker Institute of Nuclear Physics

Novosibirsk, 630090 Russia

Helical Spin Rotators and Snakes

# HELICAL SPIN ROTATORS AND SNAKES.

V.I.Ptitsin and Yu.M.Shatunov

*Budker Institute of Nuclear Physics, Novosibirsk, 630090, Russia*

## Abstract

In present paper the spin motion in helical undulator is considered. Then possible schemes of spin rotators and snakes based on the sequence of helical undulators are suggested.

## 1 Introduction.

The polarization of proton beam above 30 Gev can be only maintained with the use of Siberian Snakes, the special kind of spin rotator which rotates particle spin by  $180^\circ$  around an axis directed in horizontal plane [1]. Also for experimental purposes it is often desired to have the longitudinal beam polarization in the interaction points of a collider. In this case the spin rotator can be applied to rotate vertical spin of a proton into horizontal plane.

The schemes based on the sequence of vertical and horizontal bending magnets have been proposed recently to be used as spin rotators and snakes [2,3]. The main disadvantage of such schemes is a large orbit excursion even at the energy of some hundreds Gev. From this point of view the rotator based on the helical undulator design [4] is more appropriate and in last years some schemes that include helical undulator have been suggested [5,6].

In present paper the spin rotator design based on the sequence of helical undulators is discussed. In the chapter 2 the spin and orbital motions in helical undulator are considered. The rotation axis and rotation angle for one period spin transformation are found. Then the scheme of Siberian Snake with the use of four undulators is presented in chapter 3. In chapter 4 the variants of spin rotators to rotate vertical spin to horizontal plane is studied.

## 2 Orbital and spin motion in helical undulator.

In the helical undulator with the period  $\lambda$  and the field amplitude  $h$  the on-axis field can be written as:

$$H_x = -h \sin kz, \quad H_y = h \cos kz, \quad H_z = 0,$$

where  $k = 2\pi/\lambda$ ,  $z$  is the coordinate along undulator axis and the subscripts of  $x$  and  $y$  correspond to horizontal and vertical components respectively.

We define the so-called undulator factor  $p$  as:

$$p = \frac{q_0 h}{c|k|}$$

where  $q_0 = e/mc$ , The  $p$  is mainly used for describing the properties of undulator radiation of electrons. However, as it will be seen later, the undulator factor is also the appropriate concept when one consider the spin motion.

The particle trajectory can be obtained from the motion equation, where  $z$  is used as independent variable. We believe the condition  $|px'/\gamma| \ll 1$  is true and therefore the  $\dot{z} = const \approx c$ . Then for transverse motion we have:

$$x = -\frac{p}{\gamma|k|}(1 - \cos kz) + x'_0 z + x_0$$

$$y = \frac{p}{\gamma|k|} \sin kz + (y'_0 - \frac{p}{\gamma} \frac{k}{|k|})z + y_0 \quad (1)$$

where  $x_0, x'_0, y_0, y'_0$  are coordinates and angles of the electron at the entrance of undulator.

After one undulator period the orbital coordinates and angles are transformed accordingly to:

$$\begin{aligned} x &= x_0 + x'_0 \lambda, \\ y &= y_0 + y'_0 \lambda - \frac{p}{\gamma} \frac{k}{|k|} \lambda, \\ x' &= x'_0, \\ y' &= y'_0 \end{aligned} \quad (2)$$

For particle entering the undulator along its axis after one period the particle orbit is simply shifted on the  $\lambda p/\gamma$  in the direction which corresponds to the direction of magnetic field at the undulator entrance. This direction will be called the main direction in the following consideration.

To consider spin motion in the undulator it is a convenient way to use a rotating reference frame ( $\hat{e}_1, \hat{e}_2, \hat{e}_3$ ) that is related to the laboratory frame by the transformation:

$$\begin{aligned} \hat{e}_1 &= \hat{e}_x \cos kz + \hat{e}_y \sin kz \\ \hat{e}_2 &= -\hat{e}_y \cos kz + \hat{e}_x \sin kz \\ \hat{e}_3 &= \hat{e}_z \end{aligned} \quad (3)$$

The axes of the rotating frame coincide with the laboratory frame after each undulator period, at  $z = m\lambda$  ( $m$  is integer).

The spin motion in the rotating frame will be described by the equation:

$$\dot{\mathbf{S}} = (\Omega_{\text{lab}} - \Omega_{\text{rot}}) \times \mathbf{S},$$

where

$$\Omega_{\text{lab}} = -\frac{q_0}{\gamma} (1 + \nu_0) \mathbf{H} + \frac{q'}{c^2} (\mathbf{H} \cdot \mathbf{v}) \mathbf{v}$$

is the spin angular velocity in the laboratory frame (from the Thomas-BMT equation) and  $\Omega_{\text{rot}} = kze_z$  is the axes precession frequency. We define  $\nu_0 = \gamma q'/q_0$  as the anomalous spin precession tune, with  $q'$  standing for the anomalous part of the electron magnetic moment.

Using the longitudinal coordinate  $z$  instead of time  $t$  as the independent variable the equation of spin motion can be rewritten as:

$$\frac{d\mathbf{S}}{dz} = \mathbf{W} \times \mathbf{S} \quad (4)$$

where  $\mathbf{W} = \Omega_{\text{lab}}/\dot{z} - k\mathbf{e}_z$

In zero approximation the particle spin precesses in the rotating frame at the constant angular velocity:

$$W_1 = (1 + \nu_0) \frac{p}{\gamma} k; \quad W_2 = 0; \quad W_3 = -k;$$

and the solution of (4) is obvious. The spin vector precesses around the direction determined by the unit vector  $\mathbf{n}$ :

$$\mathbf{n} = \frac{k}{\sqrt{W_1^2 + W_3^2}} \left( (1 + \frac{1}{\nu_0}) p \frac{q'}{q_0} \mathbf{e}_1 - \mathbf{e}_3 \right) \quad (5)$$

at the spin tune  $\nu$ :

$$\nu = \sqrt{1 + \left(1 + \frac{1}{\nu_0}\right)^2 p^2 \left(\frac{q'}{q_0}\right)^2}, \quad (6)$$

and  $2\pi\nu$  gives the spin rotation angle in one period of undulator.

As the rotating frame coincides with the laboratory frame at every undulator period the same vector  $\mathbf{n}$  is also the periodic solution of spin motion in the laboratory frame and defines the axis of the one-period spin transformation. Note that  $\mathbf{n}$  lies in the plane formed by the undulator axis and the main direction. Any spin vector rotates by  $2\pi(\nu - 1)$  angle around  $\mathbf{n}$  in one undulator period.

Obtained expressions for one-period transformation for particle orbit and spin give the basis to construct the spin rotators which consist of several undulators with integer number of period but with different helicities and field amplitude. Note that accordingly to formulas (2, 5) when one changes the sign of the value of magnetic field and undulator helicity the one period orbit shift does not change but spin rotation becomes opposite. It gives an additional possibilities at the construction of spin rotator.

### 3 Siberian snake.

The so-called continuous axis snake have been discovered by K. Steffen [2]. Steffen's snake is based on dipole magnet sequence. In general form the snake configuration can be written as:

$$S = (-H, -V, mH, 2V, -mH, -V, H),$$

where H and V are respectively the horizontal and vertical bending magnets and  $m$  is the number more than 1 [3]. The internal symmetry of snake provides automatically both restoring of particle orbit at the snake exit and the snake axis lying in horizontal plane. Then the choice of the  $V$  and  $H$  determine the required spin rotation angle (  $180^\circ$  for 100% snake) and required direction of snake axis.

The continuous axis snake can be designed also on the basis of four helical undulators. It can be shown that the appropriate symmetry conditions in this case read as:

1. Helicity(1 und.) = Helicity(4 und.),  
Helicity(2 und.) = Helicity(3 und.)
2.  $p_1 = -p_4$  ,  $p_2 = -p_3$
3.  $N_1 = N_4$  ,  $N_2 = N_3$  ,  
where  $N_i$  is the period number of  $i$ th undulator.
4. The magnetic field at the entrance of each undulator is in vertical direction.

Thus the parameters of two last snake undulators are determined by the parameters of first and second undulators. It is seen that such configuration symmetry allows two families of snakes, when the first and second undulators have the same helicity or the opposite one. Each family consists of the variety of possible schemes with different number of undulator periods. The numerical analysis of these schemes shows that increasing the number of periods though reduces slightly the orbit excursion but leads to the growth of field integral and total length. Thus the use of small number of period is more preferable. Also the variant when all undulators have same helicities provides less values of field integral so that we consider the examples of two snake configurations from this family:

variant A :  $N_1 = 1, N_2 = 1$

variant B :  $N_1 = 1, N_2 = 2$

In the figure 1 the relationship between  $p_1$  and  $p_2$  and the dependence of longitudinal snake axis projection on  $p_1$  are shown for the A variant.

If one want to have the choice of snake axis to be at any angle in the interval of  $[0^\circ, 90^\circ]$  and if the maximum field of 8 T can only be used then the length of period and the total length for A and B variants are:

A : period length = 1.43 m ; total length = 5.72 m

B : period length = 1.13 m ; total length = 6.72 m

In the table the set of parameters for longitudinal ( $\phi = 0^\circ$ ), transverse ( $\phi = 90^\circ$ ) and  $45^\circ$  snake axes is presented:

	$\phi$	p1	p2	integral(Tm)	$y_{max}$ (cm)
A:	$0^\circ$	0.27	-0.352	24.5	1.3
	$45^\circ$	0.44	-0.193	24.9	2.1
	$90^\circ$	0.58	-0.161	29.1	2.8
B:	$0^\circ$	0.25	-0.24	28.8	0.9
	$45^\circ$	0.44	-0.13	27.9	1.6
	$90^\circ$	0.3	-0.45	47	2.2

The values of  $y_{max}$  are taken for  $\gamma = 30$ . In both variants maximum field of 8 T is applied to have 90° snake axis. The given data show that the A variant provides better values of field integral but larger orbit deviation.

If only 45° snake axis is to be used then by using the field of 8 T the length of A variant can be reduced to 4.4 m ( the period length = 1.1 m ). Then  $y_{max} = 1.6$  cm.

In the figures 2,3 the particle and the spin trajectories are shown for 45° snake axis.

#### 4 Spin rotator.

In this chapter spin rotator schemes to rotate vertical proton spin into horizontal plane will be described.

We will consider the variant when the rotator consists of three undulators. Such variant allows various final spin directions without changing the undulators orientation around the longitudinal axis. Assuming equal period length for all undulators for orbit restoration we have the simple condition:  $\sum_{i=1}^3 N_i \text{sign}(k_i) p_i = 0$ . At choosen undulator helicities and period numbers two parameters  $p_1$  and  $p_2$  are taken to give desired final spin direction. There are many possible schemes with different number of undulator period and with the different set of of undulator helicities. One can choose from this variety of schemes the design which provides for desired final spin direction ( or the desired range of final spin direction) with minimal values of field integral and minimal orbit excursion. We have searched for the variants of spin rotator for the RHIC ring. In this case the rotator has to provide the range of possible final spin direction (from pure horizontal to nearly longitudinal) in order to have the longitudinal polarization in the interaction point in wide energy range. The analysis of the number of variants shows that the optimal scheme which gives the minimal field integral and small orbit distortion is:

Undulator	Helicity	Number of periods
1	+	1
2	+	2
3	-	1

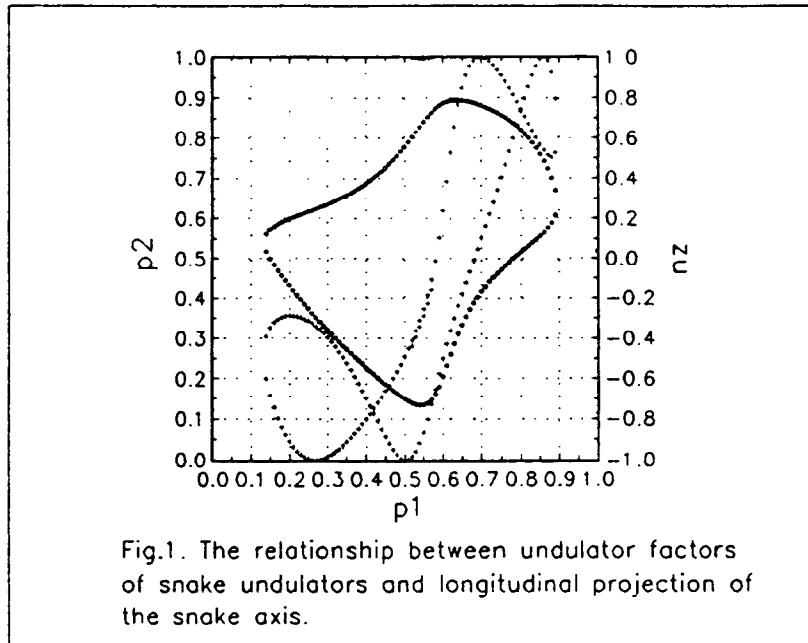
The dependences of undulator factor of second undulator  $p_2$  and the final spin direction (the angle  $\phi$  is encountered from longitudinal direction) on the  $p_1$  is shown in Fig.4. The range of possible  $\phi$  in this variant is from 1.5° to 108° that satisfies to design requirements. The undulator parameters for horizontal and nearly longitudinal final spin direction are:

$\phi$	$p_1$	$p_2$	$p_3$	integral(Tm)	$y_{max}$ (cm)
90°	0.339	-0.193	-0.053	15.3	0.17
1.5°	0.24	-0.319	-0.398	25	0.2

The value of maximum orbit deviation  $y$  is given for  $\gamma = 200$  and undulator period length of 1 meter (so that the total length of the rotator is 4 meters). The maximum field value in this variant is 8 T and is required to rotate spin to longitudinal direction. In the figures 5 and 6 the spin rotaton and orbit excursion into rotator are shown.

#### 5 Conclusion.

The main advantage of the spin rotator schemes based on helical undulators is less orbit deviation as compared with bending magnet schemes. This fact makes such schemes more attractive to use at medium energy range (from 10 to 300 Gev). In general case the value of the field integral for helical undulator rotator is some larger than for dipole magnet one for the same spin rotation. However, the stored magnetic field energy ( $\int H^2 dV$ ) for helical rotator is less than for dipole magnet rotator which consists of large aperture magnets to keep the large orbit excursion in such rotator. We can note that the insertions of dipole magnets on both sides of suggested rotator schemes can be applied that leads also to decreasing the maximum orbit excursion into the rotator.



## References

- [1] Ya. S. Derbenev and A. M. Kondratenko, Part. Accel.,8,115 (1978).
- [2] K. Steffen, DESY Report, DESY 83-124 (1983).
- [3] S. Y. Lee, Nucl. Instr. and Meth., A306 (1991).
- [4] Ya. S. Derbenev and A. M. Kondratenko, Proc. High Energy Physics with Polarized Beams and Targets, Argonne 1978, AIP Conf.Proc. 51, 292.
- [5] E. D. Courant, Proc. of 8th International Symposium on High-Energy Spin Physics, Minneapolis 1988, AIP Conf. Proc. 187, vol.2, 1085.
- [6] T. Toyama, Proc. of 10th International Symposium on High-Energy Spin Physics, Nagoya 1992, 433.

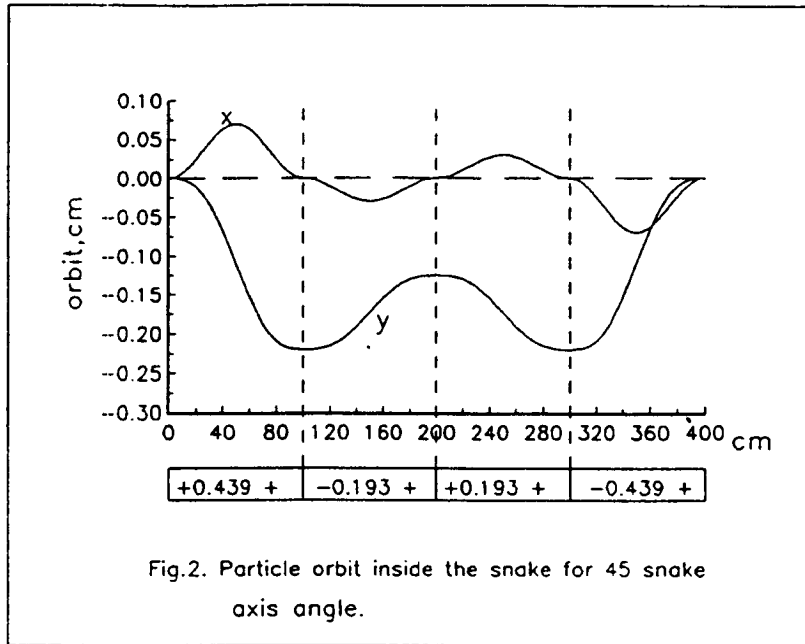


Fig.2. Particle orbit inside the snake for 45 snake axis angle.

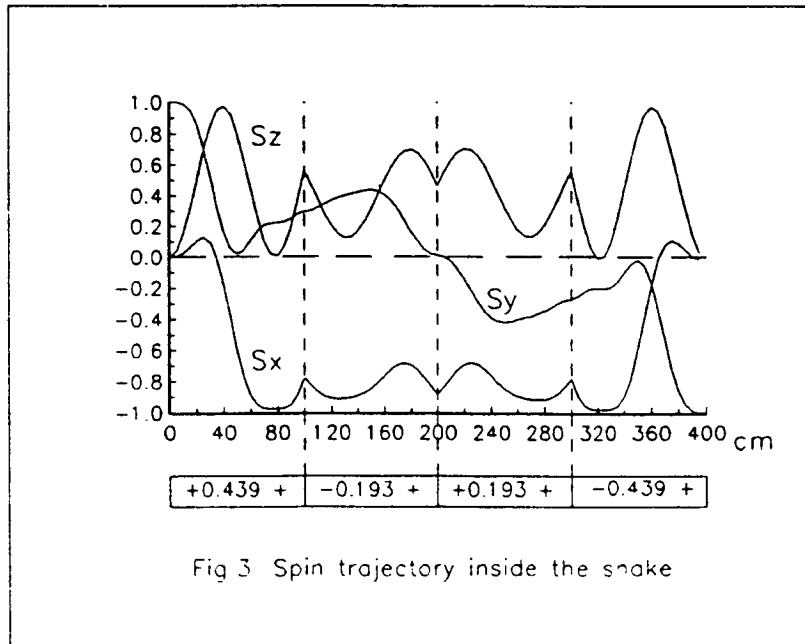
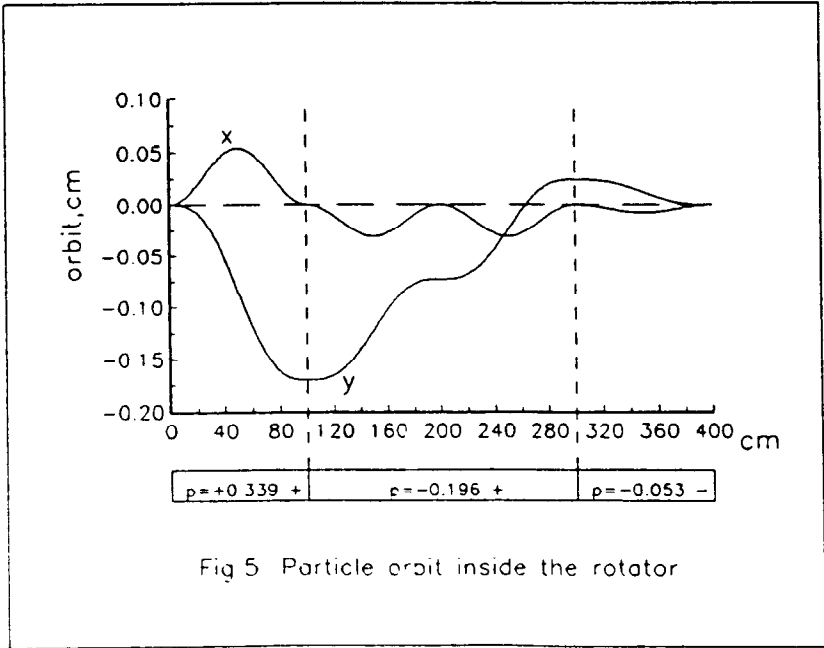
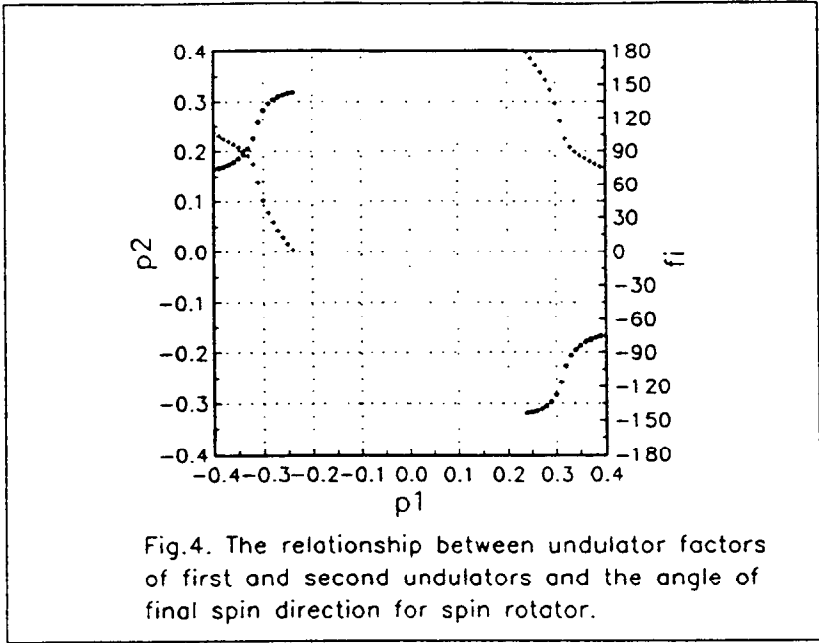


Fig 3 Spin trajectory inside the snake



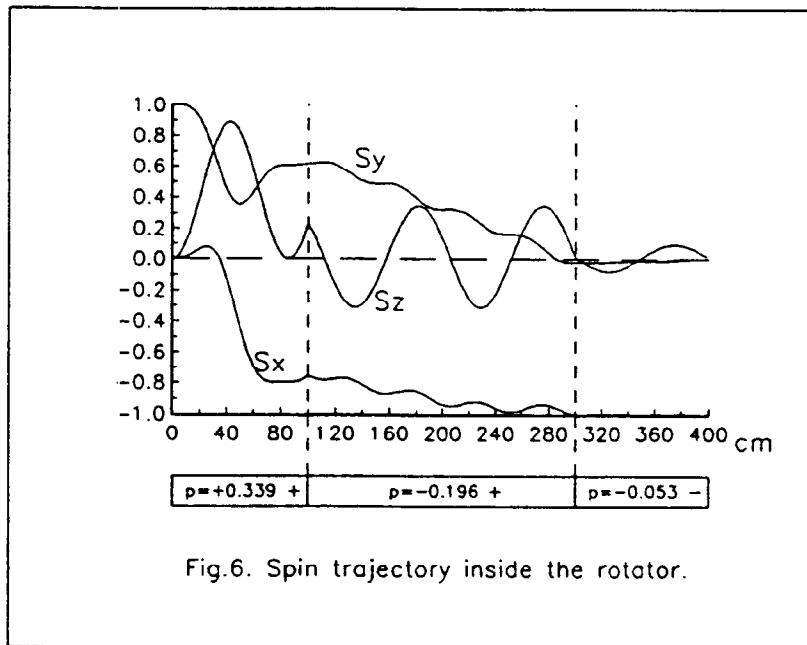


Fig.6. Spin trajectory inside the rotator.



**R. Gupta, G. Morgan and E. Willen**

**Brookhaven National Laboratory**

**Upton, NY 11973-5000**

**Design and Status of Helical Magnets at BNL**

Ramesh Gupta

Workshop Sep 12, 1994

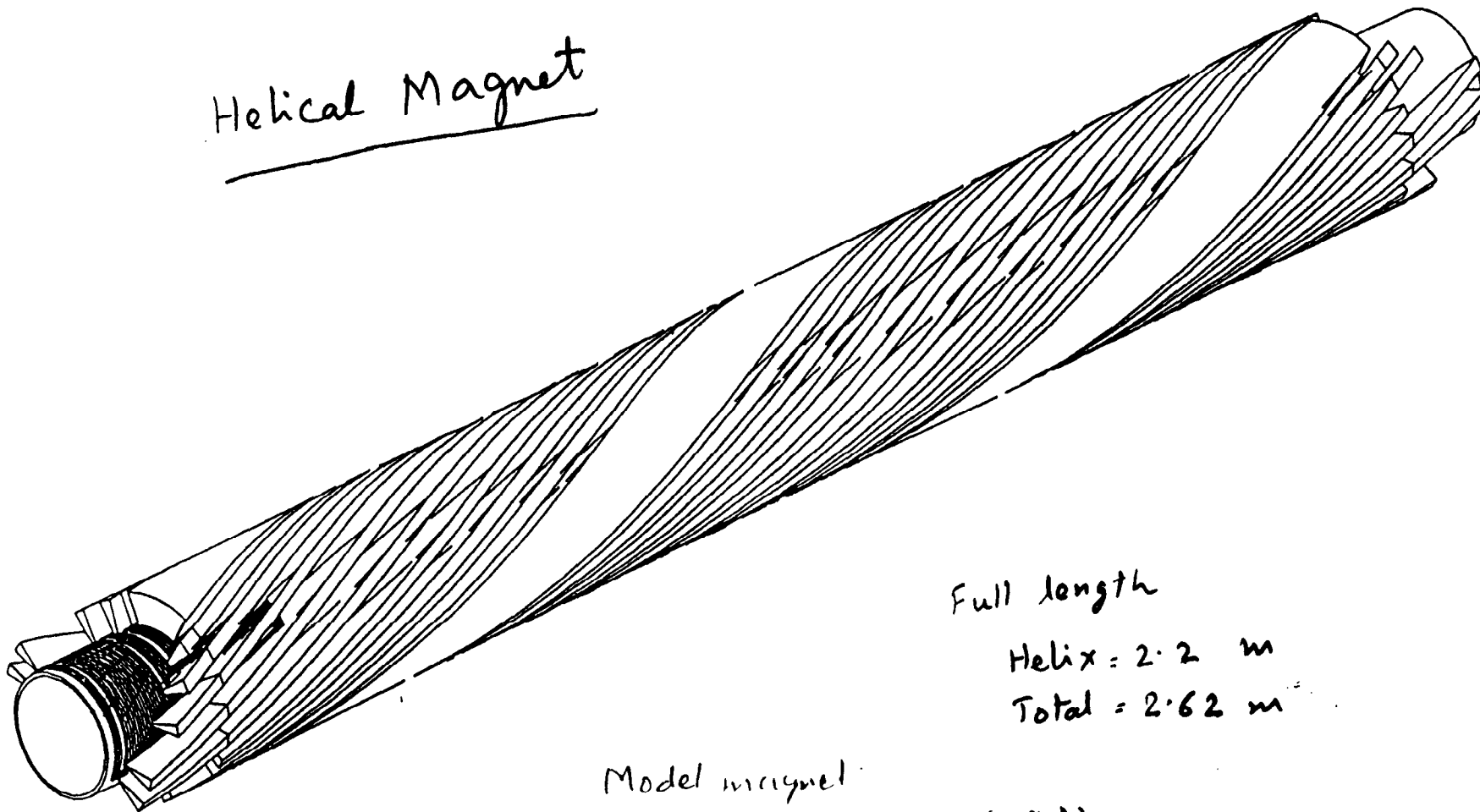
**Design and Status  
of  
Helical Magnet  
at BNL**

Ramesh Gupta

Gerry Morgan

Erich Willen

# Helical Magnet



Full length

Helix = 2.2 m

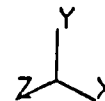
Total = 2.62 m

Model magnet:

Helix = 1.1 m (180°)

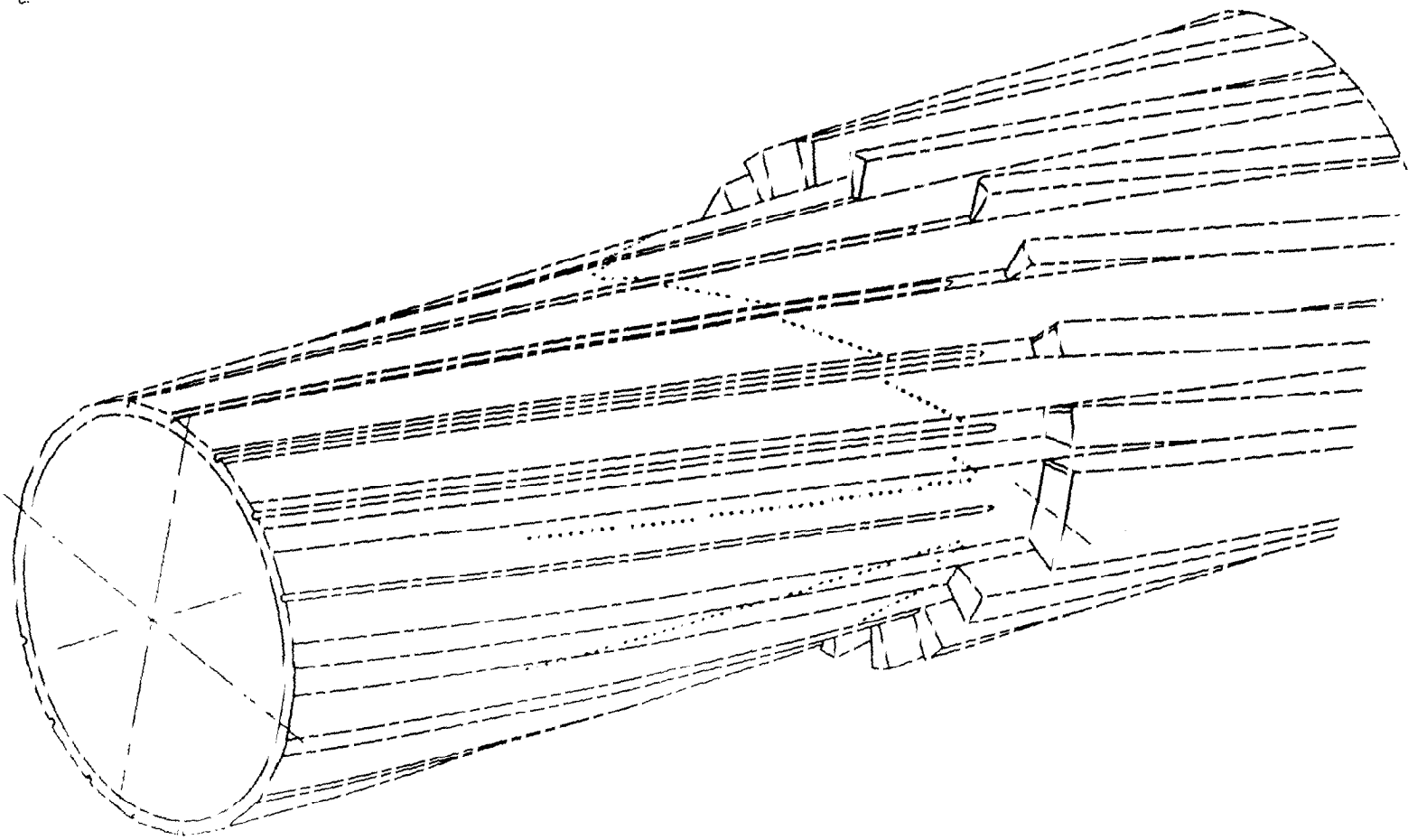
Total = 1.524 m

Ends are modified now



ALUMINIUM TUBE

Ridge & Valley after machining



SDRC I-DEAS VI.i(s): Solid\_Modeling

06-JUN-94

09:28:06

Database: rhic 8 & 10cm helical dipole for proton spin

User: LE ISO LEFT (modified)

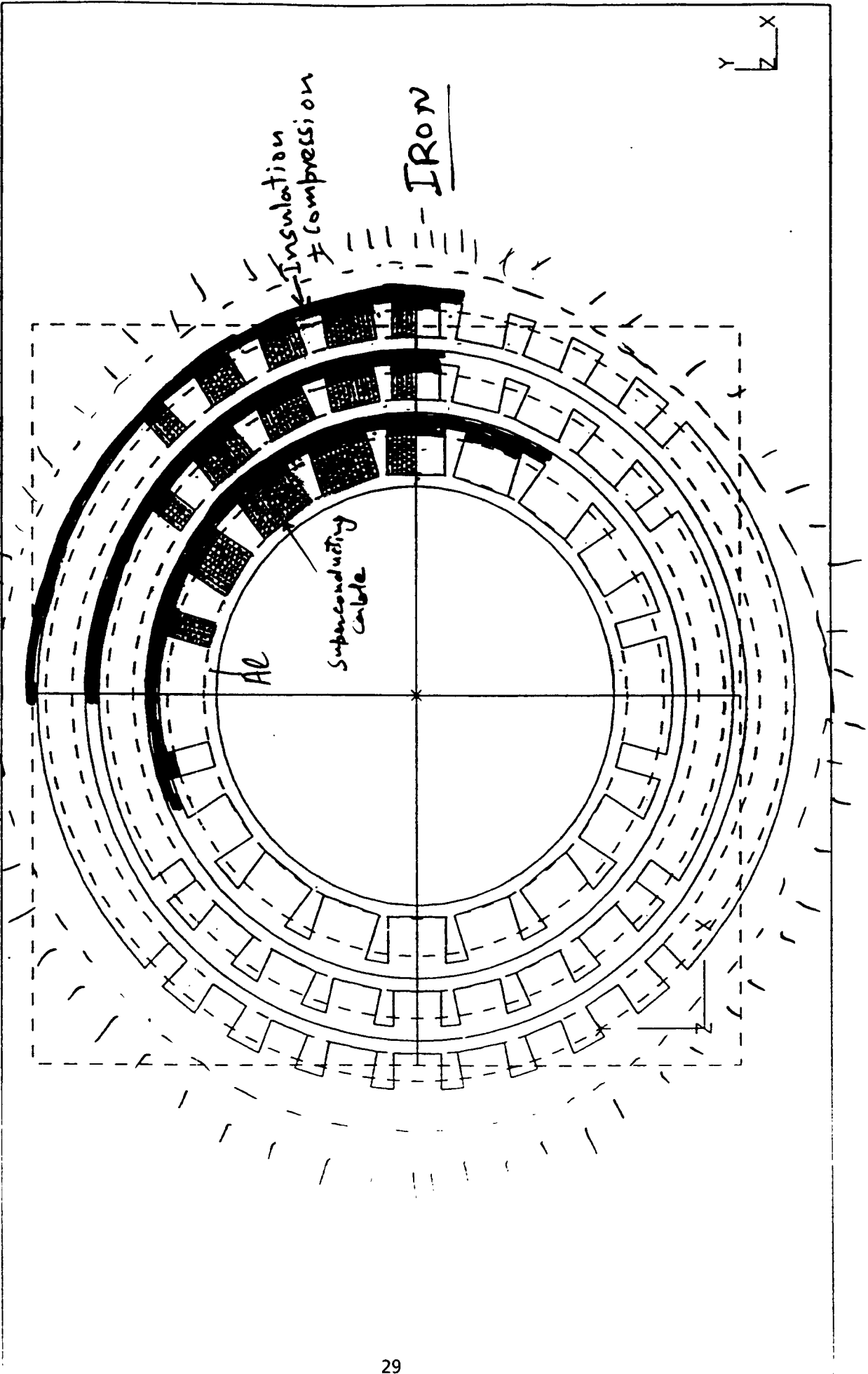
Task: Construction Geometry (3D Mde)

Skin: No current SPIN GROUP exist

Wireframe: 5-SNAKE 3 LAY XSECT (modifi  
Profile: No current PROFILE exists

Display: No stored Option

Units: MM



# Design Field in Various Magnets

Magnet Type Quench (theoretical @ 4.5

Helical = 4 Tesla

Wire 4.5 T

RHIC = 3.5 T

CABLE 4.8 T

SSC = 6.6 T

CABLE 7.4 T

Corrector (RHIC) = 0.6 T  
(Dipole, 3 layers)

Wire ~ 2 T

Sextupole (RHIC)

Pole Tip = 1.1 T

Wire ~ 2 T

Note: Lorentz forces on the conductors goes as  $I \times B$   
( $\sim I^2$  or  $B^2$ )

# Design Principles for the Helical Dipole Magnet

## *Low Current, DC Operation (<500 A)*

- Numerous magnets distributed around the ring requires that the current leads each have a low heat leak
- Magnets will be operated at a fixed current (no ramping required)

## *Use Available Superconductor If Possible*

- Design incorporates a 7 strand (6-around-1) Kapton-wrapped cable made of RHIC corrector wire
- Operating current will be 382 A
- Cable of wires is preferable to a single wire in a magnet

## *Model Construction After RHIC Sextupole*

- RHIC sextupole had a long R&D effort before satisfactory design was achieved
- Production sextupole magnets have good performance, if built according to design
- Sextupole quench current (200 A) is similar to that required in helical magnet

## *Support Each Turn Completely*

- Straight section turns are supported by fiberglass/epoxy matrix
- End turns are supported by mineral-loaded epoxy filler
- Turns are compacted with fiberglass overwrap applied under tension

## *Good Field (low harmonic content) in Body and in Ends*

- Body field optimized by adjusting thickness of wedges between current blocks
- End field optimized by controlling turning angle and turn spacing

## Parameters of the Helical Dipole Magnet - I

Parameters of the Helical Dipole Magnet - I			
<b>Selected Parameters</b>			
Operating field	T	4	•
Operating current	A	382	•
Operating temperature	K	4.2	!
Quench field @ 4.2K	T	4.67	!
Quench current @ 4.2K	A	453	!
Peak field on conductor at quench	T	5.25	!
Inductance	H	1.5	•
Stored energy at operating field	kJ	112	
<b>Length</b>			
<b>Coil</b>			
Straight section	mm	1100	•
Winding end	mm	139	
Coil end	mm	212	
Total	mm	1524	•
Lamination stack	mm	1524	
<b>Helix</b>			
Length	mm	1100	•
Rotation	deg	180	•
Pitch	deg/mm	0.1636	•
<b>Radius of yoke</b>			
Inner	mm	91.4	•
Outer	mm	250	•
Cold mass weight	kg		
<b>Superconductor Parameters</b>			
<b>Wire</b>			
<b>Mechanical</b>			
Nominal filament diameter	microns	10	•
Nominal filament spacing	microns	>1	
Nominal Cu to non-Cu ratio		(2.5 ± 0.1):1	
Number of filaments		310 ± 5	
Diameter, bare	in	0.013 ± 0.0001	•
Twist direction		right	
Twist pitch	twst/in	2.0 ± 0.2	
<b>Electrical</b>			
Minimum I(crit)@2.0T, 4.2K	A	120	
Max, I(crit)@2T/I(crit)@5T		1.9	
Minimum I(crit)@5.0T, 4.2K	A	68	
Wire max R(295K)	ohm/m	0.28	
Wire min RRR		90	
<b>Cable</b>			
<b>Mechanical</b>			
Number of wires		7	•
Type		6-around-1	•
Twist direction		right	
Twist pitch	twst/in	2.67	
Diameter, bare	in	0.039	•
Diameter, insulated	in	0.043	•
<b>Electrical</b>			
Minimum J(crit)@5.0T, 4.2K	A	476	

Operating T  
RHIC Dipole 4.5  
Bus = 4.5T

RHIC dipole 20

**Parameters of the Helical Dipole Magnet - II**

**Mechanical Parameters**

	Cylinder			Total
	Inner	Middle	Outer	
Cylinder number	1	2	3	<b>3</b>
Number of current blocks	5	5	5	<b>15</b>
Number of cable layers	7	5	5	<b>17</b>
Number of turns per layer (per block, from midplane)	6,12,12,10,5	5,10,10,10,5	5,10,8,8,5	
Number of turns per block, from midplane	42,84,84,70,35	25,50,50,50,25	25,50,40,40,25	
Total turns (upper or lower half)	315	200	180	695
Cable length per block, from midplane, m	122,233,218,170,81	79,150,176,130,60	84,158,118,110,65	
Cable length (upper or lower half), m	825	595	534	1954
Pole angle, deg	77.6	56.2	46.2	
Self inductance, mH	250	160	170	
Fractional contribution to field	0.44	0.29	0.27	
Radius of cylinder (inner, outer), mm	47, 60.4	63.4, 74.4	77.4, 88.4	
Radius of current block (inner, outer), mm	50, 58.4	66.4, 72.4	80.4, 86.4	

33

SNAKE

- Multi-layer coils like in corrector magnets.
- The wire (cable) would, however, be laid with a scheme similar (somewhat) to RHIC Sextupole in a helical path.

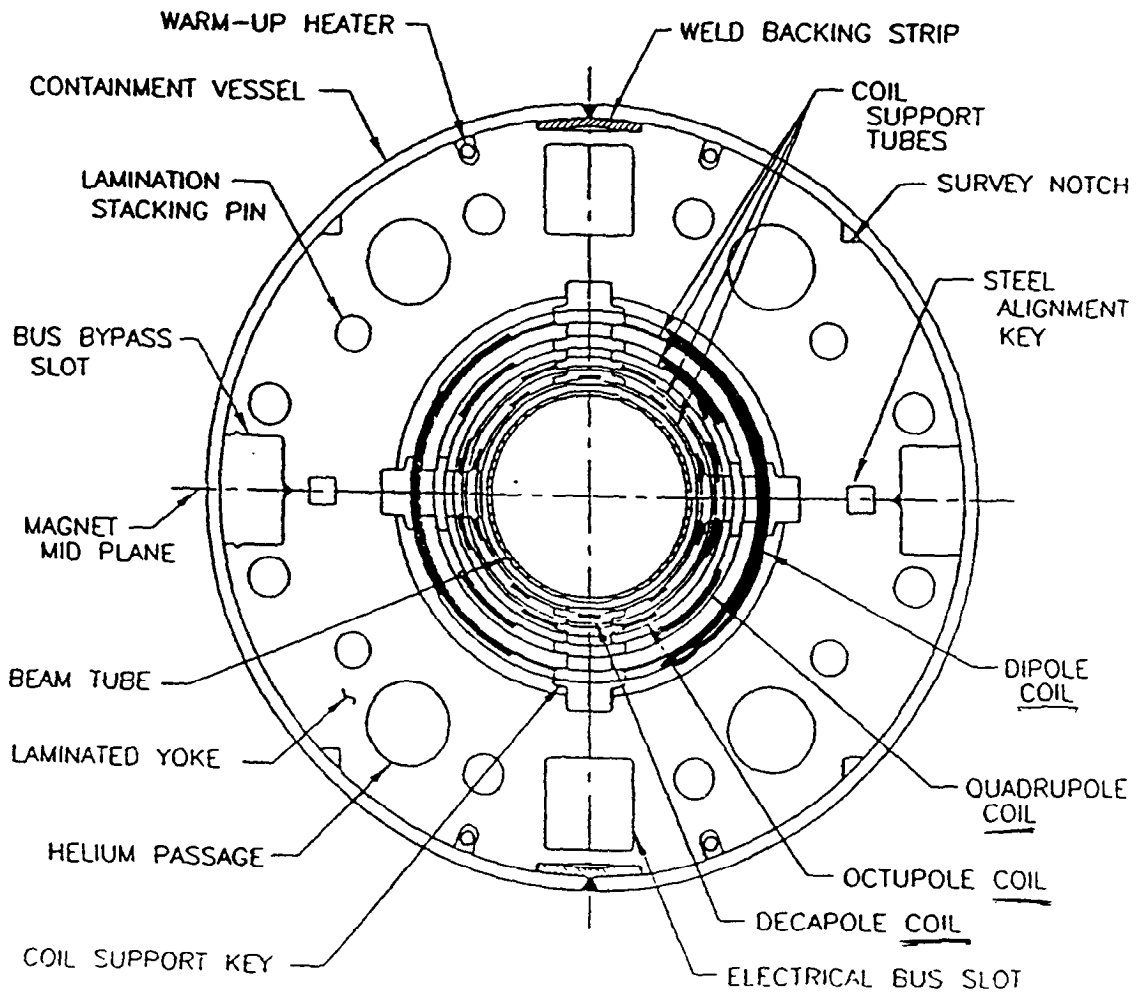


Fig. 1-10. Arc corrector cross-section (beam tube i.d. = 69 mm).

# Superconductors for Helical Magnet

6 around 1 cable using corrector wire

Corrector wire: 0.013" dia = 0.99 mm

$$I_c = 7.0 A \cdot T = 490 A (5T)$$

$$C_c / SC = 2.5 : 1$$

Ratio of areas:

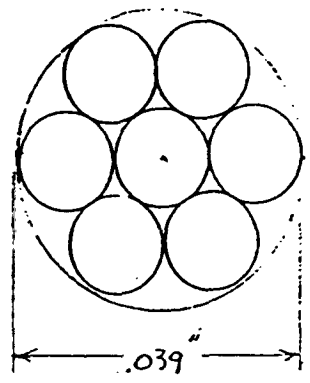
Cable wire dia = .748 mm  
(inc insulation)

Cable 6-A-1: .99 + .1 = 1.09 mm

$$\text{Ratio} = \left( \frac{.748}{1.09} \right)^2 = .471$$

Ratio of diameters:

$$\frac{.748}{1.09} = .686$$



NAPID. AL | ...

## Cross-section Design

cosine  $\theta$  Magnet to Generate Dipole Field.

However,

- Typical superconducting magnet has copper wedges inserted between cable to shape the field
- Here we would have superconducting cable inserted in a Aluminium structure.

The tooling and manufacturing concepts change accordingly.

## Cross-section Design

Three layers (cylinders) in the design.

Advantages of three small layers instead of one large one :

1. Each layer is easier to construct
2. Reduce (redistribute) Lorentz forces on cables and hence expect better performance
3. Can build, test and iterate the design in a partial magnet
4. Field quality of one layer can be iterated in the second/third layer

SNAKE 3 LVR 5 BLK each  
 file = U05:[SCHATCH.GUPTA.TEMPS]TEMPS.D07:2 Run 31-MAY-94 17:31:23  
 CRISO= 0.0491 dB/Ellipse= 0.1568 Peak Enhance= 0.184 0.165  
 TRANSFER FUNCTION= 105.13364 POLE ANGLE= 77.60550 Rfe= 9.340 Rref= 3.100  
 PARAMETERS ORIGINAL FINAL DIFFERENCE Face Angles

SNAKE 3 LVR 5 BLK each  
 file = U05:[SCHATCH.GUPTA.TEMPS]TEMPS.D07:2 Run 31-MAY-94 17:31:23  
 BegDist EndDist MidDist dAngle Radial Radius2 Radius3 Radius4 Angle14  
 (mil) (mil) (mil) (deg) (inch) (inch) (inch) (inch) (Deg) (Deg)

PARAMETERS	ORIGINAL	FINAL	DIFFERENCE	Face Angles
1	6.	6.	0.	0.000 -7.301
2	2.20000	2.48427	0.28427	18.306
3	12.	12.	0.	7.301 -7.301
4	3.30000	3.42461	0.12461	19.246
5	12.	12.	0.	7.301 -7.301
6	4.40000	5.12662	0.72662	19.628
7	10.	10.	0.	6.081 -6.081
8	5.50000	7.50249	2.00249	17.387
9	5.	5.	0.	3.039 -3.039
10	5.	5.	0.	0.000 -4.749
11	2.20000	2.55198	0.35198	12.478
12	10.	10.	0.	4.749 -4.749
13	3.30000	3.53141	0.23141	13.457
14	10.	10.	0.	4.749 -4.749
15	4.40000	4.49514	0.09514	14.421
16	10.	10.	0.	4.749 -4.749
17	5.50000	6.06339	0.56339	13.507
18	5.	5.	0.	2.373 -2.373
19	5.	5.	0.	0.000 -3.951
20	2.20000	2.77884	0.57884	10.976
21	10.	10.	0.	3.951 -3.951
22	3.30000	3.63676	0.33676	11.014
23	8.	8.	0.	3.161 -3.161
24	4.40000	4.69361	0.29361	11.250
25	8.	8.	0.	3.161 -3.161
26	5.50000	5.63933	0.13933	10.966
27	5.	5.	0.	1.975 -1.975

116.54	167.88	142.21	12.4785	2.6167	2.6167	2.8521	2.8521	12.4785	0.
161.25	216.41	188.93	13.4571	2.6167	2.6167	2.8521	2.8521	25.9352	12.
205.24	264.54	234.89	14.4209	2.6167	2.6167	2.8521	2.8521	40.3564	25.
276.71	312.25	304.48	13.5067	2.6152	2.6167	2.8521	2.8512	53.8613	40.
153.60	194.79	176.19	10.9762	3.1673	3.1673	3.4030	3.4030	10.9762	0.
200.99	246.33	223.66	11.0139	3.1668	3.1673	3.4030	3.4027	21.9899	10.
259.35	305.66	282.51	11.2508	3.1668	3.1668	3.4027	3.4027	33.2403	21.
311.54	356.68	334.11	10.9664	3.1662	3.1668	3.4027	3.4023	44.2065	33.

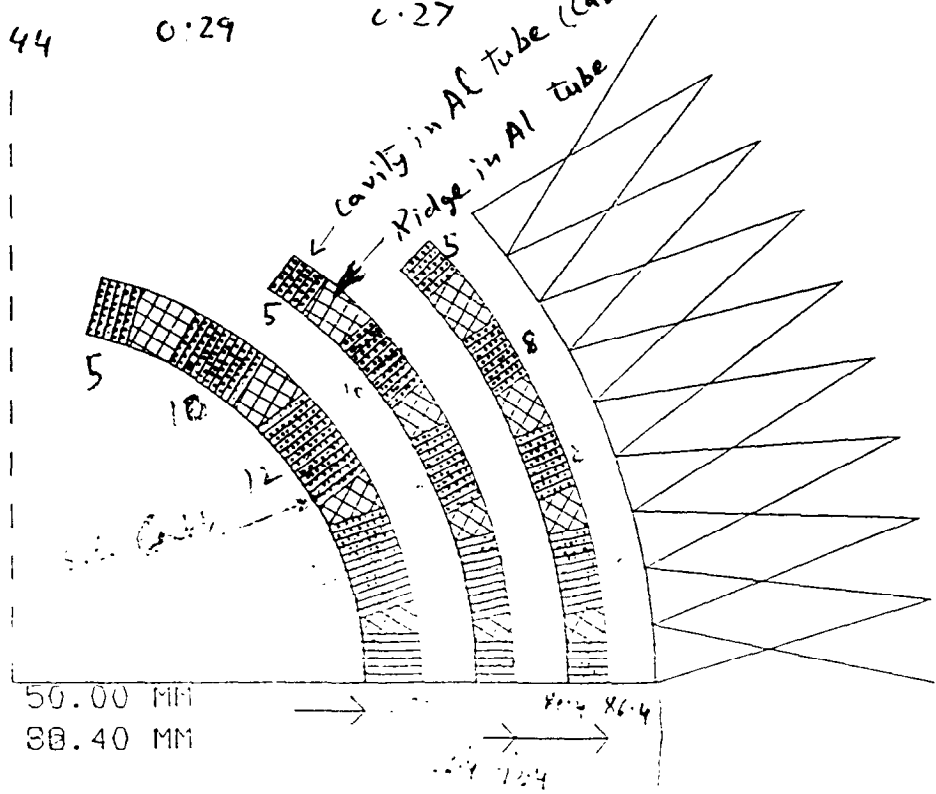
Allowed Prime Harmonics

n	bn-cal	bn-des	n	bn-cal	bn-des	In/out Cal	DESIGN
0	10000.000	0.000	10	0.150	0.000	77.860	0.000
2	-0.008	0.000	12	0.036	0.000	77.387	0.000
4	0.008	0.000	14	-0.145	0.000	56.344	0.000
6	0.011	0.000	16	0.000	0.000	56.139	0.000
8	0.065	0.000	18	0.000	0.000	46.255	0.000

All harmonics are theoretically zero.

# HELICAL MAGNET CROSS SECTION

	Layer #1	Layer #2	Layer #3	Total = (95)
Total No. of turns	315	200	150	
Fraction of total	0.45	0.29	0.26	
Fractional contribution to total field	0.44	0.29	0.27	



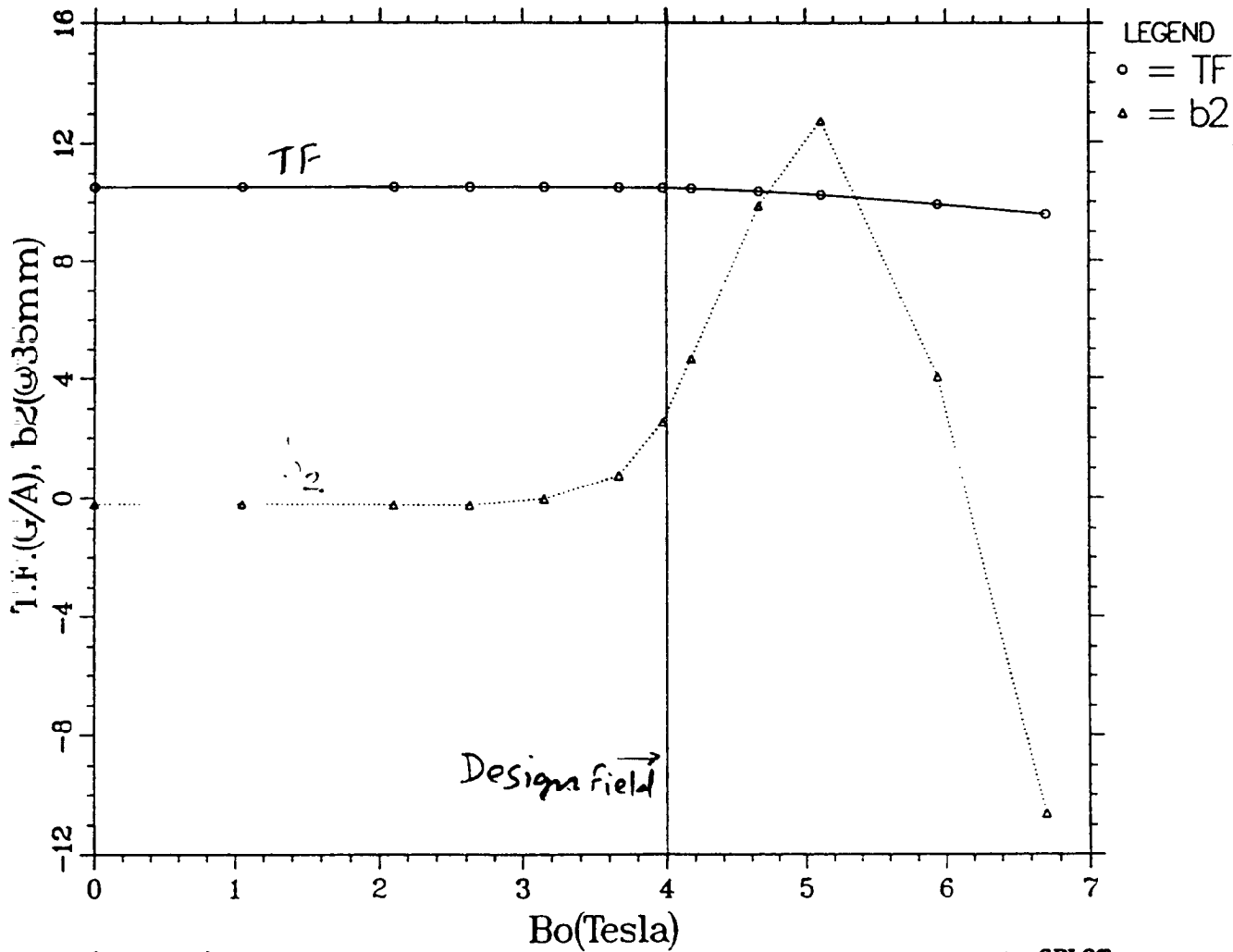
# Current dependence on Field Quality

- Not an issue since it's a fixed field operation

At Design  $\delta TF = -0.4\%$

$$\delta b_2 = +2.7 \text{ unit}$$

COIL DESIGN TO SUPPRESS SATURATION INDUCED HARMONICS.  
Current Dependence of Field Quality in Helical Magnet

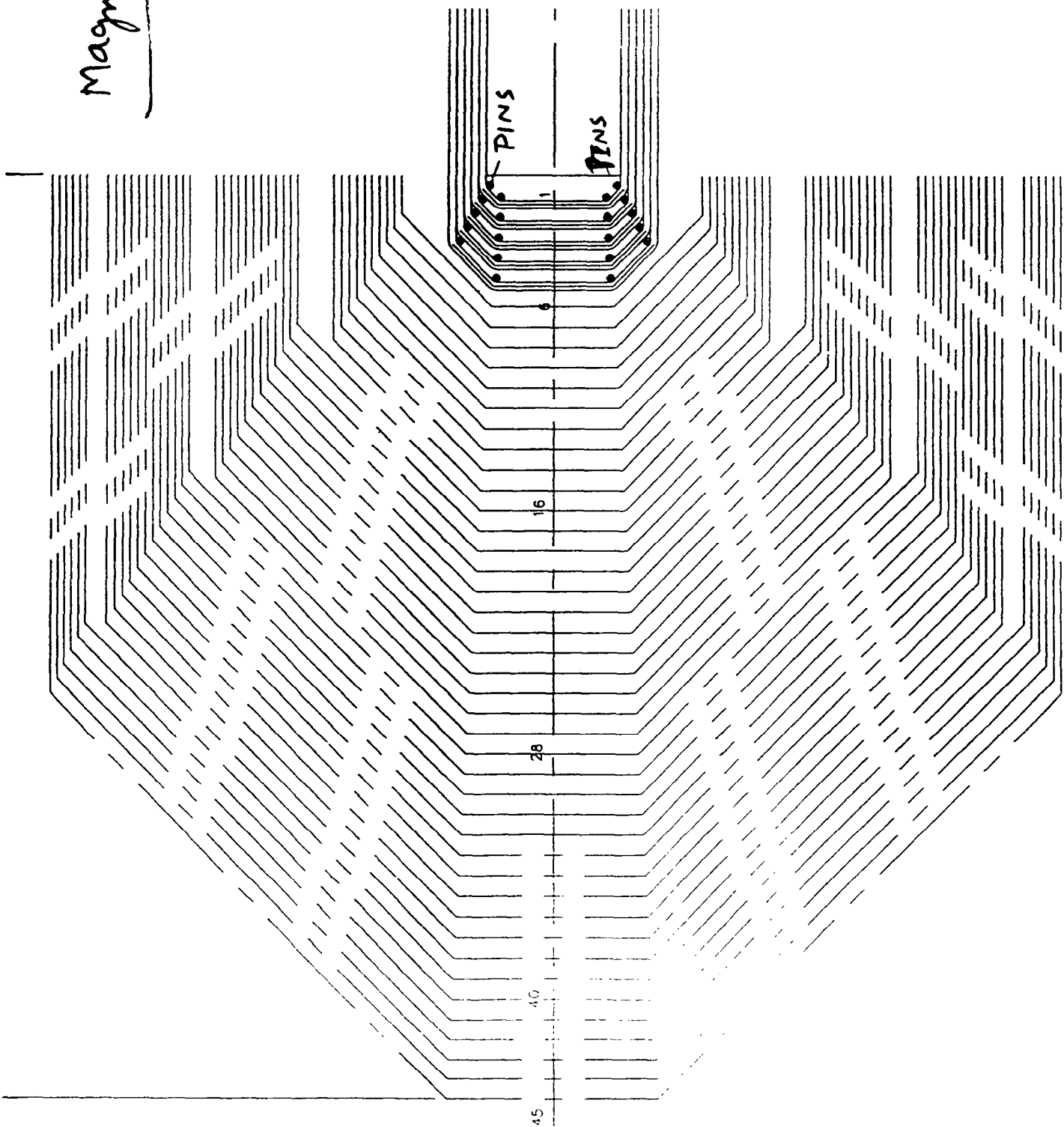


[GUPTA.SNAKE]SNAKE\_DESIGN.TFB2:1

09:36:26 . 9-SEP-94 G PLOT

Magnet End (Morgan)

Superconducting  
Cable



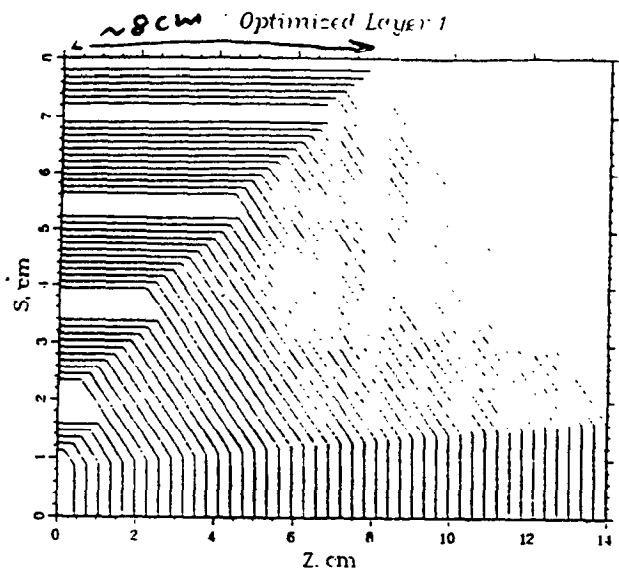


Figure 5

End Design (Morgan)

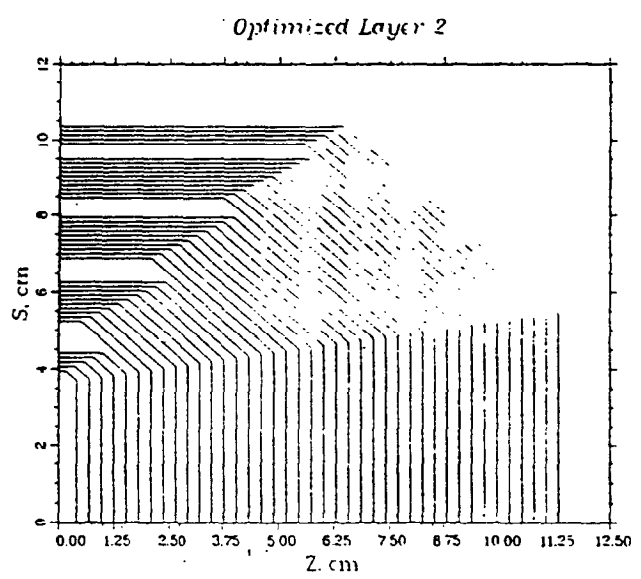


Figure 6

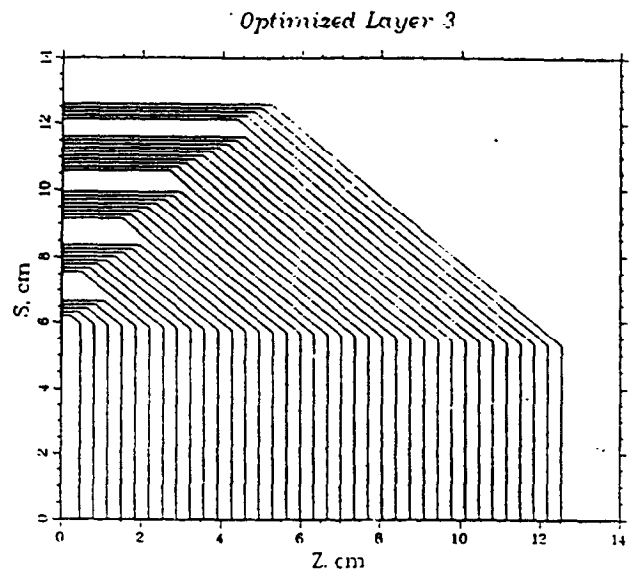


Figure 7

Plot of  $\omega$  vs  $Z$

129 rad/cm

## **Status of the Helical Dipole Magnet (August 1994)**

Parameters for a first model have been established

Superconducting cable (6-around-1) wrapped with Kapton has been manufactured at NEEW

A suitable magnetic design, including end design, has been made

Mechanical design is based on superconductor laid into spiral grooves machined into a thick-walled aluminum cylinder. Three concentric cylinders form the coils for one magnet. An iron yoke surrounds and supports the coil assembly as in other RHIC magnets

The engineering design for one cylinder has been completed, material has been procured, and the cylinder has been manufactured in the BNL shops

A technician has been assigned to begin winding superconductor into the grooves of the cylinder

## Near-Future Work for the Helical Magnet (August 1994)

### *Lab Work*

- Establish feasibility of winding the coils
- Wind one current block into cylinder, test cryogenically
- Wind complete cylinder, test cryogenically
- Modify design as required
- Build simple tooling as required

### *Design Work*

- Continue engineering design of rest of magnet
- Model quench propagation and quench temperatures in the magnet
- Establish methods for measuring field in the magnet
- Establish joint effort with industry to make a production design



**R.Baiod**

**Fermilab**

**P.O.Box 500. Batavia, Illinois 60510**

**Siberian Snakes for the Fermilab Main Injector**

# MAIN INJECTOR POLARIZED BEAM EFFORT

**CIRCA 1991-1992:**

**Yu. M. Ado, IHEP, Protvino**

**V. A. Anferov, R. Baiod, E. D. Courant, Ya. S. Derbenev,  
A. D. Krisch, D. S. Shoumkin,  
University of Michigan, Ann Arbor**

**S. Y. Lee, IUCF**

## REFERENCES:

- 1)"Acceleration of polarized protons to 120 and 150 GeV in the Fermilab Main Injector", SPIN Collaboration, University of Michigan Report, (1992).
- 2)"Acceleration of polarized protons to 1 TeV in the Fermilab Tevatron", SPIN Collaboration, University of Michigan Progress Report, (1994).
- 3)"Siberian Snakes for the Fermilab Main Injector", V. A. Anferov et al, UM HE-16, 1994, being submitted to Physical Review. Other references therein.

# MAIN INJECTOR

- Accelerates p and pbar from 8 GeV to 150 GeV
- Slow extraction @ 120 GeV with half integer scheme  
(horizontal tune = 1/2, beware of coupling resonance)
- two superperiods
- 14 m between quadrupoles, space available for each snake

# DESIGN PROCEDURE

- Evaluate resonance strength to get necessary number of snakes:

$$N_s > 5 \cdot \epsilon_{int} \quad (\text{S.Y. Lee \& Courant, Physical Review D41, 292})$$

- Choose location to get energy independent spin tune
- Choose snake precession axis so that spin tune is away from resonances (  $1/2$  ). Favor solutions, that can be implemented with snakes of same engineering design.
- Fix snake configuration, ie, type and number of magnets, arrangement and symmetry of the arrangement. Symmetry will relax some of the constraints
- Solve for magnet integrated strengths to have  $180^\circ$  spin rotation and proper horizontal precession axis
- Solve for the beam directions to be restored in both planes, and orbit to be recentered in both planes
- Optimize orbit excursions inside snake

# GENERAL REQUIREMENTS ON MAGNETIC FIELD SYMMETRY AND TRAJECTORY

- To restore beam direction in both planes:

$$\int_{\text{snake}} \vec{B} \, d\mathbf{l} = 0$$

- To recenter the orbit vertically and horizontally

$$\int_{\text{snake}} \left( \int_0^1 B_x \, dy \right) d\mathbf{l} = 0$$

$$\int_{\text{snake}} \left( \int_0^1 B_z \, dy \right) d\mathbf{l} = 0$$

- If a component is symmetric w.r.t snake center, displacement in the other direction is zero

- If a component is antisymmetric w.r.t. snake center, displacement in the other direction must be zero at the snake center

## SYMMETRY WITHIN A SNAKE AND SPIN MOTION

" If a snake is such that component  $\alpha$  is antisymmetric w.r.t snake center, and components  $\beta$  and  $\gamma$  are symmetric, then the snake axis has no  $\alpha$  component "

$$\begin{aligned} \text{Trace} \left[ \sigma_{\alpha} e^{(\alpha, \beta, \gamma)} \cdot e^{(-\alpha, \beta, \gamma)} \right] &= \text{Trace} \left[ e^{(\alpha, -\beta, -\gamma)} \cdot \sigma_{\alpha} e^{(-\alpha, \beta, \gamma)} \right] \\ &= \text{Trace} (\sigma_{\alpha}) = 0 \end{aligned}$$

### Consequences:

- \* snakes with symmetric radial field and antisymmetric vertical field, have horizontal precession axes.
- \* snakes with transverse fields, symmetric w.r.t. center, may be assumed as having symmetric (zero) longitudinal field. The precession axis is transverse, and becomes radial after adequately rotating the whole snake structure around the beam axis.

# SYMMETRY BETWEEN CONFIGURATIONS AND SPIN MOTION

## Trivial:

**" If we identically rotate the fields of all magnets in a snake, then the result is still a snake but with its axis rotated the same way as each individual magnet"**

**As a consequence, to make snakes that are different but have same engineering design:**

- \* switching the current of the vertical components only changes the snake axis to its mirror image w.r.t. the beam ( rotation around radial axis )**
  
- \* switching currents of both transverse components accomplishes the same thing ( rotation around beam axis )**
  
- \* switching the current of radial components only results in no change of axis (rotation around vertical axis)**

# MAIN INJECTOR SNAKE STRUCTURE

- Normalized emittance:  $10 \cdot \pi$  mm-mrad

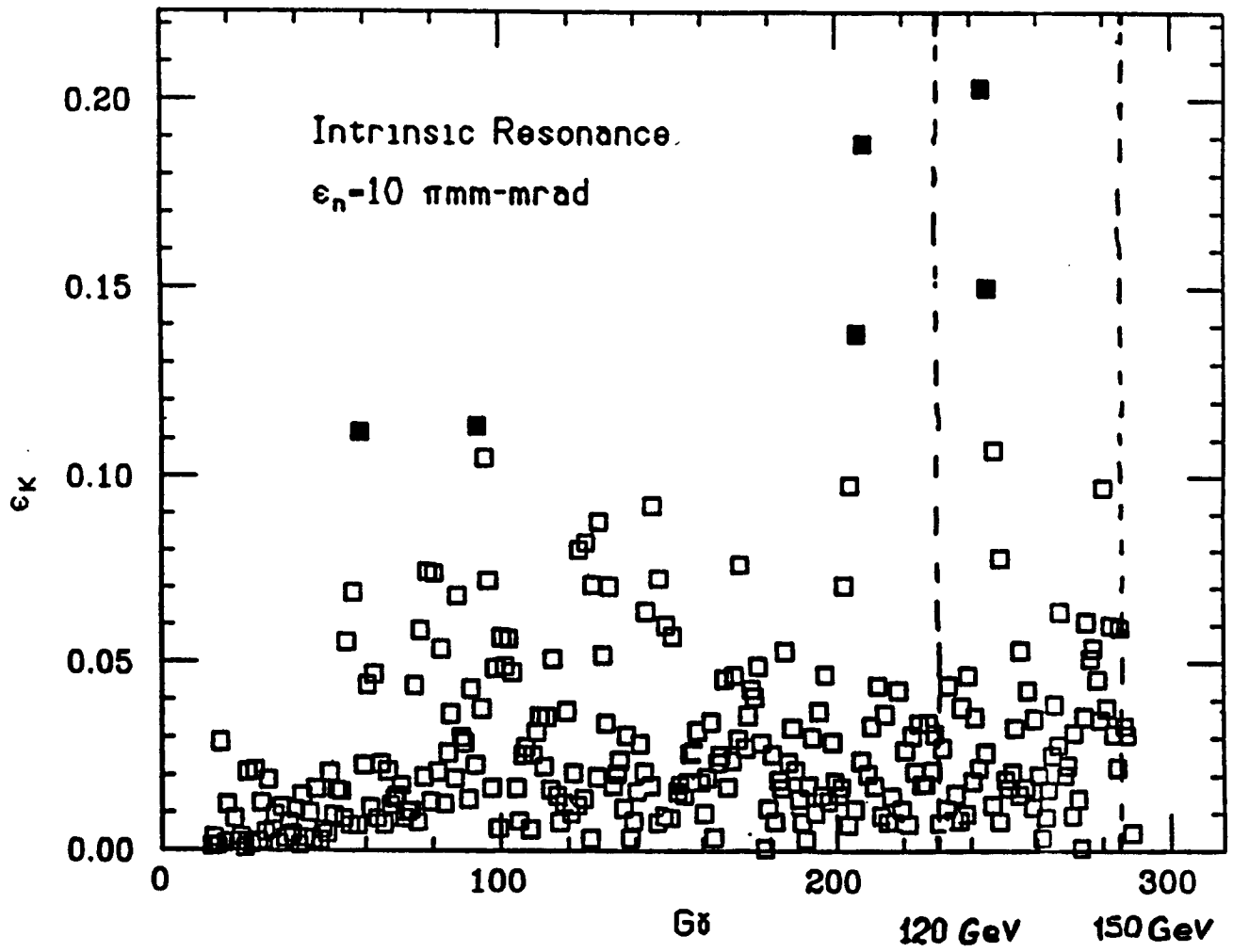
Closed orbit distortion: 2 mm

**As a result, the intrinsic resonance strength is of the order of 0.20 and the imperfection resonance strength is of the order of 0.26. Two snakes will overcome these resonances as well as provide for vertically polarized beam.**

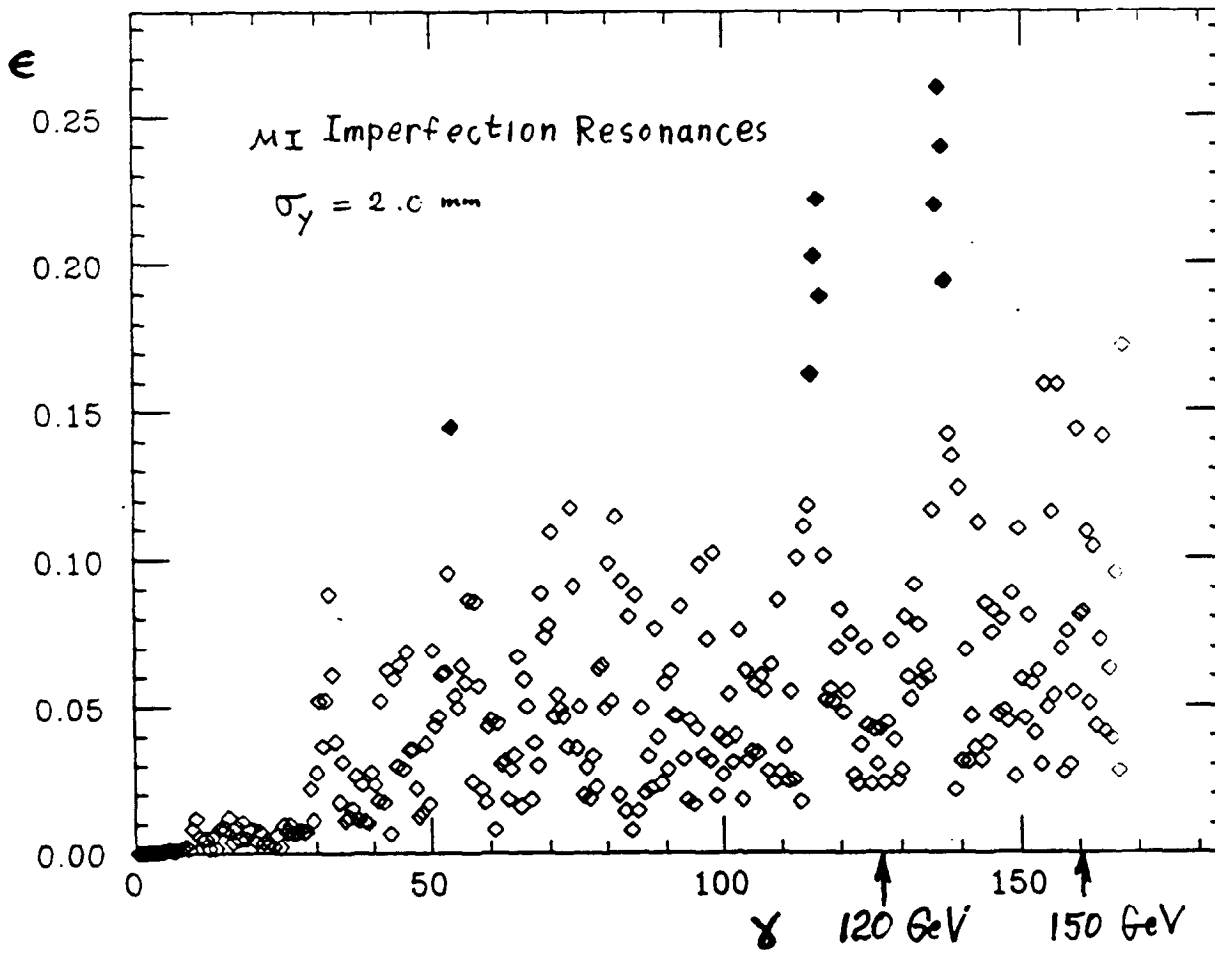
- Snakes are oppositely located in the ring to get energy independent tune

- Snake axis are orthogonal to get spin tune at 0.5, and are of identical designs. This requires each snake axis to be  $45^\circ$  away from the beam

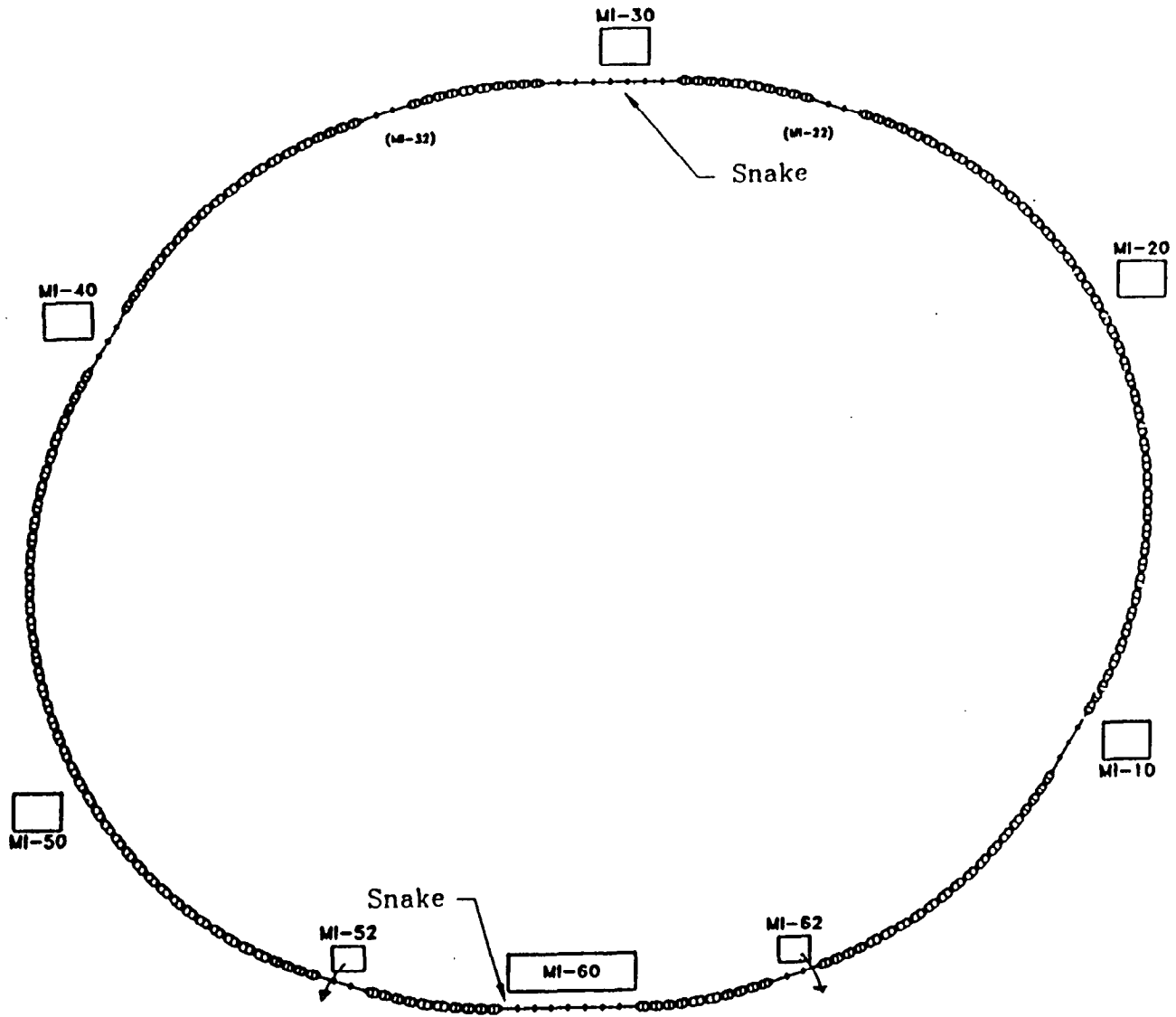
- Restrict our search to symmetric radial fields and antisymmetric vertical fields. ( Nice effects of symmetry previously discussed )



The strength  $\epsilon$  of the Intrinsic Depolarizing Resonances in the Fermilab Main Injector.



The strength  $\epsilon$  of the Imperfection Depolarizing Resonances in the Fermilab Main Injector.



Proposed snake locations in the Fermilab Main Injector Ring.

# STEFFEN-LEE SNAKE SCHEME

- Arrangement symmetry implies that :

- \* snake axis is horizontal
- \* beam direction restored in both planes
- \* no vertical orbit offset

Horizontal orbit needs to be recentered

- Maximum vertical excursion:

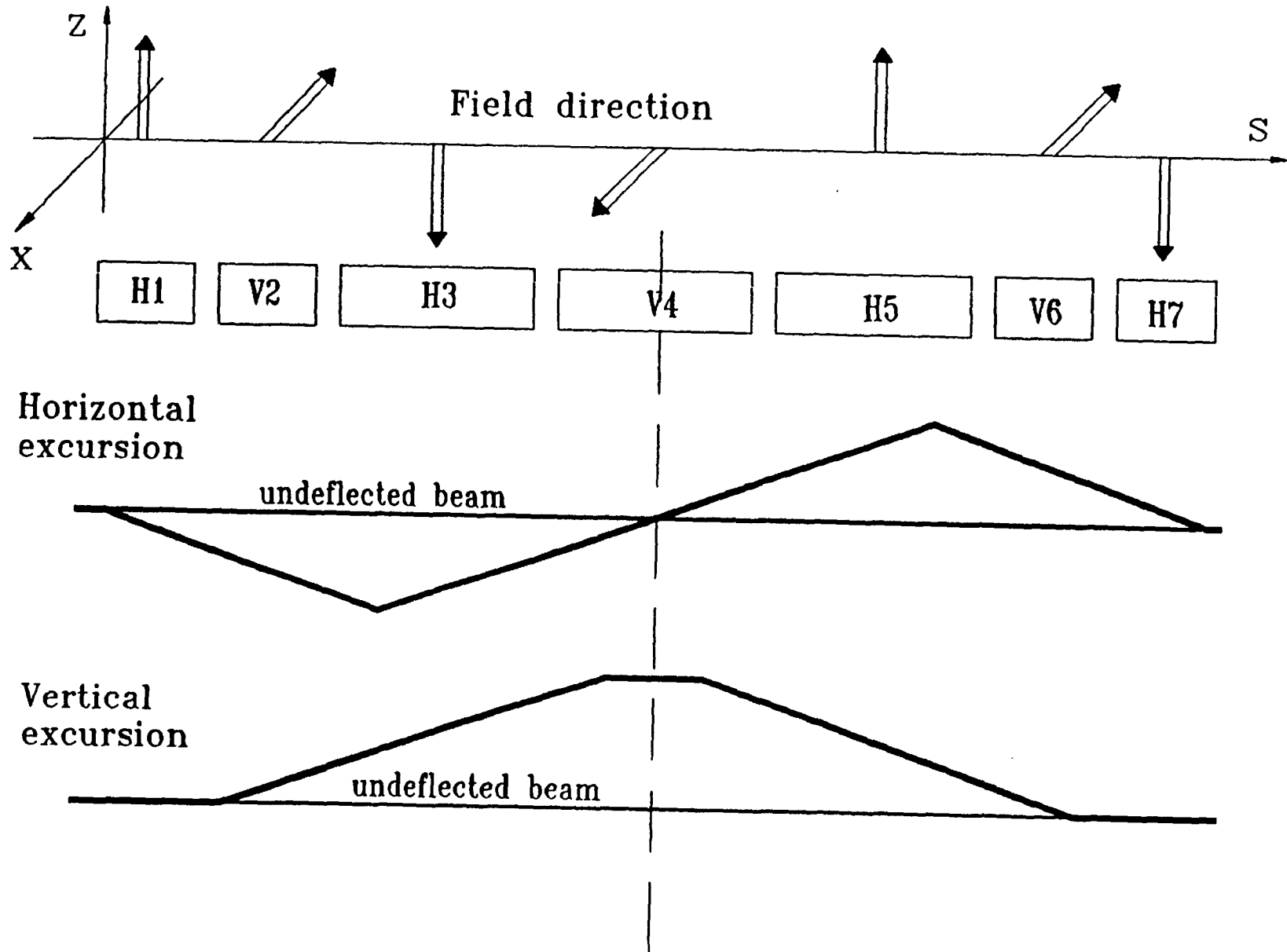
$$D_z = \frac{\Psi_y}{G \cdot \gamma} \cdot (l_y + l_m + 2 \cdot l_g) - D_{v.\text{correction}}$$

- Maximum horizontal excursion, starting from the snake center:

$$D_m = \frac{\Psi_m - \Psi_x}{G \cdot \gamma} \cdot \left( \frac{l_m - l_x}{2} + l_y + l_g \right)$$

This is to be matched to the incoming orbit, with the help of a corrector:

$$D_m = \frac{\Psi_x}{G \cdot \gamma} \cdot (l_x + l_y + 2 \cdot l_g) + D_{h.\text{correction}}$$



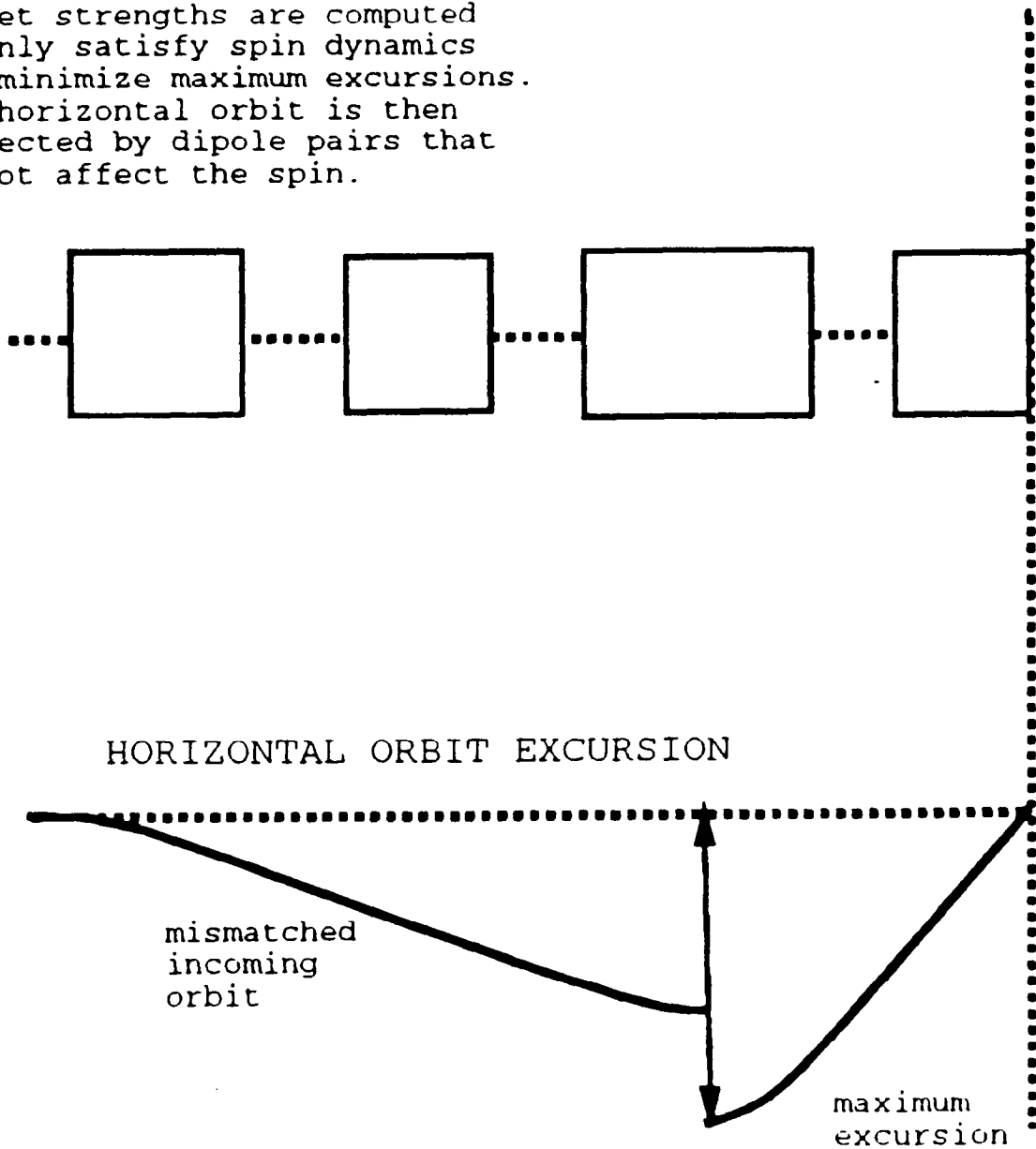
57

Magnet configuration and orbit excursions in the Steffen-Lee snake.

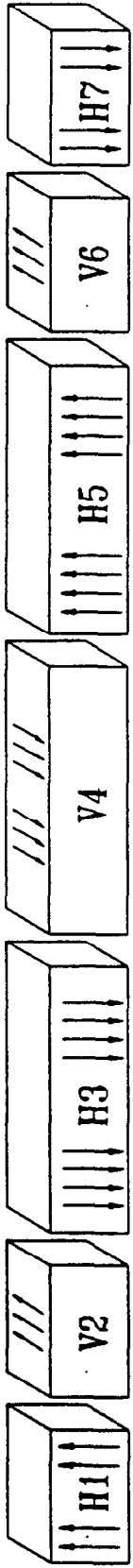
# Steffen-Lee Snake

SNAKE CENTER

Magnet strengths are computed to only satisfy spin dynamics and minimize maximum excursions. The horizontal orbit is then corrected by dipole pairs that do not affect the spin.



# Warm Steffen-Lee snake



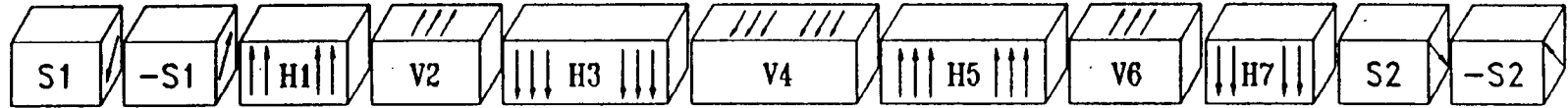
Magnet length (m)	1.00	1.00	2.15	2.15	2.15	1.00	1.00
Field (T)	1.58	1.67	1.70	1.55	1.70	1.67	1.58
$\int Bdl$ (Tm)	1.58	1.67	3.66	3.34	3.66	1.67	1.58
Horizontal Excursion (cm)	2.6	10.0	14.6	7.5	14.6	10.0	2.6
Vertical Excursion (cm)	0.0	2.8	17.1	22.3	17.1	2.8	0.0
Spin Rotation (deg)	51.7	54.8	120	109	120	54.8	51.7

Total length: 12.9 m      Gap Between Magnets: 40 cm

Total  $\int Bdl$ : 17.2 T.m      AXIS: 7 degrees from beam

Warm magnet Steffen-Lee snake scheme with horizontal axis 7° from the beam direction.

# Cold magnet Steffen-Lee snake



Magnet length (m)	0.7	0.7	0.4	0.48	0.62	0.95	0.62	0.48	0.4	0.7	0.7
Field (T)	4.7	4.7	4.7	4.7	4.7	4.7	4.7	4.7	4.7	4.7	4.7
$\int Bdl$ (Tm)	3.29	3.29	1.89	2.24	2.9	4.48	2.9	2.24	1.89	3.29	3.29
Horizontal Excursion (cm)	2.1	5.5	5.5	3.0	2.6	1.6	2.6	3.0	5.5	5.5	2.1
Vertical Excursion (cm)	2.1	5.5	5.5	5.5	2.3	5.7	2.3	5.5	5.5	5.5	2.1
Spin Rotation (deg)	108	108	62.2	73.6	95.0	147	95.0	73.6	62.2	108	108

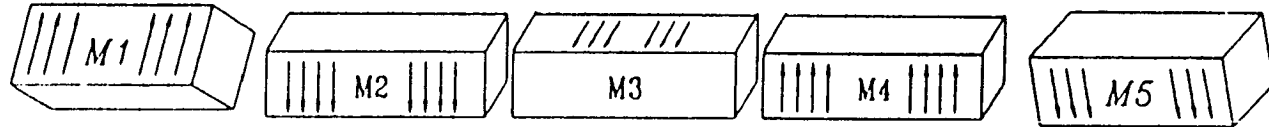
Total length: 8.75 m

Gap Between Magnets: 20 cm

Total  $\int Bdl$ : 31.7 T.m

AXIS: 45° from beam

Cold magnet Steffen-Lee snake scheme modified with two correction dipoles at each end of the snake; the snake axis is 45°.



Magnet length (m)	0.589	0.689	0.909	0.689	0.589
Field (T)	6.0 at 140.5 deg	6.0	6.0	6.0	6.0 at -140.5 deg
Bdl (T·m)	3.534	4.134	5.454	4.134	3.534
Horizontal Excursion (mm)	1.3	3.0	± 1.7	-3.0	-1.3
Vertical Excursion (mm)	1.6	6.4	8.7	6.4	1.6
Spin Rotation (degrees)	115.97	135.66	178.98	135.66	115.97

Total length: 4.265 m

Gap Between Magnets: 20 cm

Total Bdl: 20.79 T·m

AXIS: 45 degrees from beam

Proposed five magnet snake for the Tevatron.

# HELICAL MAGNET

- Field:  $\alpha_i < \alpha < \alpha_f$  ,  $d\alpha = \frac{ds}{\lambda_h}$   $\psi_h = \alpha_f - \alpha_i$

$$B_x = B_0 \cdot \cos(\alpha)$$

$$B_z = B_0 \cdot \sin(\alpha)$$

- Spin rotation:  $\psi_s = \frac{B_0 \cdot l}{1.746}$

$$d\psi_s = \frac{B_0}{1.746} \cdot ds = \frac{ds}{\lambda_s}$$

$$e^{\frac{i}{2} \cdot \sigma_y \alpha_f} \cdot e^{-\frac{i}{2} \cdot (\sigma_x \psi_s + \sigma_y \psi_h)} \cdot e^{-\frac{i}{2} \cdot \sigma_y \alpha_i} \quad \text{(notice ends contribution)}$$

- Trajectory= helix + drift  $r_0 = \frac{\lambda_h^2}{\lambda_s \cdot G \cdot \gamma}$  (helix radius)

Stretched helices have much more orbit excursion.

- Orbit direction:  $\Delta x p = \frac{\lambda_h}{G \cdot \gamma \cdot \lambda_s} \cdot (\cos(\alpha) - \cos(\alpha_i))$

$$\Delta z p = \frac{\lambda_h}{G \cdot \gamma \cdot \lambda_s} \cdot (\sin(\alpha) - \sin(\alpha_i))$$

- Orbit excursion:

$$\Delta x p = r_0 \cdot (\sin(\alpha) - \sin(\alpha_i)) + (\alpha - \alpha_i) \cdot (\lambda_h \cdot x p_0 - r_0 \cdot \cos(\alpha_i))$$

$$\Delta z p = r_0 \cdot (\cos(\alpha) - \cos(\alpha_i)) + (\alpha - \alpha_i) \cdot (\lambda_h \cdot z p_0 - r_0 \cdot \sin(\alpha_i))$$

# HELICAL SNAKES

- **Orbit excursion is smaller when orbit is matched to a helix centered at  $x=z=0$ , and with no drift. However it is costly:  $45^\circ$  precession axis are more difficult to get, in general with larger excursions and longer snakes.**
- **Search is restricted to antisymmetric schemes, ie, antisymmetric vertical field; and symmetric radial field. The orbit is matched only to restore the horizontal orbit (at the center or at the end, symmetry provides the rest) using vertical end dipoles.**
- **Incomplete helices (no full twist), require compensating horizontal field dipoles, located either at the end or in the center so that:**

$$\int_{\text{snake}} B_x \mathbf{d} = 0$$

## HELICAL FIELD HOMOGENEITY

With helical field along the axis, other components may be found offcenter, such as sextupole and longitudinal components:

(from M.W. Poole, "Synchrotron Radiation and Free Electron lasers", CERN 90-03,p 195)

$$B_r = 2B_o \left[ I_0(kr) - (kr)^{-1} I_1(kr) \right] \cos(kz)$$

$$B_\phi = -2B_o (kr)^{-1} I_1(kr) \sin(kz)$$

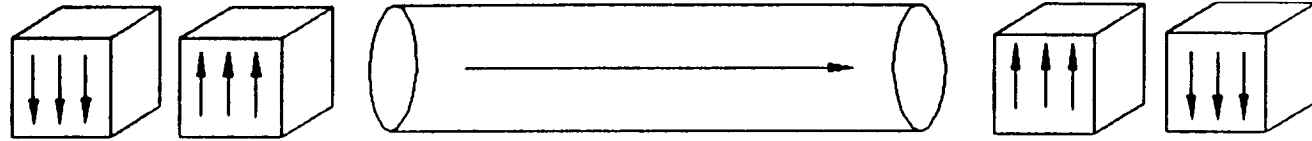
$$B_z = 2B_o I_1(kr) \sin(kz)$$

$$B_x \approx -B_o \left[ \left( 1 + \frac{1}{8} k^2 (3x^2 + y^2) \right) \sin(kz) - \frac{1}{4} k^2 xy \cos(kz) \right]$$

$$B_y \approx B_o \left[ \left( 1 + \frac{1}{8} k^2 (x^2 + 3y^2) \right) \cos(kz) - \frac{1}{4} k^2 xy \sin(kz) \right]$$

$$B_s \approx -B_o \left[ \left( 1 + \frac{1}{8} k^2 (x^2 + y^2) \right) (x \cos(kz) + y \sin(kz)) \right]$$

## Helical snake with 45° axis.



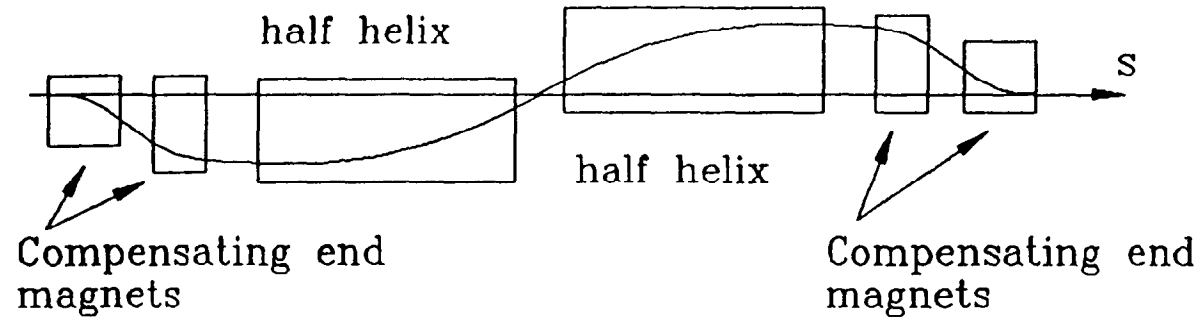
magnet length (m)	1.49	1.44	6.13	1.44	1.49
magnetic field (T)	2.0	2.0	2.0	2.0	2.0
$\int Bdl$ (Tm)	2.98	2.88	12.26	1.88	2.98
horizontal excursion (cm)	7.5	18.9	19.1	18.9	7.5
vertical excursion (cm)	0	0	13.1	0	0
spin rotation (deg)	97.8	94.6	Reversed around 45° axis	94.6	97.8
field direction/z (deg)	0	180	-90 $\xrightarrow{\text{one turn}}$ -90	180	0

helix wavelength: 6.133 m.  
total length: 14.01 m.

gap between magnets: 0.40 m.  
total  $\int Bdl$  : 24.02 Tm.

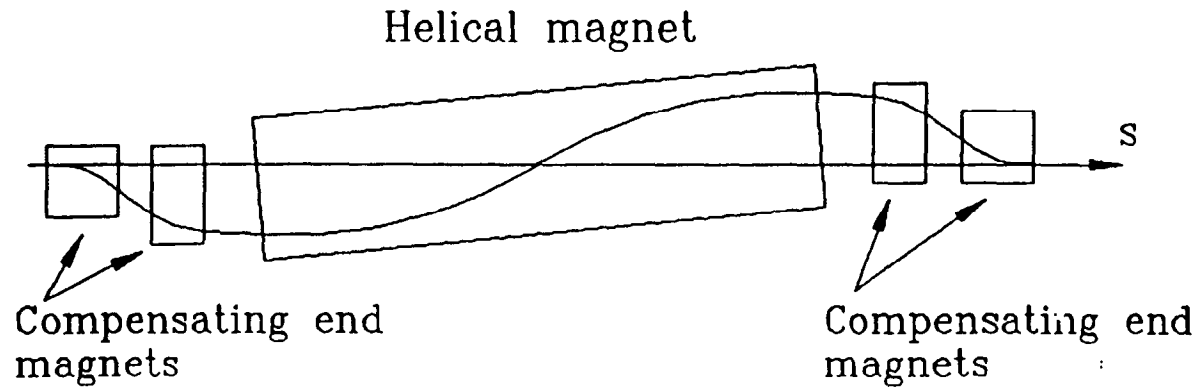
45° snake with one helix and a pair of correction dipoles at each end of the snake.

## Separated halves of helical magnet



99

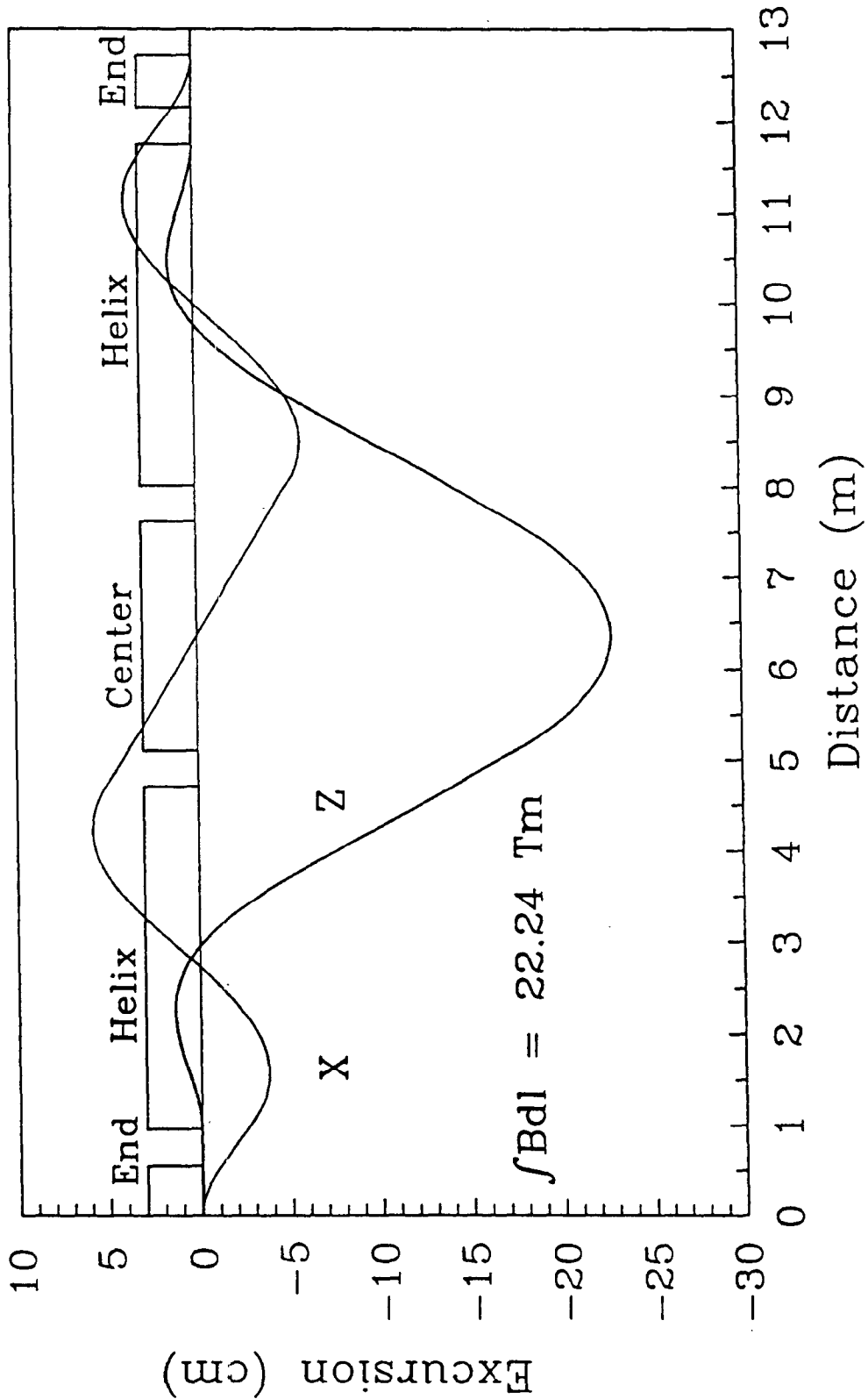
## Snake with tilted helix



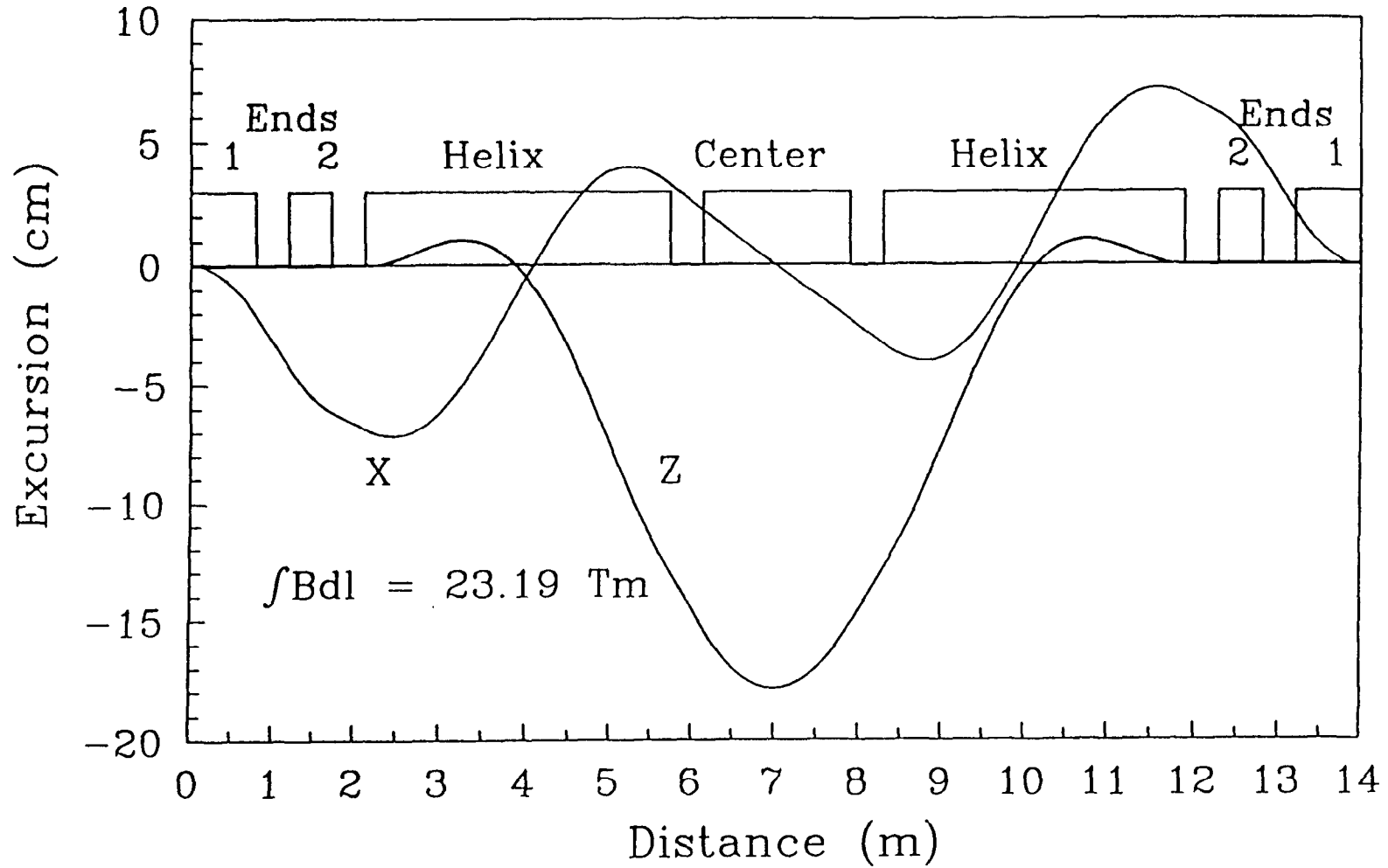
Modifications to the one-helix snake scheme for reducing the helix aperture.

Fig. a shows two half-helices separated by a small gap.

Fig. b shows a single tilted helix.



Orbit excursion profile at 8 GeV in the 45° helical snake with the central dipole and a pair of correction magnets; twist angle in the helix is 260°; gap between magnets is 0.4 m.



Orbit excursion profile at 8 GeV in the 45° helical snake with central dipole and two correction magnets on each side of the snake; twist angle in the helix is 285°; gap between magnets is 0.4 m.

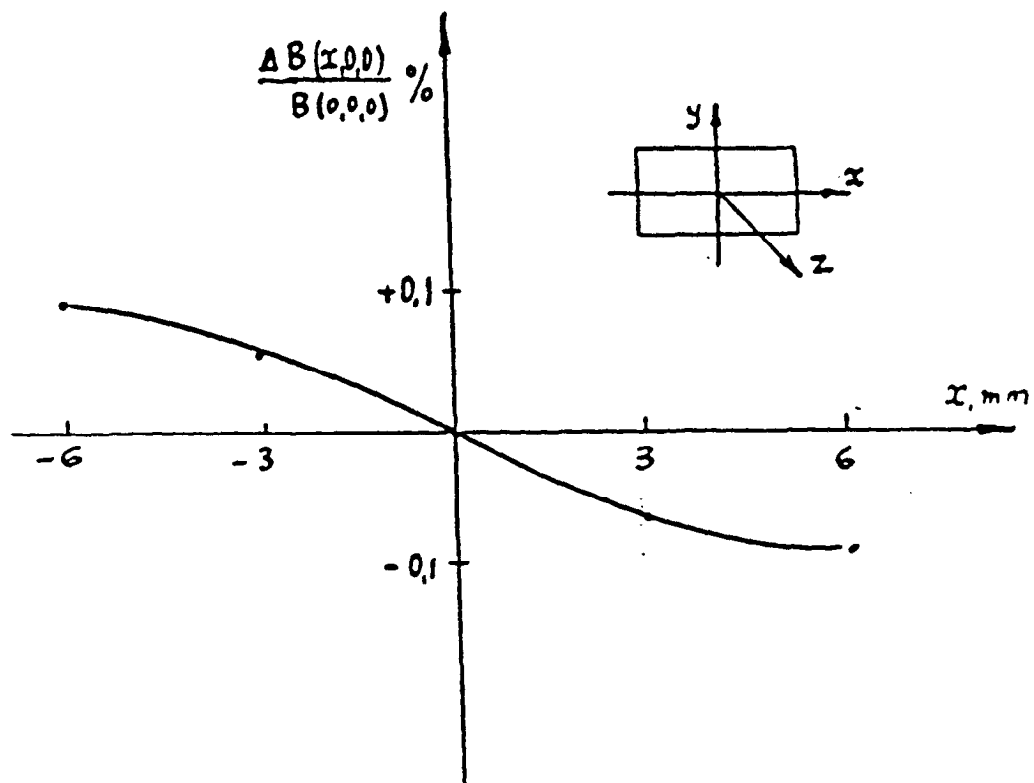
TABLE I. Snake with one helix and two end dipoles ( $l_g = 0.4$  m).

Field integral ( $\int B dl$ )	24.02 Tm
Field strength	2 Tesla
Snake axis $\varphi_s$	45°
Total length	13.61 m
Orbit excursion: $z_{max} = z_{helix}$ $x_{max} = x_{helix}$	13.1 cm $\pm 19.1$ cm
Length of the snake magnets (field direction from horiz.)	
End 1	1.49 m (90°)
End 2	1.44 m (-90°)
Helix	6.13 m (from -180° to 180°)

TABLE II. Parameters of the helical snakes with horizontal field dipole in the snake center ( $l_g = 0.4$  m).

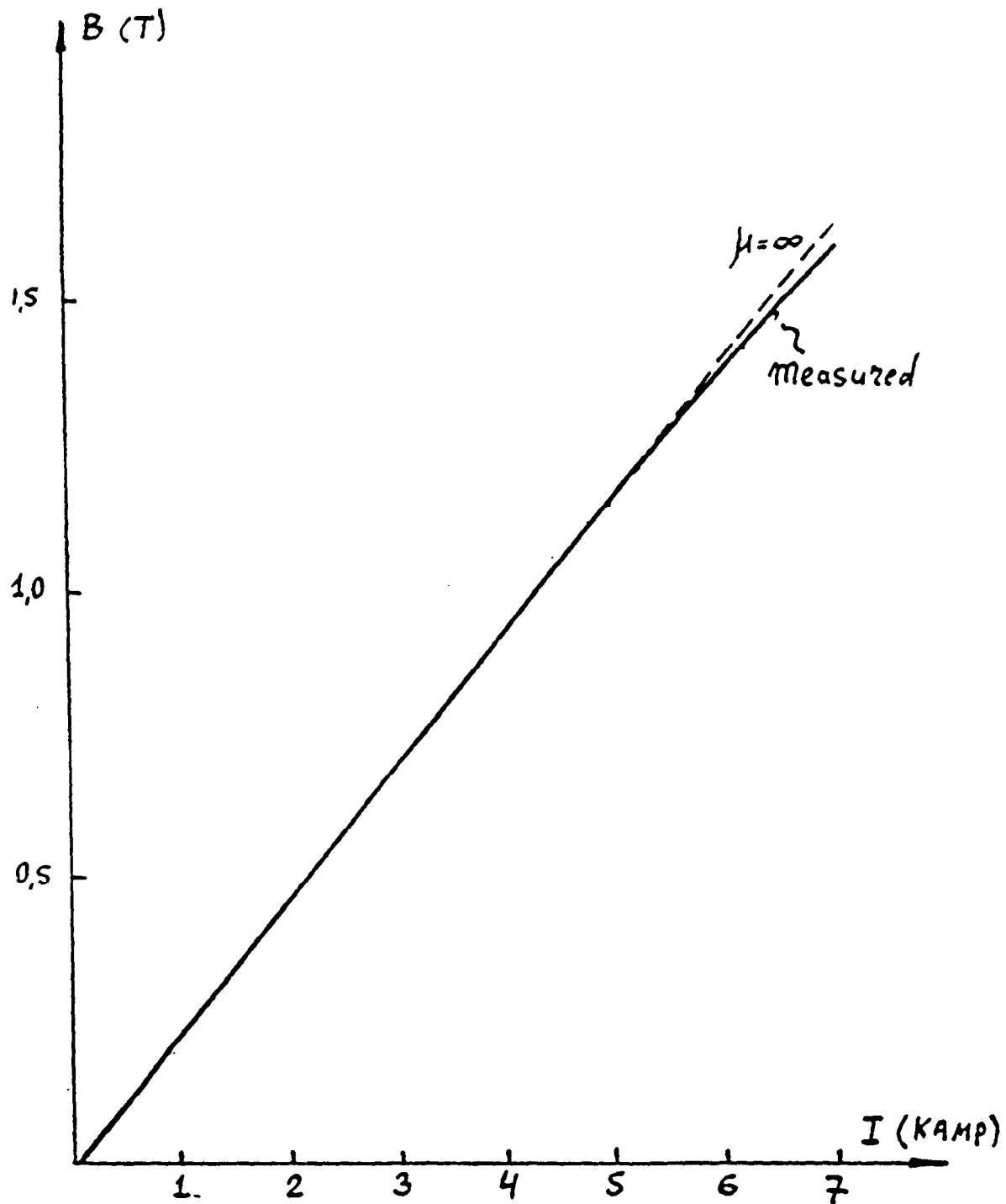
Snake scheme	with one end dipole	with two end dipoles
Field integral ( $\int B dl$ )	22.24 Tm	23.19 Tm
Field strength	2 Tesla	2 Tesla
Snake axis $\varphi_s$	45°	45°
Total length	12.72 m	13.99 m
Orbit excursion: $z_{max} (z_{helix})$ $x_{max} (x_{helix})$	22.81 cm (14.1 cm) 5.78 cm (5.78 cm)	17.85 cm (12.94 cm) 7.1 cm (7.1 cm)
Length of the snake magnets (field direction from horiz.)		
End 1	0.558 m (-90°)	0.794 m (-90°)
End 2	—————	0.525 m (90°)
Center	2.518 m (180°)	1.749 m (180°)
Helix	3.743 m (from -135° to 125°)	3.604 m (from -135° to 150°)

# Reduced Scale Helical Dipole Prototype



Field uniformity about the centerline ( $B \approx 1.61 \text{ T}$ ).

# Reduced Scale Helical Dipole Prototype



Main field versus current.



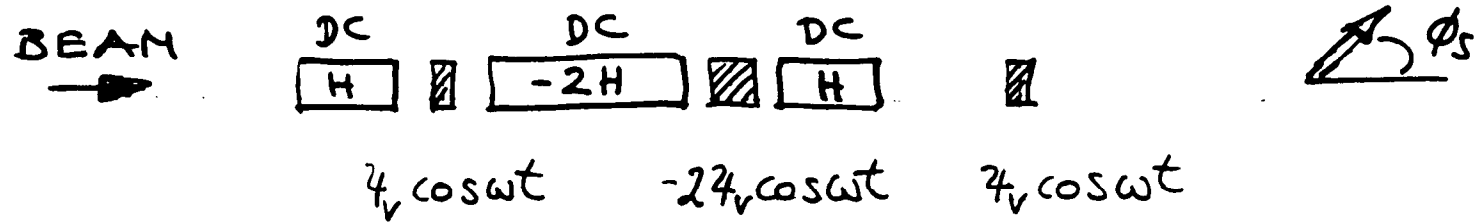
**T. Roser**

**Brookhaven National Laboratory**

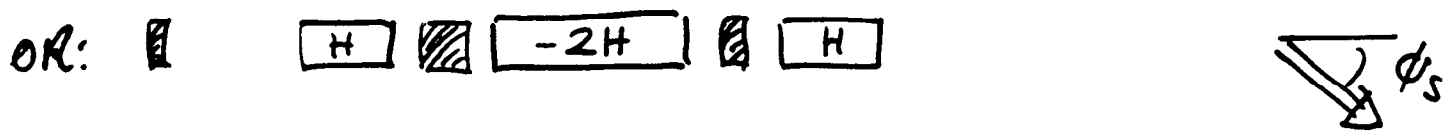
**Upton, NY 11973-5000**

**Fully Compensated Spin Flipper**

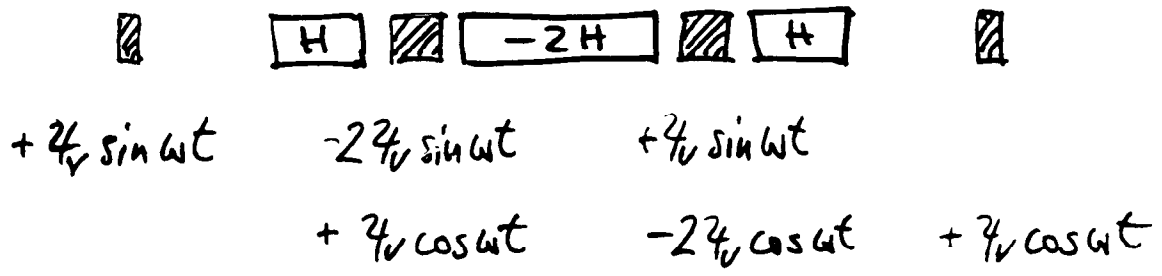
# FULLY COMPENSATED SPIN FLIPPER



$7_H = 143^\circ \rightarrow 7_S = 2.55 7_v, \phi_s = +45^\circ$

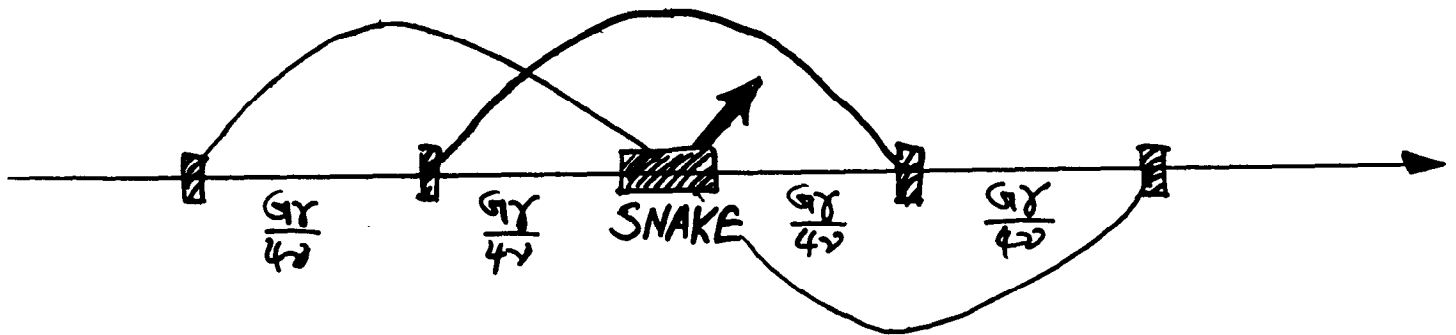


# ROTATING FIELD FLIPPER:



$\Rightarrow$  WORKS FOR ANY SPIN TUNE AND ANY ENERGY!!

# FLIPPER USING SIBERIAN SNAKE



$$2\gamma \sin \omega t$$

$$2\gamma \cos \omega t$$

$$2\gamma \cos \omega t$$

$$-2\gamma \sin \omega t$$



→ ROTATING FIELD !!

→ WORKS FOR ANY SPIN TUNE  
AND ANY ENERGY!

→ DEPENDS ON BETATRON TUNE.



M. Böge

DESY

Notkestrasse 85. D-22603 Hamburg, Germany

## Spin Tracking Calculations for the HERA electron ring

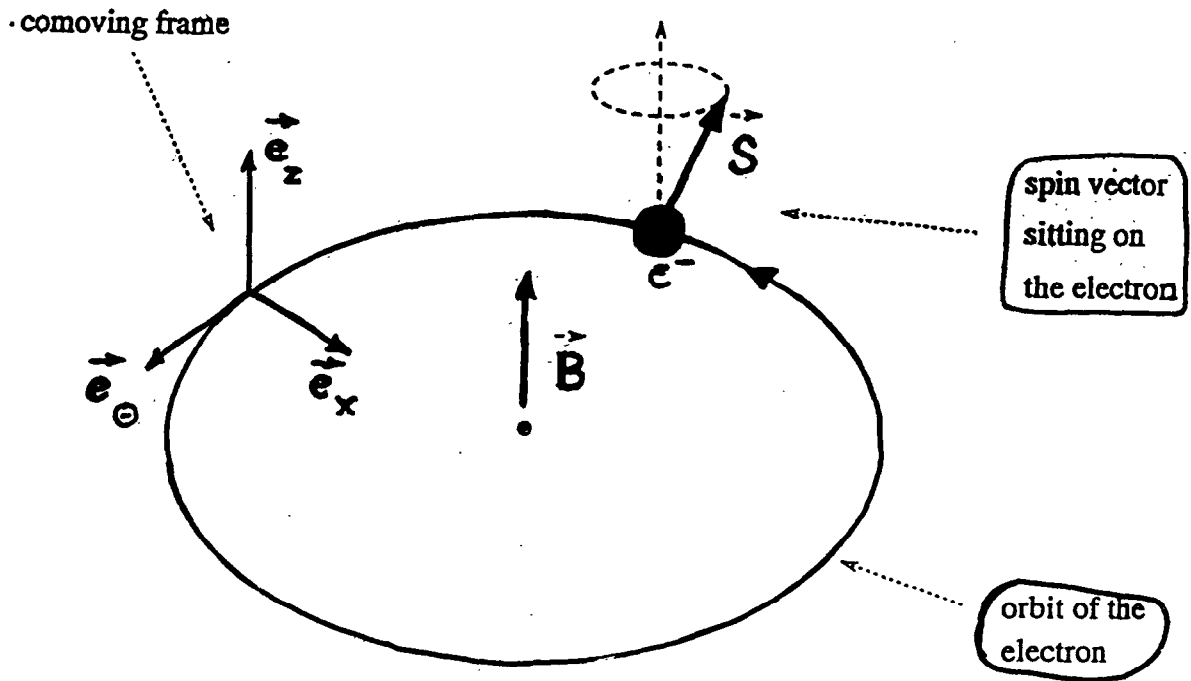
# Spin Tracking Calculations for the HERA electron ring

BNL 13th Sept '99

M. Böge

1. Short Introduction  
Radiative Polarization, Spin Diffusion,  
Resonance Structures ( $\tau_p, \tau_0$ )
2. Ways to calculate  $\tau_0$
3. The Monte-Carlo Treatment:  
SITROS Advantages / Drawbacks
4. Presentation of some results for  
HERA

# Spin Dynamics



Thomas - BMT equation:

$$\frac{d\vec{s}}{d\theta} = \vec{\Omega} \times \vec{s}$$

with  $\vec{\Omega} = \vec{\Omega}(\vec{B}, \vec{E}, \gamma)$

$\theta$  = azimuthal coord.

$\vec{B} \parallel \vec{e}_z, \vec{E} = \vec{0}: \downarrow \bar{\omega}_0$  Spin Tune

$a = \frac{g-2}{2}$

electron  $a$ -factor

$$\vec{\Omega} = \frac{e \vec{B}}{c m_e \gamma} \frac{R}{2\pi} a \gamma$$

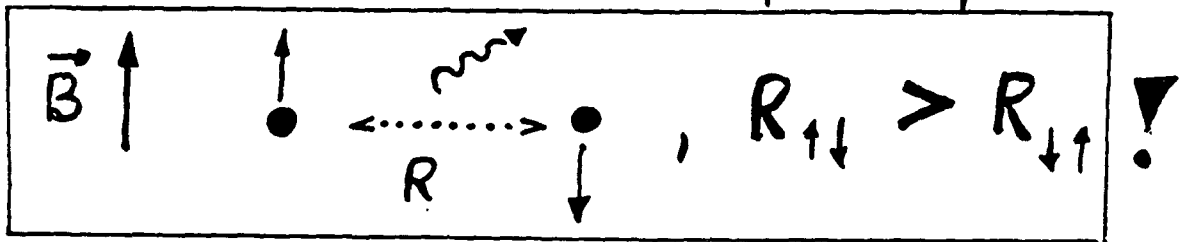
! HERA  
 $a\gamma \sim 60$

# Raditive Polarization

Synchrotron radiation:

VERY SMALL Fraction ( $< 10^{-11}$ )

Causes UP/DOWN Spin Flip:



→ Polarization  $\neq 0\%$  !

( Ternov, Loskutov, Korovina, Sokolov 1962-64)

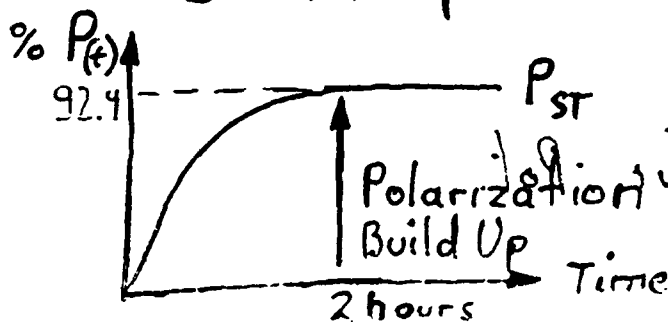
Flat Machine:

$$P_{ST} = \underline{92.4\%}$$

$$\tau_p^{-1} \propto \gamma^5 / \rho^3$$

!  $\rho =$  Bend. Radius

Build Up Time HERA at 26.6 GeV



$\tau_p \approx \underline{42 \text{ min}}$

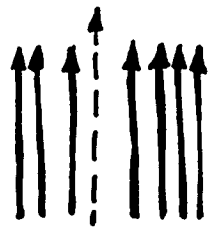
# Depolarization Effects

STOCHASTIC Motion of  $e^-$

## → Spin Diffusion

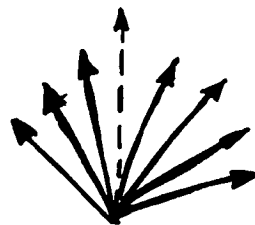
Under Presence of Horizontal Magnetic Fields ( $\perp \vec{e}_z$ ) eg.

Alignment Errors of Magnets  
( $\Delta$  Quad's,  $\Delta$  Sextupoles  $< \underline{0.3 \text{ mm}}$ )

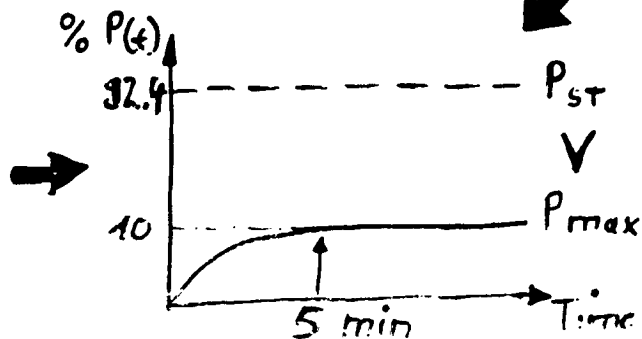
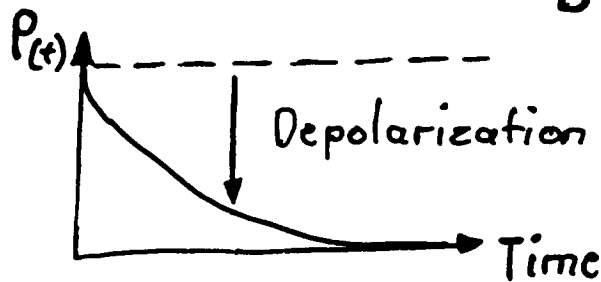


Equilibrium  
Polarization  
Direction

Diffusion



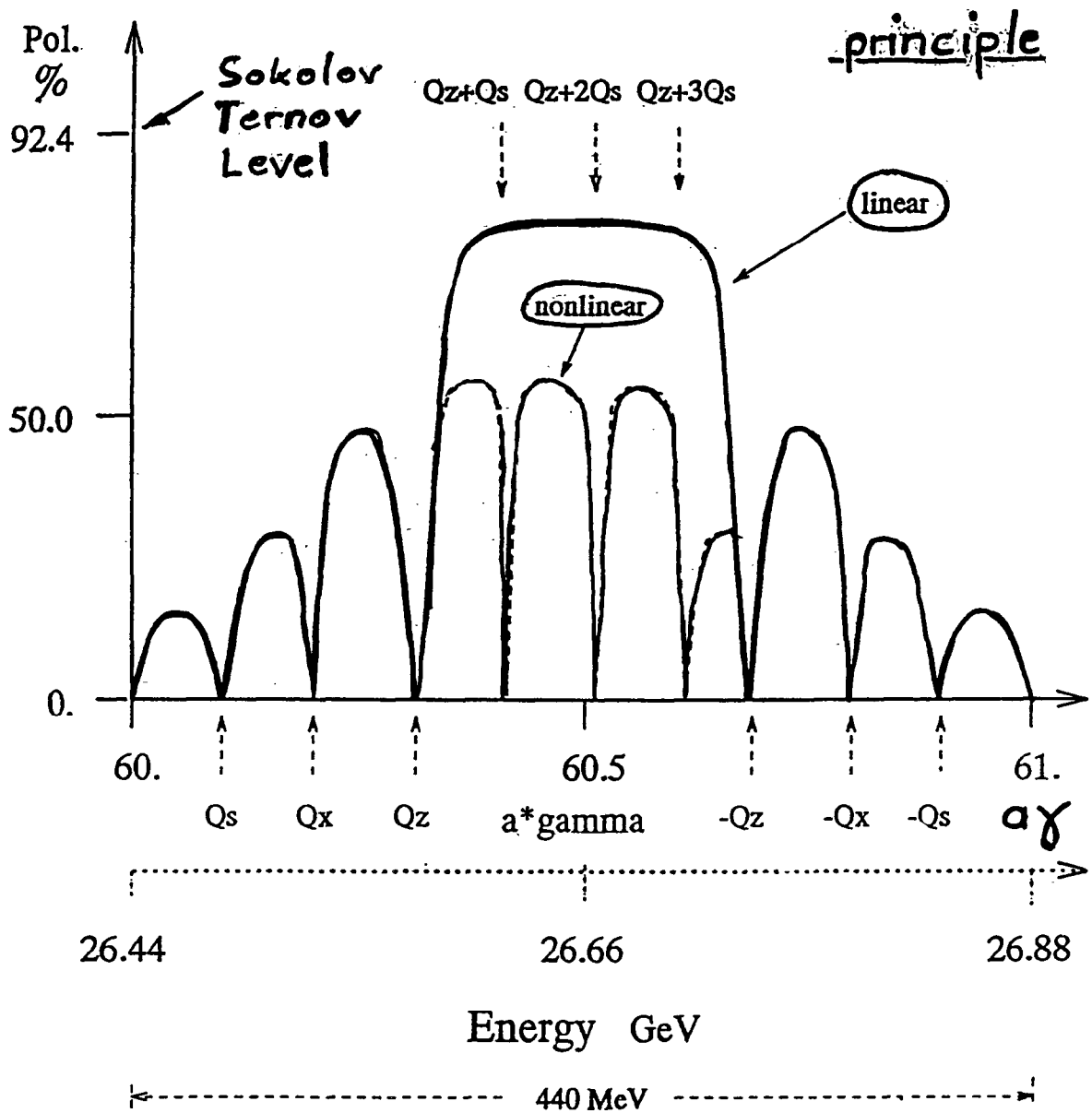
character.  
time  
 $\tau_D$



$$P(t) = P_{ST} \frac{\tau_0}{\tau_p + \tau_D} \left( 1 - e^{-\frac{\tau_p + \tau_D}{\tau_p \tau_D} t} \right)$$

$\tau_{eff} < \tau_p$

# Resonance Structure



Resonance Condition:

$\nu_i, m_i$  integer

!!

$$\nu = m + m_x Q_x + m_z Q_z + m_s Q_s$$

# Calculation of $\tau_D$

Available Programs :

- SLIM by A. CHAO

Perturbation Theory to (1th) order

(Resonances :  $|m| = |m_x| = |m_z| = |m_s| = 1$ )  
(SITF Thick Lens Version of SLIM)

- SMILE by S. MANE

Perturbation Theory to (nth) order

(Resonances :  $|m| = |m_x| = |m_z| = |m_s| = n$ )

- SODOM by K. YOKOYA

"One Turn Maps"

(Resonances :  $|m| = |m_x| = |m_z| = |m_s| = -n$ )



- SITROS by J. Kewisch, M. Böge

"Monte-Carlo", Spinor formalism  
to Integrate BMT-equation

(Resonances :  $|m| = |m_x| = |m_z| = |m_s| = n$ )  
- Harmonic Surfs

## Determination of $\tau_0$

① 1st order perturbation theory  
SITF

② classical Diffusion model  
SITROS

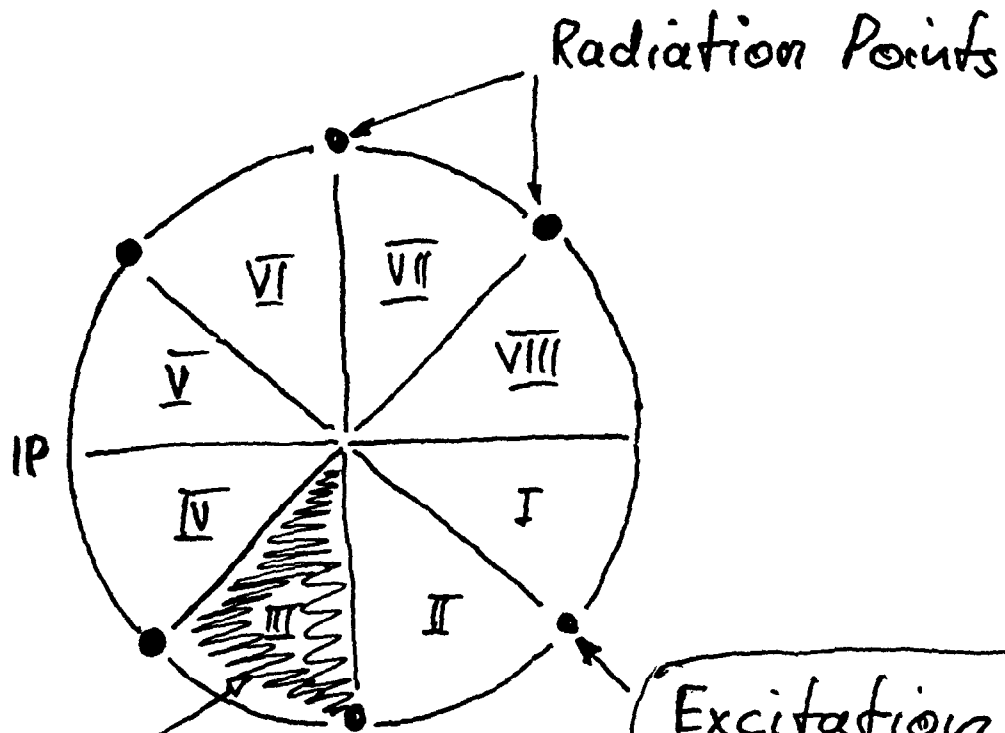
➔ nonlinear 6-dim Orbit motion

➔ 3 dim Rotations for the Spin

➔ Simulation of the Orbit motion  
with Radiation damping and  
Quantum excitation

➔ Tracking of a Particle (Spin)  
ensemble ( $N \geq 50$ ) over several  
Synchrotron damping times  
(5000 turns)

# A few Details



Transfer matrices collecting a lot of elements !

1. Contain Chromaticity and Sextupoles up to 2nd order in the Orbit vector  $\vec{X}$
2. Contain effective Spin rotation vectors up to 2nd order in  $\vec{X}$

Excitation with Gaussian distributed random kicks representing quantum fluctuations

Spin Tracking with  $3 \times 3$  rotation matrices

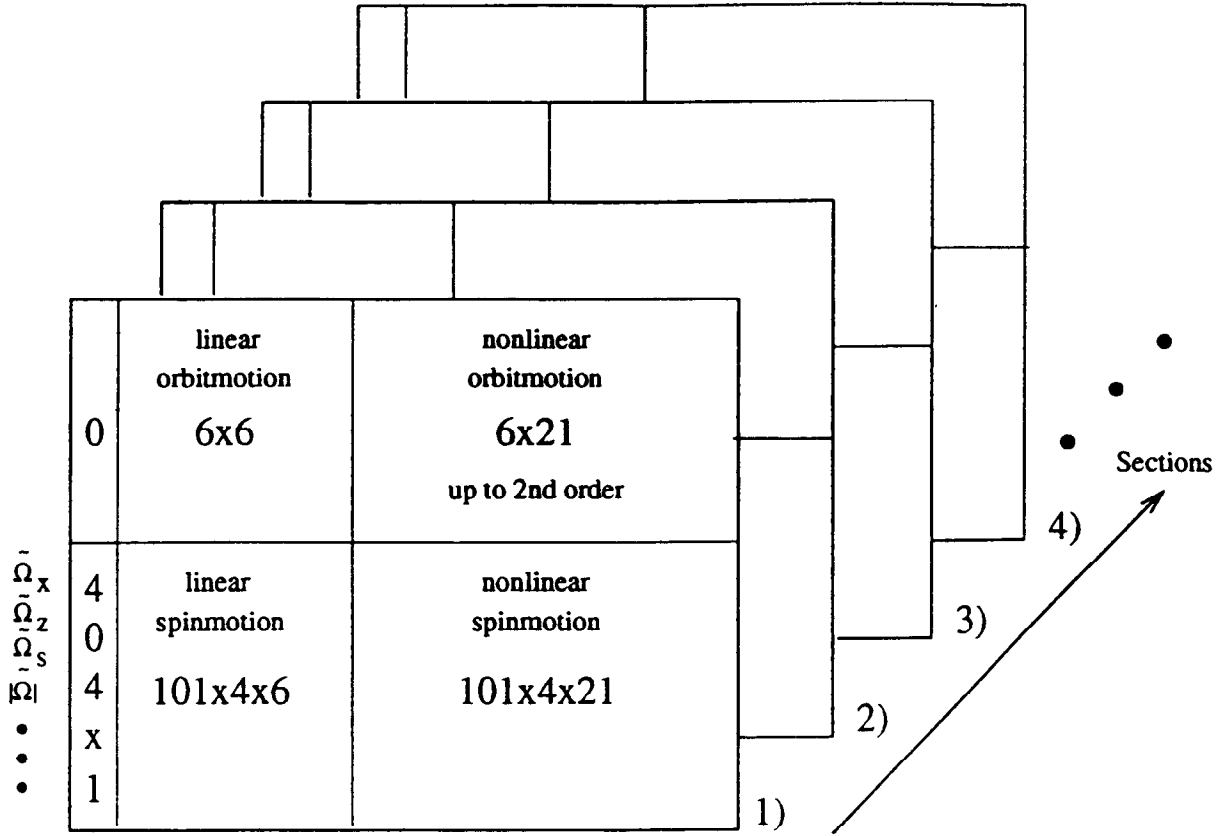


Figure 6: Structure of the matrices representing the sections for the orbital and spin tracking. The orbital tracking is performed with respect to the closed orbit and the rotation vector  $\vec{\Omega}_{sec}$  is determined with respect to the design orbit

trajectory to second order terms one can describe the rotation  $\vec{\Omega}_{sec}$  for a section by a  $4 \times 27$  matrix  $\hat{M}_{sec}^{spin}$ :

$$\begin{pmatrix} \hat{\Omega}_x \\ \hat{\Omega}_z \\ \hat{\Omega}_s \\ |\hat{\Omega}| \end{pmatrix}_{sec} = \begin{pmatrix} \hat{\Omega}_x^{co} \\ \hat{\Omega}_z^{co} \\ \hat{\Omega}_s^{co} \\ |\hat{\Omega}|^{co} \end{pmatrix}_{sec} + \hat{M}_{sec}^{spin} \vec{X}, \quad (3.23)$$

where  $\vec{\Omega}_{sec}^{co}$  represents the rotation vector of the particle on the closed orbit.

For a detailed analysis of the resonance structure given by the conditions of eq. (2.9) it is necessary to calculate the equilibrium polarization for a certain energy range covering several resonances. Normally the range between two integer values of spin tune which are  $\sim 440$  MeV apart is appropriate (see section 4).

In SITROS spin vectors are tracked simultaneously at different beam energies by including these vectors in an enlarged transformation matrix. For the spin tracking at these energies SITROS uses the particle orbits for the middle point in the chosen energy interval because the change in the orbital motion of the particles is negligible for an energy range of 440 MeV ( the variation of the radiated power is of the order of a few percent and the tune change is a second order effect ). Using eq. (3.22) for the central energy and eq. (3.23) for 101 energies one can construct a matrix consisting of  $(6 + 4 \cdot 101) \times (1 + 27)$  elements (see fig. (6)).

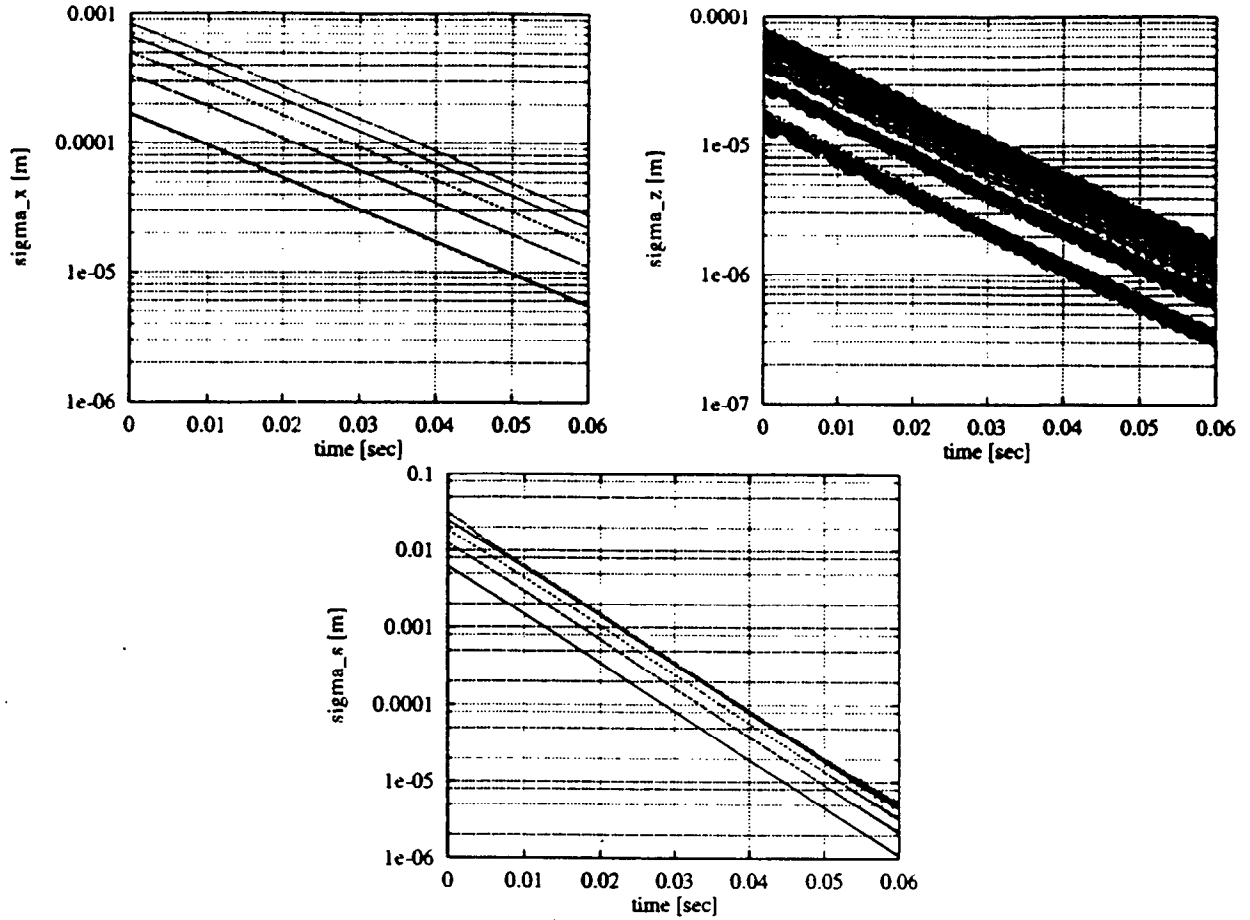


Figure 7: Determination of the damping times  $\tau_y$  ( $y = x, z, s$ ) for five starting Gaussian particle distributions with  $1, 2, 3, 4, 5\sigma_y^{lin}$ , where the  $\sigma_y^{lin}$  are given by linear theory. The beam excitation by quantum emission is switched off in the simulation. The ratio of  $\sigma_z$  and  $\sigma_x$  corresponds to 2% emittance coupling

### 3.5.4 Problems induced by approximations

Even if no damping is included, the quadratic matrices  $\hat{M}_{sec}^{orbit}$  are nonsymplectic. This can lead to an artificial growth of the phase space volume covered by the particles. To be sure that this effect is insignificant one has to check the damping times for the modes  $k$  which should be close to the values of  $\tau_k$  expected from the linear theory. In fig. (7) the results of a simulation without beam excitation by quantum emission for a HERA optic at 26.666 GeV and an RF voltage of 150 MV with 2% emittance coupling between the  $x$  and  $z$  mode are shown. The curves correspond to starting Gaussian distributions of 500 particles with different mean beam sizes ( $1\sigma_y^{lin} \rightarrow 5\sigma_y^{lin}$ ,  $y = x, z, s$ ), which are given by linear theory. The method to determine the beam sizes in the simulation is described in section 3.5.6. The damping times calculated from the simulation are  $\tau_x = 17.5$  msec,  $\tau_z = 15.1$  msec and  $\tau_s = 7.0$  msec. These values are identical to the damping times given by linear theory within the expected precision. In addition the slope of the "straight" lines in logarithmic scaling does not change with increasing variance of the starting distribution, although one expects that the nonsymplecticity gets more important for particles with large amplitudes. One can conclude that for the phase space region covered in the simulation the nonsymplecticity of the matrices does not lead to an artificial excitation or damping.

For the determination of the matrices  $\hat{M}_{sec}^{spin}$  another problem occurs. The calculation of  $\vec{\Omega}_{sec}$ ,

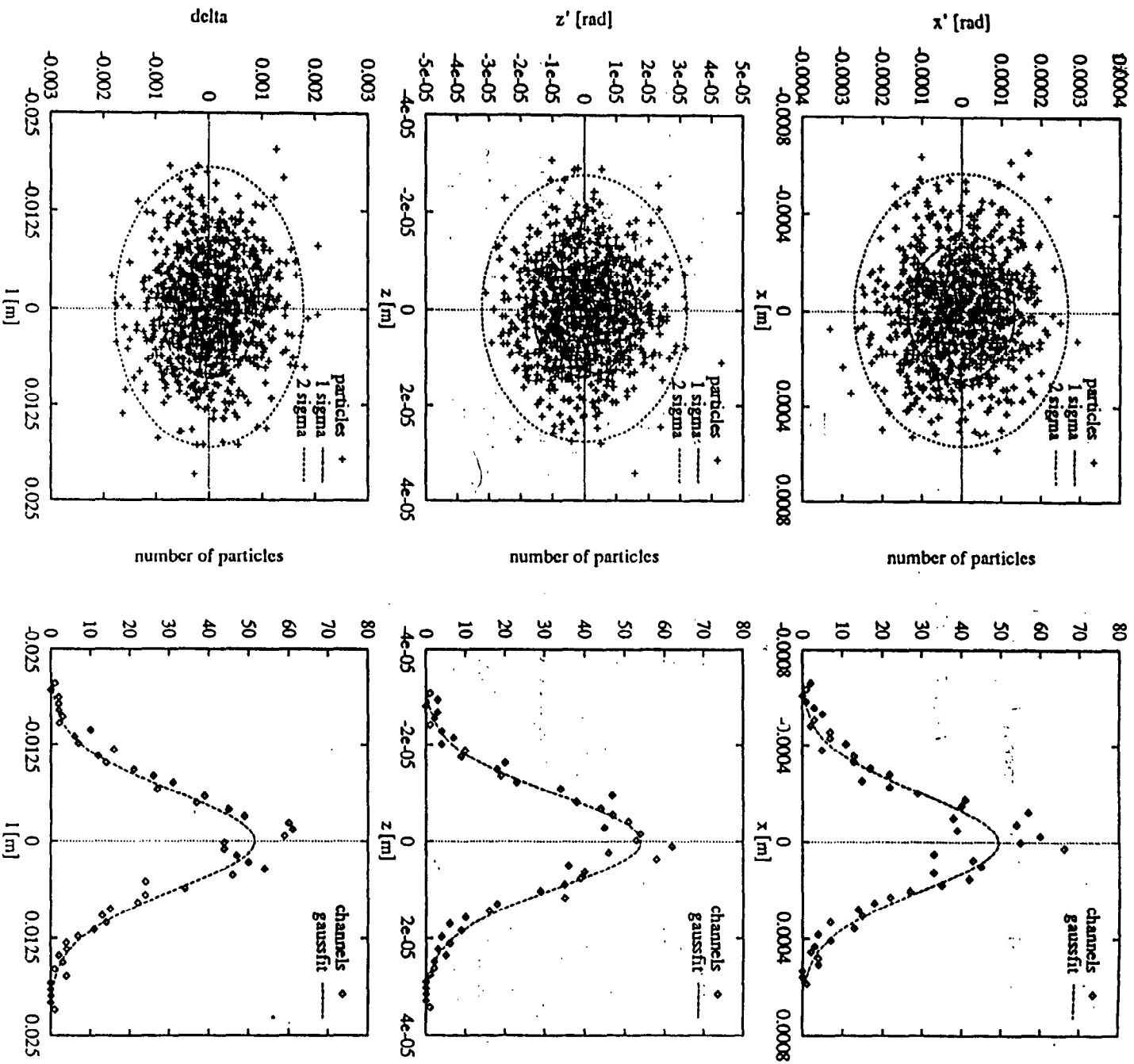


Figure 12: Left: Phase space projections for  $N = 1000$  particles onto the  $(x, x')$ ,  $(z, z')$ ,  $(l, \delta)$  plane, Right: Particle distribution functions for  $x$ ,  $z$ ,  $l$

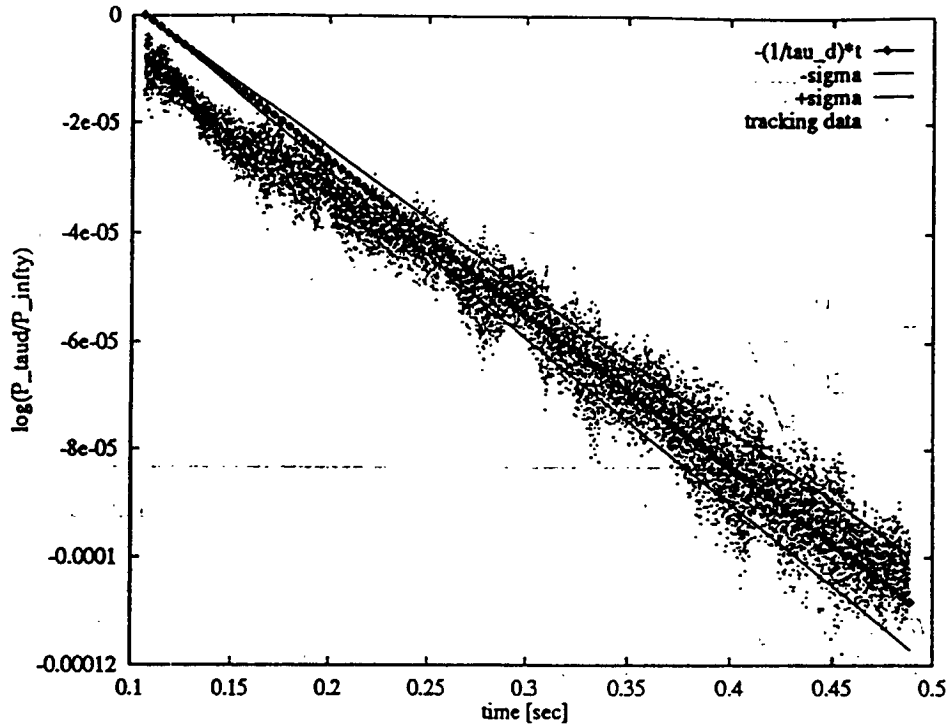


Figure 14: *Simulation of the depolarization process in a logarithmic scale  $\log(P_{\tau_d}(t)/P_{\infty})$  for a HERA optic with one rotator pair at an energy of 28 GeV. All spins are started parallel to the  $\bar{n}_0$ -axis at  $t_0 = 0.11$  sec. The tracked time interval corresponds to  $2 \times 10^4$  turns. The samples are taken every turn*

where  $\sigma_y^2 = 2 \langle y^2 \rangle$  is the equilibrium beam size and  $\tau_y$  denotes the damping time of the  $y$  motion. For  $y = x$  using  $\tau_x \sim 15$  msec and  $\sigma_x = 3 \times 10^{-4}$  m,  $\tau_{diff_x}(x_b)$  is shown as a function of the boundary  $x_b$  in fig. (15). After  $1 \times 10^4$  turns 63% of the particles have passed the  $3\sqrt{\langle x^2 \rangle}$  boundary. To push the same percentage of particles through the  $5\sqrt{\langle x^2 \rangle}$  boundary  $1 \times 10^7$  turns would be necessary in order to test the effect of the tails of the distribution beyond  $\sim 3.5\sigma_x$  on the polarization. It is not generally practical in SITROS to track the spins for long enough so that they have been out in the tails of the approximately Gaussian phase space distribution and have experienced the stronger diffusion to be expected at large amplitudes. How important are the particles in the tails ?

An answer can be given by a diffusion model introduced by T. Limberg [22]. In the one dimensional case the depolarization time constant  $\tau_d$  can be approximated by:

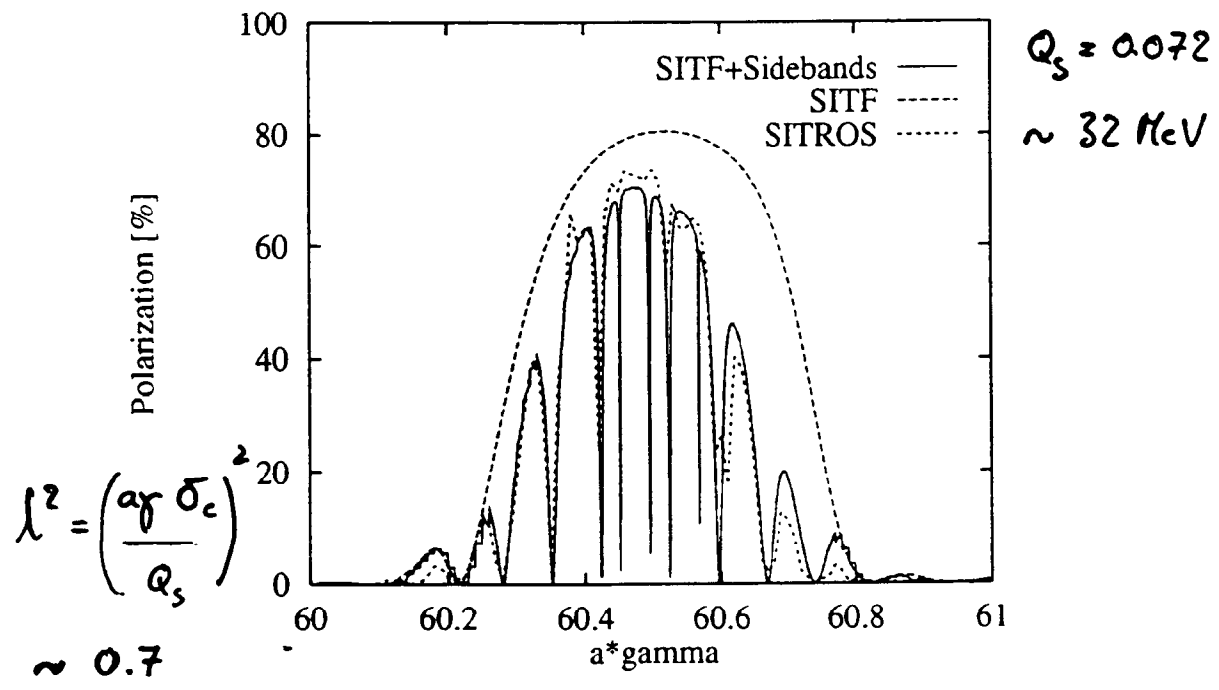
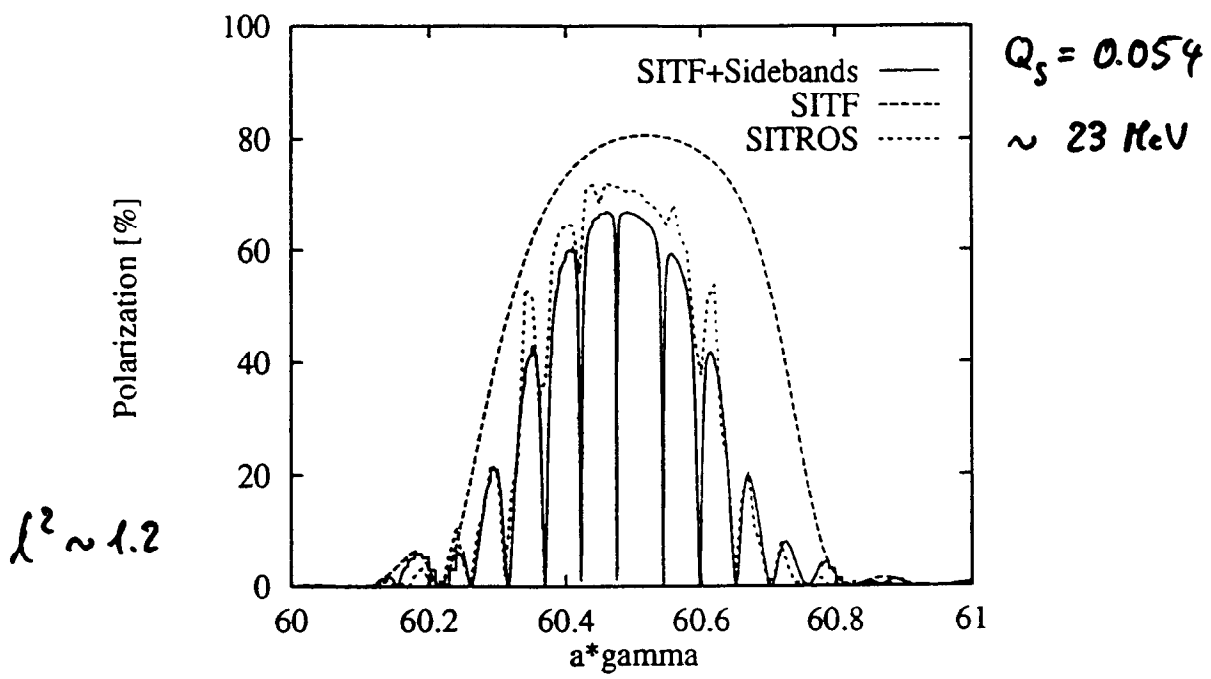
$$\frac{1}{\tau_d} = \int_{n_1}^{n_2} dn \frac{\exp(-n)}{\tau_{d(n_1, n_2)}} + \int_{n_2}^{n_3} dn \frac{\exp(-n)}{\tau_{d(n_2, n_3)}} + \dots \quad (3.36)$$

with  $n = y^2/\sigma_y^2$ .  $\tau_{d(n_i, n_j)}$  is an average depolarization time for the interval  $(y_i^2/\sigma_y^2, y_j^2/\sigma_y^2)$ . This is a phase space weighted depolarization rate appearing also in [55][54]. For two intervals  $(n_1, n_2) = (0, 8)$  (corresponding to  $(0, 4\sqrt{\langle y^2 \rangle} = 2.8\sigma_y)$ ) and  $(n_2, n_3) = (8, \infty)$   $\tau_d$  is calculated to be:

$$\frac{1}{\tau_d} = \frac{1 - \exp(-8)}{\tau_{d(0,8)}} + \frac{\exp(-8)}{\tau_{d(8,\infty)}}$$

For  $\tau_{d(0,8)} = 3600$  sec,  $\tau_{d(8,\infty)}$  has to be of the order of one second to contribute to  $1/\tau_d$  significantly ! In practice it is not easy to determine the local depolarization rates specified in eq. (3.36). But the previous calculation indicates that it is "unlikely" that the contributions from the tails are important.

SITROS  $\longleftrightarrow$  SITF + Side Band model



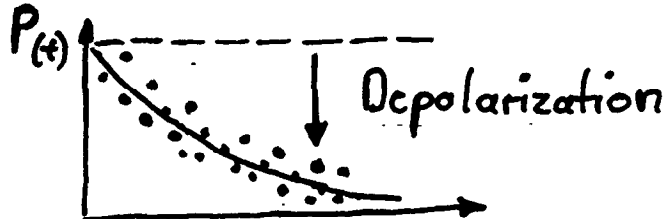
$\Rightarrow$  SITROS is in good agreement with the Sideband model applied on the basis of SITF

$\Rightarrow$  High  $Q_s$  does not really help! Much more important are positions of certain sidebands!

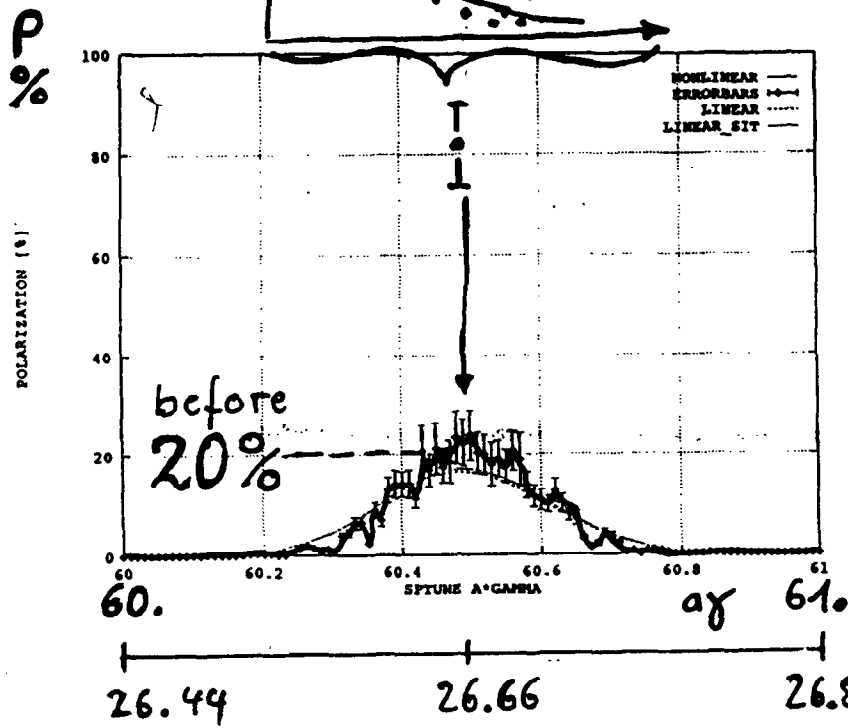
# SITROS Calculations

Beam = 50 e<sup>-</sup>, Photons =  Random Kicks

Time = 5000 Turns (0.1 sec)



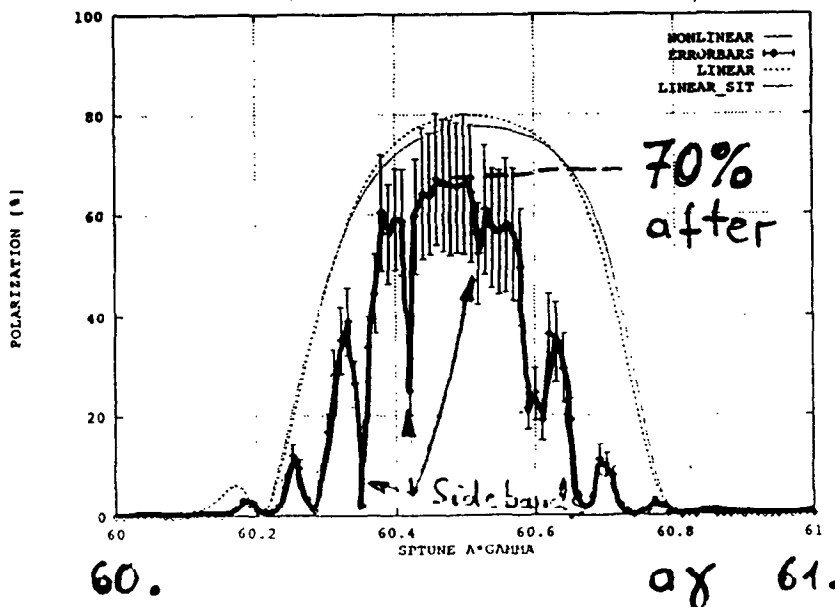
FIT  $\tau_D$  !



- Standard HERA Optic - with distortions

Prediction

20%



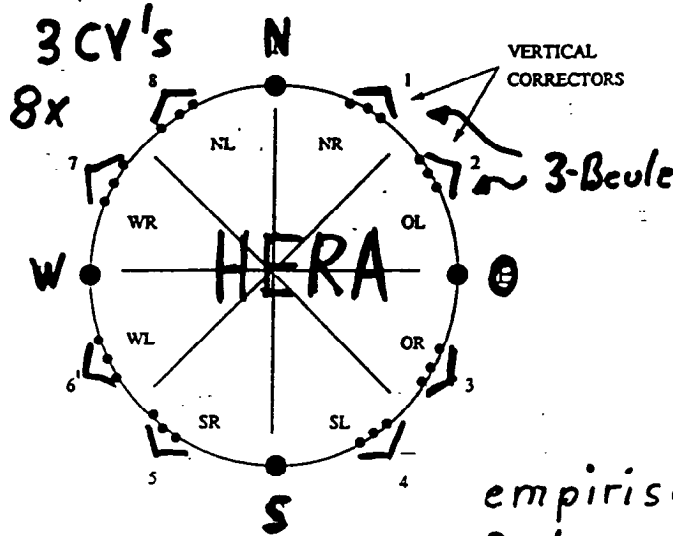
- Standard HERA Optic - with distortions
- Harmonic Bump Correction !

Prediction

70%

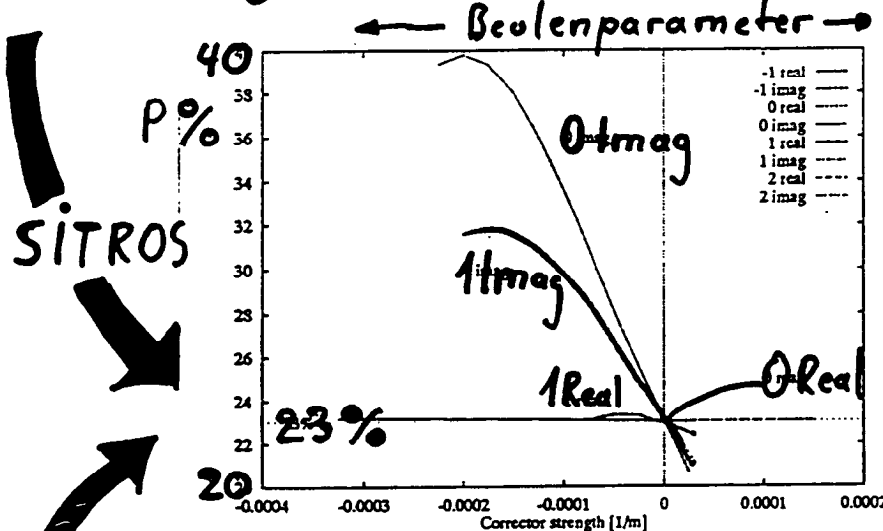
# (2.) Polarisationsoptimierung 1992:

## Harmonische Beulen



## Ausgangsposition:

1. Realignment der Quadrupole im Shut down 91/92
2. Entkopplungsbeule über alle Bögen
3. Tunes geschoben:  
 $Q_x = 0.19 \rightarrow 0.12$   
 $Q_z = 0.28 \rightarrow 0.2$   
 $Q_s = 0.072$

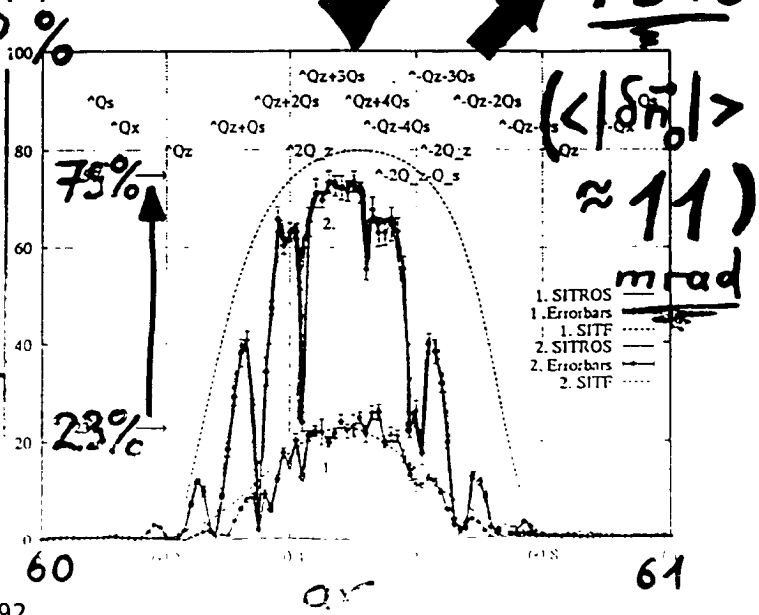


→ 25%  
Polarisation  
( $\langle |\delta \vec{n}_0| \rangle \approx 20$ )  
mrad  
Was tun ??

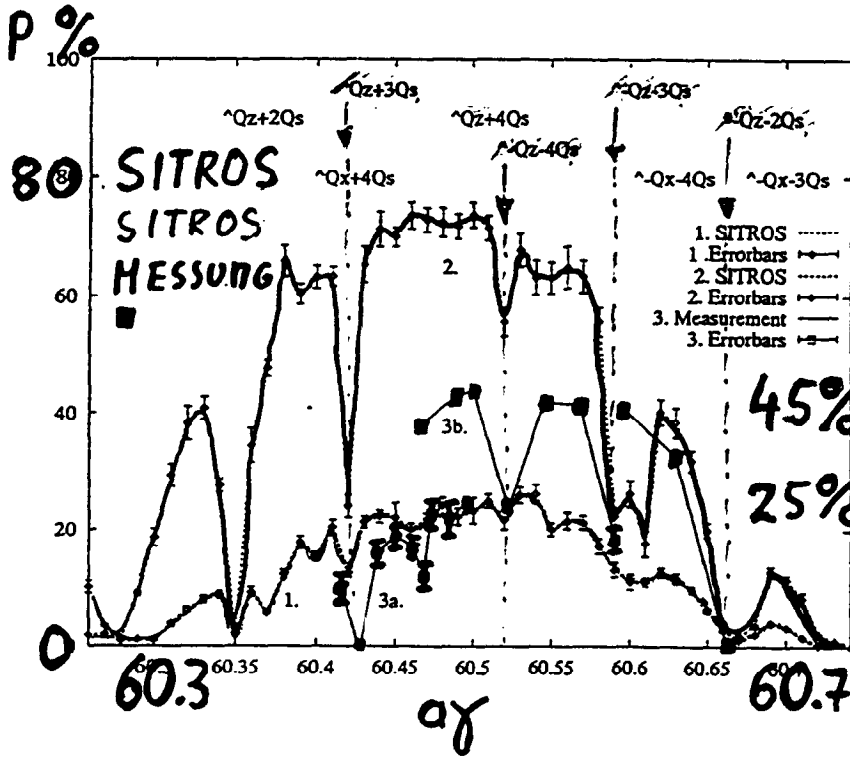
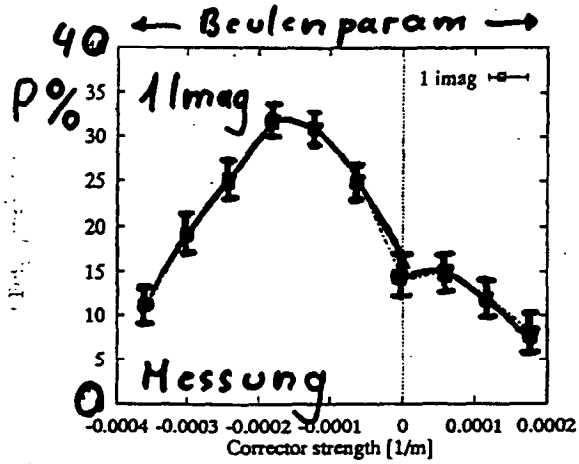
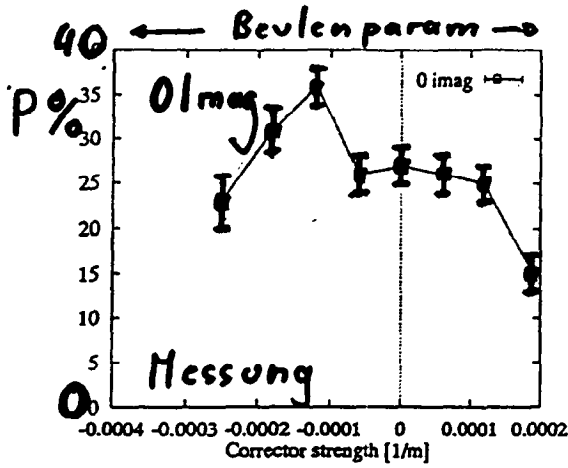
SITROS

$$\delta \vec{n}_0(s) \propto \sum_m \frac{f_m}{m - \gamma} e^{-i 2\pi m \frac{s}{L}}$$

$f_m =$  Fourier harmon.  
 $(m - \gamma)$  Resonanznenner  
 $f_m$  mit  $m = 60 +$   
 Komplex  $(-1, 0, 1, 2)$



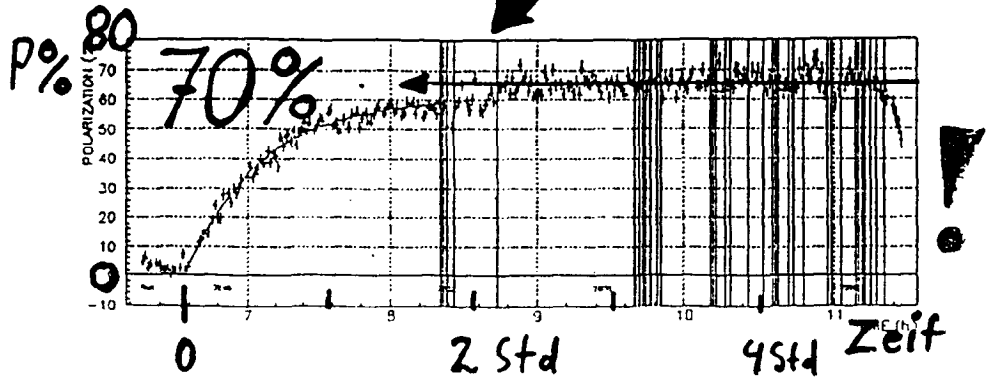
# Vergleich mit Messungen:



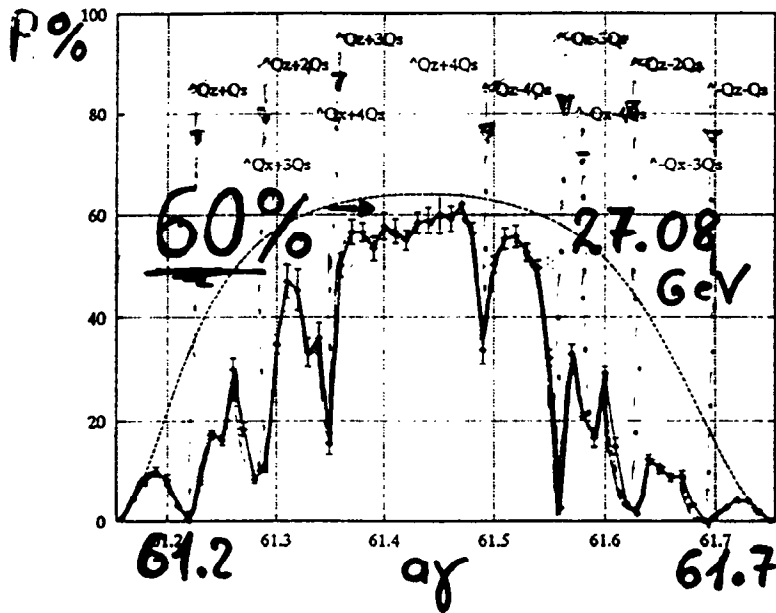
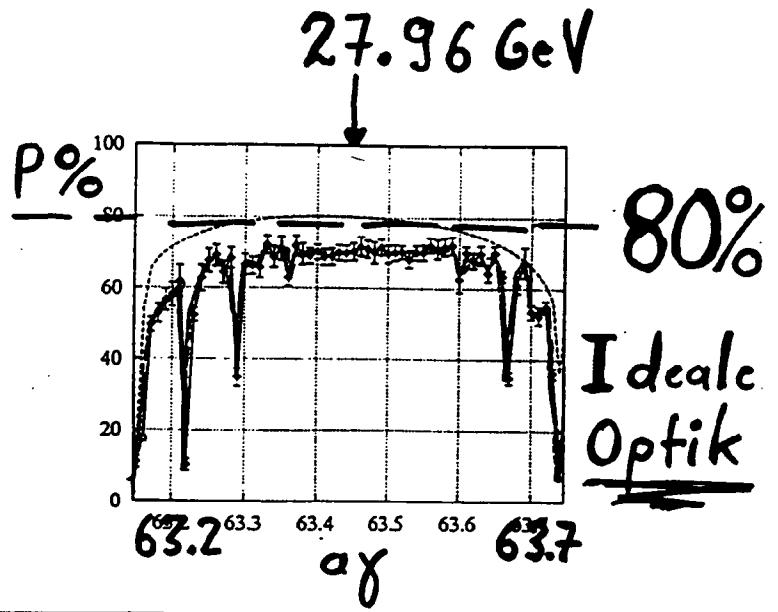
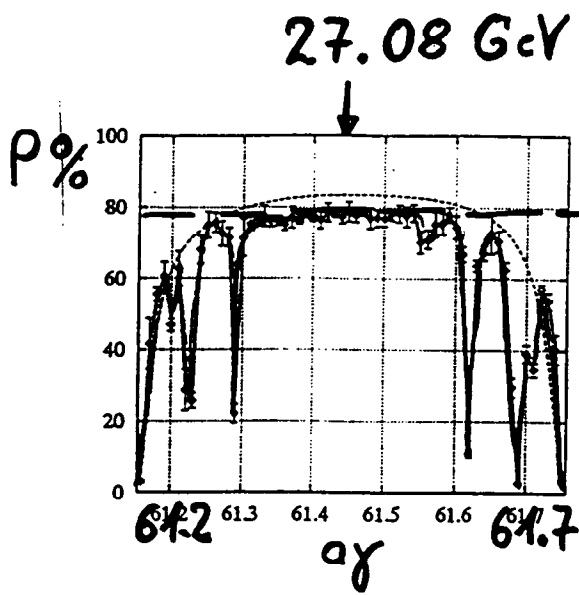
In Messung und Simulation **STARKE** Seitenänderung zu  $\pm Q_z$  !

Diskrepanz nach Optimierung:  
75%  $\leftrightarrow$  45%  
Simulation Messung

Messung '93



# Simulationen: für 2 Energieintervalle



STARKE

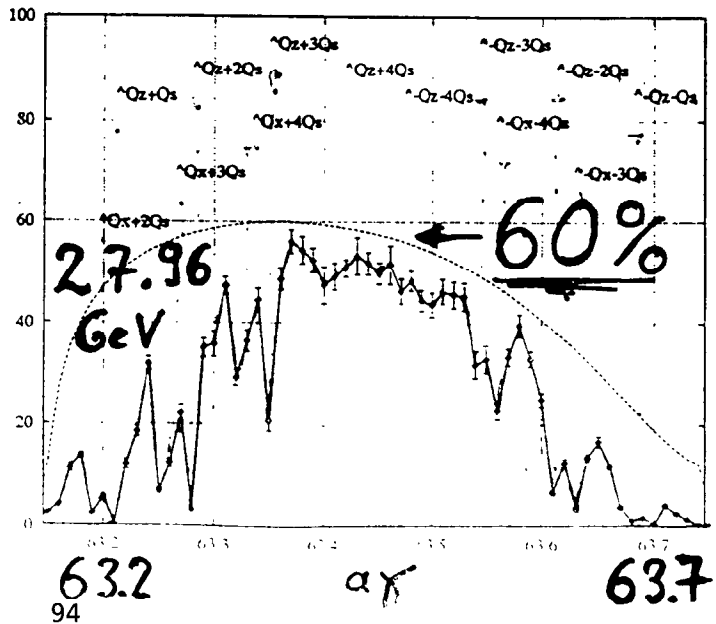
Seitenfelder:

$$\nu = \pm Q_z + m_s Q_s$$

$$\nu = \pm Q_x + m_s Q_s$$

Optimiert  
mit harmonischen  
Beulen!

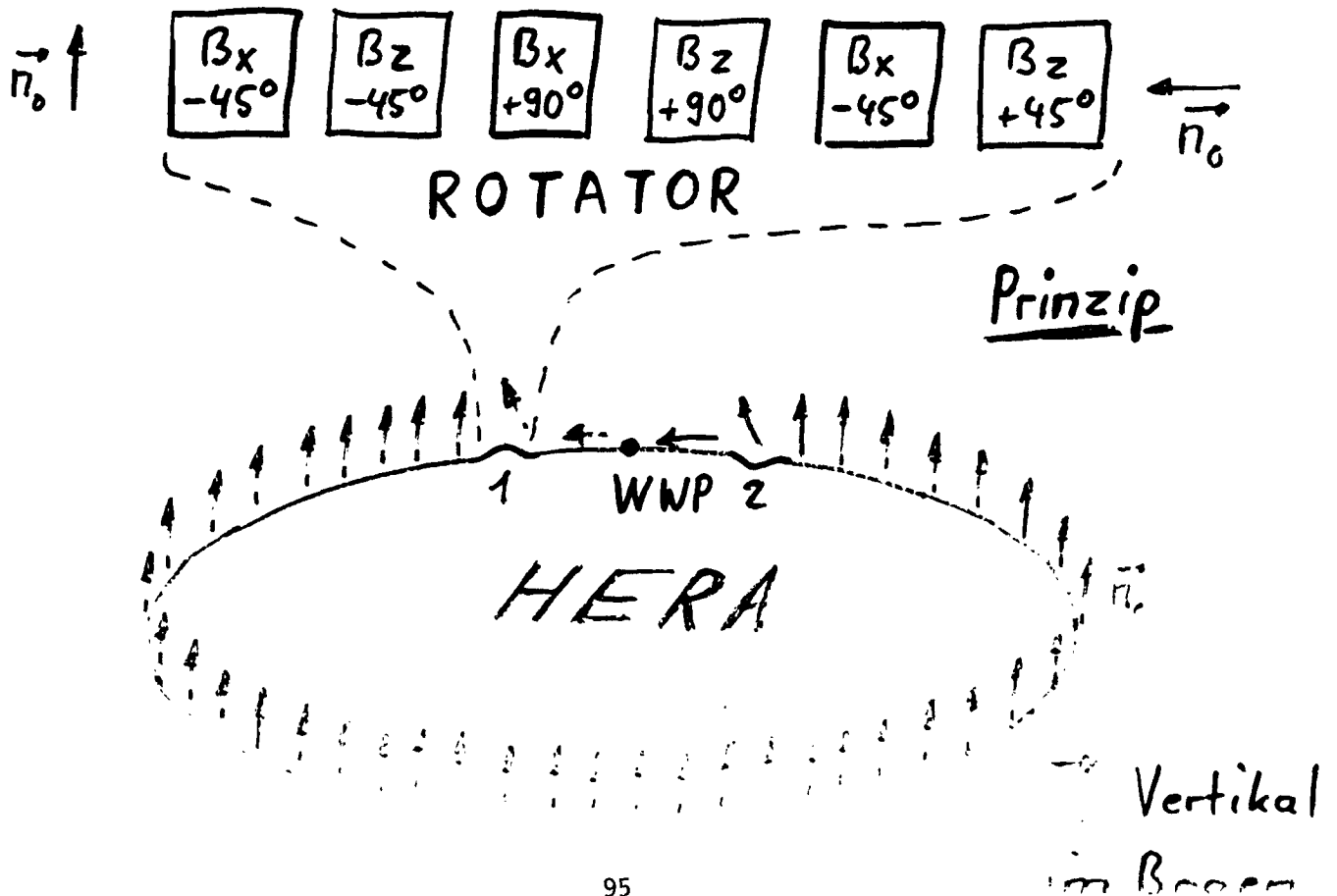
~ 60%



# HERA mit einem Rotatorpaar für HERMES

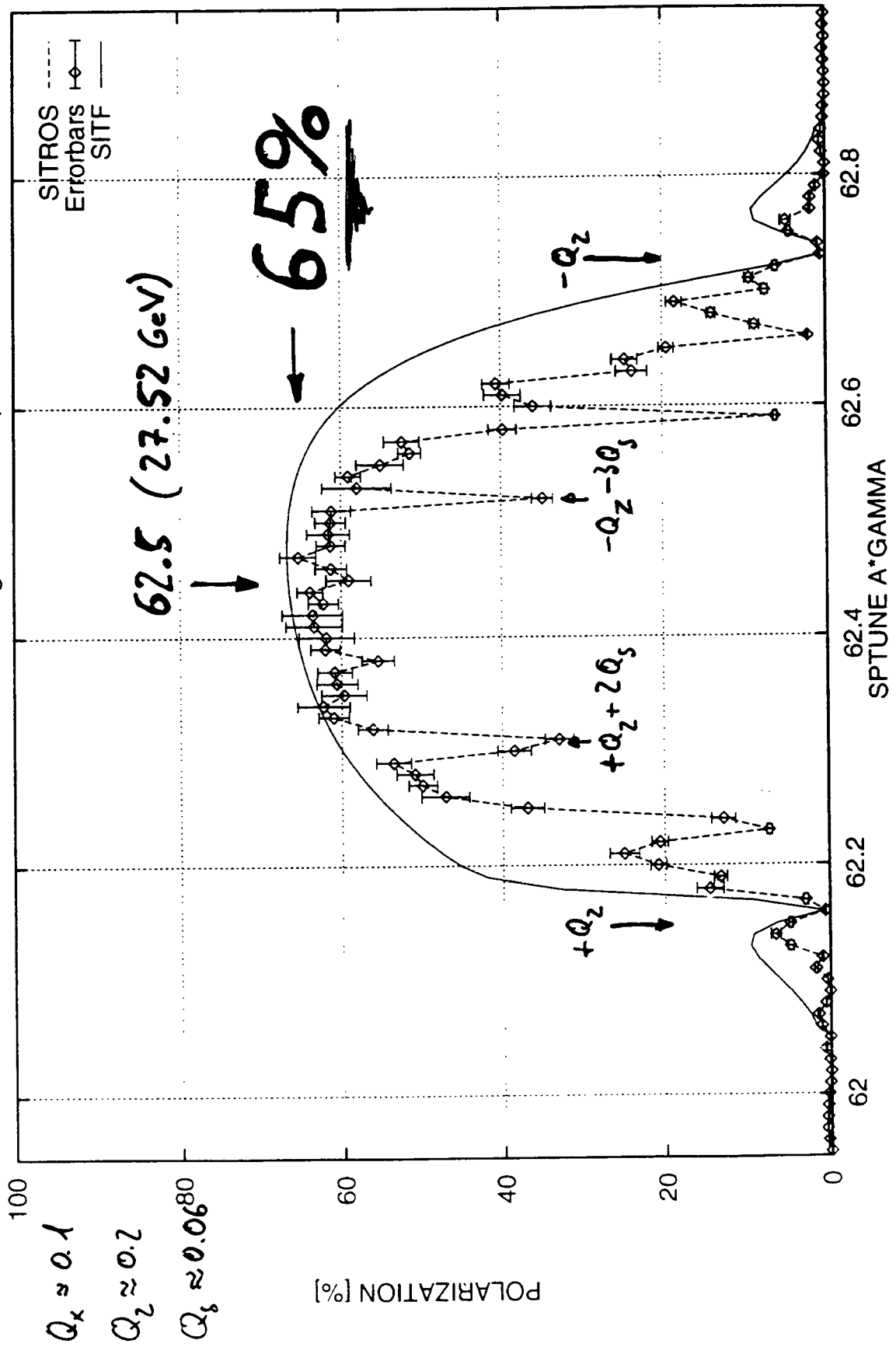
- Longitudinale Polarisation für HERMES
- Wie kann man das erreichen?
- Man benutzt Spin rotatoren!

☀️ 2 Spinrotatoren im Geraden Stück Ost (Mini-Rotator Schema)



SITROS calculation for HERA with one spin-motator pair

SITROS: 5000 TO 10000 TS - gnu/hermes.27p519.03123nn.dat



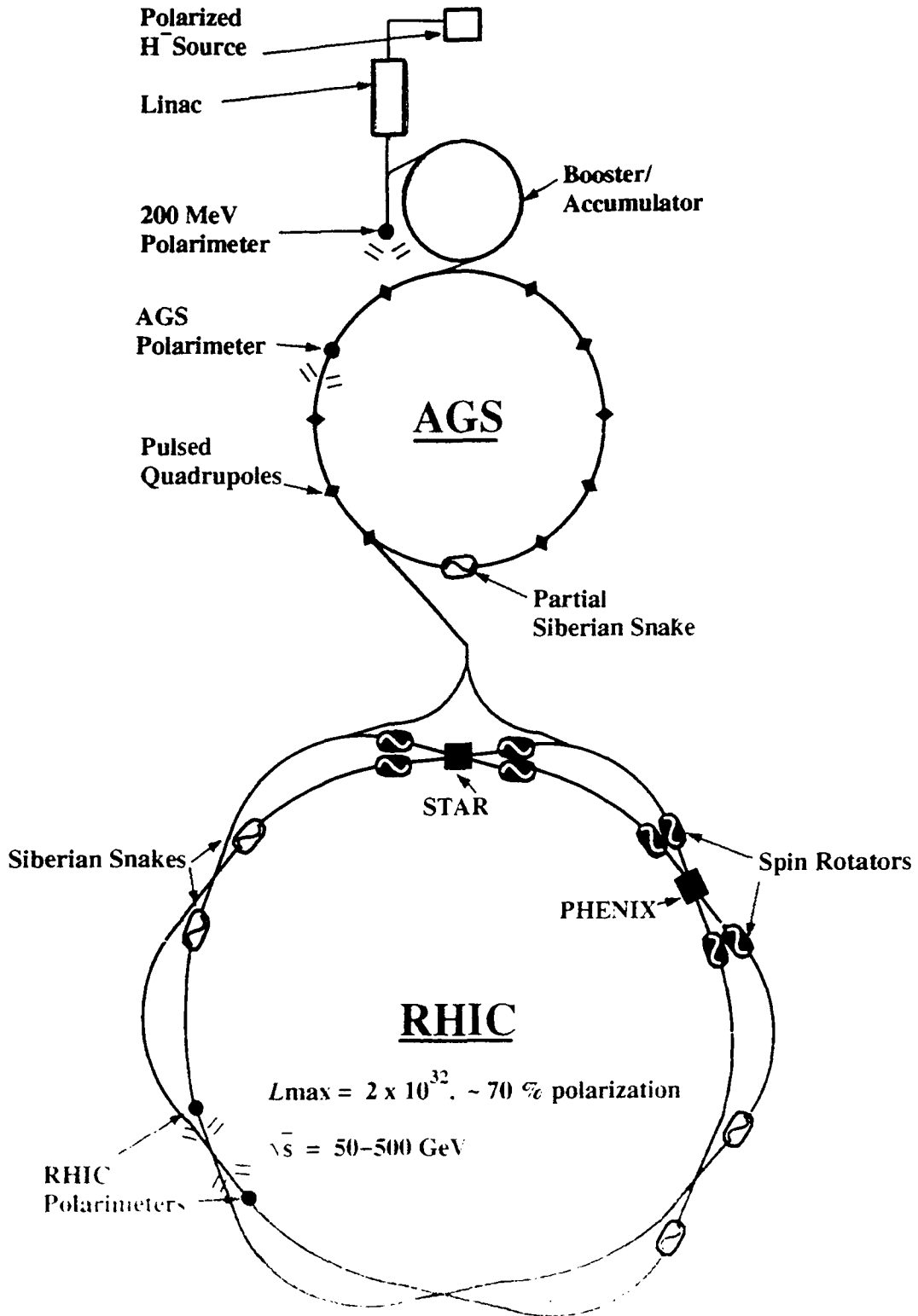
T. Roser, K. Brown, G. Bunce, E. Courant, R. Fernow, S.  
Y. Lee, A. Luccio, Y. Makdisi, S. Mane, L. Ratner, H.  
Spinka, S. Tepikian, A. G. Ufimtsev and D. Underwood

Brookhaven National Laboratory

Upton, NY 11973-5000

Conceptual Design for the Acceleration of Polarized  
Protons in RHIC

# Polarized Proton Collisions at BNL



# POLARIZED COLLIDER PHYSICS (RSC)

- SPIN EFFECTS IN DIRECTY, JET,  $W^{\pm}$ ,  $Z$ , ... PRODUCTION

- $A_{LL}(a+b \rightarrow c+X)$

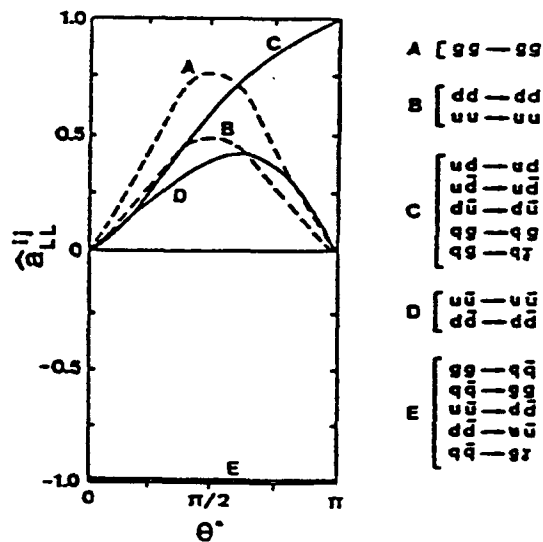
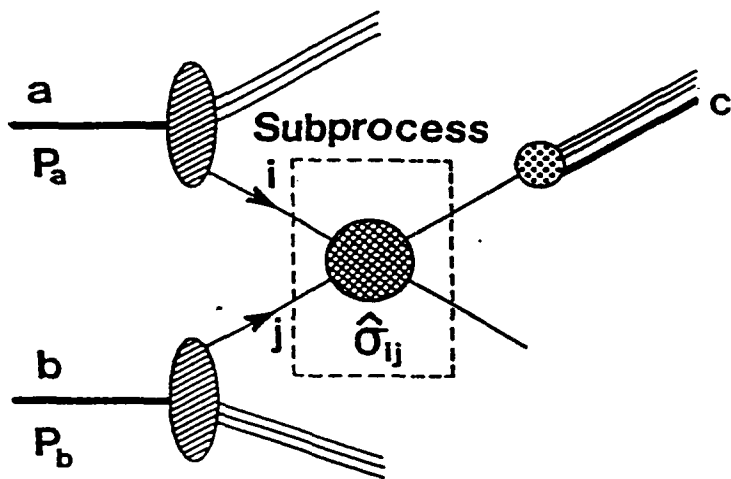
$$= \frac{d\sigma(\Rightarrow) - d\sigma(\Leftarrow)}{d\sigma(\Rightarrow) + d\sigma(\Leftarrow)}$$

$$= \sum_{ij} \int dx_a dx_b \underbrace{\Delta f_i^{(a)} \Delta f_j^{(b)}}_{\text{SPIN STRUCTURE FUNCTIONS}} \underbrace{\hat{a}_{LL}^{ij}}_{\text{PARTON ASYMMETRY}} \frac{d\hat{\sigma}_{ij}}{d\sigma}$$

SUM OVER PARTONS

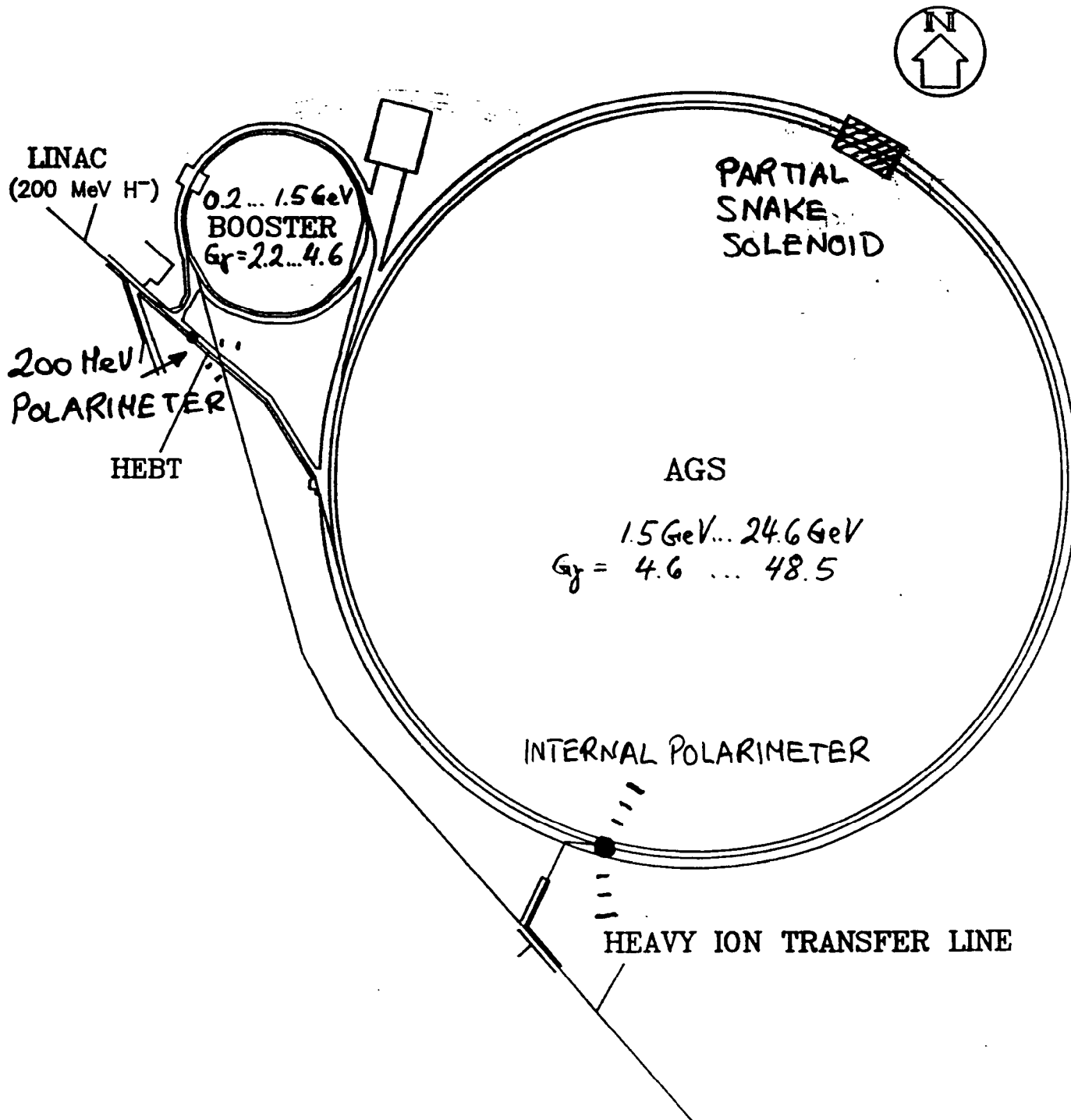
SPIN STRUCTURE FUNCTIONS

PARTON ASYMMETRY

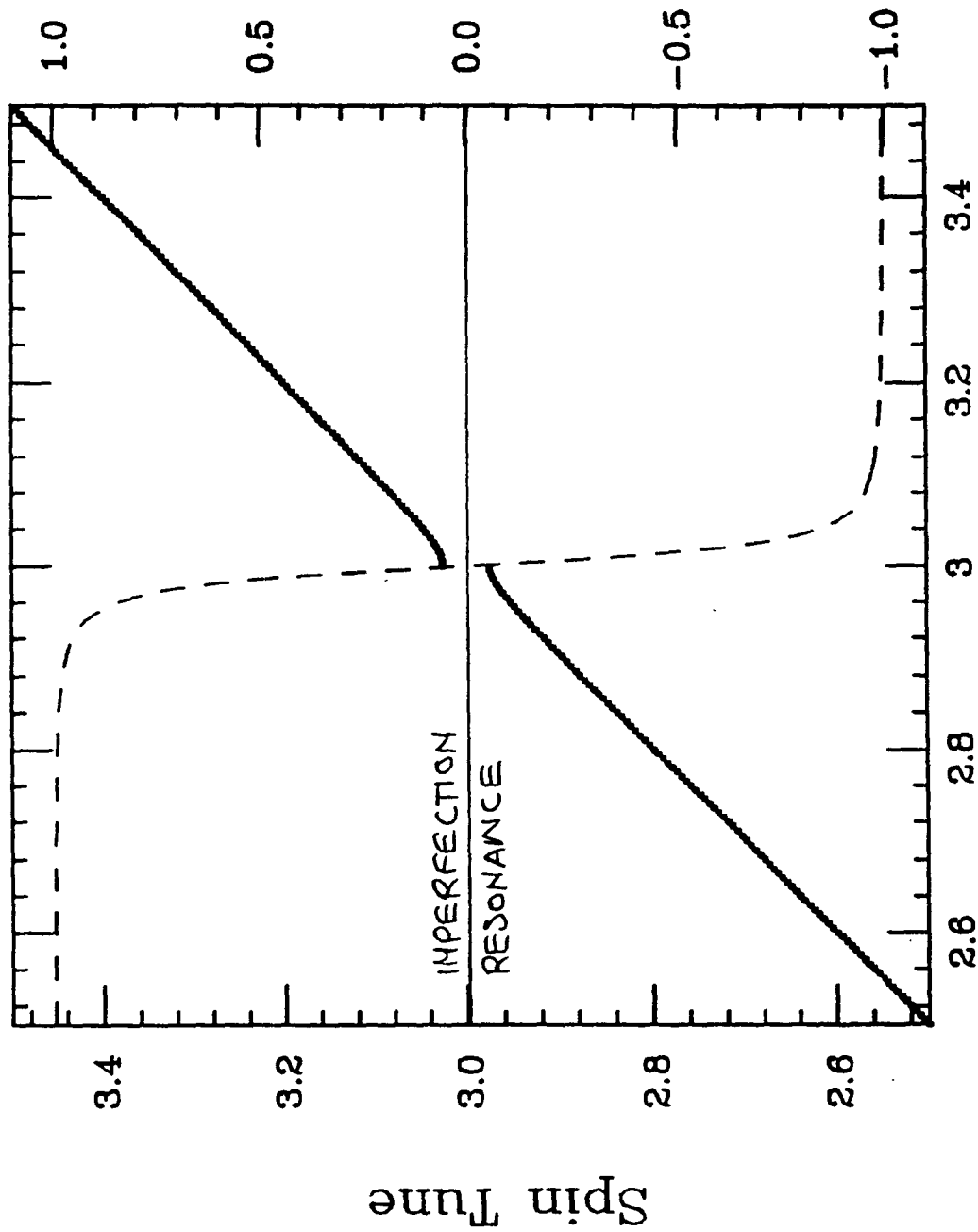


- $x \approx 0.1 \rightarrow$  QUARK POLARIZATION LARGE

# AGS PARTIAL SNAKE TEST, E-880



9° (5%) PARTIAL SNAKE



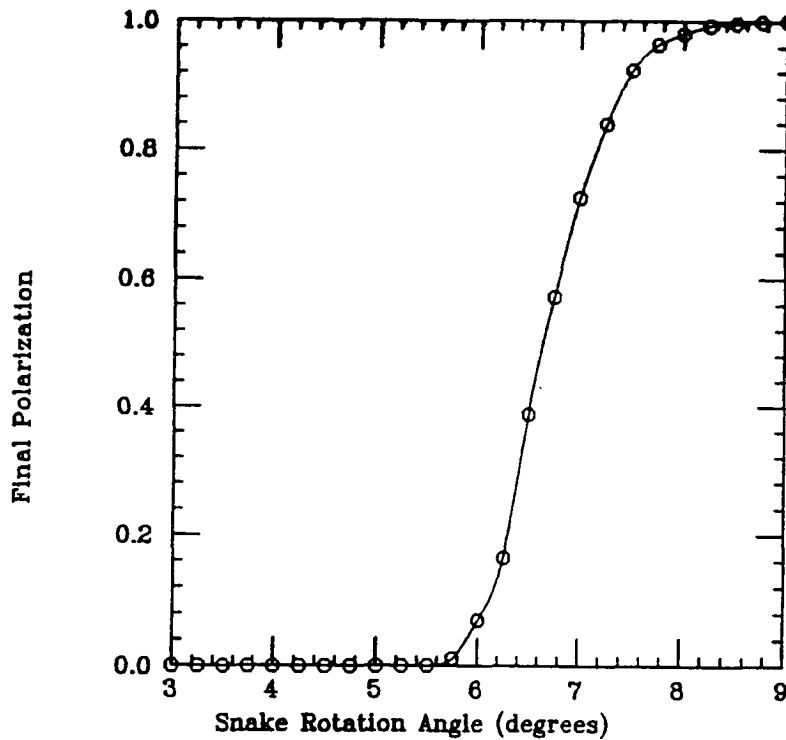
INJECTION:  $G\gamma = 4.6$  EXTRACTION TO RHIC:  $G\gamma = 48.5$

G γ

$$\frac{P_{FINAL}}{P_{INITIAL}} = 2 \exp \left[ -\frac{\pi}{2\alpha} \left| \epsilon e^{i\varphi} + \frac{\delta}{2\pi} \right|^2 \right] - 1$$

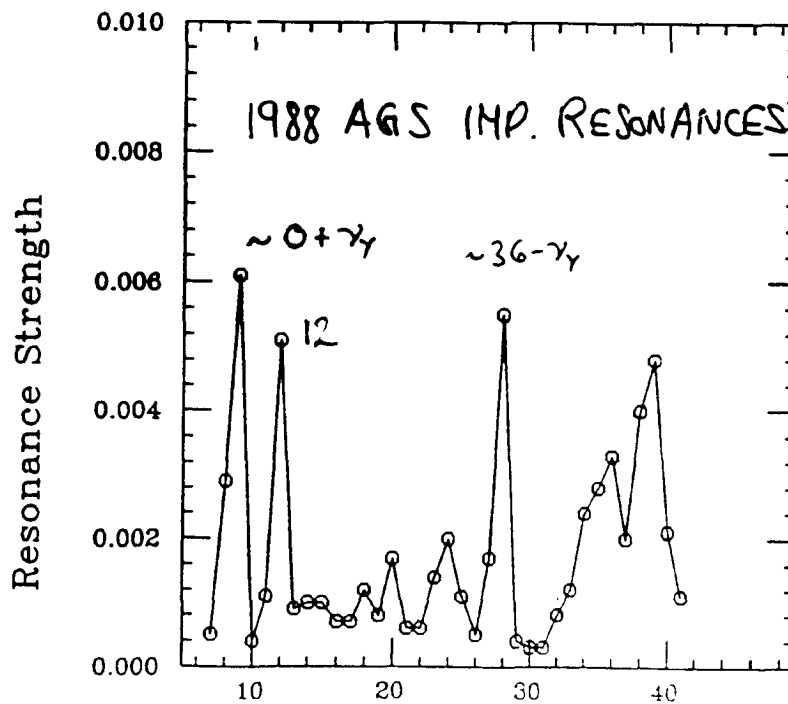
$$\alpha \approx 4 \times 10^{-5} \text{ (AGS)}$$

ACCELERATION THROUGH 40 IMP. RESONANCES ( $\epsilon = 0.01$ )



WORST CASE!

$$\Rightarrow \delta = 9^\circ$$



# 'NEW' AGS POLARIMETER

ELASTIC PP SCATTERING

AT  $t = -0.15 [\text{GeV}/c]^2$

$A_N = 13\% (6 \frac{\text{GeV}}{c}) \dots 3\% (24 \frac{\text{GeV}}{c})$

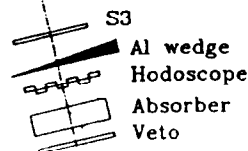
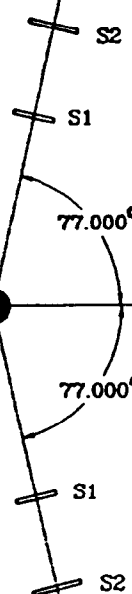
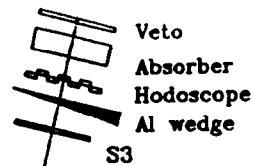
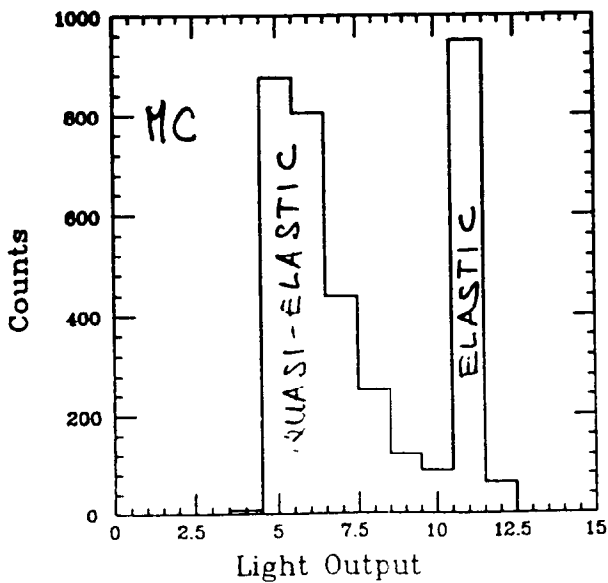
0.003" NYLON STRING TARGET

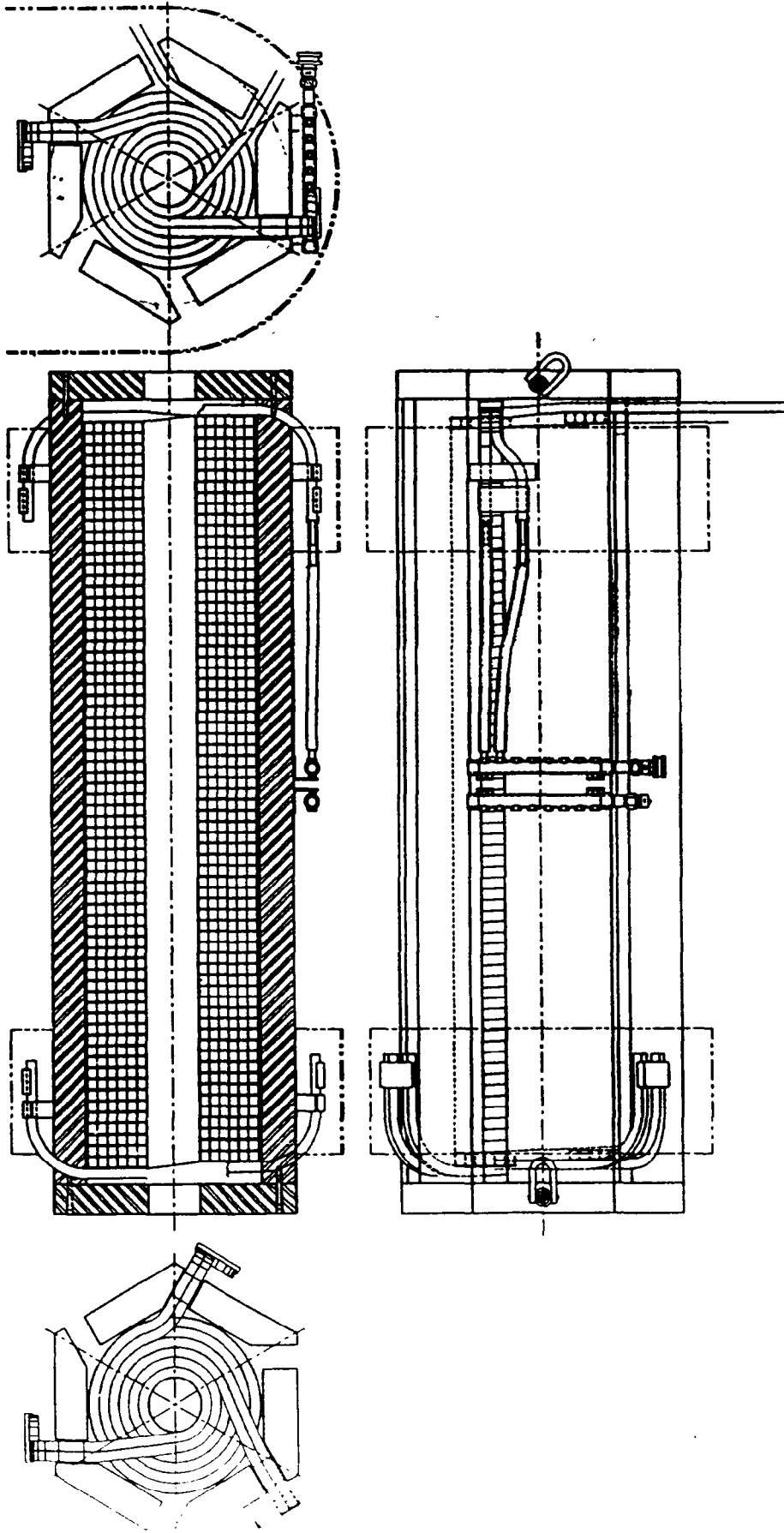
CIRC. BEAM

ABSOLUTE POLARIMETER

⇒ IDENTIFICATION

OF ELASTIC SCATTERING!





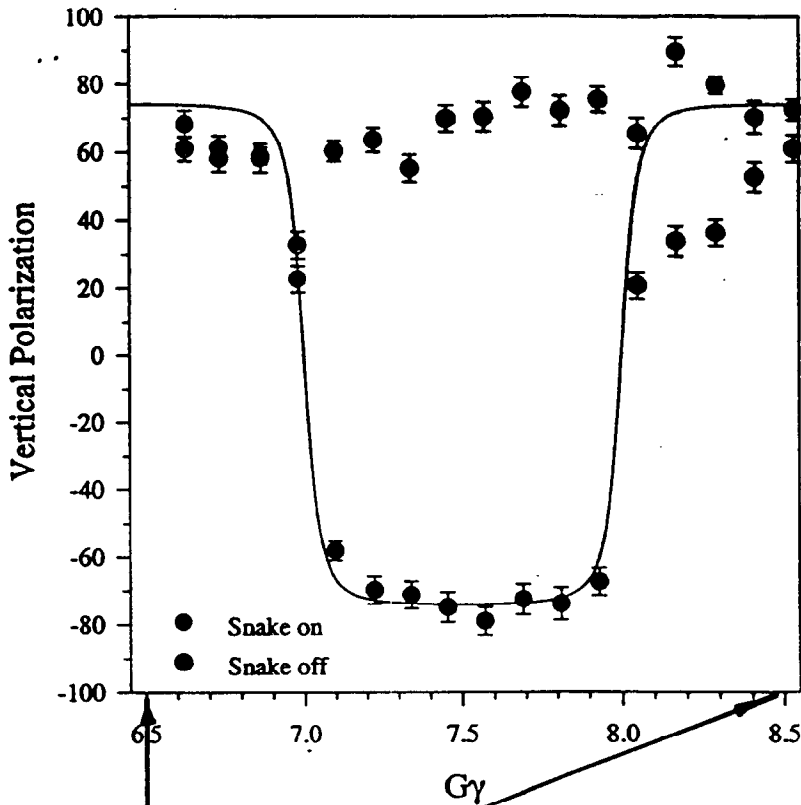
## PARTIAL SNAKE SOLENOID

$$\int B_{dL} = \frac{25 \text{ GeV}/c \times 9^\circ}{\epsilon (1+G)} = 4.7 \text{ Tm}$$

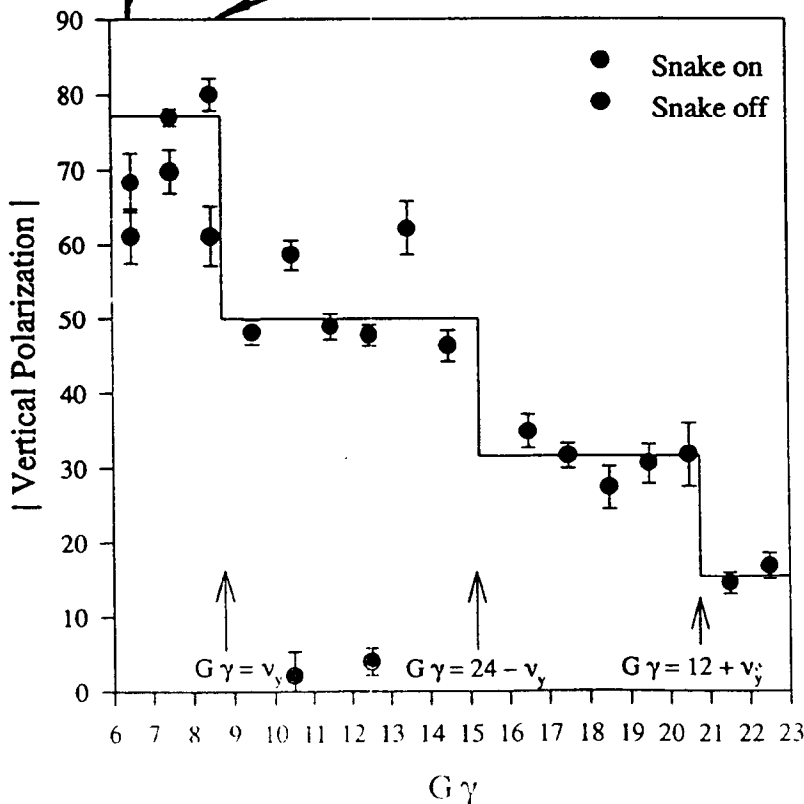
$$I_N = \frac{1}{\mu_0} \int B_{dL} = 3.7 \times 10^6 \text{ A turns}$$

$$L \approx 6 \text{ mH} \quad P_{\text{PEAK}} \approx 1.4 \text{ MW} \quad (\Delta t \approx 0.6 \text{ sec})$$

# PARTIAL SIBERIAN SNAKE TEST



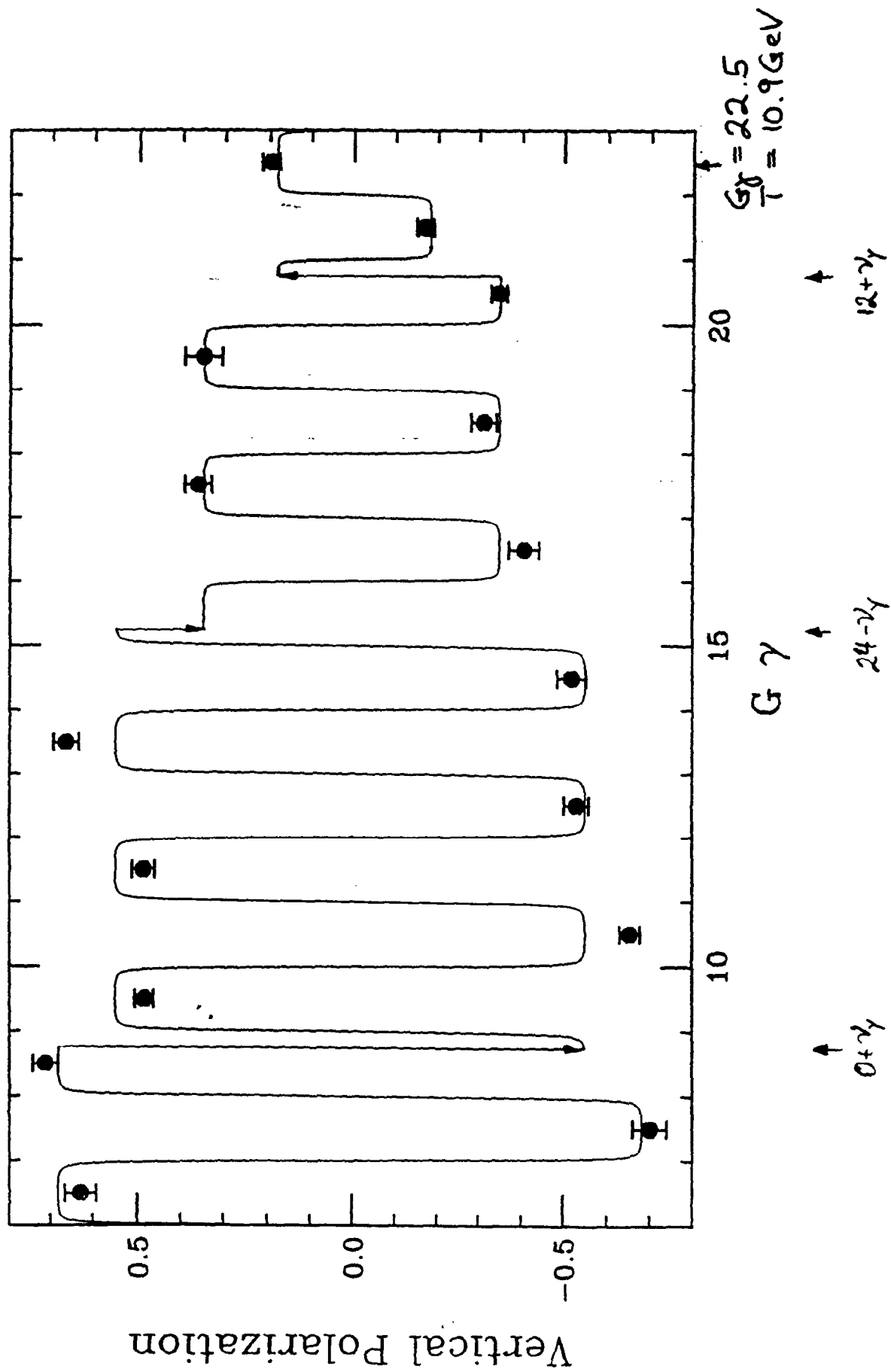
PARTIAL SNAKE  
DRIVES SPIN-FLIP  
AT  $G\gamma = n$



POLARIZATION  
LOSS ONLY AT  
INTRINSIC RES.

WITH PULSED QUAD  
FULL POLARIZATION  
FOR RHIC INJECTION  
→ SPIN COLLIDER

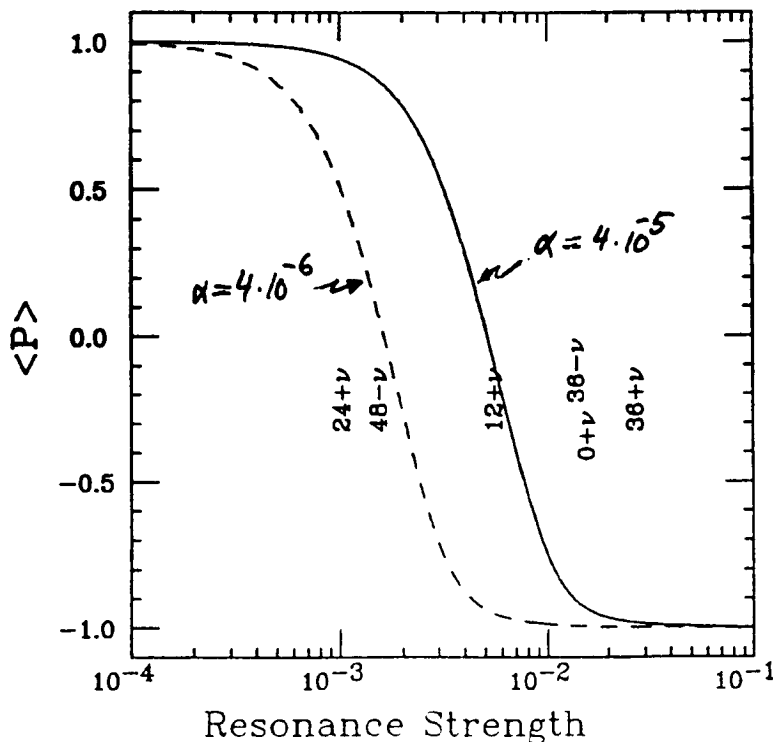
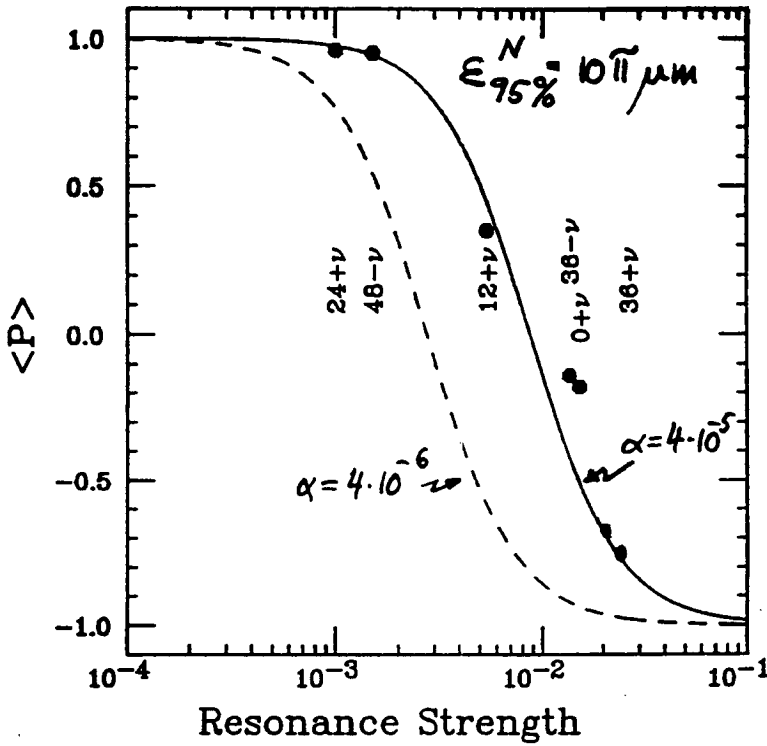
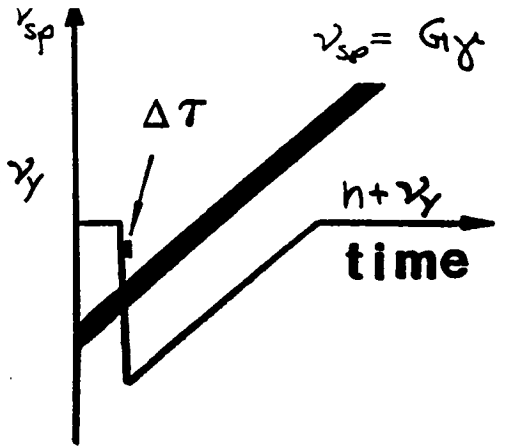
E-880 PRELIMINARY



# INTRINSIC RESONANCES

- DRIVEN BY VERT.  $\beta$  OSCILLATIONS :  $\nu_{sp} = n \pm \gamma$
- $\gamma$  JUMP  $\rightarrow \alpha$  LARGE  $\rightarrow \frac{P_p}{P_T} = 2e^{-\frac{\pi \epsilon^2}{2\alpha}} - 1 \approx 1$

BUT: BEAM ENITTANCE GROWTH



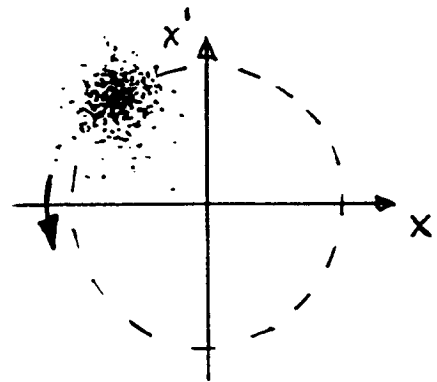
## SPIN FLIP

- $\epsilon$  LARGE OR  $\alpha$  SMALL (NEED PARTIAL SNAKE!)
- AVERAGE OVER BEAM DISTR.

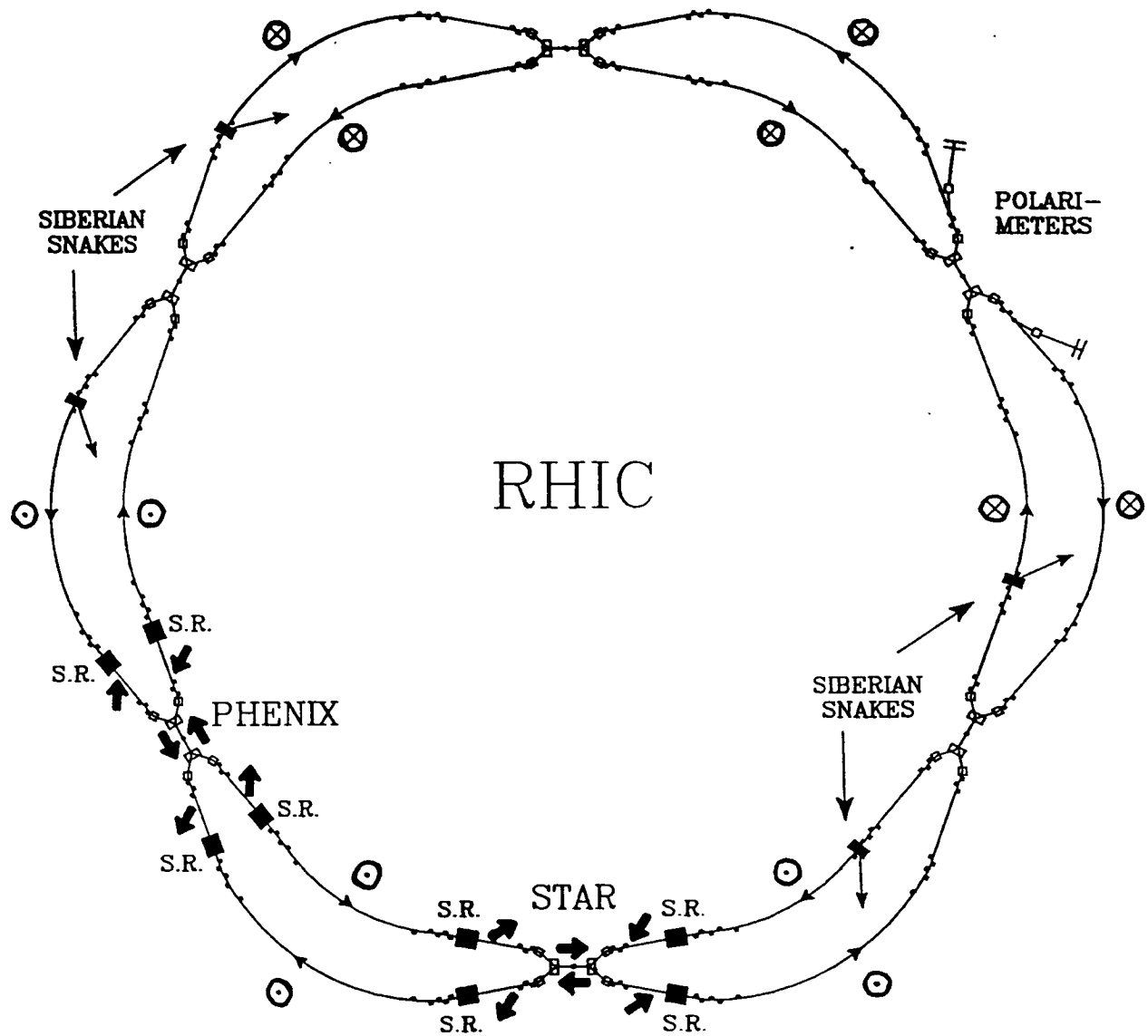
$$\langle P \rangle = \frac{1 - \frac{\pi \epsilon_{95}^2}{6\alpha}}{1 + \frac{\pi \epsilon_{95}^2}{6\alpha}}$$

$\epsilon_{95}$ : STRENGTH OF PARTICLE  
WITH  $\epsilon = \epsilon_{95\%}$

- COHERENT  $\beta$  OSCILLATION

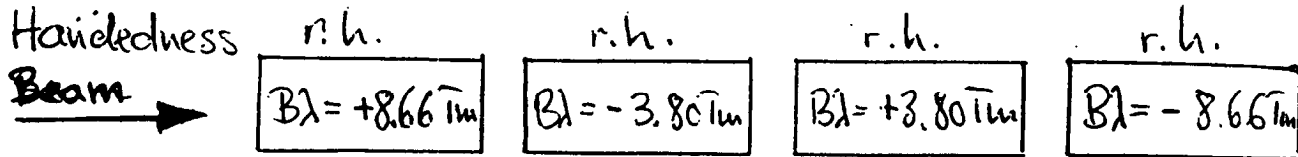


← AMPLITUDE =  $2\sigma$



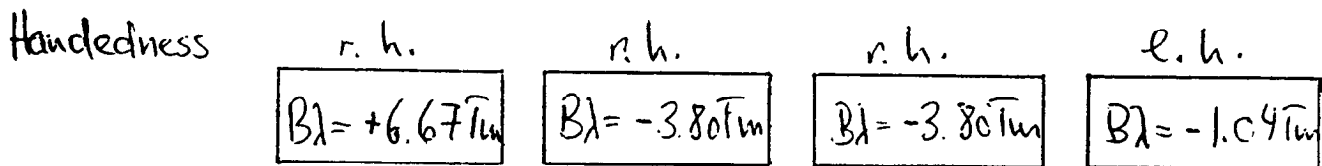
## Designs of Shatunov et al:

### Snake with 45° axis:



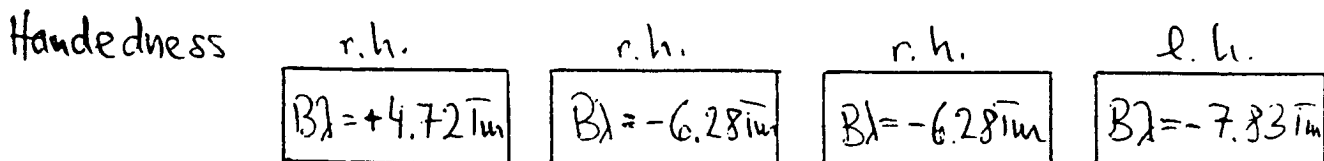
$$Y_{\max}(B=4\text{T}, \gamma=27) = 35.2 \text{ mm}$$

### Spin Rotator to produce radial polarization:

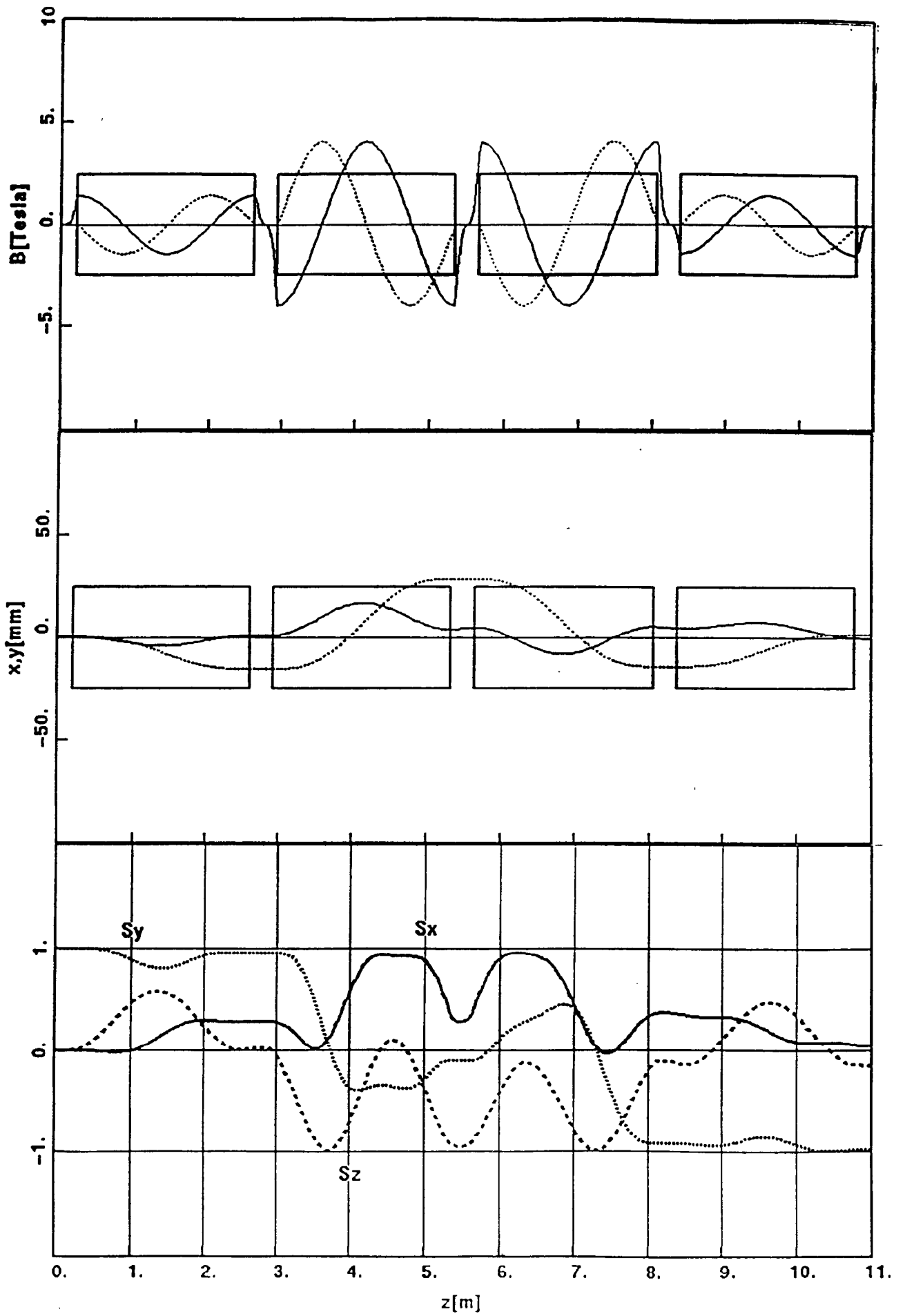


$$Y_{\max}(B=4\text{T}, \gamma=27) = 27.1 \text{ mm}$$

### Spin Rotator to produce longitudinal polarization:



$$Y_{\max}(B=4\text{T}, \gamma=27) = 31.8 \text{ mm}$$



SDRC I-DEAS VI.1(s): Solid Modeling

22-MAR-94

15:28:43

Database: rhic 8cm helical dipole coil/magnet for proton spin experime

View : COIL ASSY ISO

Task: Assembly

System: 2-COIL DRUM ASSY (modified)

Display : No stored Option

Units : MM

Bin: 3-COIL ASSY

Update Level: Full

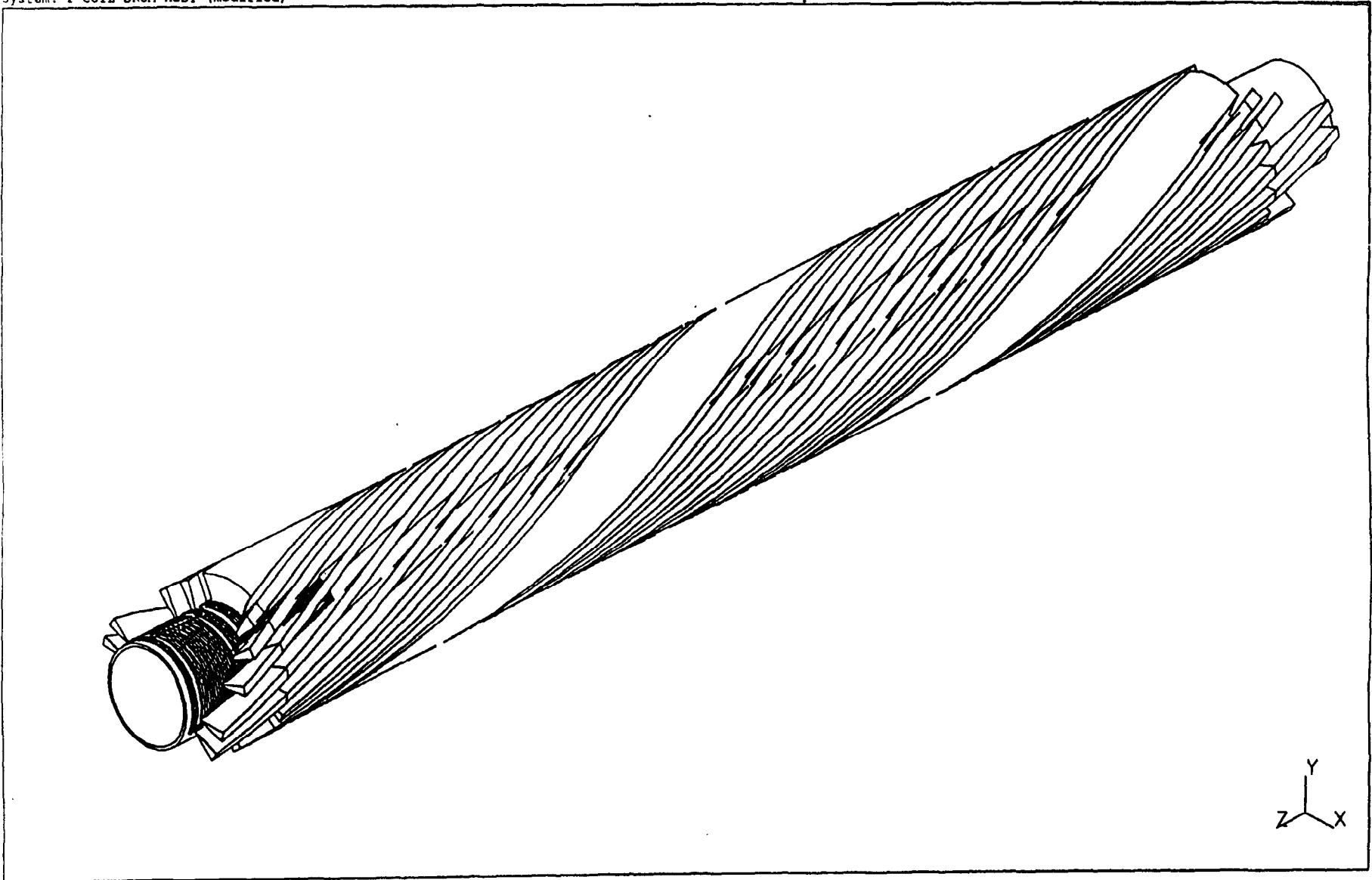
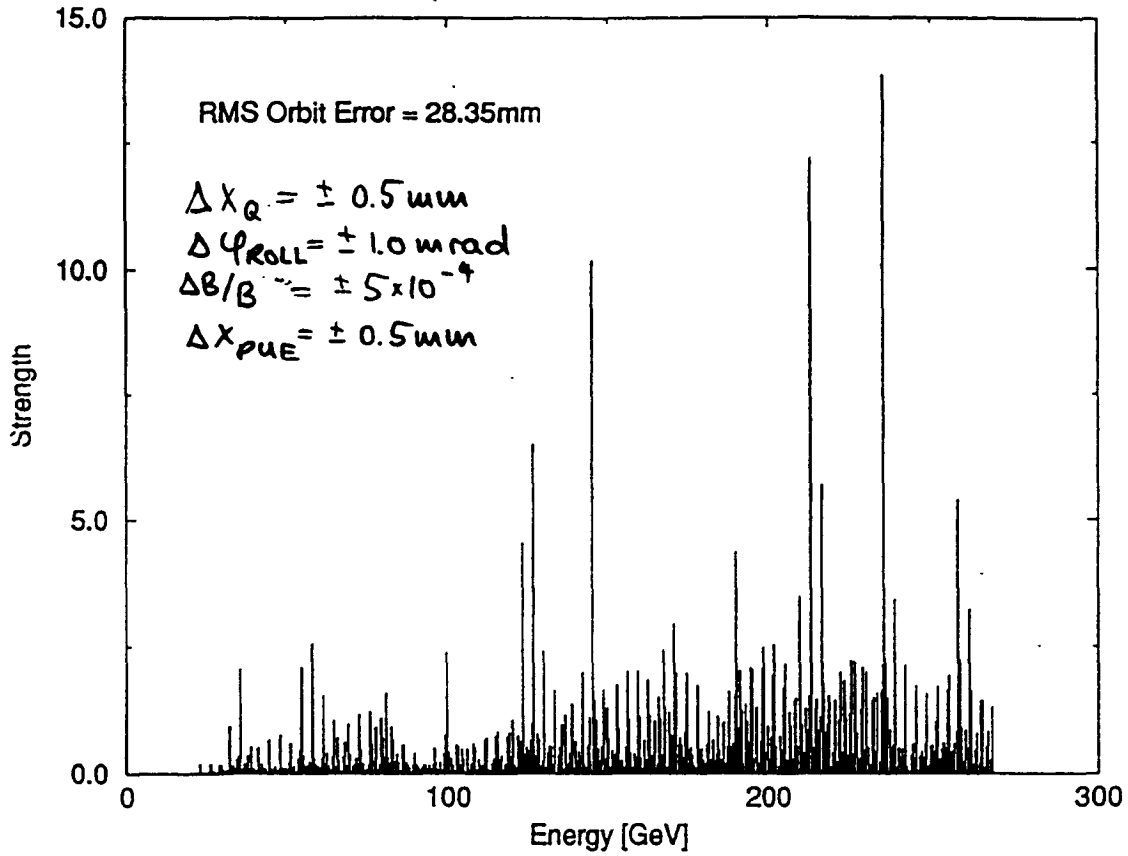


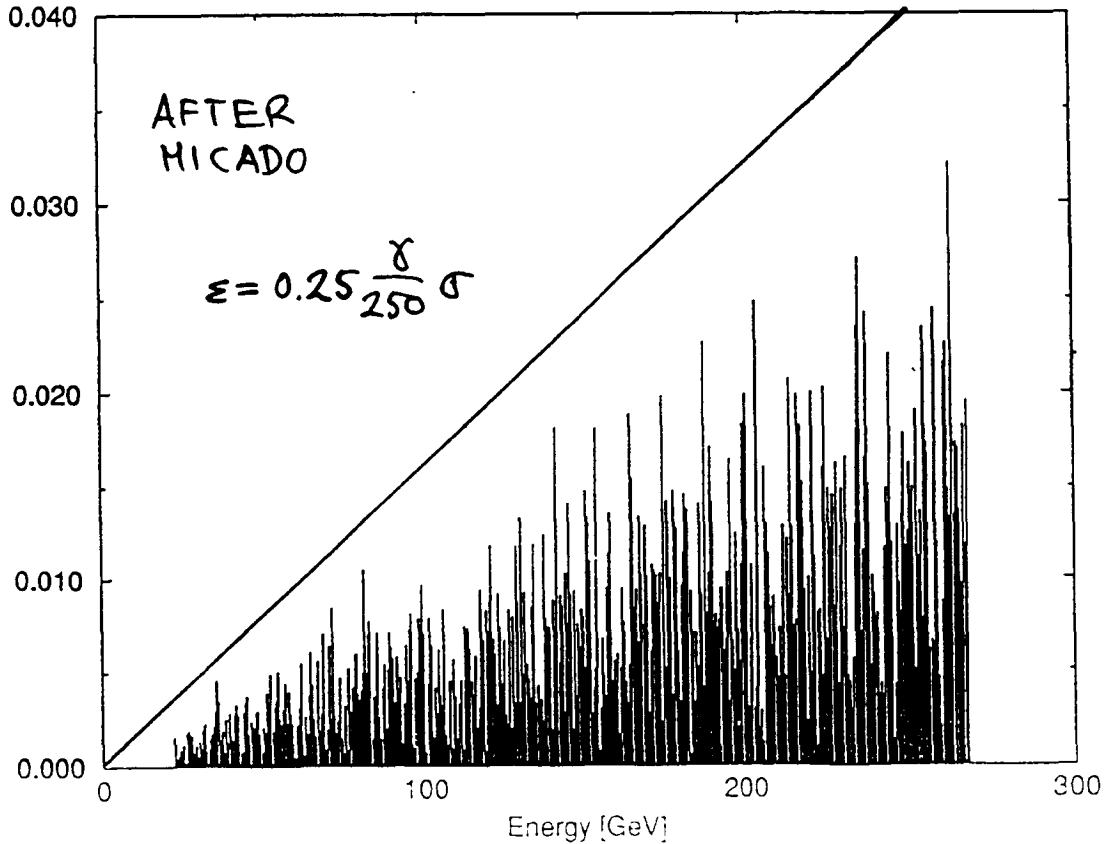
Fig. 4

# Imperfection Depolarizing Resonances

$\beta^* = 10\text{m}$ , Uncorrected Orbit



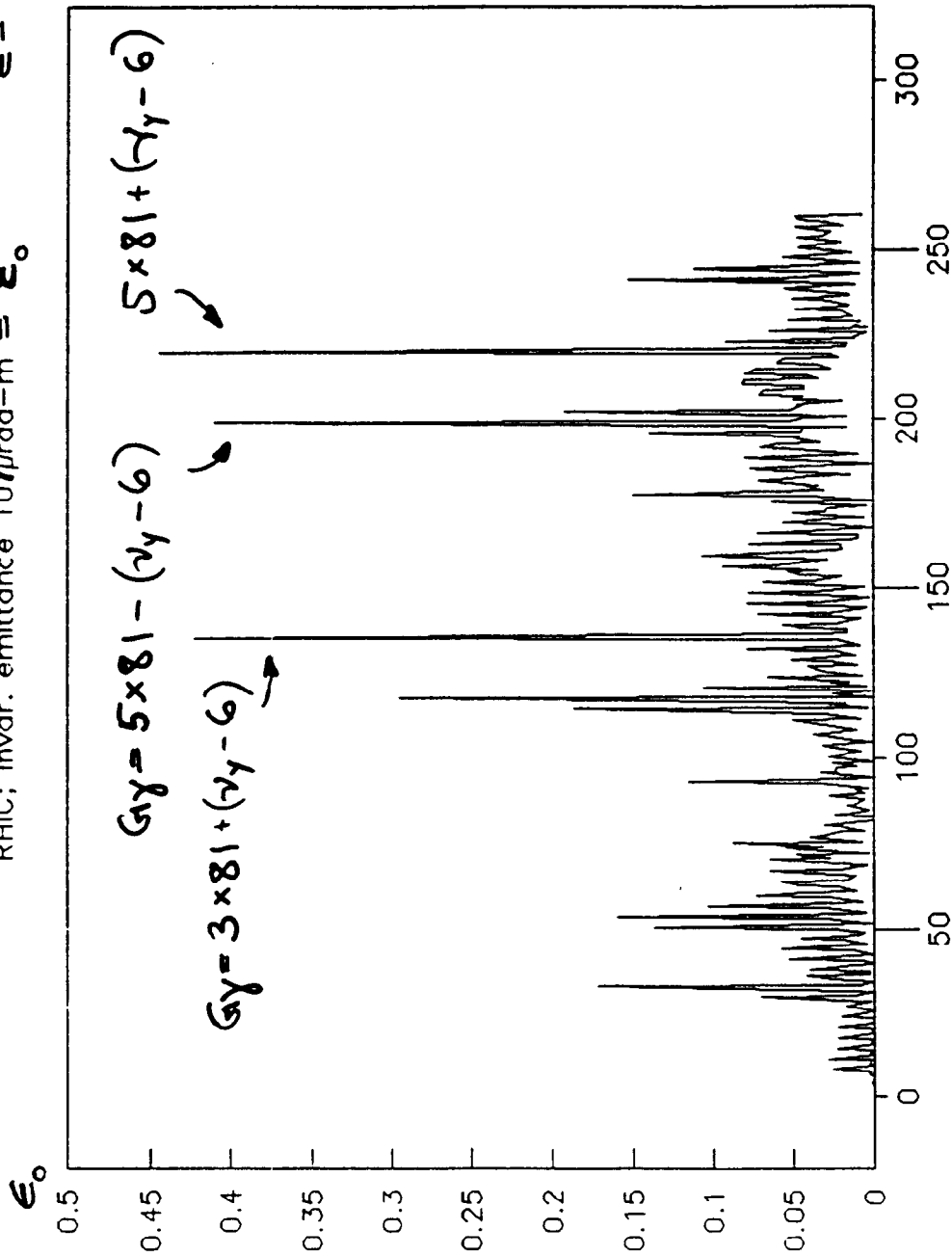
$\beta^* = 10\text{m}$ , Orbit Error = 0.155mm =  $\sigma$



# Intrinsic resonance strength

RHIC; invar. emittance  $10^7 \mu\text{rad-m} = \epsilon_0$

$$\epsilon = \epsilon_0 \sqrt{\frac{\epsilon'}{\epsilon_0}}$$



Energy

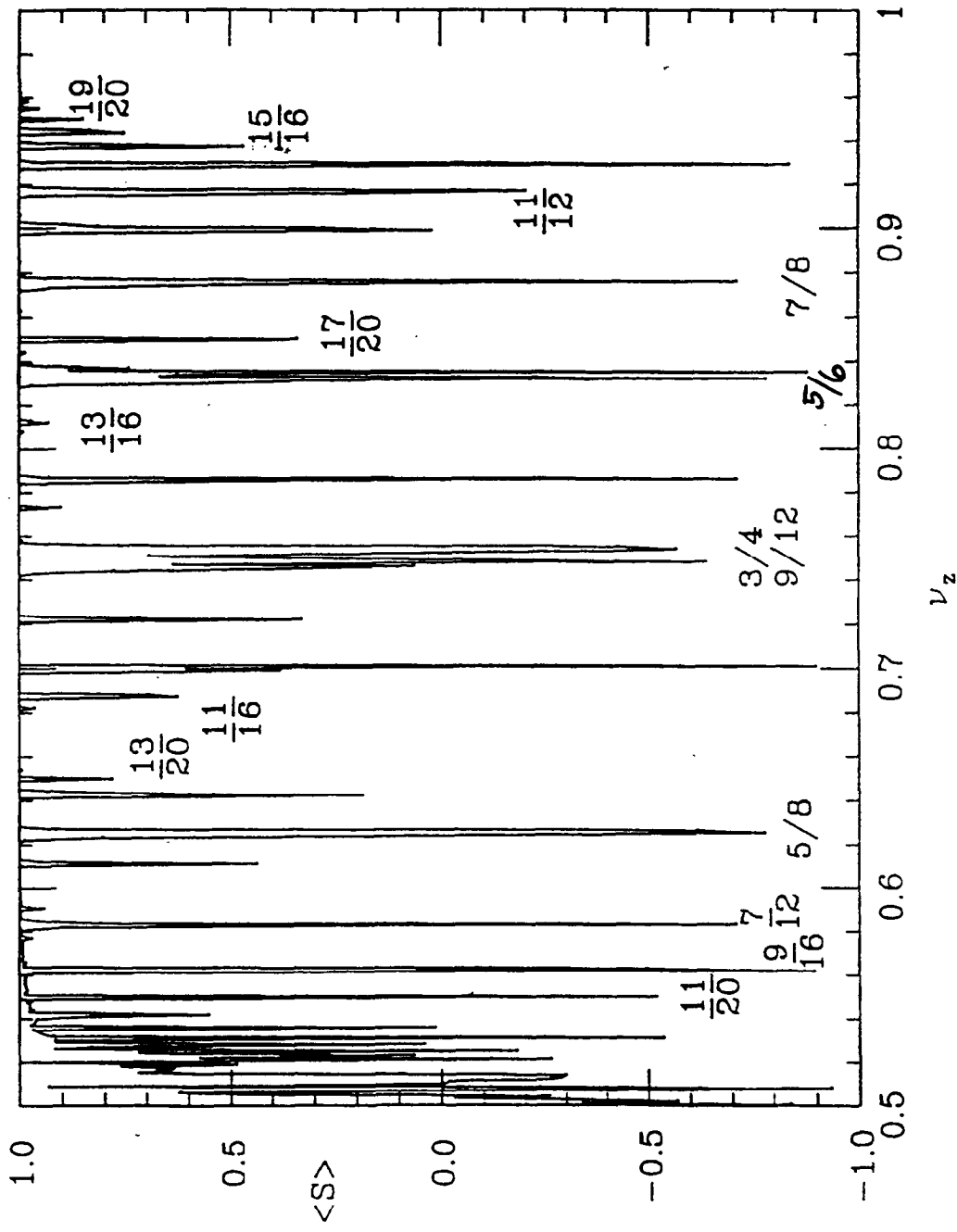
—  $\beta^* = 10\text{m}$  (ALL  $\phi$  INTERACTION REGIONS)

~ SAME FOR  $\beta^* = 1\text{m}$

$$\Delta \nu = \frac{\nu_{sp} \pm k}{n}$$

ACCELERATION THROUGH INTRINSIC RESONANCE WITH SNAKE

$\epsilon_{int} = 0.5$   $\epsilon_{imp} = 0.05$   $N_p = 2$   $\nu_p = 1/2$



$\rightarrow \Delta \nu = 0.815 \dots 0.830 = 0.015$

Figure 10

# SPIN TUNE SPREAD

			SHIFT	SPREAD
IMPERFECTION RESONANCE	$\epsilon_{imp} \leq 0.05$	$\Delta\nu_{sp} = \frac{\pi \epsilon ^2}{4}$		$< 0.002$
ORBITAL ANGLE BETWEEN SNAKES	$\Delta\theta \leq 1 \times 10^{-4}$ rad	$\Delta\nu_{sp} = \frac{G\gamma\Delta\theta}{\pi}$	$< 0.010$	
CLOSED ORBIT ERROR	$\Delta\theta \leq 2 \times 10^{-5}$ rad		$< 0.002$	
BETATRON MOTION	$\Delta\theta \leq 7 \times 10^{-5}$ rad			$< 0.007$
			$< 0.012$	$< 0.009$

→  $\Delta\nu_y < 0.006$

WHEN ACCELERATING THROUGH THE  
3 STRONG RESONANCES.

⇒ NO DEPOLARIZATION!

TRACKING CALCULATION FOR  
BEAM DISTRIBUTION OVERLAPPING  
SNAKE RESONANCE :

- 10% OVERLAPPING  $\Delta y_y = \beta/16$

- $\dot{\gamma} = 3.9 \text{ sec}^{-1}$

- $\epsilon_N = 20 \pi \text{ mm mrad}$

$\rightarrow \frac{\Delta P_{\text{final}}}{\Delta P_{\text{initial}}} \gtrsim 0.95, 3 \text{ RES.} \rightarrow \frac{\Delta P_{\text{final}}}{\Delta P_{\text{initial}}} \gtrsim 0.86$

NOTE: NO POLARIZATION DIFFUSION  
IN PROTON BEAMS!

# STORAGE MODE

(> 5 GeV)

- CHOOSE ENERGY FAR FROM STRONG INTRINSIC RESONANCES: 139 GeV, 200 GeV, 224 GeV  
→ VERY WEAK SNAKE RESONANCES

- TRACKING CALCULATION ON SNAKE RESONANCE

$$\Delta\nu_y = 13/16, \epsilon = 0.15 \rightarrow \frac{P_{\text{final}}}{P_{\text{initial}}} = 0.90 \text{ STABLE}$$

FOR  $> 8 \times 10^9$  TURNS.

$$\text{REALITY: } \Delta\nu_y \neq \frac{\nu_{sp} \pm k}{n}, \epsilon \ll 0.15$$

ALSO: NO POLARIZATION DIFFUSION

- RF NOISE:

$$\text{DEPOLARIZING RESONANT NOISE: } \nu_{sp} f_{\text{rev}} = 39 \text{ kHz}$$

$$\text{NOISE KICK: } \theta_k \rightarrow N_p = \frac{\cos(0.80)}{G_\gamma \theta_k}$$

$$\text{ORBITAL RESONANT NOISE: } \nu_{x,y} f_{\text{rev}} \approx 14 \text{ kHz}$$

$$\rightarrow N_o = \frac{A}{\langle \beta \rangle \theta_k}$$

$$\rightarrow \frac{N_p}{N_o} = \frac{\cos(0.8) \langle \beta \rangle}{G_\gamma A} = 3.2$$

## SPIN FLIPPER FOR RHIC

GOAL: REVERSE POLARIZATION OF STORED BEAM

SOLUTION: "SLOW" ADIABATIC PASSAGE THROUGH  
ARTIFICIAL RESONANCE

- ARTIFICIAL RESONANCE DRIVEN BY LOCAL RF

SPIN ROTATOR  $\epsilon = \frac{\delta}{2\pi} \approx 10^{-4}$ ,  $f = f_{REV} / 2 = f_{PRECESSION}$   
 $= 40 \text{ kHz}$

- RF MINI SNAKE: V H -2V -2H V H

$\chi_V: 90^\circ \text{ DC}$ ,  $\chi_H: 0.5^\circ \text{ RF} \rightarrow \chi_S = \sqrt{10} \chi_H = 1.6^\circ$ ;  $\epsilon = 4 \times 10^{-3}$

- "SLOW" ADIABATIC PASSAGE: RAMP FREQUENCY  
OF SPIN ROTATOR THROUGH RESONANCE  
CONDITION,  $\tau \approx 1 \text{ sec}$

# EMITTANCE GROWTH DUE TO SPIN FLIPPER

- 40 kHz FIELD:  $0.017 \mu\text{m} \rightarrow$  DEFLECTION  $\approx 100 \mu\text{rad}$
- RESIDUAL ORBIT DEFLECTION:  $\sim 1 \mu\text{rad}$  @ 25 GeV

- $$\begin{pmatrix} X_n \\ X'_n \end{pmatrix} = \sum_{m=1}^n \left[ \begin{pmatrix} 1 & 0 \\ 0 & 1 \end{pmatrix} \cos((n-m)2\pi\nu_y) + \begin{pmatrix} \alpha & \beta \\ -\gamma & -\alpha \end{pmatrix} \sin((n-m)2\pi\nu_y) \right] \times \begin{bmatrix} 0 \\ \cos(m2\pi\nu_{sp}) \cdot \Delta x' \end{bmatrix}$$

- $$X_n = \beta \Delta x' \sum_{m=1}^n \cos(m2\pi\nu_{sp}) \sin((n-m)2\pi\nu_y)$$

$$= \frac{1}{2} \beta \Delta x' \left[ \cos(2\pi n \nu_y) - \sin 2\pi \nu_y \frac{\cos(2\pi n \nu_{sp}) - \cos(2\pi n \nu_y)}{\cos(2\pi \nu_{sp}) - \cos(2\pi \nu_y)} \right]$$


---

$$X_{\max} \approx 1.2 \beta \Delta x' \text{ FOR } \nu_{sp} = \frac{1}{2}, \nu_y = 0.8$$

$$\underline{\underline{\Delta \epsilon_N}} = \gamma \cdot (1.2 \Delta x')^2 \beta = \underline{\underline{0.0007 \pi \text{ mm} \mu\text{rad}}}$$

- DECOHERENCE IN  $> 100$  TURNS ( $\Delta \nu_y < 0.01$ ):

$$\Delta \epsilon_N(t) = \frac{t \cdot f_{REV}}{100} 7 \cdot 10^{-4} \pi < 0.6 \pi \text{ mm} \mu\text{rad s}^{-1} t$$

# POLARIMETERS

ABSOLUTE MEASUREMENT:

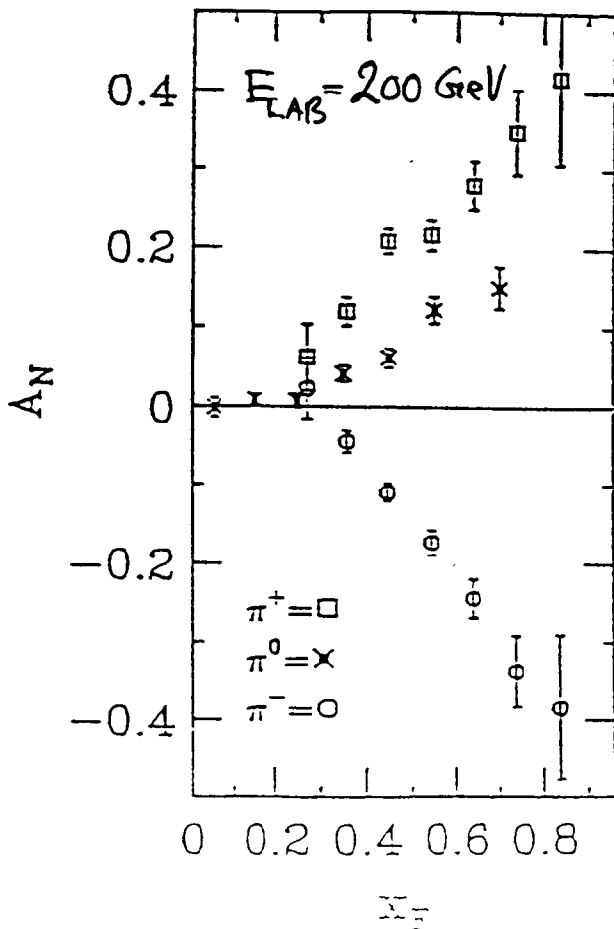
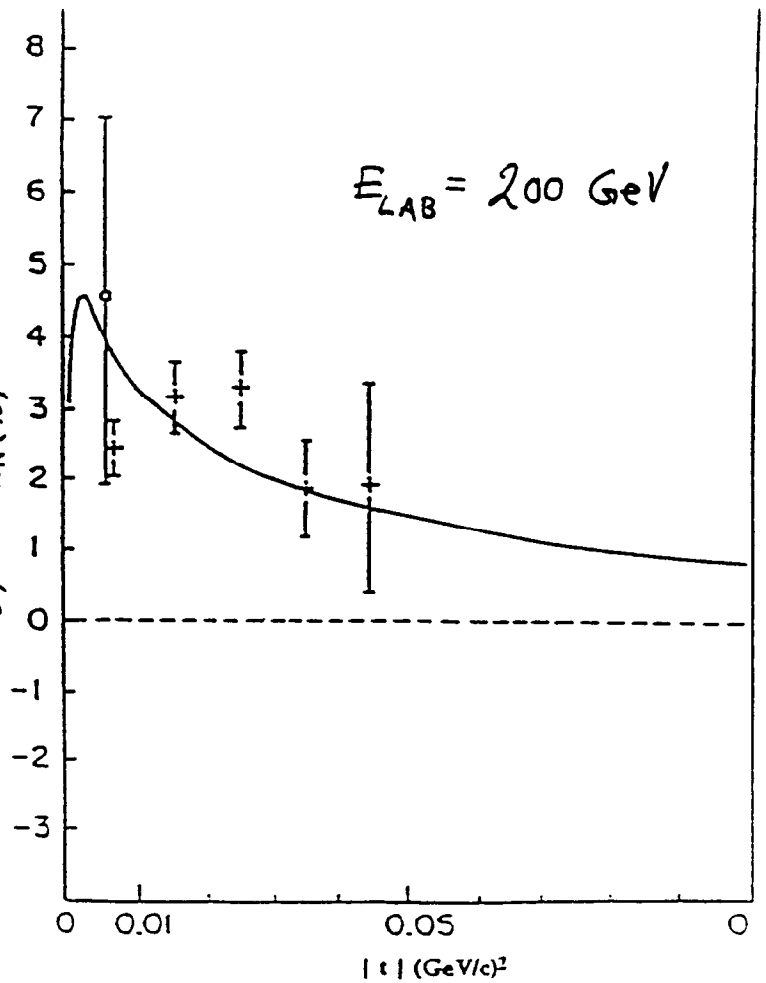
COULOMB-NUCLEAR-INT.

IN SMALL ANGLE EL. SCATT.

$$A_N \approx 5\% \text{ AT } |t| = 2 \times 10^{-3} \left(\frac{\text{GeV}}{c}\right)^2$$

→ HIGH  $\beta$  SECTION, ROMAN POTS

(RLOI 1)



RELATIVE MEASUREMENT:

INCLUSIVE PION PRODUCTION

AT LARGE  $x_F$

$A_N$  LARGE

POL. MONITOR AT STAR & PHENIX

DETECTION OF HIGH  $p_T$   $\pi$ 'S ?

D. P. Barber, K. Heinemann and G. Ripken

DESY

Notkestrasse 85. D-22603 Hamburg, Germany

Spin tune shift due to closed orbit distortion

Spin tune shift due to closed orbit distortion.

D.P. Barber, K. Heinemann and G. Ripken.  
DESY Hamburg.

Based on DESY Report M-94-05

### **Introduction**

A perturbative formalism, up to second order, for calculating spin tune shift on the closed orbit of a storage ring due to misalignment. This is based on the familiar concepts of the SLIM formalism and can treat rings of arbitrary geometry. The final formulae agree with those already given using another approach by K. Yokoya (SSC-189 1988)

Why?

1. Measure beam energy using resonant depolarization :  $\nu_0 = a\delta \Rightarrow E$

$$\nu = \nu_0 + \Delta\nu \xrightarrow{?} E$$

2.  $\Delta\nu$  for TeV protons

3. Looking for a simple formula :  $\sum_j \frac{|V_{ij}|^2}{\lambda_i - \lambda_j}$  ?  
as in Q.M.?

- self education

- check the others

= Previous : Derbenev + Kondratenko

Yokoya

Assmann + Koutchouk.

Using the usual notation the motion of a spin vector  $\vec{\xi}$  on the design orbit is described by the Thomas-BMT equation:

$$\begin{aligned} \frac{d}{ds} \vec{\xi} &= \vec{\Omega} \times \vec{\xi} \\ &= \underline{\Omega} \cdot \vec{\xi} \end{aligned} \tag{1}$$

where we write the spin as

$$\vec{\xi} = \begin{pmatrix} \xi_s \\ \xi_x \\ \xi_z \end{pmatrix}$$

and where the precession vector  $\vec{\Omega}$

$$\vec{\Omega} = \begin{pmatrix} \Omega_s \\ \Omega_x \\ \Omega_z \end{pmatrix}; \quad \underline{\Omega} = \begin{pmatrix} 0 & -\Omega_z & \Omega_x \\ \Omega_z & 0 & -\Omega_s \\ -\Omega_x & \Omega_s & 0 \end{pmatrix}$$

We calculate in the machine coordinate system. In the presence of misalignments the closed orbit deviates from the design orbit and we write:

$$\begin{aligned} \frac{d}{ds} \vec{\xi} &= [\vec{\Omega} + \vec{\omega}] \times \vec{\xi} \\ &= [\underline{\Omega} + \underline{\omega}] \cdot \vec{\xi} \end{aligned} \quad (2)$$

where

$$\vec{\omega} = \begin{pmatrix} \omega_s \\ \omega_r \\ \omega_z \end{pmatrix}; \quad \underline{\omega} = \begin{pmatrix} 0 & -\omega_z & \omega_r \\ \omega_z & 0 & -\omega_s \\ -\omega_r & \omega_s & 0 \end{pmatrix}$$

is the contribution to the precession vector due to closed orbit distortions and is assumed to be small compared with  $\vec{\Omega}$ .

Denoting the 3x3 orthogonal rotation transfer matrix solving by  $M_0(s + L, s)$ , the corresponding matrix in the presence of distortions is written as:

$$\underline{M}(s + L, s) = \underline{M}_0(s + L, s) + \delta \underline{M}(s + L, s) .$$

with:

$$\frac{d}{ds} \underline{M}_0(s, s_0) = \underline{\Omega} \cdot \underline{M}_0(s, s_0) ;$$

$$\underline{M}_0(s_0, s_0) = \underline{1}$$

and the initial condition :

$$\delta \underline{M}^{(1)}(s_0, s_0) = \underline{0} .$$

The spin tune is extracted from the corresponding one turn eigen problem.

The eigen problem for a perfectly aligned machine of arbitrary geometry takes the form:

$$(3) \quad \overline{M}^0(s_0 + L, s_0) \vec{u}^\mu(s_0) = \alpha^\mu \cdot \vec{u}^\mu(s_0) ;$$

$$(\mu = 1, 2, 3)$$

with

$$(4) \quad \begin{aligned} \alpha_1 &= 1 ; \\ \alpha_2 &= e^{+i \cdot 2\pi Q^{spin}} ; \\ \alpha_3 &= e^{-i \cdot 2\pi Q^{spin}} \end{aligned}$$

and

$$(5) \quad \vec{u}_1(s_0) = \vec{u}^0(s_0) ;$$

$$(6) \quad \vec{u}_2(s_0) = \frac{\sqrt{2}}{1} [m^0(s_0) + i \cdot l^0(s_0)] ;$$

$$(7) \quad \vec{u}_3(s_0) = \frac{\sqrt{2}}{1} [m^0(s_0) - i \cdot l^0(s_0)] ;$$

The  $(\vec{u}_0, m_0, \vec{l}_0)$  are real vectors and the spin tune is the real number  $Q^{spin}$ .

We will develop the perturbation theory around  $\overline{M}^0, \vec{u}_1, \vec{u}_2$  and  $\vec{u}_3$ .

Further properties:

$$\vec{n}_0(s) = \underline{M}_0(s, s_0) \vec{n}_0(s_0); \tag{8}$$

$$\vec{m}_0(s) = \underline{M}_0(s, s_0) \vec{m}_0(s_0); \tag{9}$$

$$\vec{l}_0(s) = \underline{M}_0(s, s_0) \vec{l}_0(s_0) \tag{10}$$

Obviously the orthonormality relations remain unchanged:

$$\vec{n}_0(s) = \vec{m}_0(s) \times \vec{l}_0(s) \tag{11}$$

$$\vec{m}_0(s) \perp \vec{l}_0(s); \tag{12}$$

$$|\vec{n}_0(s)| = |\vec{m}_0(s)| = |\vec{l}_0(s)| = 1. \tag{13}$$

and the eigenvectors  $\vec{v}_\mu(s)$

$$\vec{v}_\mu(s) = \underline{M}_0(s, s_0) \vec{v}_\mu(s_0)$$

obey the orthonormality relations:

$$\vec{v}_\mu^+(s) \cdot \vec{v}_\nu(s) = \delta_{\mu\nu}. \tag{14}$$

In a perfectly aligned planar machine  $\vec{n}_0$  is vertical and  $\vec{m}_0, \vec{l}_0$  are horizontal.

**The perturbed part of the revolution matrix:**

We have by definition:

$$\frac{d}{ds} [\underline{M}_0(s, s_0) + \delta \underline{M}(s, s_0)] = [\underline{\Omega} + \underline{\omega}] \cdot [\underline{M}_0(s, s_0) + \delta \underline{M}(s, s_0)] ; \tag{15}$$

$$\underline{M}_0(s_0, s_0) + \delta \underline{M}(s_0, s_0) = \underline{1} . \tag{15}$$

Furthermore we write :

$$\delta \underline{M} = \delta \underline{M}^{(1)} + \delta \underline{M}^{(2)} + \delta \underline{M}^{(3)} + \dots , \tag{16}$$

where  $\delta \underline{M}^{(\nu)}$  denotes the  $\nu^{th}$  order in  $\underline{\omega}$  of  $\delta \underline{M}$ .

$$\delta \underline{M}^{(1)}(s + L, s) = \underline{M}_0(s + L, s) \cdot \int_s^{s+L} d\tilde{s} \cdot \underline{M}_0^{-1}(\tilde{s}, s) \cdot \underline{\omega}(\tilde{s}) \cdot \underline{M}_0(\tilde{s}, s) . \tag{17}$$

$$\delta \underline{M}^{(2)}(s + L, s) = \underline{M}_0(s + L, s) \cdot \int_s^{s+L} d\tilde{s} \cdot \underline{M}_0^{-1}(\tilde{s}, s) \cdot \underline{\omega}(\tilde{s}) \cdot \delta \underline{M}^{(1)}(\tilde{s}, s) \tag{18}$$

### Perturbation theory for the spin tune shift:

The sum of the eigenvalues of a diagonalisable matrix is given by its trace:

$$\text{Sp} [\underline{M}(s_0 + L, s_0)] = \alpha_1 + \alpha_2 + \alpha_3 \quad (19)$$

So we get:

$$\text{Sp} [\delta \underline{M}(s_0 + L, s_0)] = \delta\alpha_1 + \delta\alpha_2 + \delta\alpha_3 \quad (20)$$

with

$$\delta\alpha_1 = 0; \quad (21)$$

$$\begin{aligned} \delta\alpha_2 &= e^{+i \cdot 2\pi [Q_{spin} + \delta Q_{spin}] - i \cdot 2\pi Q_{spin}} \\ &= \alpha_2 \cdot [e^{i \cdot 2\pi \delta Q_{spin}} - 1]; \end{aligned} \quad (22)$$

$$\begin{aligned} \delta\alpha_3 &= e^{-i \cdot 2\pi [Q_{spin} + \delta Q_{spin}] - i \cdot 2\pi Q_{spin}} \\ &= \delta\alpha_2^*. \end{aligned} \quad (23)$$

In the spirit of the series expansion (?) we write:

$$\delta Q_{spin} = \delta Q_{spin}^{(1)} + \delta Q_{spin}^{(2)} + \dots \quad (24)$$

Finally after some manipulation:

$$\delta Q_{spin}^{(1)} = \frac{1}{2\pi i \cdot (\alpha_2 - \alpha_3)} \cdot Sp [\delta \underline{M}^{(1)}(s_0 + L, s_0)] ; \quad (25)$$

$$\delta Q_{spin}^{(2)} = \frac{1}{2\pi i \cdot (\alpha_2 - \alpha_3)} \cdot \left\{ Sp [\delta \underline{M}^{(2)}(s_0 + L, s_0)] + 2\lambda^2 \cdot (\delta Q_{spin}^{(1)})^2 \cdot (\alpha_2 + \alpha_3) \right\} . \quad (25)$$

Now use the orthogonality (completeness) relations:

$$\vec{v}_\mu^+(s) \cdot \vec{v}_\nu(s) = \delta_{\mu\nu} . \quad (26)$$

Then the trace of  $Sp [\delta \underline{M}^{(n)}]$  is:

$$\begin{aligned} Sp [\delta \underline{M}^{(n)}] &= Sp \left\{ (\vec{v}_1, \vec{v}_2, \vec{v}_3) \cdot \begin{pmatrix} \vec{v}_1^+ \\ \vec{v}_2^+ \\ \vec{v}_3^+ \end{pmatrix} \cdot \delta \underline{M}^{(n)} \right\} \\ &= Sp \left\{ \begin{pmatrix} \vec{v}_1^+ \\ \vec{v}_2^+ \\ \vec{v}_3^+ \end{pmatrix} \cdot \delta \underline{M}^{(n)} \cdot (\vec{v}_1, \vec{v}_2, \vec{v}_3) \right\} \\ &= \sum_{\nu=1}^3 \vec{v}_\nu^+ \cdot \delta \underline{M}^{(n)} \cdot \vec{v}_\nu . \end{aligned} \quad (27)$$

Calculation of  $\delta Q_{spin}^{(1)}$ :

$$\begin{aligned}
 Sp[\delta \underline{M}^{(1)}] &= \sum_{\nu=1}^3 \alpha_{\nu} \cdot \vec{v}_{\nu}^{+}(s_0) \cdot \underline{M}_0^{-1}(s_0 + L, s_0) \cdot \delta \underline{M}^{(1)}(s_0 + L, s_0) \cdot \vec{v}_{\nu}(s_0) \\
 &= \sum_{\nu=1}^3 \alpha_{\nu} \cdot \vec{v}_{\nu}^{+}(s_0) \cdot \int_{s_0}^{s_0+L} d\bar{s} \cdot \underline{M}_0^{-1}(\bar{s}, s_0) \cdot \underline{\omega}(\bar{s}) \cdot \underline{M}_0(\bar{s}, s_0) \cdot \vec{v}_{\nu}(s_0) \\
 &= \sum_{\nu=1}^3 \alpha_{\nu} \cdot \int_{s_0}^{s_0+L} d\bar{s} \cdot \vec{v}_{\nu}^{+}(\bar{s}) \cdot \underline{\omega}(\bar{s}) \cdot \vec{v}_{\nu}(\bar{s}) \\
 &= \sum_{\nu=1}^3 \alpha_{\nu} \cdot \int_{s_0}^{s_0+L} d\bar{s} \cdot \vec{v}_{\nu}^{+}(\bar{s}) \cdot [\vec{\omega}(\bar{s}) \times \vec{v}_{\nu}(\bar{s})] \\
 &= \int_{s_0}^{s_0+L} d\bar{s} \cdot \vec{\omega}^T(\bar{s}) \cdot \{ \alpha_2 \cdot [\vec{v}_2(\bar{s}) \times \vec{v}_2^*(\bar{s})] + \alpha_3 \cdot [\vec{v}_3(\bar{s}) \times \vec{v}_3^*(\bar{s})] \} \\
 &= \frac{1}{2} \cdot \int_{s_0}^{s_0+L} d\bar{s} \cdot \vec{\omega}^T(\bar{s}) \cdot \left\{ \alpha_2 \cdot [\vec{m}_0(\bar{s}) + i \cdot \vec{l}_0(\bar{s})] \times [\vec{m}_0(\bar{s}) - i \cdot \vec{l}_0(\bar{s})] \right. \\
 &\quad \left. + \alpha_3 \cdot [\vec{m}_0(\bar{s}) - i \cdot \vec{l}_0(\bar{s})] \times [\vec{m}_0(\bar{s}) + i \cdot \vec{l}_0(\bar{s})] \right\} \\
 &= -i \cdot (\alpha_2 - \alpha_3) \cdot \int_{s_0}^{s_0+L} d\bar{s} \cdot \vec{\omega}^T(\bar{s}) \cdot \vec{n}_0(\bar{s})
 \end{aligned} \tag{28}$$

leading to:

$$\delta Q_{spin}^{(1)} = -\frac{1}{2\pi} \cdot \int_{s_0}^{s_0+L} d\bar{s} \cdot \vec{\omega}^T(\bar{s}) \cdot \vec{n}_0(\bar{s}). \tag{29}$$

This expression agrees with that given by K. Yokoya.  
Similarity with quantum mechanics.

If  $\underline{\omega} \perp \hat{n}$  : no first order shift  
- eg. VCO. distn in flat ring.

Calculation of  $\delta Q_{spin}^{(2)}$  :

$$Sp [\delta \underline{M}^{(2)}] = \sum_{\mu=1}^3 \alpha_{\mu} \cdot \vec{v}_{\mu}^{+}(s_0) \cdot \underline{M}_0^{-1}(s_0 + L, s_0) \cdot \delta \underline{M}^{(2)}(s_0 + L, s_0) \cdot \vec{v}_{\mu}(s_0) \quad (30)$$

Using the completeness relation again twice over:

$$\begin{aligned} Sp [\delta \underline{M}^{(2)}] &= \sum_{\mu=1}^3 \sum_{\nu=1}^3 \alpha_{\mu} \cdot \int_{s_0}^{s_0+L} ds' \cdot \vec{v}_{\mu}^{+}(s') \cdot \underline{\omega}(s') \cdot \vec{v}_{\nu}(s') \\ &\quad \times \int_{s_0}^{s'} ds'' \cdot \vec{v}_{\nu}^{+}(s'') \cdot \underline{M}_0(s', s'') \cdot \underline{\omega}(s'') \cdot \vec{v}_{\mu}(s'') \\ &= - \sum_{\mu=1}^3 \sum_{\nu=1}^3 \alpha_{\mu} \cdot \int_{s_0}^{s_0+L} ds' \cdot \vec{v}_{\mu}^{+}(s') \cdot [\vec{\omega}(s') \times \vec{v}_{\nu}(s')] \\ &\quad \times \int_{s_0}^{s'} ds'' \cdot \{ \vec{v}_{\mu}^{+}(s'') \cdot [\vec{\omega}(s'') \times \vec{v}_{\nu}(s'')] \}^{+} \\ &= - \sum_{\mu=1}^3 \sum_{\nu=1}^3 \alpha_{\mu} \cdot \int_{s_0}^{s_0+L} ds' \cdot \vec{\omega}^T(s') \cdot [\vec{v}_{\nu}(s') \times \vec{v}_{\mu}^{*}(s')] \\ &\quad \times \int_{s_0}^{s'} ds'' \cdot \{ \vec{\omega}^T(s'') \cdot [\vec{v}_{\nu}(s'') \times \vec{v}_{\mu}^{*}(s'')] \}^{+} \quad (31) \end{aligned}$$

Using the complete set of relations of the form:

$$\begin{aligned} \vec{v}_1 \times \vec{v}_1^* &= \vec{n}_0 \times \vec{m}_0 \\ &= 0; \end{aligned} \tag{32}$$

$$\begin{aligned} \vec{v}_1 \times \vec{v}_2^* &= \vec{n}_0 \times \frac{1}{\sqrt{2}} [\vec{m}_0 - i \cdot \vec{l}_0] \\ &= \frac{1}{\sqrt{2}} [\vec{l}_0 + i \cdot \vec{m}_0] \\ &= +i \cdot \frac{1}{\sqrt{2}} [\vec{m}_0 - i \cdot \vec{l}_0] \\ &= +i \cdot \vec{v}_3; \end{aligned} \tag{33}$$

etc,  
etc,  
etc,

and a lot of tedious manipulation

the final answer comes out as:

$$\delta Q_{spin}^{(2)} = \frac{1}{4} \cdot \text{Im} \left\{ \frac{1}{e^{-2\pi i Q_{spin}} - 1} \cdot \int_{s_0}^{s_0+L} ds' \cdot [\vec{\omega}^T(s') \cdot \vec{v}_2(s')]^* \right. \\ \left. \times \int_{s_0}^{s'} ds'' [\vec{\omega}^T(s'') \cdot \vec{v}_2(s'')] \right\} . \quad (34)$$

This is similar to the form given by K. Yokoya

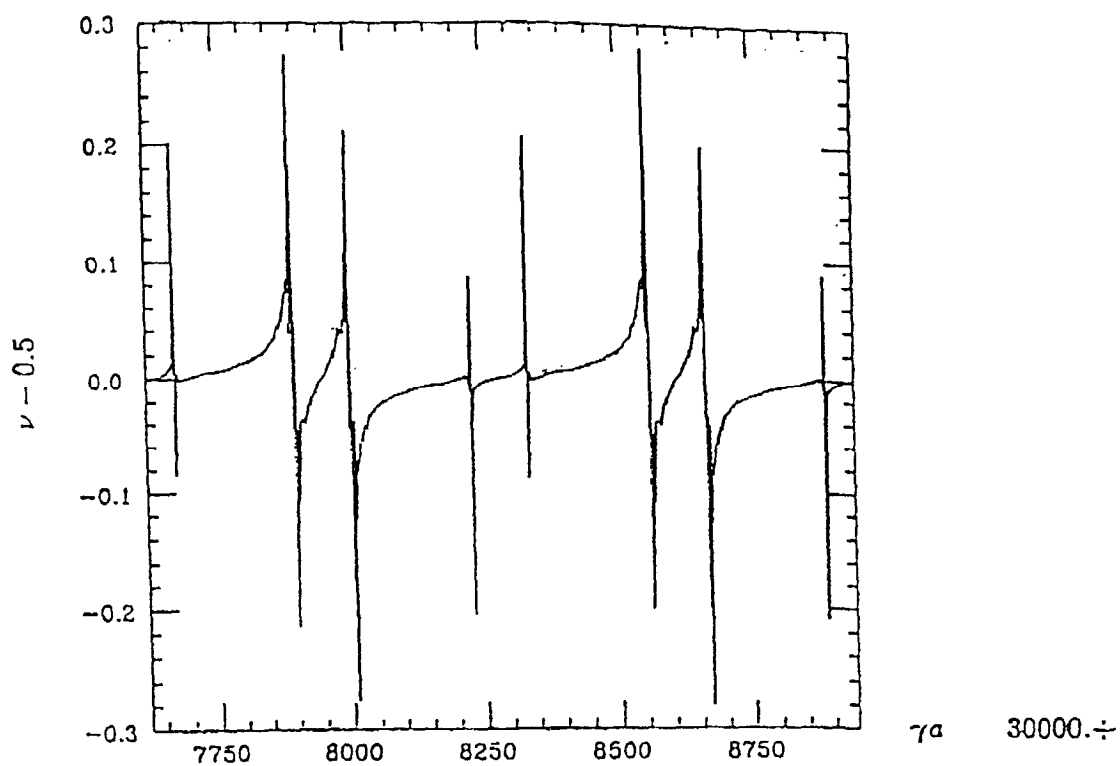


Fig.2a. Spin tune shift due to imperfection without correction. Quadrupole misalignment  $\pm 10\mu\text{m}$  (uniform).

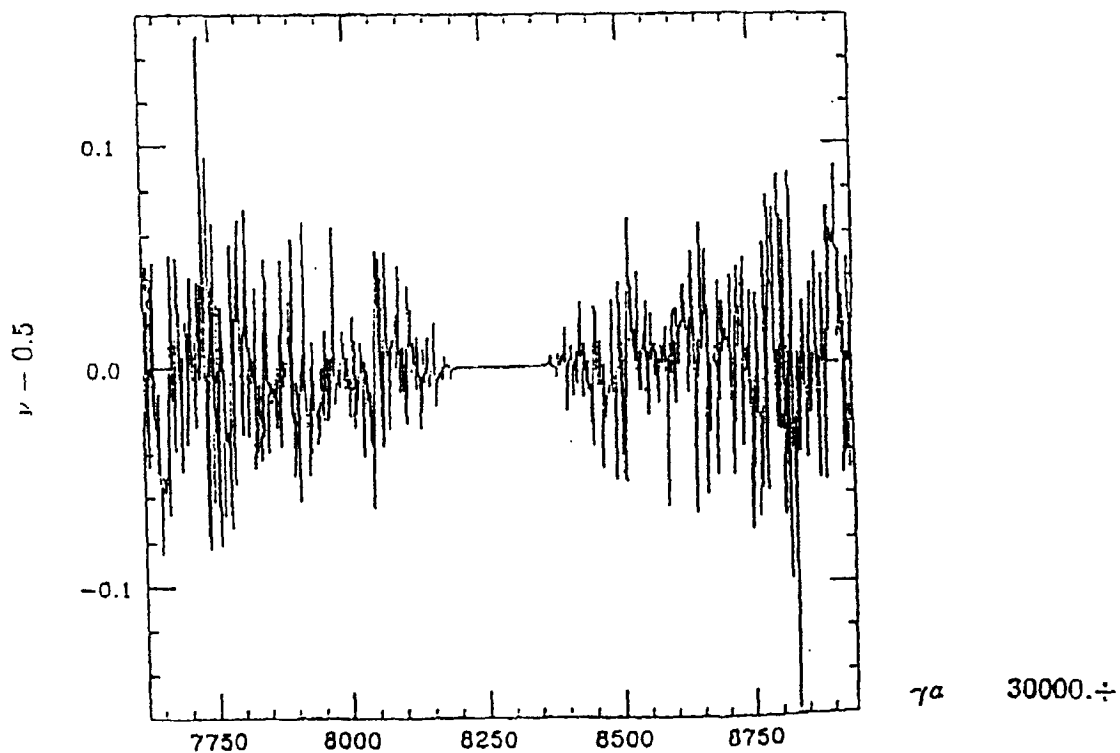


Fig.2b. Spin tune shift due to imperfection with correction. Quadrupole misalignment  $\pm 100\mu\text{m}$  (uniform) and residual  $y_{\text{cod}} = 25\mu\text{m}$ .

D. P. Barber

DESY

Notkestrasse 85. D-22603 Hamburg, Germany

Longitudinal Polarization at HERA: Rotators + Spin  
Matching

Brookhaven Sept '94.

Longitudinal Polarization  
at

HERA:

Rotators + Spin Matching

D.P. Barber - DESY

for the HERA Polarization Group.

## Summary

1. Electrons in storage rings can become spin polarized due to sync. rad'n (Sokolov-Ternov)
2. Sync. rad'n also excites orbit motion  $\rightarrow$  spin diffusion (mainly in quads)  $\rightarrow$  depolariz'n.
3. Depolarization can be very strong if the polarization vector is horizontal in parts of the ring - as when rotators are on.
4. Then "spin matching" is essential for making  $G_{2 \times 6}$  small.  $\rightarrow$  lots of independent quad circuits
5. The success at HERA shows that longitudinal polarization can be achieved!

## LONGITUDINAL POLARIZATION

- First time in the history of high energy electron storage rings!



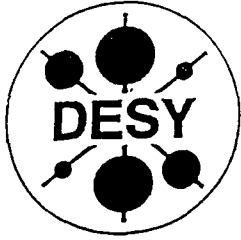
Parameters:

	p	e	
Energy	820	30	GeV
Number of I.P.		3(4)	
Bending field	4.53	0.185	Tesla
Bunches	220	220	
Av. Current	163	58	mA
Luminosity		$1.5 \times 10^{31}$	$\text{cm}^{-2} \text{s}^{-1}$

Injection:

e:  $e \text{ linac} \xrightarrow{200 \text{ MeV}} \text{DESY II} \xrightarrow{9 \text{ GeV}} \text{PETRA} \xrightarrow{14 \text{ GeV}} \text{HERA}$

p:  $\text{H}^+ \xrightarrow{750 \text{ KeV}} \text{RFQ} \xrightarrow{50 \text{ MeV}} \text{LINAC} \xrightarrow{\rightarrow e^+} \text{DESY III} \xrightarrow{7.5 \text{ GeV}} \text{PETRA} \xrightarrow{40 \text{ GeV}} \text{HERA}$



# DESY TELEGRAMM

vom 5. Mai 1994

## **HERA ist einmalig**

**Zum ersten Mal longitudinal polarisierter Elektronenstrahl**

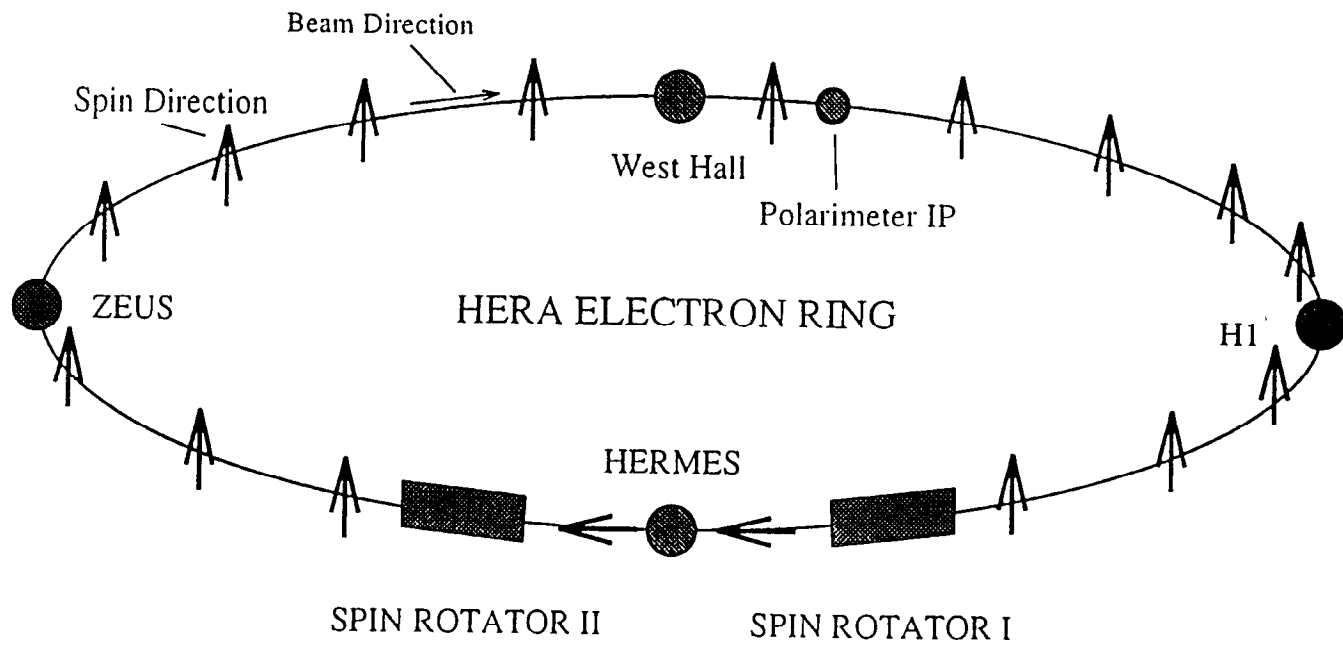
Gestern nachmittag wurde im Elektronenring von HERA zum ersten Mal ein longitudinal polarisierter Teilchenstrahl erzeugt. Das ist überhaupt weltweit das erste Mal, daß ein longitudinal polarisierter Elektronenstrahl in einem Speicherring erzeugt wurde. Um dies zu erreichen, wurde bei DESY unter der Federführung des - leider schon verstorbenen - Maschinenphysikers Klaus Steffen, ein Spinrotator entwickelt, der aus einer Vielzahl von Ablenkmagneten besteht. In ihnen wird die Richtung des "Spins" der Elektronen gedreht. In der vergangenen Winterunterbrechung wurden die Magnete im Bereich Ost des HERA-Tunnels eingebaut und jetzt zum ersten Mal mit einem Elektronenstrahl betrieben. Dabei werden die Spins bei jedem Umlauf, also 47.300 Mal in der Sekunde, aus der senkrechten in die parallele oder antiparallele Flugrichtung gekippt und anschließend wieder zurückgedreht.

Lange Zeit wurde die technische Durchführbarkeit dieses Projekts unter den Experten kontrovers diskutiert, da die Spins auf kleine Störungen in den Speicherringen sehr empfindlich reagieren und die theoretische Be-

rechnung ihres Verhaltens sehr schwierig ist. Um so erfreulicher ist es, daß beim ersten Anschalten der Rotatormagnete in HERA sofort eine hohe longitudinale Polarisation von über 55% erreicht werden konnte.

Unter dem Spin eines Teilchens versteht man die Achse seiner Eigendrehung. Die Spins der in HERA gespeicherten Elektronen richten sich nach einiger Zeit zu etwa 60% von selbst antiparallel zum Feld der Speicherringmagnete aus. Der Teilchenstrahl ist dann "transversal polarisiert". Er wird als "longitudinal polarisiert" bezeichnet, wenn die Spins in der Flugrichtung der Elektronen oder entgegengesetzt zu ihr ausgerichtet sind. Der longitudinal polarisierte Elektronenstrahl wird für das HERMES-Experiment benötigt, mit dem das "Spin-Verhalten" von Protonen und Neutronen untersucht werden soll und das 1995 in Halle Ost beginnen soll. Später sollen auch für die beiden Kollisionsexperimente H1 und ZEUS Spinrotatoren in HERA eingebaut werden, um weitere wichtige Fragestellungen der Teilchenphysik untersuchen zu können.

Herausgegeben von DESY/PR, Aushang bis 16.5.1994



Spin rotators :

Natural  $\text{pol}^n$  is vertical

Need  $\bar{P} \parallel \bar{B}$  in most of ring: Drive  $\text{pol}^n$  mechanism.

But need  $\bar{P}$  longitudinal at I.P.

$\Rightarrow$  Rotate  $\bar{P}$  ( $\hat{n}_0$ )

Vertical  $\rightarrow$  longitudinal : just before I.P.

L  $\rightarrow$  V : just after I.P.

$\Rightarrow$  Recall:  $\Delta\theta_s = a\gamma\Delta\theta_{\text{orbit}}$

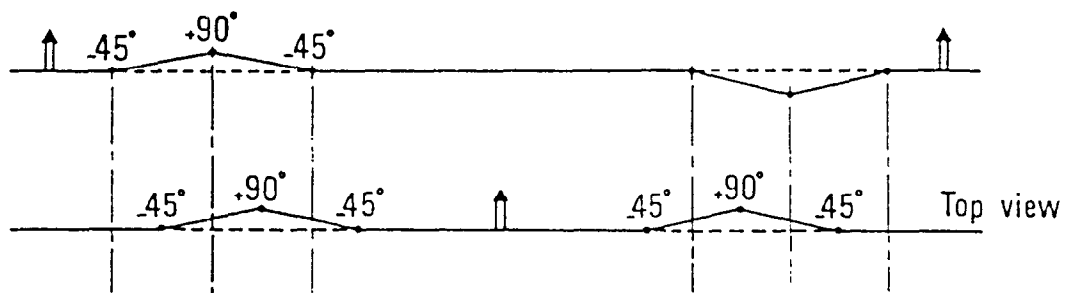
Use interleaved string of vertical and horizontal bends.

Finite rotations do not commute.

$\Rightarrow$  Mini-rotator : Buon, Steffen HERA

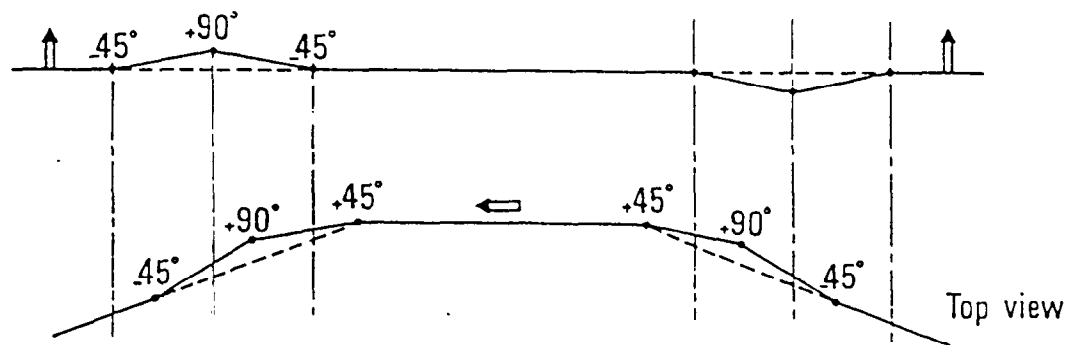
Siberian snake of 1<sup>st</sup> kind

Side view



HERA mini rotator (principle)

Side view

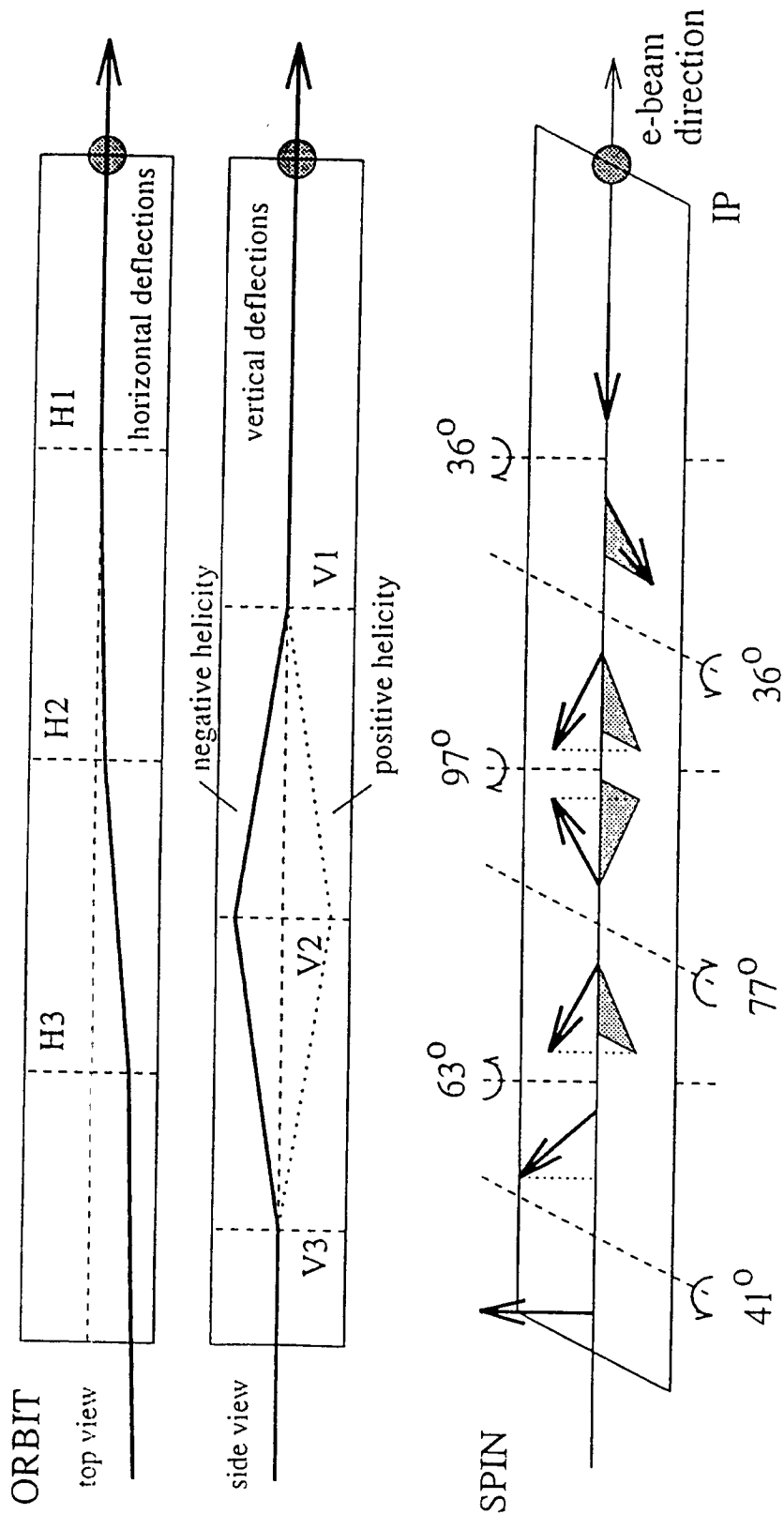


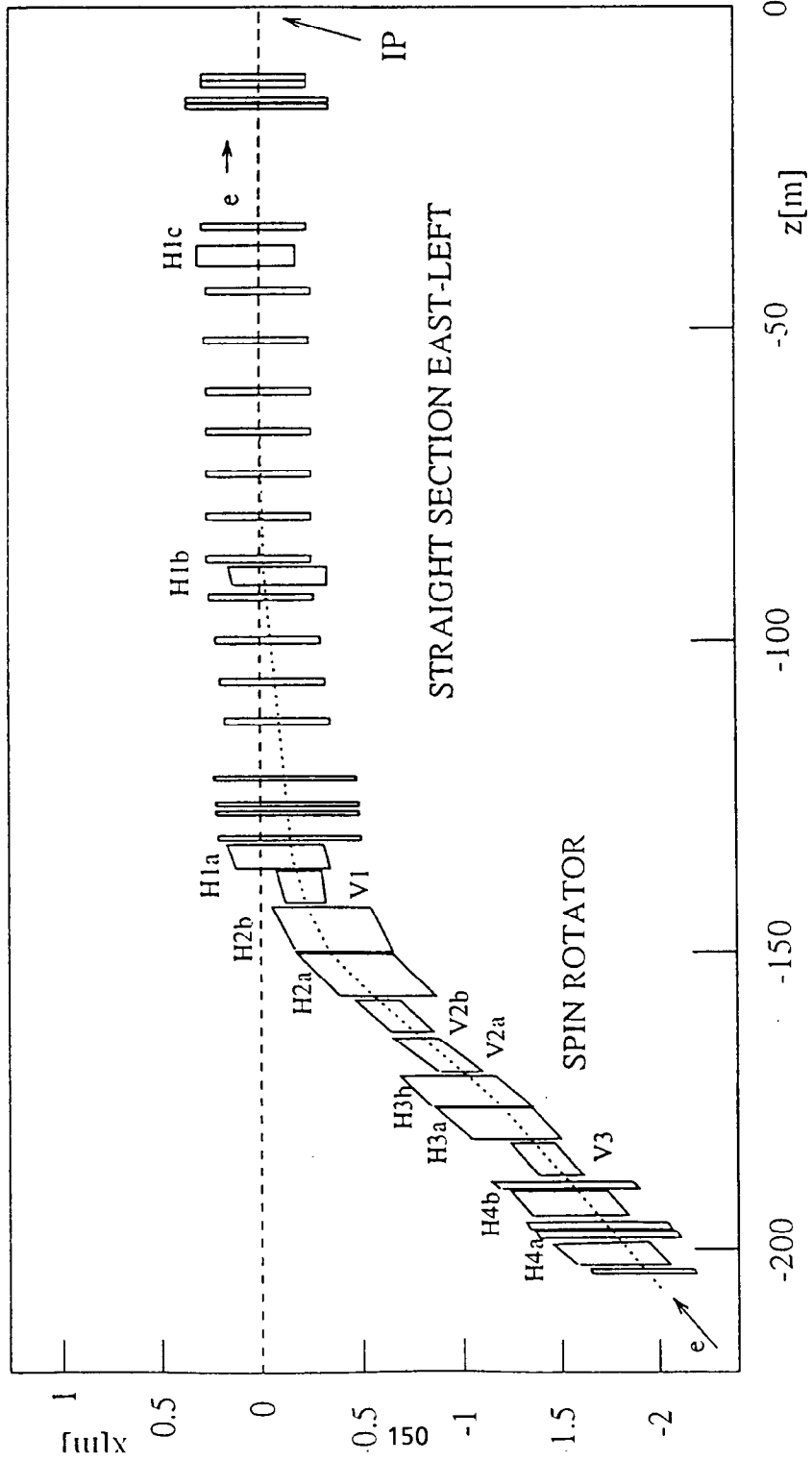
Chief features: Buon+Steffen.

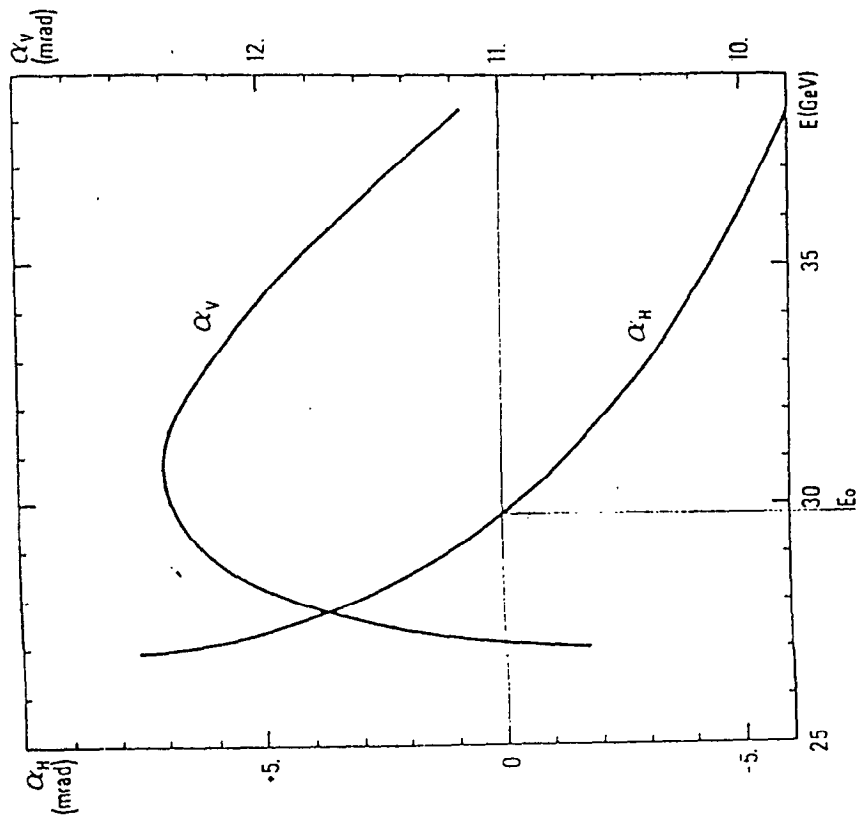
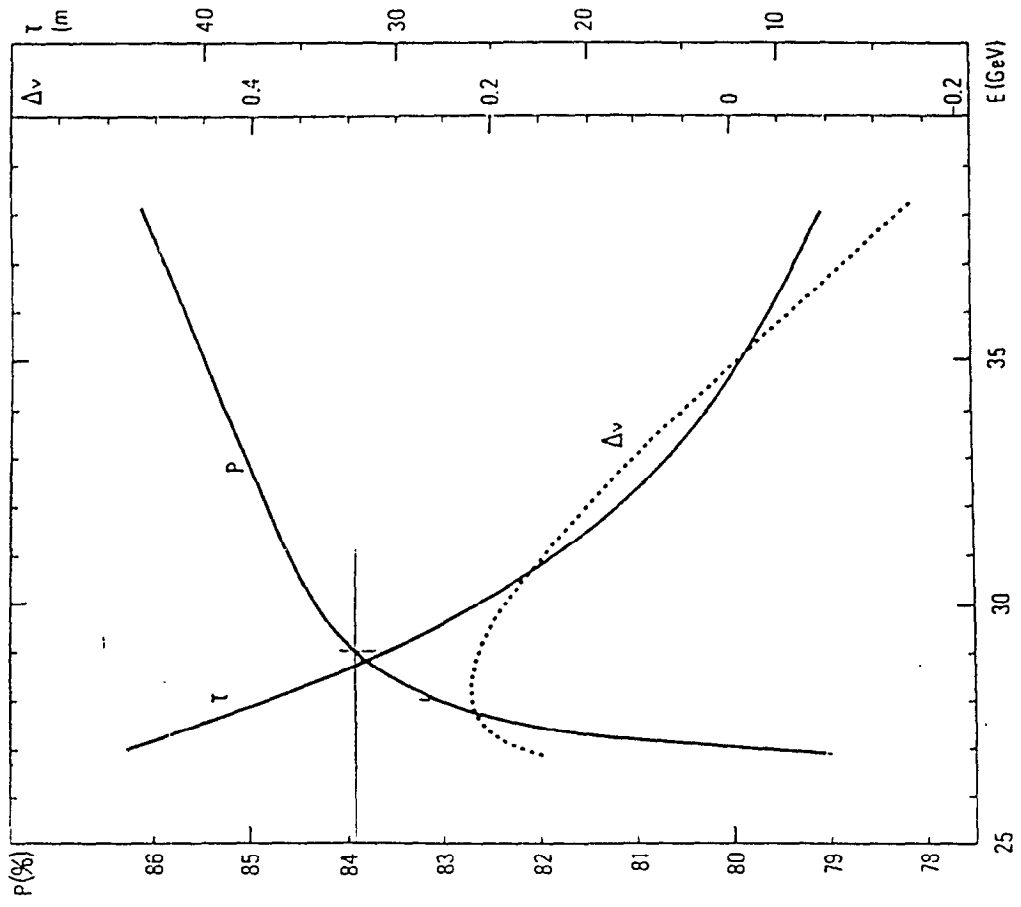
- 1) Length limited to 56m :  $\Delta P \sim L^{-2}$ , no quads. needed.
- 2) Variable energy: 27-35 GeV: adjust orbit deflections. ( $\alpha\delta$ )
- 3) Total vertical bend is zero, slope at IP. = 0.
- 4) Symmetric in hor. plane, antisym. in vert. plane
- 5)  $P_{35} > P_{27}$ ,  $P_{s/T}$  maximised
- 6) +/- helicity: reverse vertical bends.
- 7) Ends fixed: middle section must be movable.  
field adjustment: small corrections.  
Vert + hor shifts small
- 8) Total hor. bend  $\neq 0$ , include in arc, save space
- 9)  $\Delta$ (spin tune): small

2 rotator pairs:

$$P_{s/T} \sim 89\% \text{ at } 35 \text{ GeV}$$







# HERA POLARIZATION

Date 20.11.93

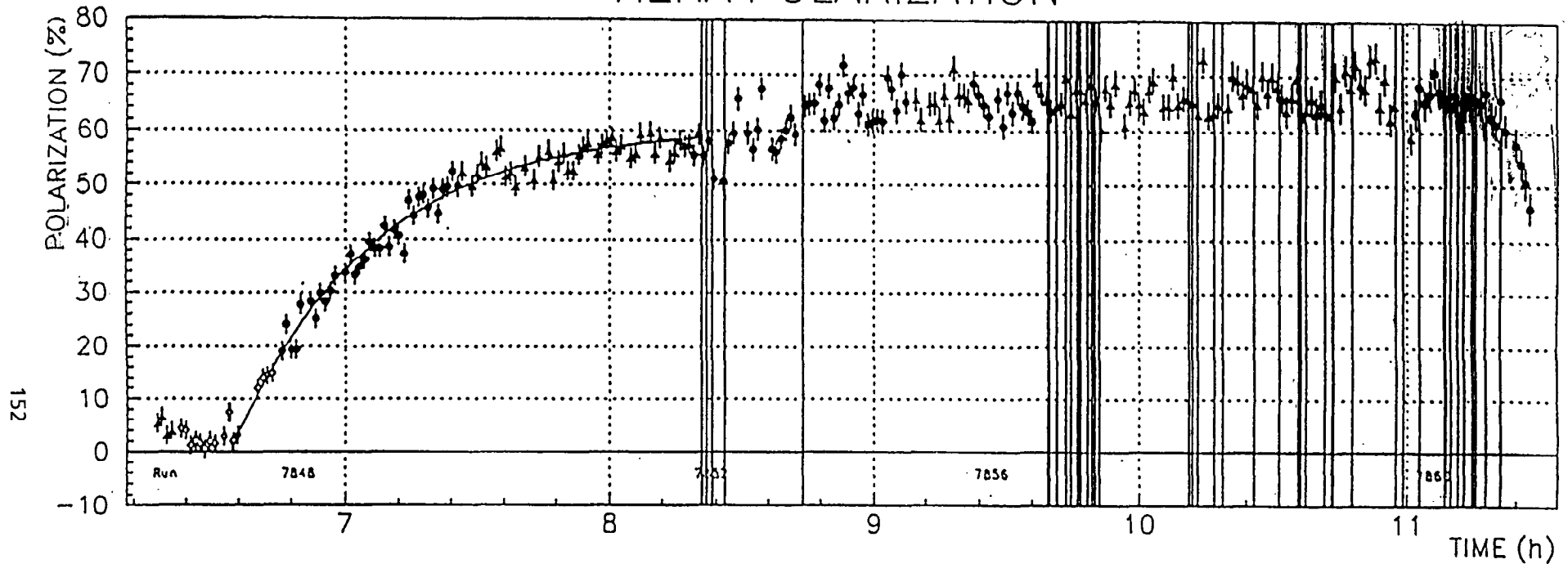
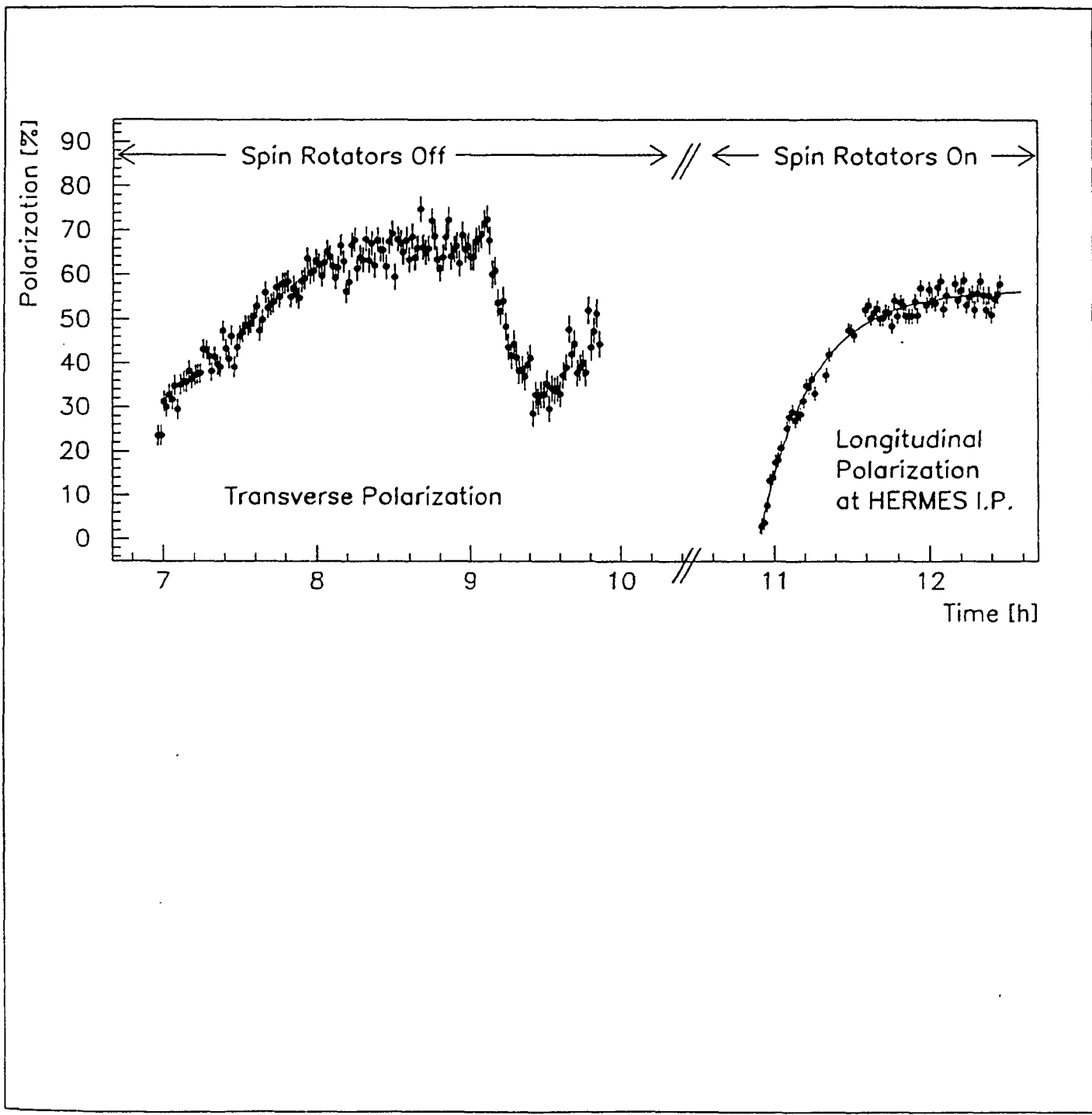


Figure 6: The rise time of  $\tau = 30.8 \pm 1$  min translates to an asymptotic value of  $P = 65 \pm 2\%$  which agrees with the measured value of  $P = 60.5 \pm 0.6\%$ . After changing the tunes at 8:26 h polarization increased to maximum values close to  $P = 70\%$ .



# HERA POLARIZATION (statistical errors only)

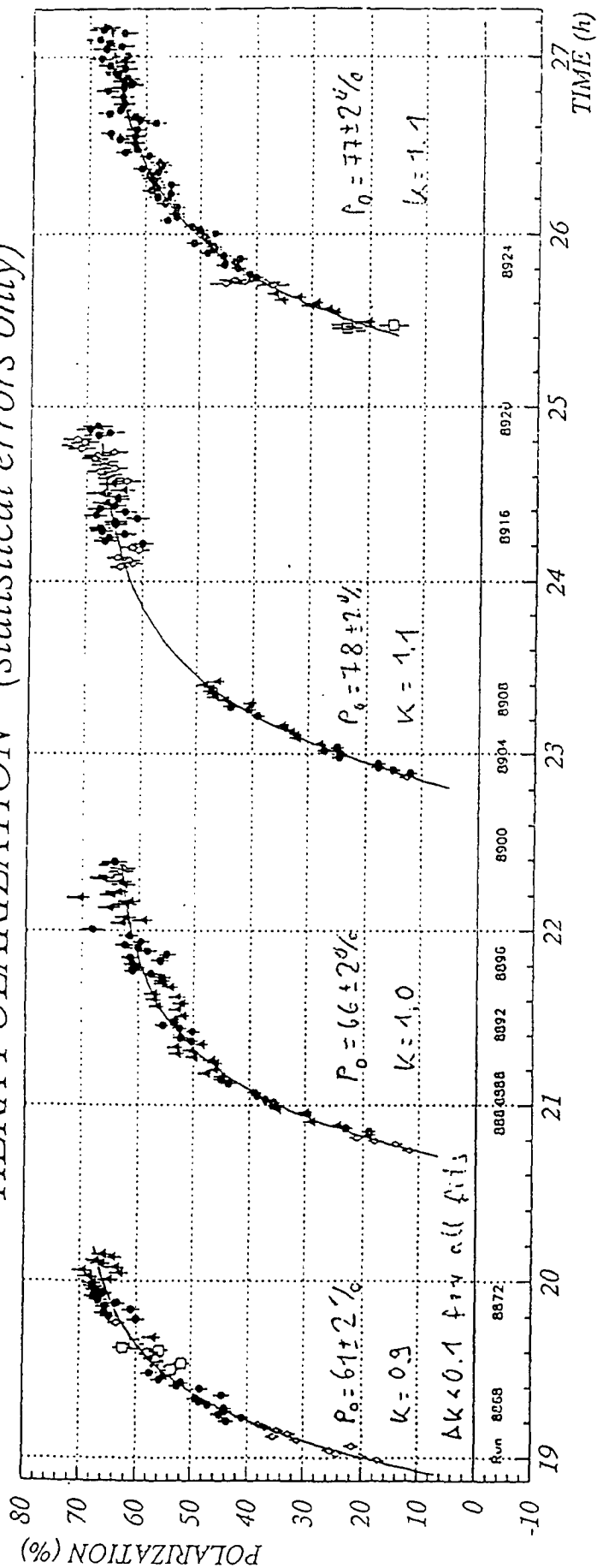
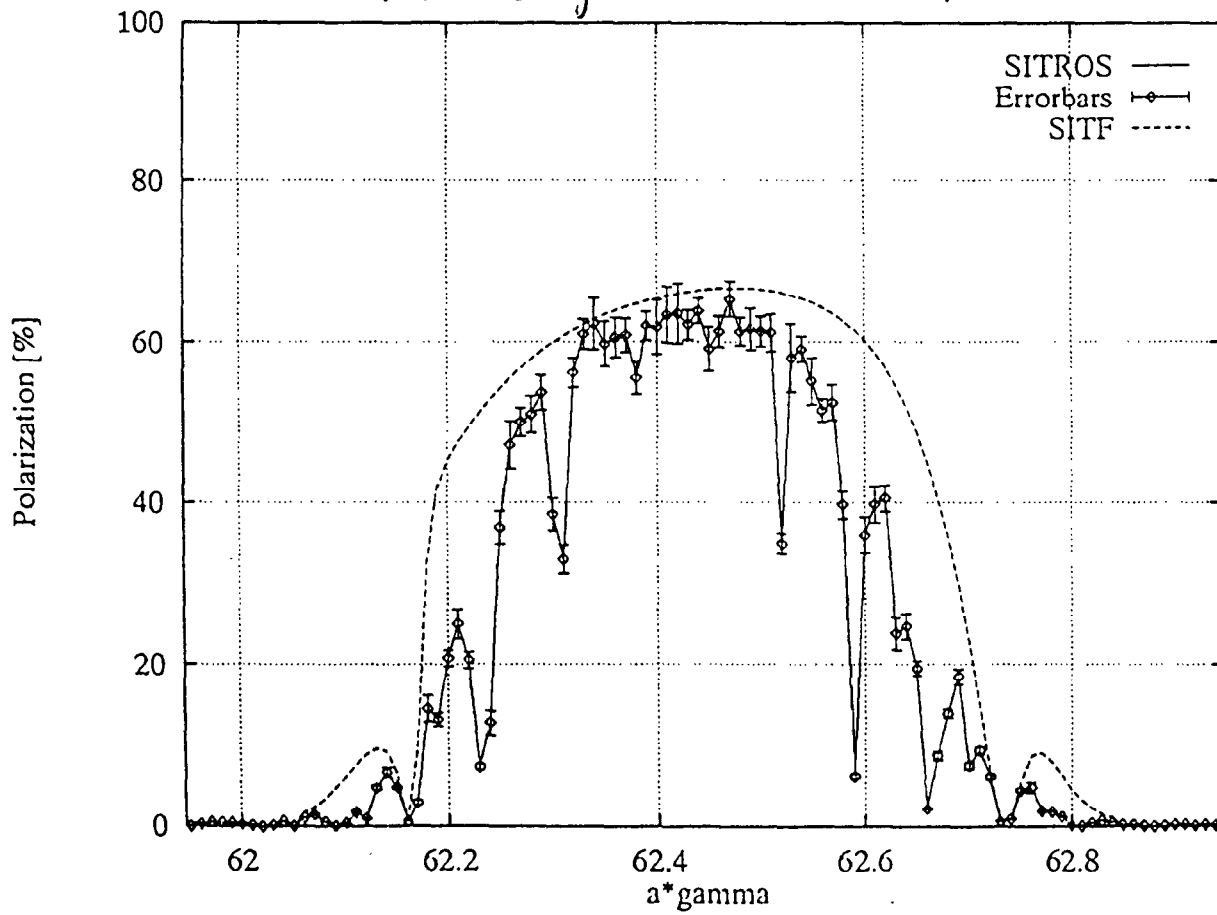


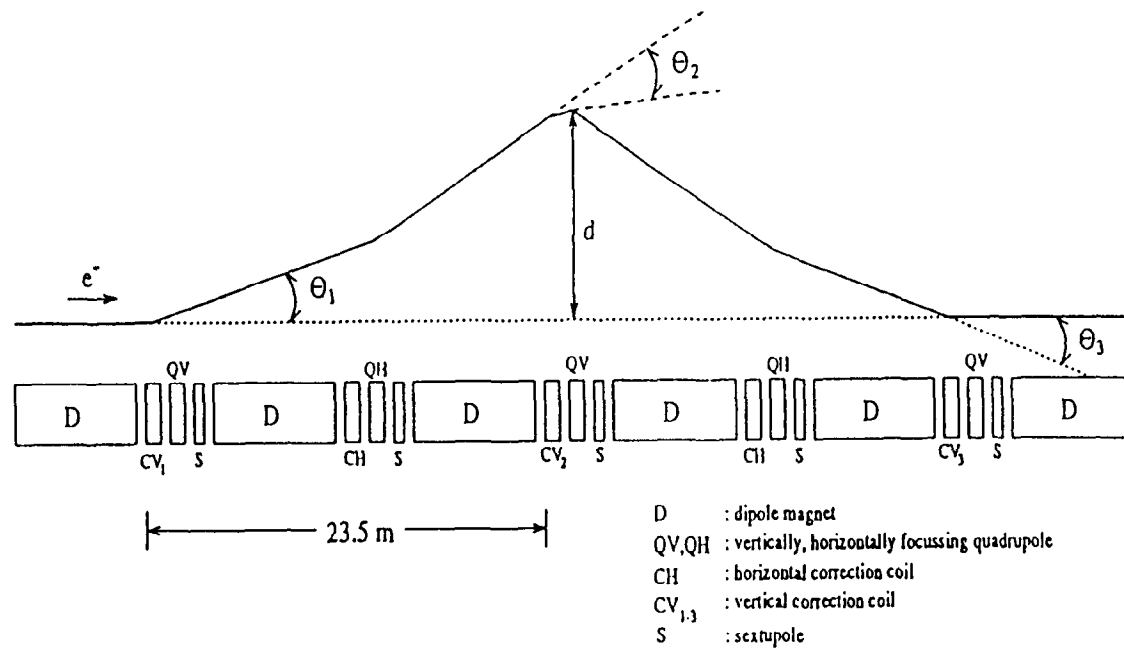
Fig 3: Longitudinal Polarization during HERA bake-out.

Fit  $P_{\text{meas}} = \frac{P_0}{k} (1 - e^{-\frac{t-t_0}{\tau}})$  with  $\tau = 2.47 \frac{\text{h}}{\text{min}}$  fixed  $k = \text{Calibration constant of the polarization}$

The fits do not account for changes of Hevac conditions during the po-c, rise!

M. Böge: SITROS.





1. The periodic magnet lattice in the HERA arcs. A single "FODO cell" contains two dipole magnets, two quadrupoles, and two correction coils. The length of one cell is 23.5 m, and the phase advance of the betatron oscillations is  $\pi$ . Also shown is a schematic drawing of a vertical closed orbit bump utilizing three consecutive vertical correction coils. The first dipole magnet produces a kick  $\theta_1$  and the subsequent coils produce kicks  $\theta_2 \approx -\theta_1$  and  $\theta_3 = \theta_1$ ; the kicks produced by the quadrupoles are also indicated. The maximum orbit deviation is denoted by  $d$ . The total length of a bump is 47.0 m.

SPIN MATCHING  
+  
POLARISATION CALCULATIONS  
for  
HERA

D. P. Barber  
DESY

Generalities :

Derbenev, Kondratenko 1973 :

$$P_{eq} = 92.4\% \frac{\langle |\rho|^{-3} \hat{B} \cdot (\hat{n} - \underline{d}) \rangle}{\langle |\rho|^{-3} \left( 1 - \frac{2}{9} (\hat{n} \cdot \hat{v})^2 + \frac{11}{18} \underline{d}^2 \right) \rangle}$$

$\hat{n}(I, \Psi)$  : solution to BMT eqn on trajectory

$$\underline{d} = \gamma \partial \hat{n} / \partial \gamma$$

$\langle \rangle$  - ring + ensemble average

: Linear orbit, "spherical" spin motion

For each orbit  $\underline{d}$  can be calculated

$\underline{d}$  is large  $\rightarrow$  P small if resonance:

$$\nu = k \pm n_x Q_x \pm n_z Q_z \pm n_s Q_s$$

↑  
spin tune.

N/C

To design a storage ring with high pol<sup>n</sup> :

Adjust lattice to make  $\langle \frac{d^2}{|p_i|^2} \rangle$  small

Calculation to all orders complicated :

D/K, Yokoya

⇒ Begin with linearised representation of  $\hat{H}$

⇒ Practical formalism for storage ring design

⇒ Perhaps use higher order later: But:

What about non-linear orbit motion? YOKOYA  
-lie Algebra

# Linear formalism: summary!

Periodic solution to B.M.T. equation on periodic orbit:

$$\hat{n}_0(s+L) = \hat{n}_0(s) \quad , \quad \frac{d\hat{n}_0}{ds} = \underline{\Omega}(s) \wedge \hat{n}_0$$

+ orthogonal vectors  $\hat{m}_0, \hat{l}_0$  - also BMT sol<sup>n</sup>.

$$\Rightarrow \quad \hat{n} = \hat{n}_0 + \alpha \hat{m}_0 + \beta \hat{l}_0 \quad \alpha, \beta \ll 1$$

$$\frac{d\hat{n}}{ds} = (\underline{\Omega} + \underline{\omega}) \wedge \hat{n}$$

↖  $\underline{\omega}(s, x, x', \dots)$ : linearised

$$\Rightarrow \quad \frac{d\alpha}{ds} = \underline{\omega} \cdot \hat{l}_0 \quad , \quad \frac{d\beta}{ds} = -\underline{\omega} \cdot \hat{m}_0 \quad (\text{linearised!})$$

Orbit vector:  $(x, x', z, z', \sigma, \frac{\delta E}{E}) = \bar{y}(s)$

||  
?

$$\Rightarrow \begin{bmatrix} x \\ x' \\ z \\ z' \\ \sigma \\ \frac{\delta E}{E} \\ \alpha \\ \beta \end{bmatrix}_s = \begin{bmatrix} M_{6 \times 6}(s, s_0) & O_{6 \times 2} \\ G_{2 \times 6}(s, s_0) & D_{2 \times 2} \end{bmatrix} \begin{bmatrix} x \\ x' \\ z \\ z' \\ \sigma \\ \frac{\delta E}{E} \\ \alpha \\ \beta \end{bmatrix}_{s_0}$$

A. Chao  
(SLIM)

160 'BMT' basis:  $D = \begin{pmatrix} 1 & 0 \\ 0 & 1 \end{pmatrix}$

Matrix approach to spin matching: Minimize  $G_{2 \times 6}$

1. Direct connection to SLIM (SLICK)
2. Necessary for coupled systems (skew quads, solenoid)
3. Evaluation (numerical) of integrals in an optimisation pgm. is too slow (thick lens)  
→ analytic integration → but  $\int$  already contained in  $G_{2 \times 6}$  matrix
4. "Locality": once  $G$  is zero for a section of ring it remains zero no matter what changes are made to the optics outside.
5. Provides a systematic basis for investigation of algebraic properties eg. REDUCE (solenoids)
6. Interpretation usually transparent.  
eg. arbitrary string of quadrupoles + drifts

C 31/01/94 401311630 MEMBER NAME BLPROP (V2.S) M FORTRAN

- Fit arc to middle of rotator east. Fit VERSION 2.

- 1st part: fit to the east rotator at the BG-BF join.

#F1 ;DKL5 TWISS-H=(1. 8.0185 0.000101)
#F2 ;DKL5 TWISS-V=(1. 8.0466 0.000101)
#F3 ;DKL5 TWISS-H=(2. 0.2771 0.000011)
#F4 ;DKL5 TWISS-V=(2. 0.3518 0.000011)
#F5 ;DKL5 TWISS-H=(3. 31.4035 0.001101)
#F6 ;DKL5 TWISS-V=(3. 35.7105 0.001101)
#F7 ;DKL5 TWISS-H=(5. -0.5479 0.000111)
#F8 ;DKL5 TWISS-H=(6. 0.0334 0.000011)

SPINOR (L Hand et al, input)

- 2nd part: fit to the start of the WR periodic section.

#F9 ;DKL8 TWISS-H=(2. 1.7291 0.000011)
#F10 ;DKL8 TWISS-V=(2. -0.6113 0.000011)
#F11 ;DKL8 TWISS-H=(3. 39.9302 0.001101)
#F12 ;DKL8 TWISS-V=(3. 13.5073 0.001101)
#F13 ;DKL8 TWISS-H=(5. -0.8895 0.000111)
#F14 ;DKL8 TWISS-H=(6. 0.0387 0.000011)

- 3rd part: fix the tunes to integers across the West quadrant.

#F15 ;DKL9 TWISS-H=(1. 3.0000 0.000101)
#F16 ;DKL9 TWISS-V=(1. 3.0000 0.000101)

- 4th part: fit the spin matrix elements.

#F17 ;DKL5 TMATRIX=(7. 4. 0.0 0.011011)
#F18 ;DKL5 TMATRIX=(8. 3. 0.0 0.011010)

- 5th part: allow the North area to adjust.

#F19 ;IPN2 TWISS-H=(2. 0.0 0.000100)
#F20 ;IPN2 TWISS-V=(2. 0.0 0.000100)
#F21 ;IPN2 TWISS-H=(3. 2.2 0.010000)
#F22 ;IPN2 TWISS-V=(3. 0.88 0.010000)
#F23 ;IPN2 TWISS-H=(5. 0.0 0.000100)
#F24 ;IPN2 TWISS-H=(6. 0.0 0.000100)

- 6th part: keep the Betas small.

#F25 DKL1;DKL8 MAXBETAV=(70. 0.051011)

- 7th part: test new fits.

#F26 ; SPIN-H=(1. 2. 0. 10.000000)
#F27 ; SPIN-V=(1. 2. 0. 10.000000)
#F28 ; SPIN-E=(1. 1. 0. 10.000000)
-#F26 DKL1;DKL8 HARMGMAT=(2. 0.051011)
-#F27 DKL3;DKL4 MAXBETAV=(50. 0.051011)
-#F30 ;DKL7 TWISS-V=(3. 150.0 0.051110)
-#F30 DKL2;DKL6 MAXBETAV=(70. 0.511010)
-#F29 DKL1;DKL8 RMSBETAH=(50. 0.011011)
-#F30 DKL2;DKL7 RMSBETAH=(50. 0.011010)

FIT \* A B C D E F G H I J K L M N O P Q R S T U V W X Y Z
& a b c d e f g h i j k l m n o p q r s t u v w x y z
& F1+F2+F3+F4+F5+F6+F7+F8+F9+F10+F11+F12+F13+F14+F15+F16+F17+F18
& +F19+F20+F21+F22+F23+F24+F25

- Starting Twiss parameters.

- IP WEST
TWISS 0. 0. 0.0 0.0 10.0060 21.9275 -.0143 0. 0. 0.

- Starting spin basis vectors:

- For vertical n in arc: Using new(Aug 93) input spin basis definition.

- MX LX MZ LZ MS LS
SPINBAS -1.0 0.0 0.0 0.0 0.0 -1.0

- Starting spin integrals.

- HLC HMC HLS HMS VLC VMC VLS VMS EL EM
SPININT 0. 0. 0. 0. 0. 0. 0. 0. 0. 0.

- VARIOUS OPTIONS

:MINIMIZER 1 { (1): NAG gradient minimizer. (2) LNR minimizer.
:TWISSOUTPUT { Print Twiss list.
:SPINOUTPUT 0 { List/dont list(1/0) spin basis at each point.

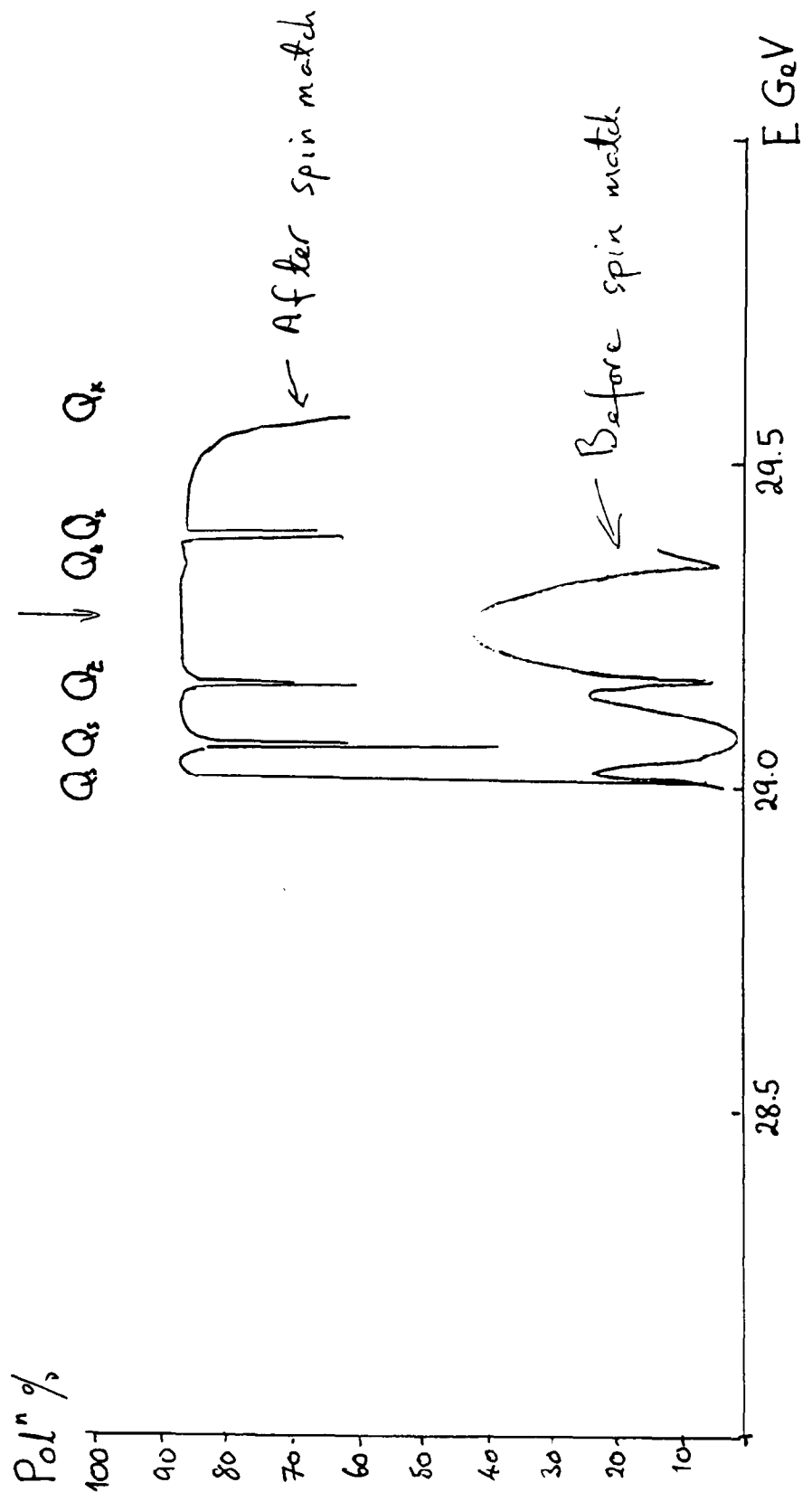
Spin matching  $\iff \hat{n}_{\text{D.K.}}$

1st order COSY T.C.'s for  $\Omega_{3 \times 3}$

$\equiv$   
SLIM  $G_{2 \times 6}$

SLIM: perfect, 2 rotator pairs.

Match



**Yu. Shatunov**

**Budker Institute of Nuclear Physics**

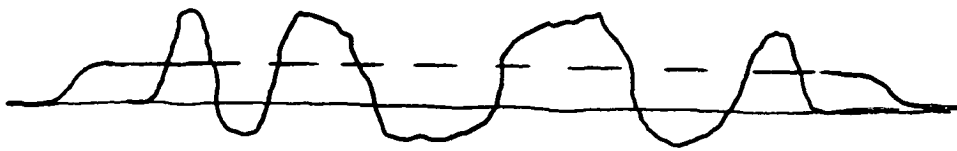
**Novosibirsk, 630090 Russia**

**Motivation for high field**

# Motivations for high field

Yu. Skatunov

1. C.O. excursions
2. no restrictions for insertion
3. free space for { BPM,  
dipole bridge  
quadrupoles

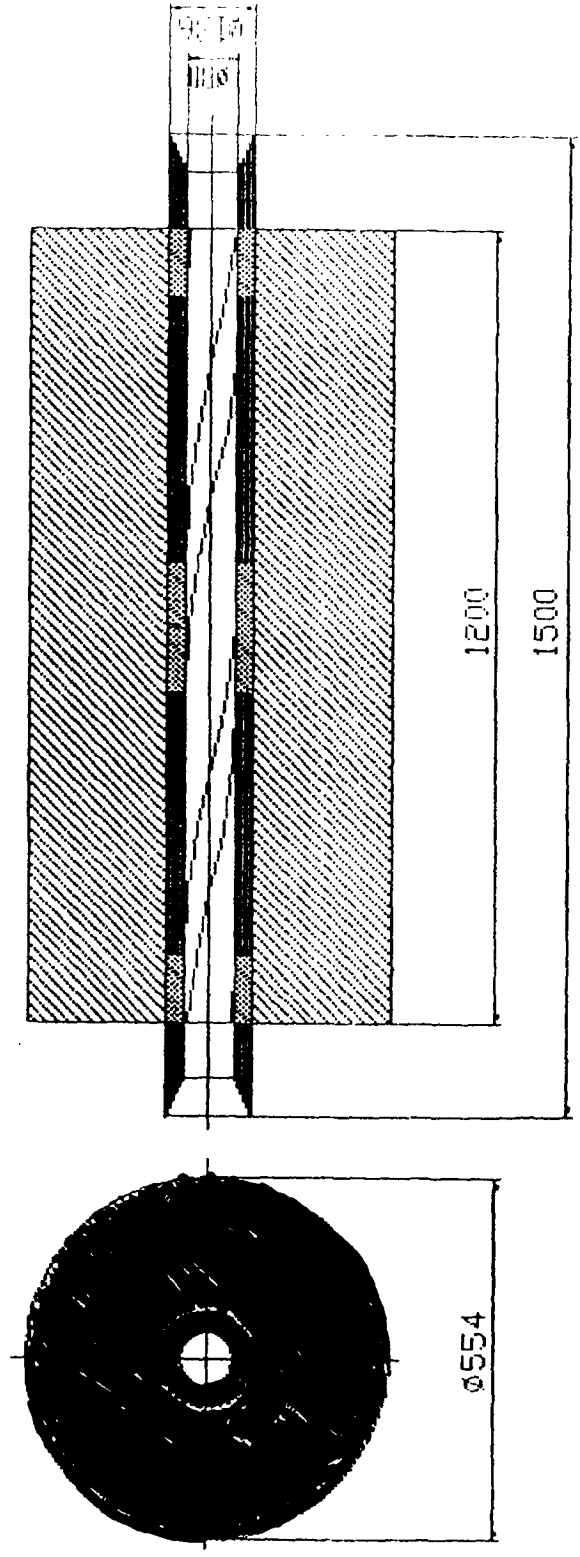


quads ?

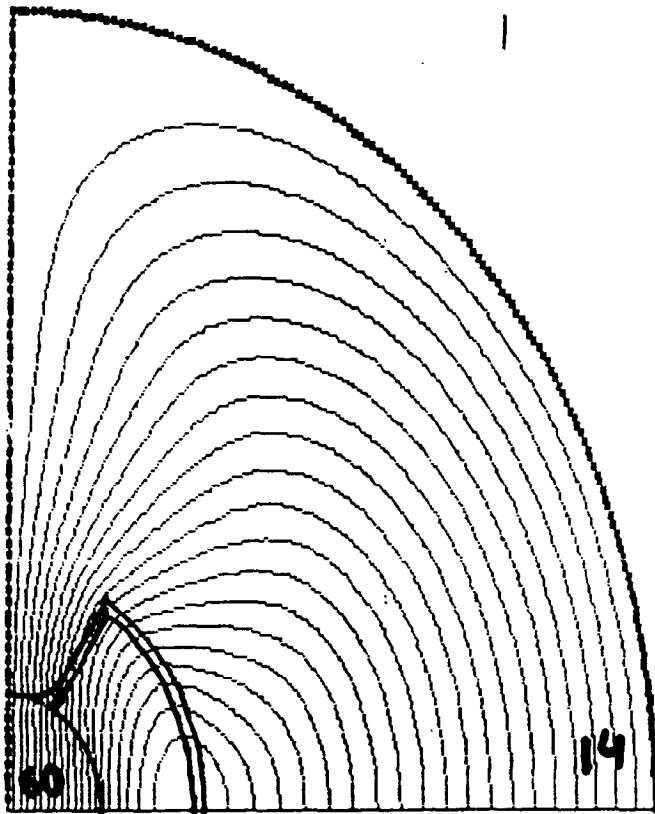
betatron tunes phase advanced on snake  
may be important for resonance  
strength

Technical parameters:

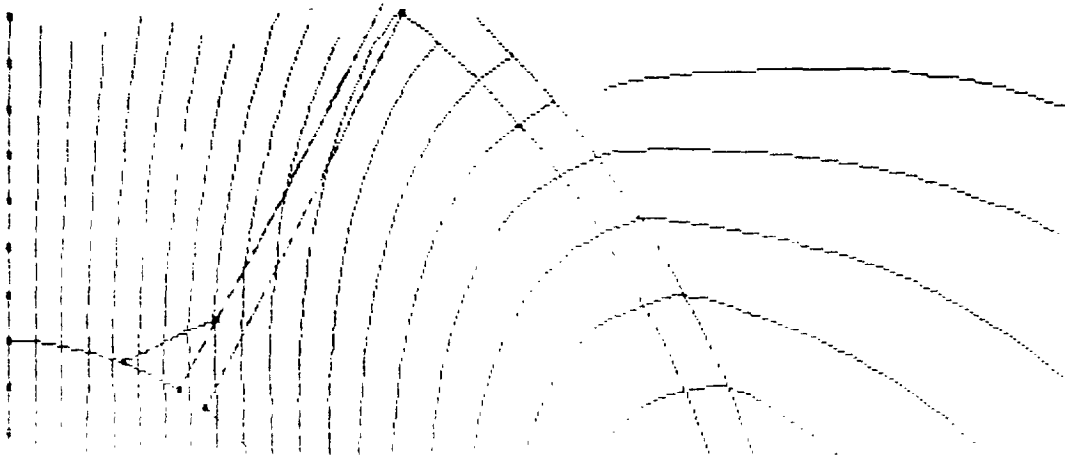
- Current :  $I_c = 200 \text{ A}$
- Number of turns : 3300
- Diameter of wire :  $d = 0,85 \text{ mm}$
- Magnetic field amplitude :  $6.0 \text{ T}$
- Superconductor at  $4,2 \text{ K}$  ;  
Nb-Ti alloy NT-50.

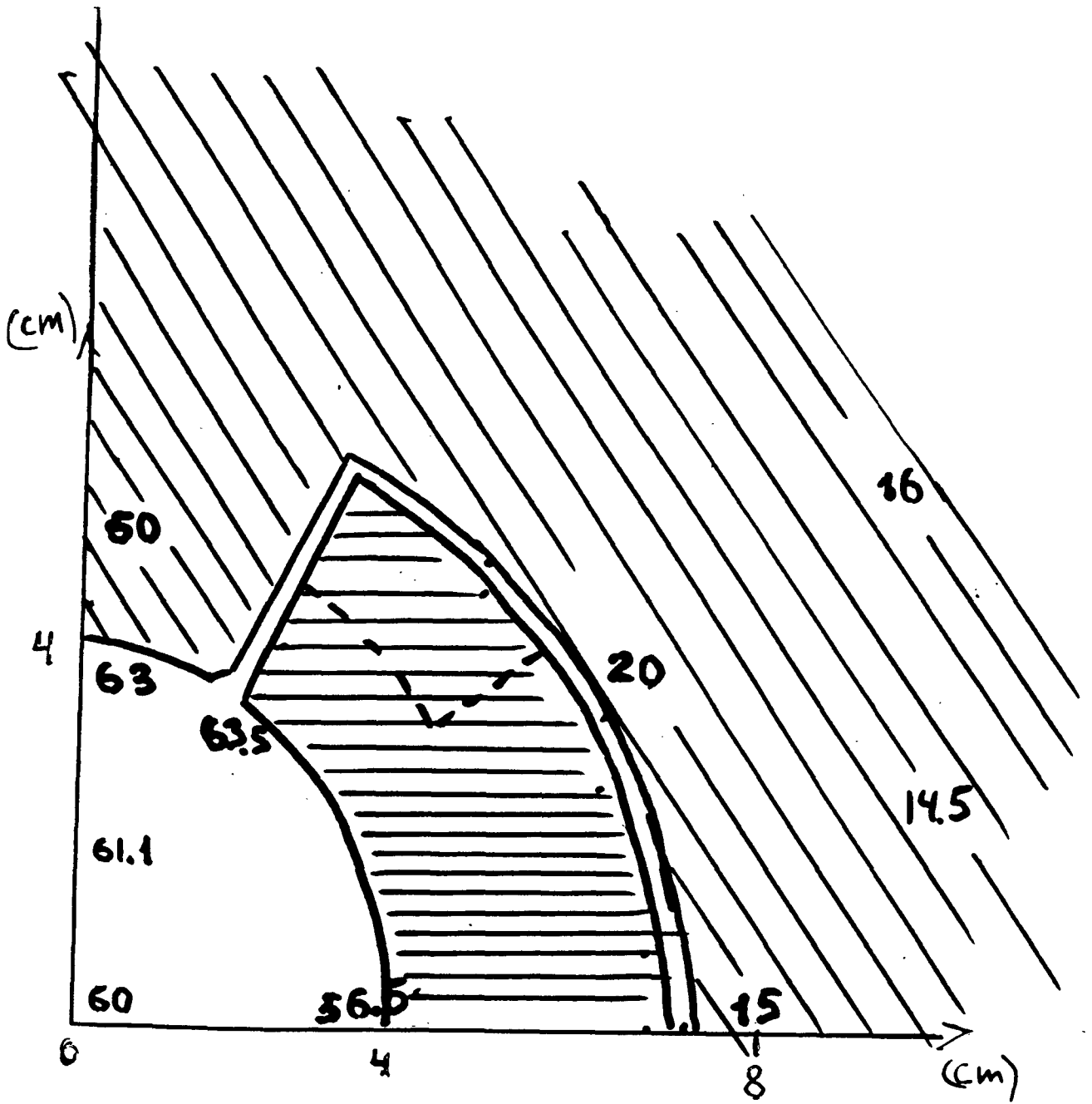


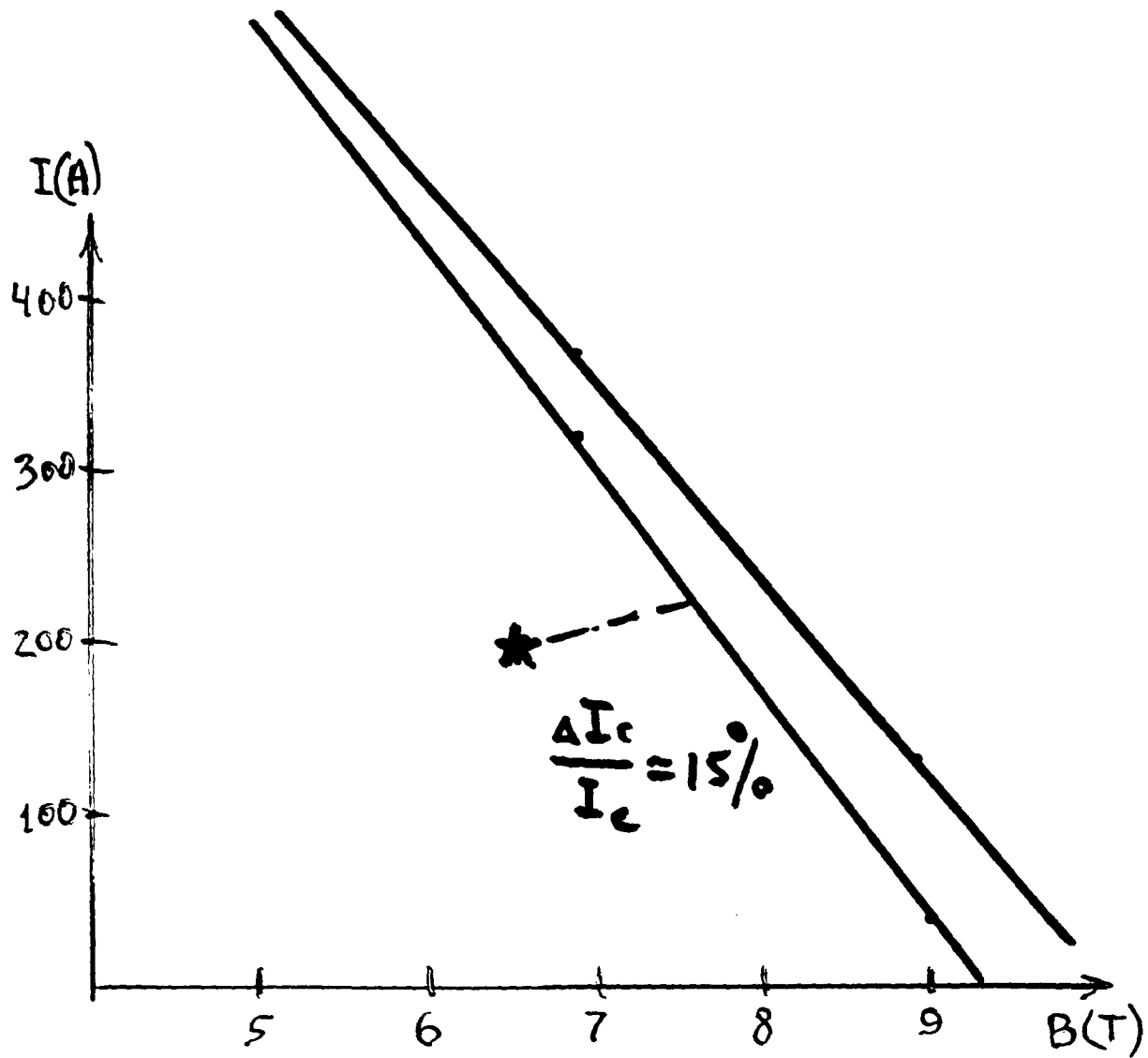
Flux from: -402.144 To: -3.996420E-07 Step: 20.1072  
Xmin= .000000 Ymin= .000000  
Xmax= 27.6000 Ymax= 27.6000



Flux from: -402.144 To: -2.934282E-38 Step: 20.1072  
Xmin= .000000 Ymin= .000000  
Xmax= 11.3138 Ymax= 6.90000







**F. Pilat**

**Brookhaven National Laboratory**

**Upton, NY 11973-5000**

**Models for the Helical Snake**

## MODELS FOR THE HELICAL SNAKE

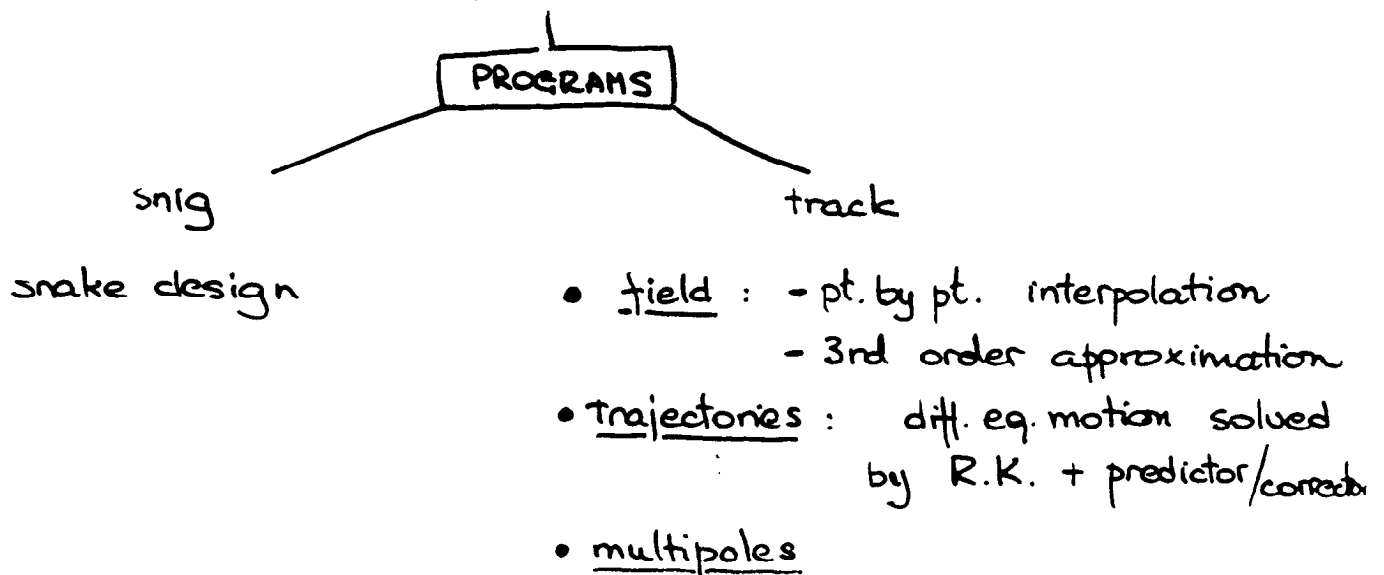
( F. PILAT / RAP )

goal evaluate effect of snakes (+ spin rotators) on  
RHIC beam dynamics  
(coupling ?) [ not SPIN ]



model of helical snake in TERPOT  
(code used for performance analysis of RHIC, errors,  
corrections, tracking, etc.)

starting point mathematical model for the snake field (AL.)  
("superposition of wigglers").



## FIELDS in TEAPOT

(approx) SNAKE FIELD: (2 wigglers phase shifted by  $\pi/2$ )

$$\begin{cases} B_x = B_0 \left( \frac{k_x}{k_y} S_x S_y \cos kz + C_x C_y \sin kz \right) \\ B_y = B_0 \left( C_x C_y \cos kz + \frac{k_y}{k_x} S_x S_y \sin kz \right) \\ B_z = B_0 \left( \frac{k}{k_y} C_x S_y \sin kz - \frac{k}{k_x} S_x C_y \cos kz \right) \end{cases} \quad \begin{aligned} C_x &\equiv \cosh(k_x x) \\ C_y &\equiv \cosh(k_y y) \\ S_x &\equiv \sinh(k_x x) \\ S_y &\equiv \sinh(k_y y) \end{aligned}$$

TEAPOT multipole expansion

$$B_y + iB_x = B_0 \sum_{n=0}^{\infty} (b_n + ia_n) (x + iy)^n$$

one cannot express the snake field in  $\uparrow$  form

because of the longitudinal field.

i.e. the simple model for the snake

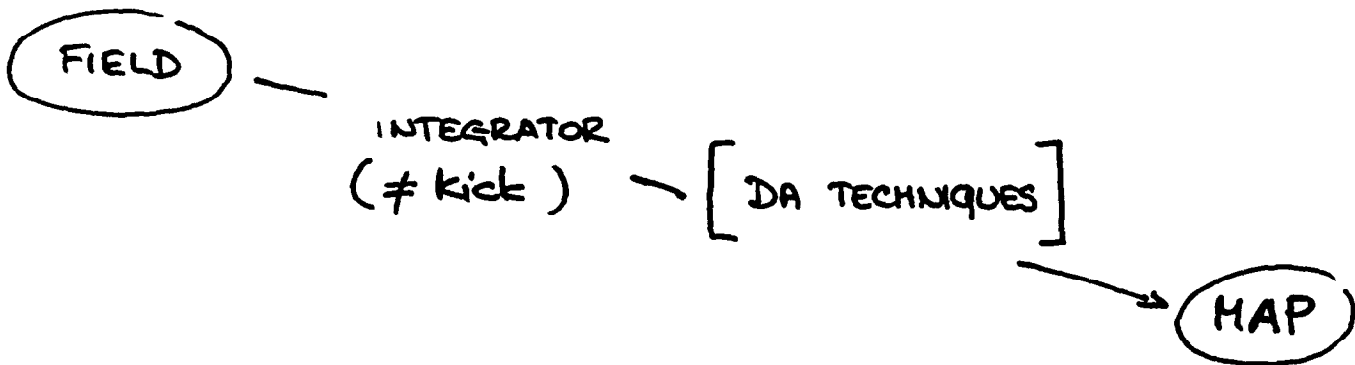


kick - multipoles - kick + ...

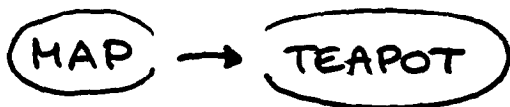
does NOT work.

GENERAL WAY TO SOLVE THE PROBLEM :

\* MAP \*



map will not be symplectic  
adequate order / truncated Taylor series



work in progress :

existing  
DA package PACT+

- write a Runge/Kutta integrator
- extract a snake map

map in TEAPOT :

- map up to 2<sup>nd</sup> order possible in the default version of TEAPOT
- version of TEAPOT which allows maps up to  $n^{\text{th}}$  order obtained by the ZUB package.

## SIMPLER MODELS FOR THE SNAKE

- verify the results of the programs
- give an order of magnitude of problems (coupling?)

### ■ Results of the programs for a helical snake

similar to the one which is going to be built.

+ comparison of trajectories integrated through the exact field to simple solutions of the field on axis.

### ■ LINEAR MATRIX for the SNAKE (status report)

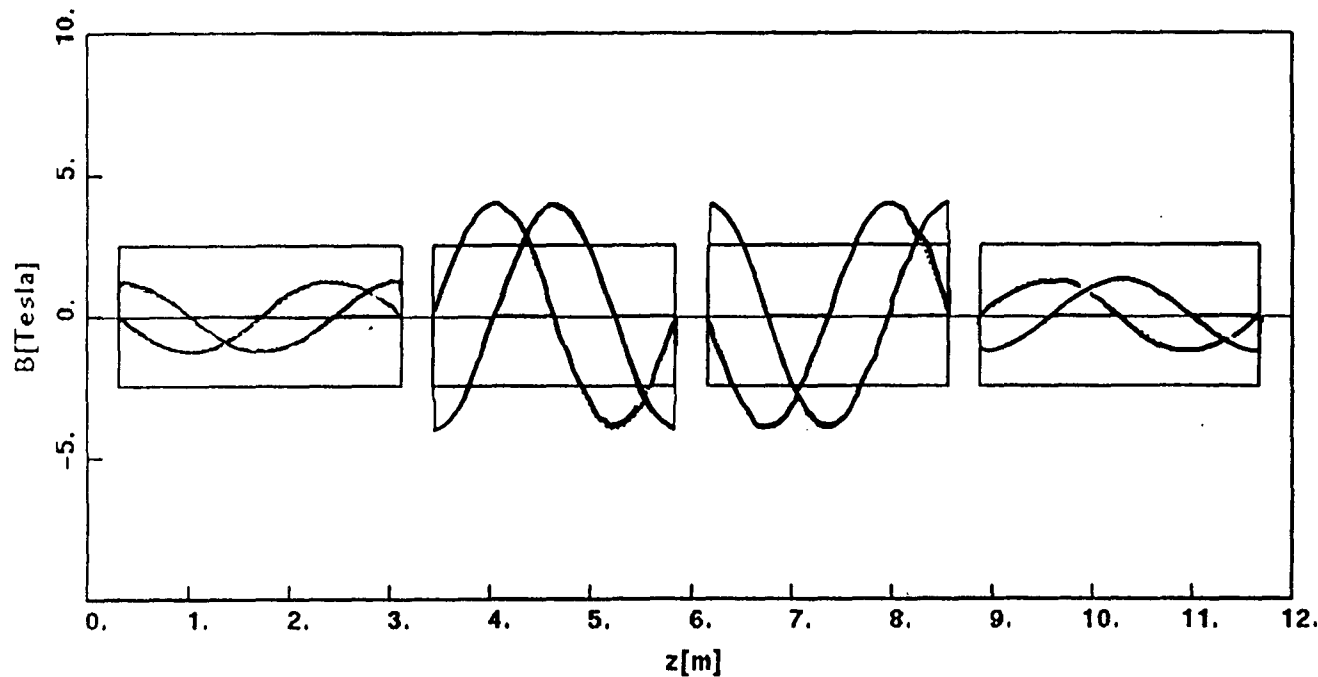
- extension to '2 dim' of the techniques being used by Talman.

'1 dim' wiggler

$R$  and  $T$  matrices.

- projection matrix

alternative way to calculate the transfer matrix (S. Peggs).



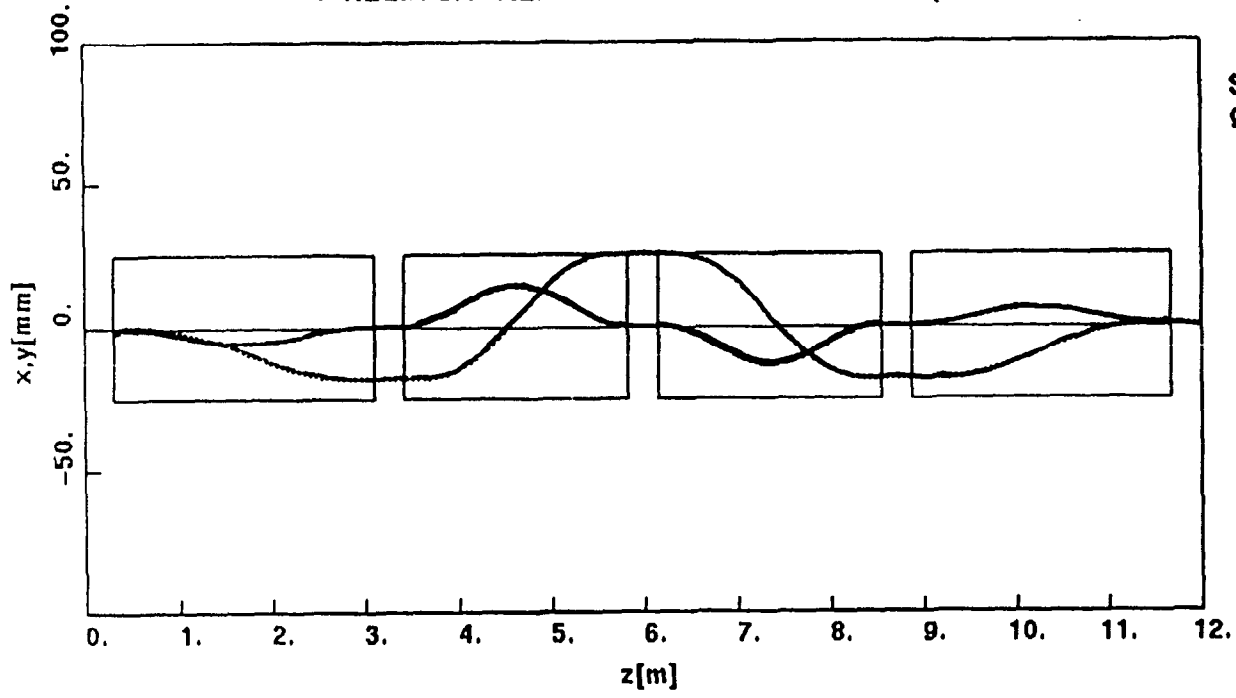
gamma=27  
B=1.25/4./4./1.25 [T]

$B_x$   
 $B_y$

176

realistic model of a helical snake for RHIC

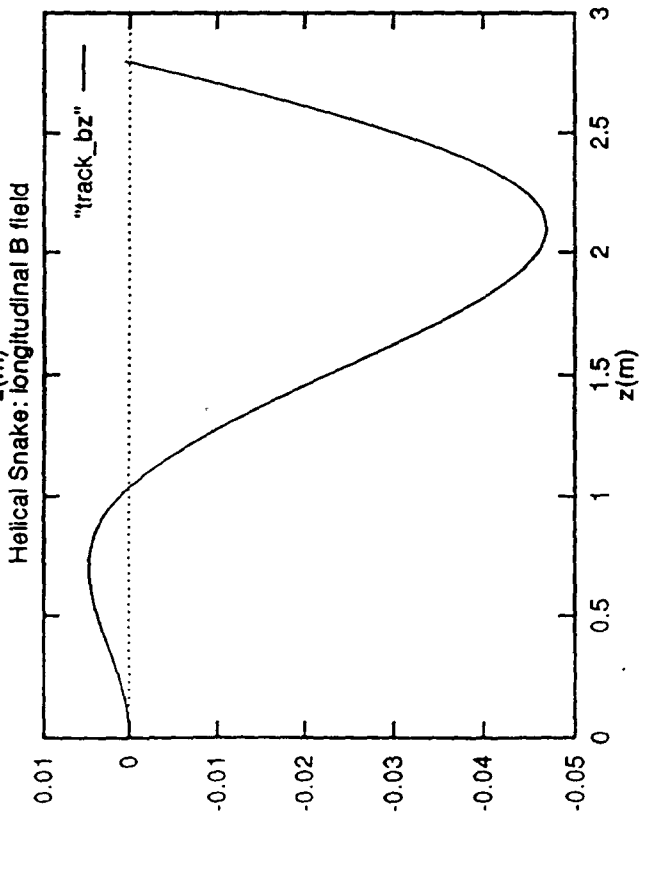
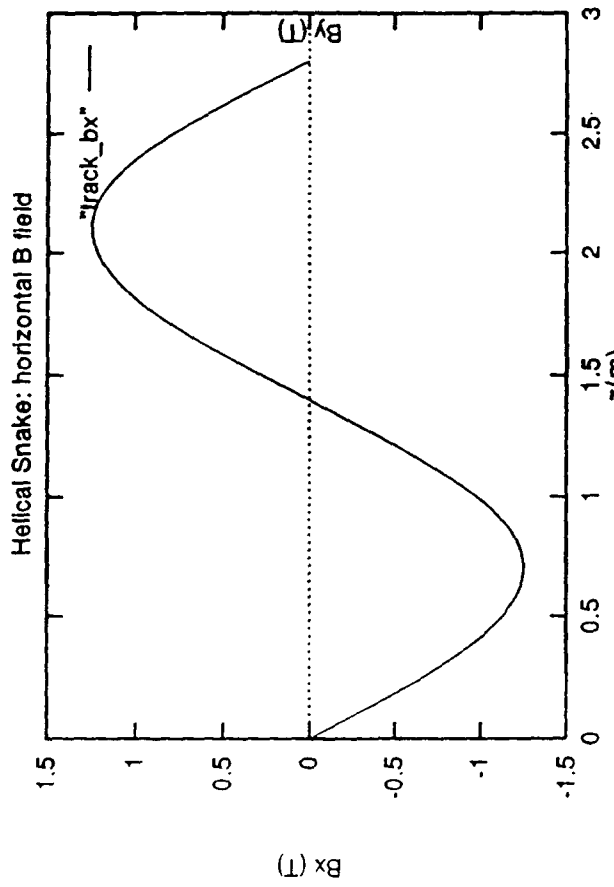
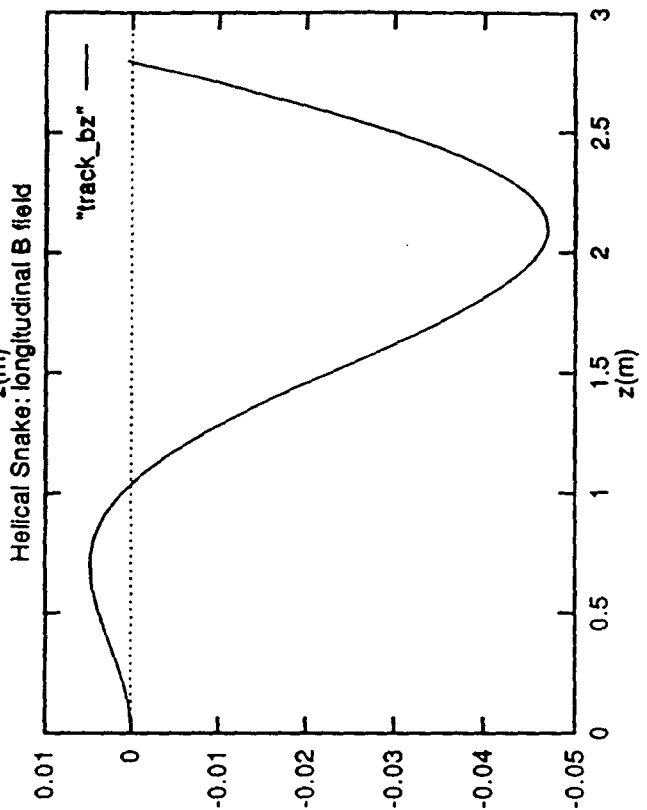
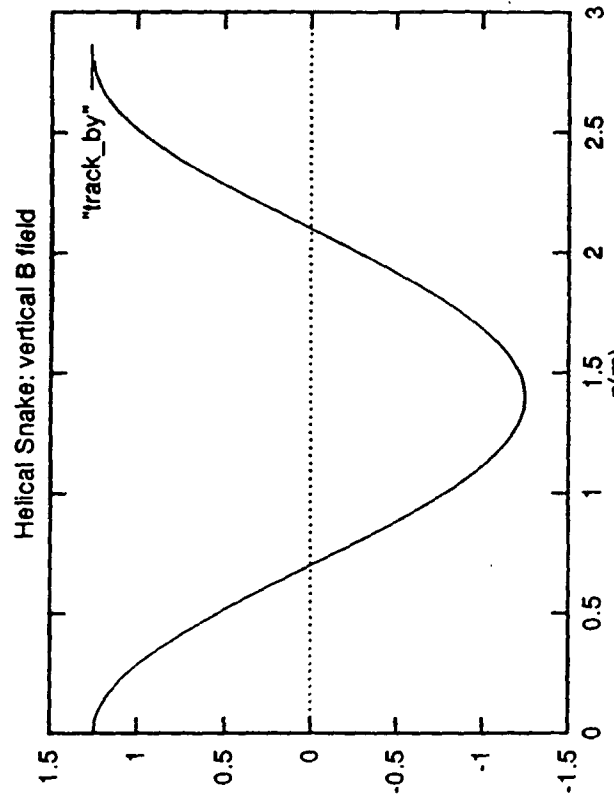
module	1	2.8 m	1.25 T
module	2	2.4 m	4.0 T
module	3	2.4 m	4.0 T
module	4	2.8 m	1.25 T



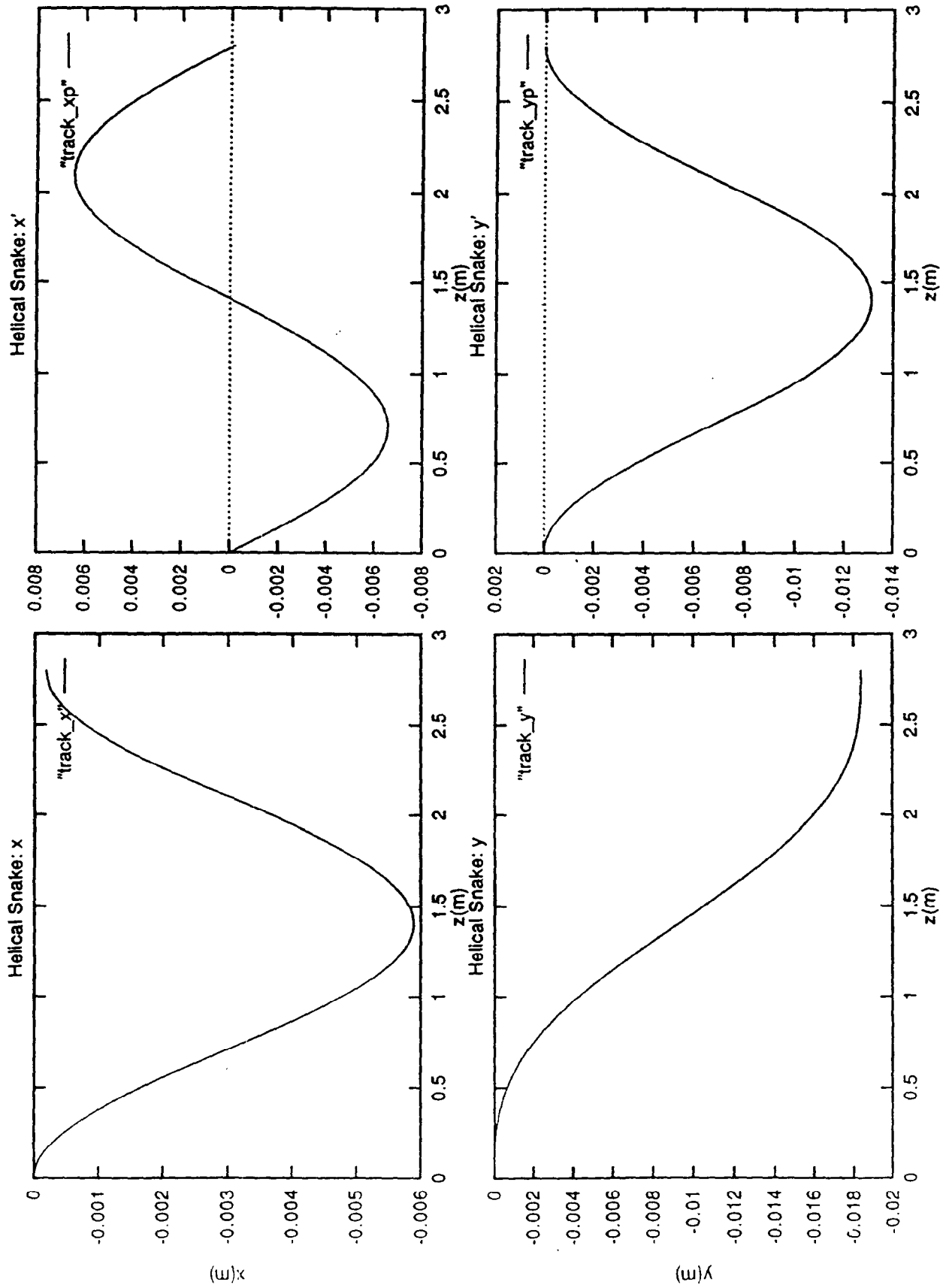
Shatunov  
gamma=27

x  
y

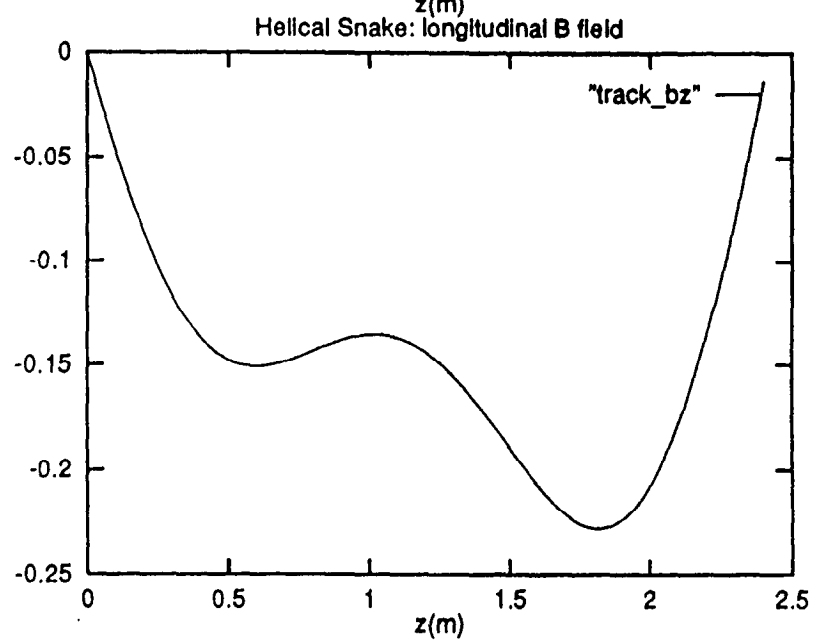
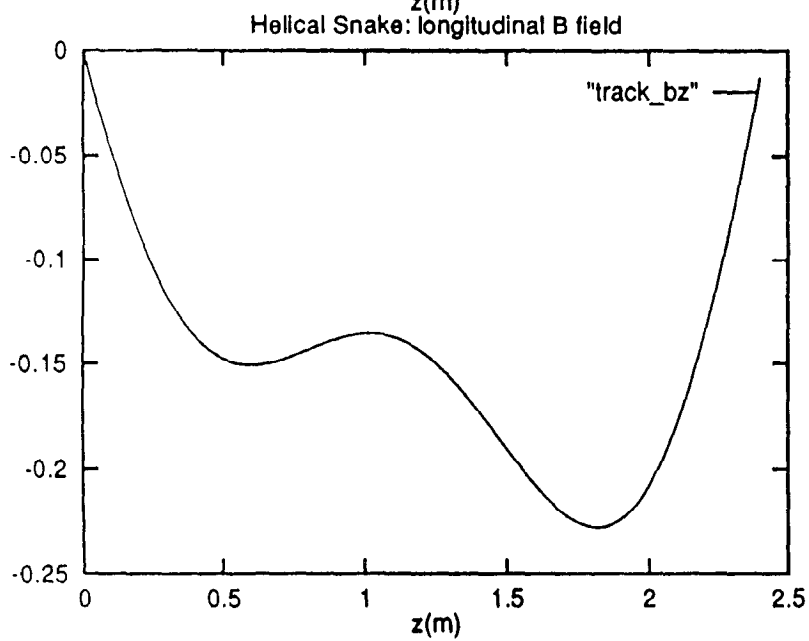
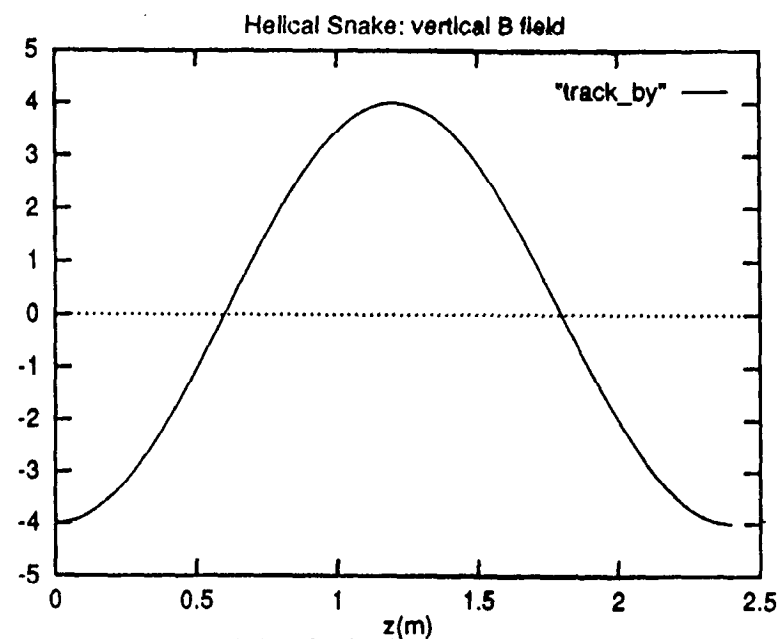
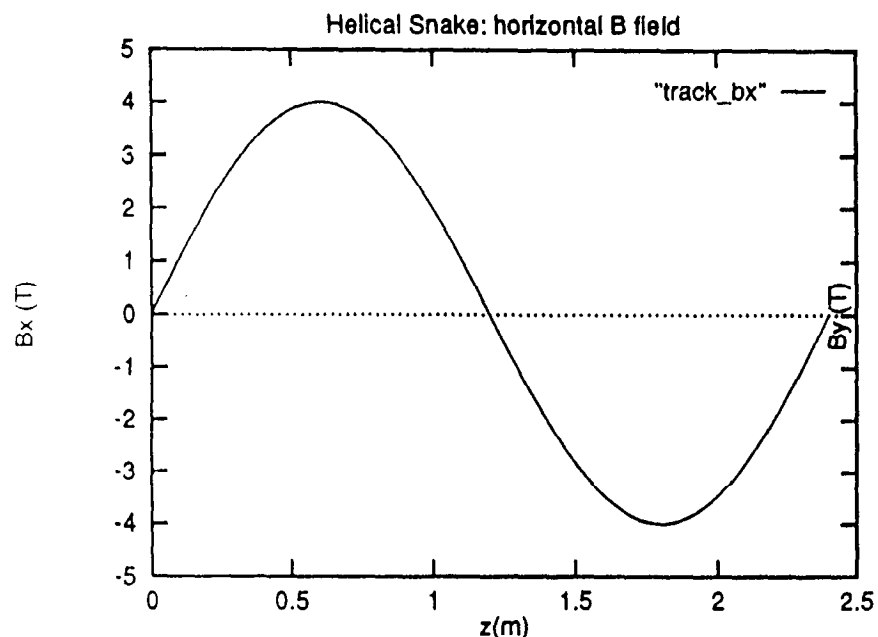
module 1



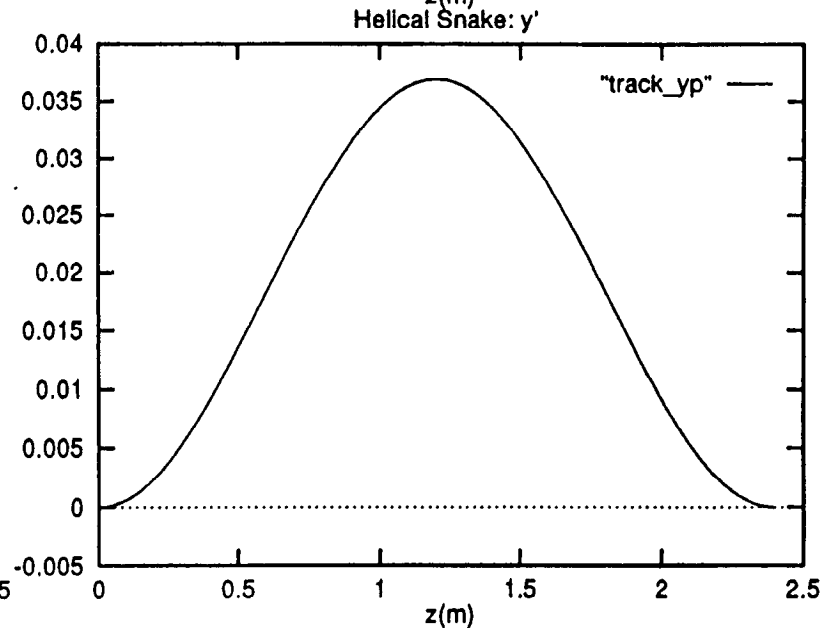
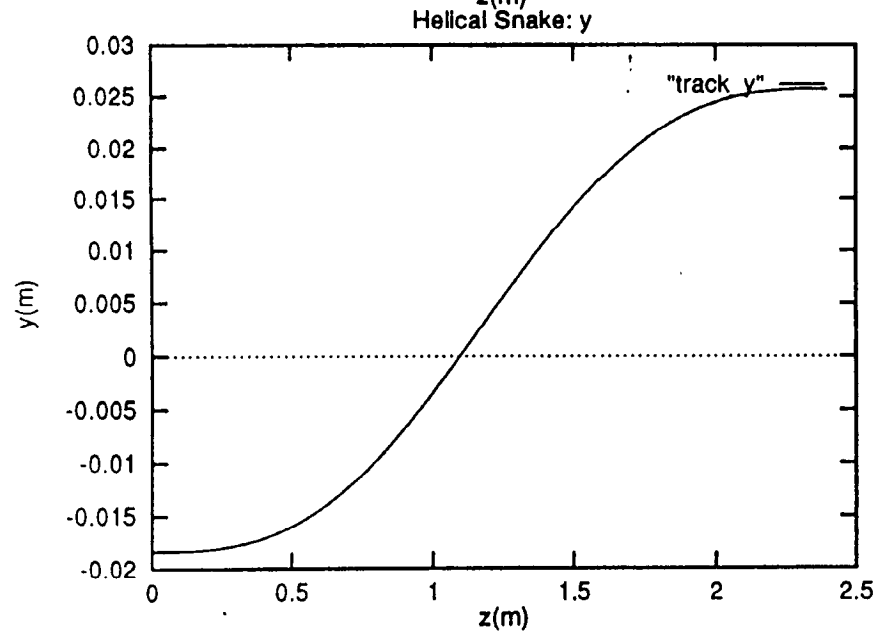
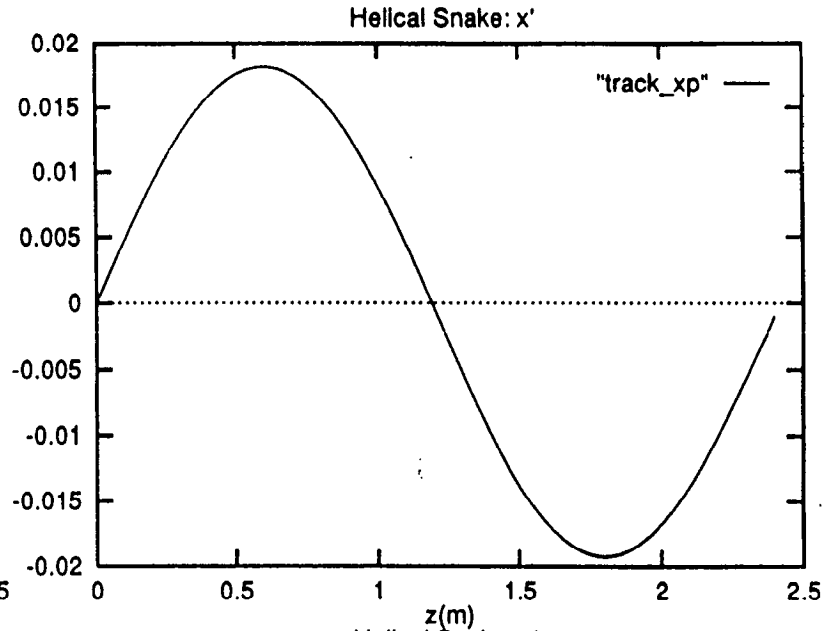
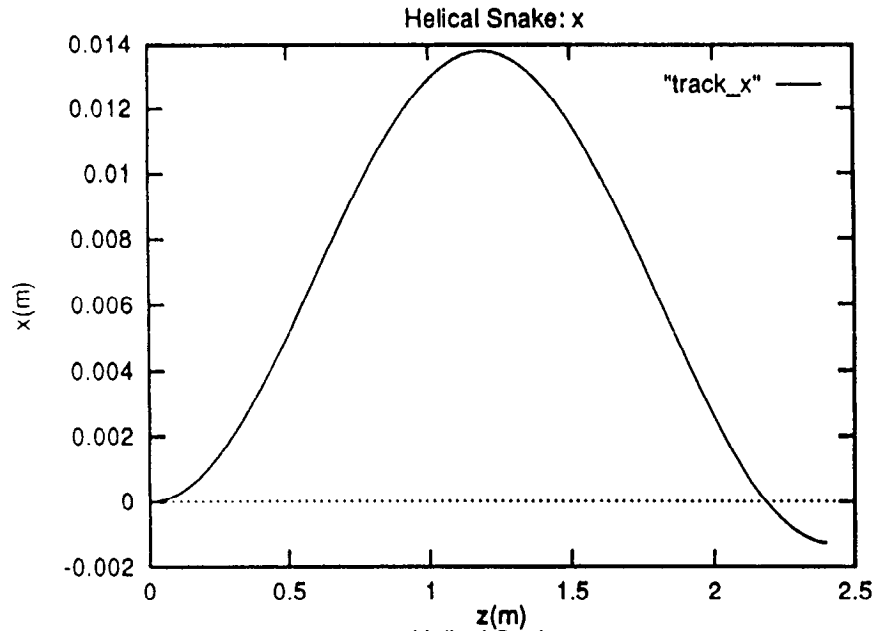
module 1



module 2



module 2



comparison trajectories.

take the field on axis

$$\begin{cases} B_x = \frac{e}{mc\gamma} B_0 \sin(kz + \phi) \\ B_y = \frac{e}{mc\gamma} B_0 \cos(kz + \phi) \\ B_z = 0 \end{cases}$$

solution

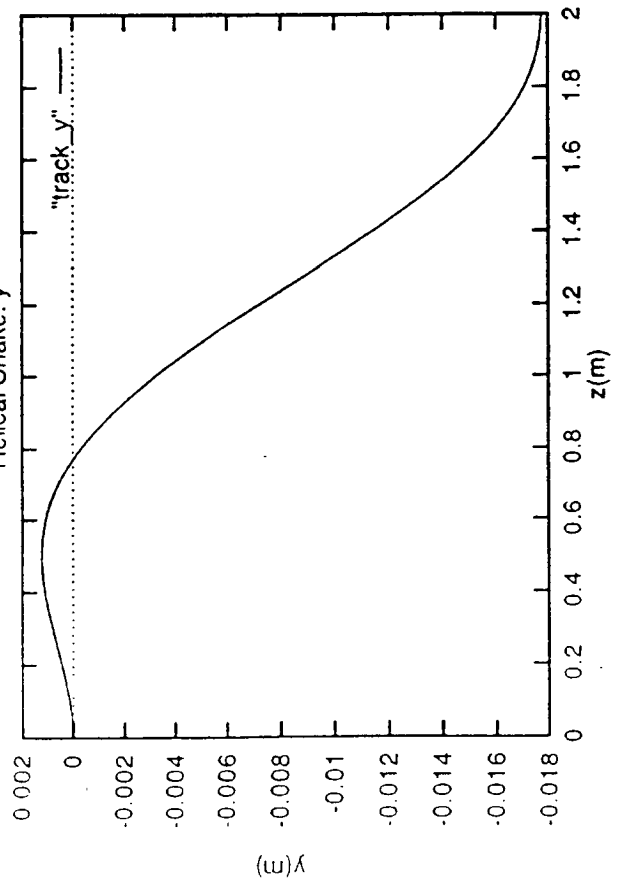
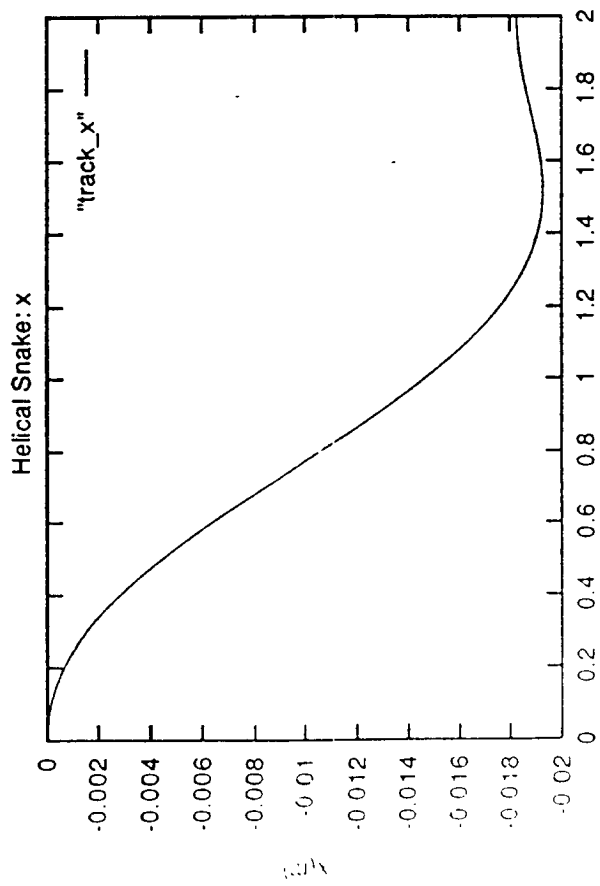
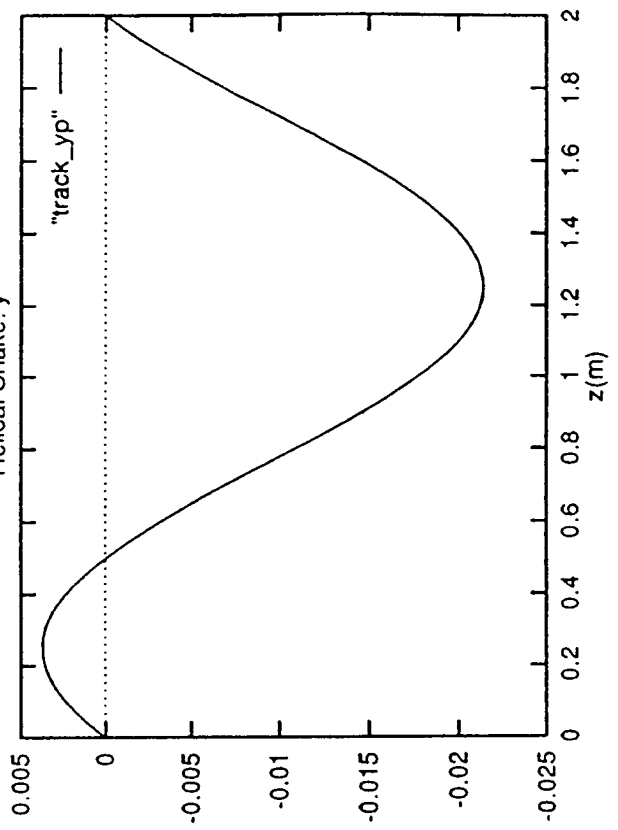
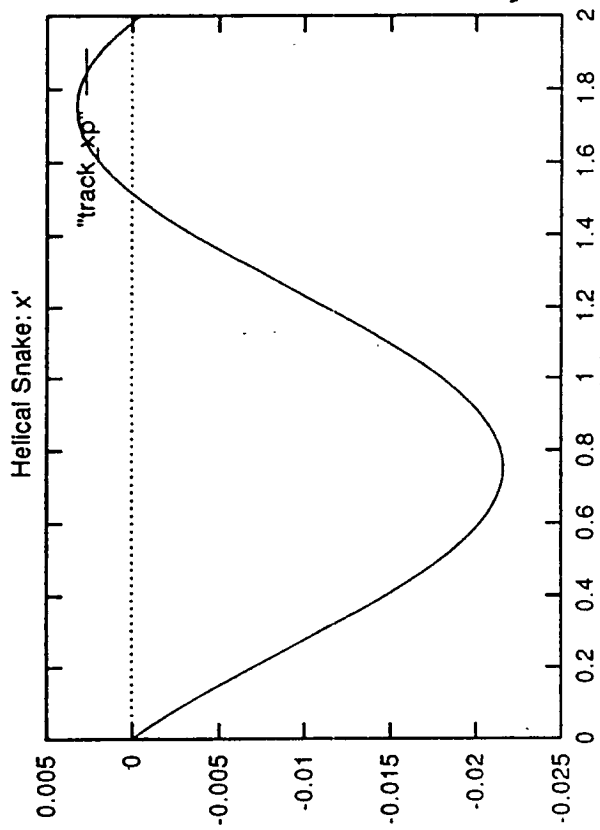
$$\begin{cases} x = x_0 + \left( x'_0 - \frac{e}{mc\gamma k} \sin\phi_0 \right) z - \frac{e}{mc\gamma k^2} \left( \cos(kz + \phi_0) - \cos\phi_0 \right) \\ y = y_0 + \left( y'_0 + \frac{e}{mc\gamma k} \cos\phi_0 \right) z - \frac{e}{mc\gamma k^2} \left( \sin(kz + \phi_0) - \sin\phi_0 \right) \end{cases}$$

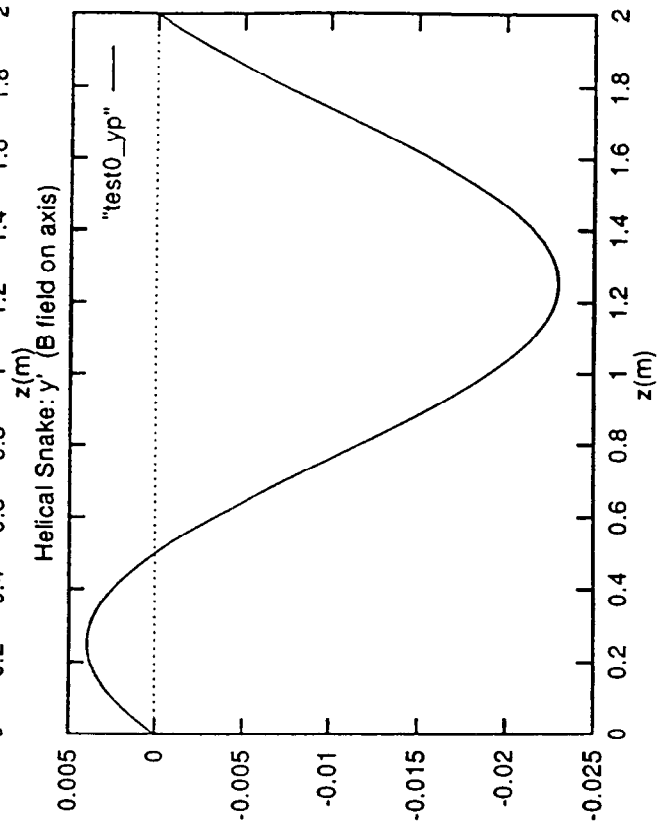
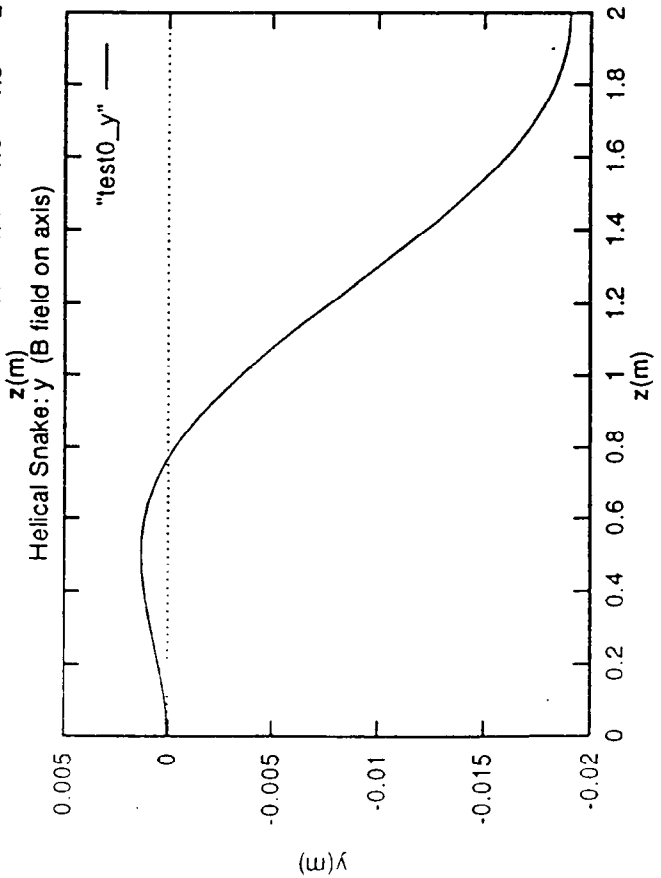
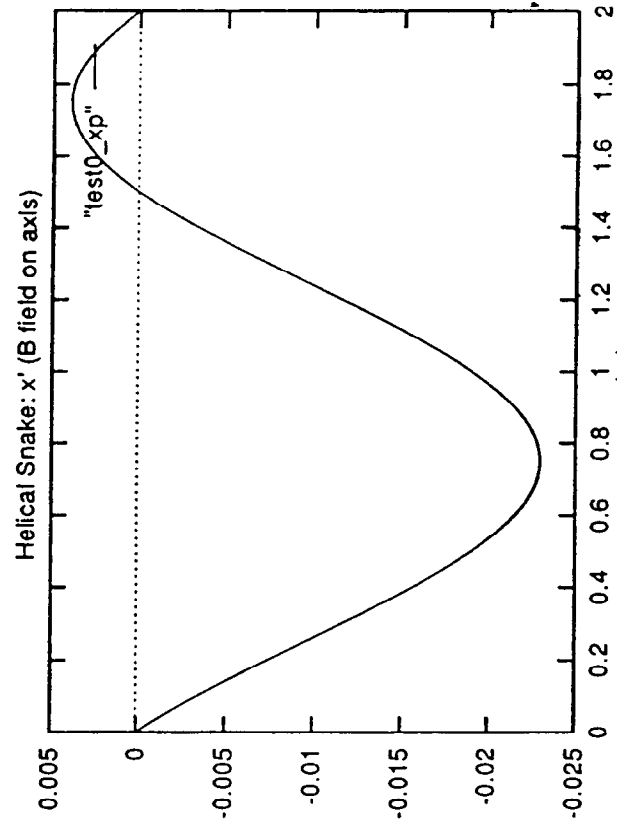
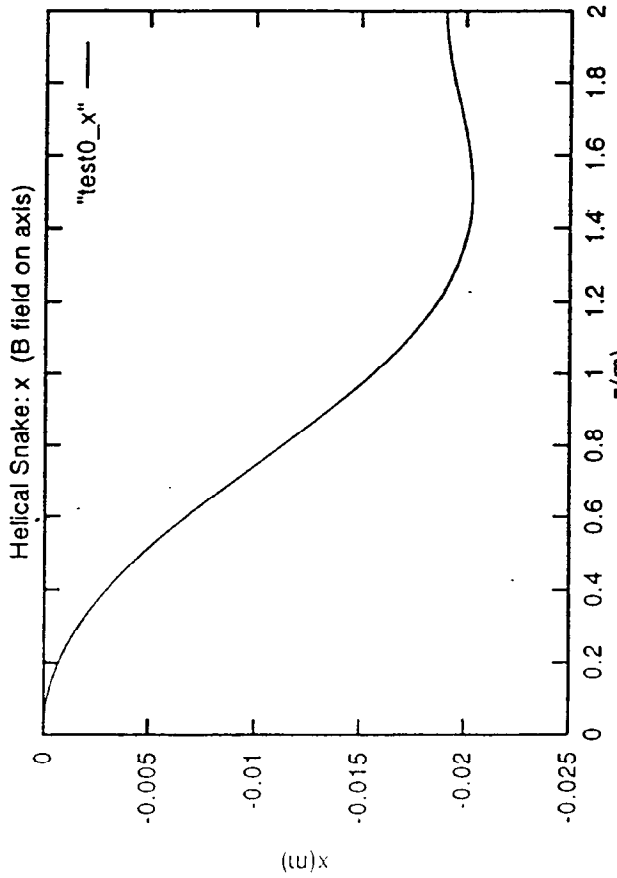
case ( $k_x = k_y$ )      $k = \pi$      take  $\boxed{\phi_0 = \frac{3}{4}\pi}$

↳ case in the program     → compare trajectories.

N.B. take  $\boxed{\phi_0 = \pi, 0.}$

↳ analytical expressions for the trajectories same as Richard wiggler (but in 2 dim.).





## LINEAR MATRICES FOR THE HELICAL SNAKE



$$M = M_4 \times D(\Delta) \times M_3 \times D(\Delta) \times M_2 \times D(\Delta) \times M_1$$

TALMAN : 1 DIM WIGGLER

calculate matrix for 1 wavelength of wiggler

postulate solution for  $x(z), y(z) \rightarrow x'(z), y'(z)$

$$\text{calculate } x'' \hat{x} + y'' \hat{y} + 0 \hat{z} = \alpha \bar{v} \times \bar{B} = \tilde{\alpha} \begin{pmatrix} \hat{x} & \hat{y} & \hat{z} \\ x'(z) & y'(z) & 1 \\ B_x & B_y & B_z \end{pmatrix}$$

substitute  $x \rightarrow x(z)$      $y \rightarrow y(z)$

expand  $\cosh, \sinh$  to first order

integrate  $\int_0^L dz$  over 1 wavelength

$$\text{obtain } \Delta x' = \int_0^L x''(z) dz \quad \Delta y' = \int_0^L y''(z) dz$$

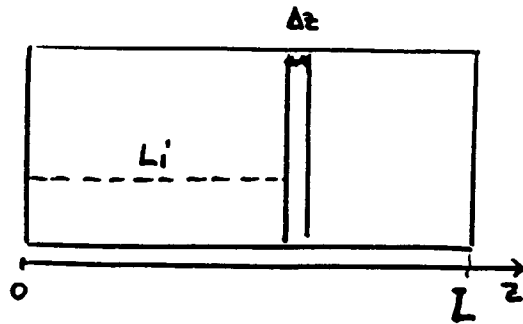
↓  
TRANSFER MATRIX

[ for the snake (2dim problem) the calculation becomes quickly complicated ]

# PROJECTION MATRIX

on axis in the rotating frame we have a pure dipole field.

↓ module of the snake.



calculate projection  $P_i$  of 'slice'  $i$

to first order  $M = I + \text{Sum } P_i \rightarrow I + \int_0^L dz P(z)$

calculation of  $P_i$

\* kick matrix at  $z=0$   $\tilde{K}$

\*  $P_i : D(-L_i) R(-\theta_i) \tilde{K}(\tilde{r}_i) R(\theta_i) D(L_i)$   
 $r_0 = r_0(z)$

integration over  $z$ .

**A. Luccio**

**Brookhaven National Laboratory**

**Upton, NY 11973-5000**

**SNIG Formalism**

## SNIG FORMALISM

A.Luccio

AGS Dept. Brookhaven National Laboratory, Upton, NY 11973-5000

### Introduction

To characterize and design Snakes and Spin Rotators for spin polarized proton beams in a fast and easy way, a computer code SNIG has been developed. SNIG solves the problem by simultaneous integration of the equation of motion and the equation of precession of the spin.

Input is the configuration of the field, generated by an array of purely transverse or helical dipoles, with their edge field. We made the approximation that the transverse components of the field are not a function of the transverse coordinate, and that the longitudinal field is a linear function of the displacement of the beam. These assumptions are to a good degree justified by the present technology of "cosine" dipoles, like the ones employed in high energy proton colliders.

To characterize the device as an optical element in the accelerator lattice, once a "central" beam has been tracked, we integrate the motion of an ensemble of particles in phase space. The transport map between final and initial coordinates of the beam is then statistically evaluated, and the focusing parameters of the snake or rotator are estimated.

## Differential Equations

The vector equations for the motion and for the spin (treated as an ordinary vector) precession are:

Motion: 
$$\frac{d\beta}{dt} = \beta \times \Omega$$

with the definitions

$$\Omega = \frac{e\mathbf{B}}{m\gamma} \quad \beta^2 = 1 - \frac{1}{\gamma^2} \quad \gamma = E/mc^2$$

Spin precession: 
$$\frac{ds}{dt} = C_1 \mathbf{s} \times \Omega + C_2 (\beta \cdot \Omega) \mathbf{s} \times \beta$$

with the definitions

$$C_1 = 1 + G\gamma \quad C_2 = -\frac{G\gamma^2}{1 + \gamma} \quad G = \frac{1}{2}g - 1$$

Call  $x$  (radial) and  $y$  (vertical) the transverse coordinates, and  $z$  the longitudinal coordinate (the prevalent direction of propagation of the beam). Using  $z$  as the independent variable, and the following definitions

$$\frac{dz}{dt} = \beta_z c \quad \beta_z = \frac{\beta}{\sqrt{1 + x'^2 + y'^2}} \quad \begin{cases} x' = \beta_x / \beta_z \\ y' = \beta_y / \beta_z \end{cases}$$

write the following scalar d.equations

for the motion:

$$\begin{cases} \frac{dx'}{dz} = [x' y' \Omega_x - (1 + x'^2) \Omega_y + y' \Omega_z] / \beta_z \\ \frac{dy'}{dz} = [(1 + y'^2) \Omega_x - x' y' \Omega_y - x' \Omega_z] / \beta_z \\ \frac{dx}{dz} = x' \\ \frac{dy}{dz} = y' \end{cases}$$

$$\left\{ \begin{array}{l} \frac{ds_x}{dz} = [p_z s_y - p_y s_z] / \beta_z \\ \frac{ds_y}{dz} = [p_x s_z - p_z s_x] / \beta_z \\ \frac{ds_z}{dz} = [p_y s_x - p_x s_y] / \beta_z \end{array} \right. \quad \text{or:} \quad \frac{ds}{dz} = [-\mathbf{p} \times \mathbf{s}] / \beta_z$$

and for the spin:

where:

$$\begin{cases} p_x = C_1 \Omega_x / \beta_z + C_2 x' \Gamma \\ p_y = C_1 \Omega_y / \beta_z + C_2 y' \Gamma \\ p_z = C_1 \Omega_z / \beta_z + C_2 \Gamma \end{cases}$$

$$\Gamma = \beta_z (x' \Omega_x + y' \Omega_y + \Omega_z) \quad s_x^2 + s_y^2 + s_z^2 = 1$$

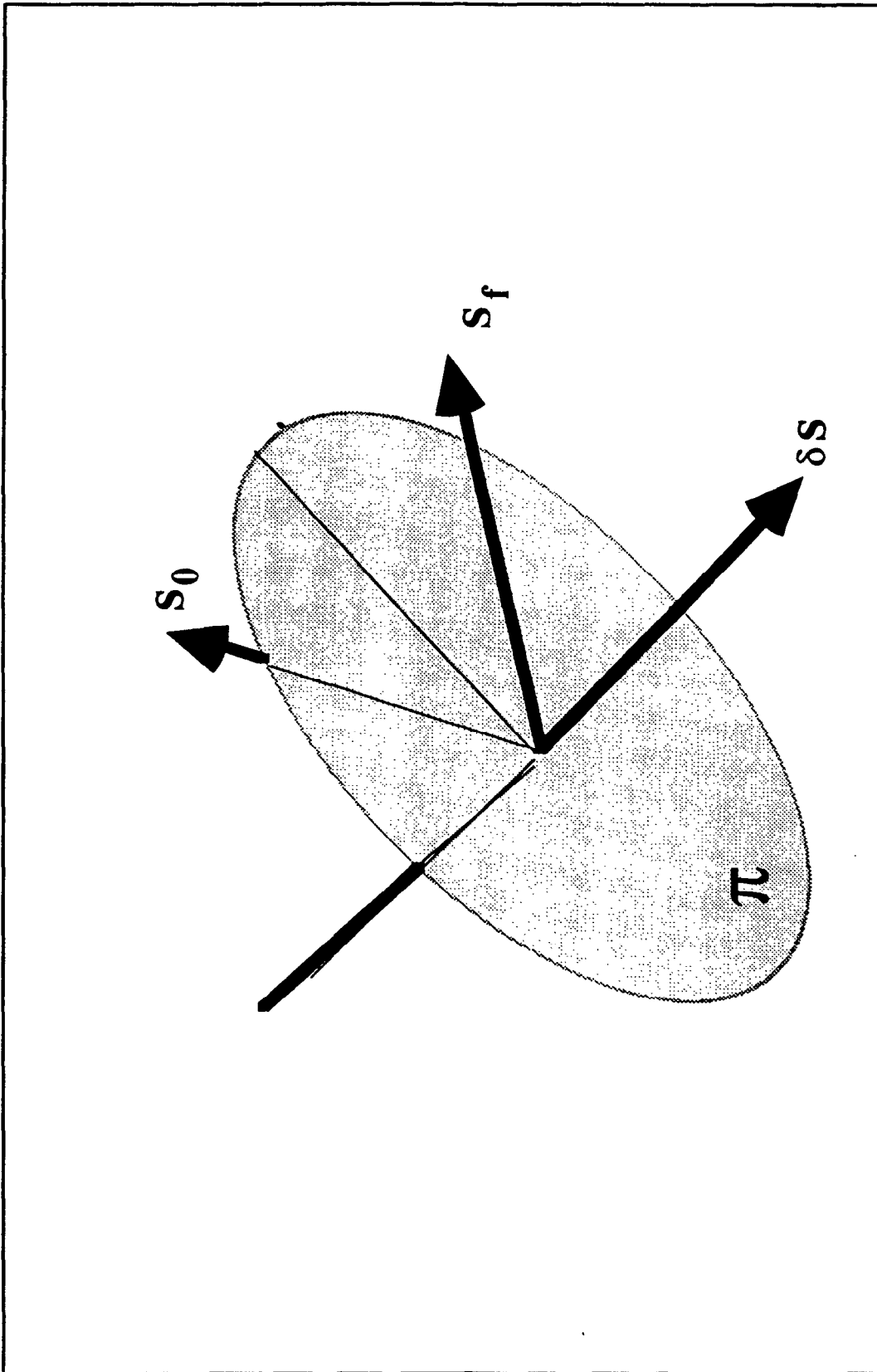
## Axis of Spin Precession

3 more equations, formally identical to the latter, are used to calculate the orientation of the axis of precession  $\sigma$

$$\frac{ds^A}{dz} = -\mathbf{p} \times \mathbf{s}^A$$

The idea -admittedly not too elegant- is the following:

if a spin vector  $\mathbf{s}$  precesses from  $\mathbf{s}_0$  to  $\mathbf{s}_f$ , the axis of precession must belong to the plane  $\pi$  bisecting the  $(\mathbf{s}_0 \mathbf{s}_f)$  angle

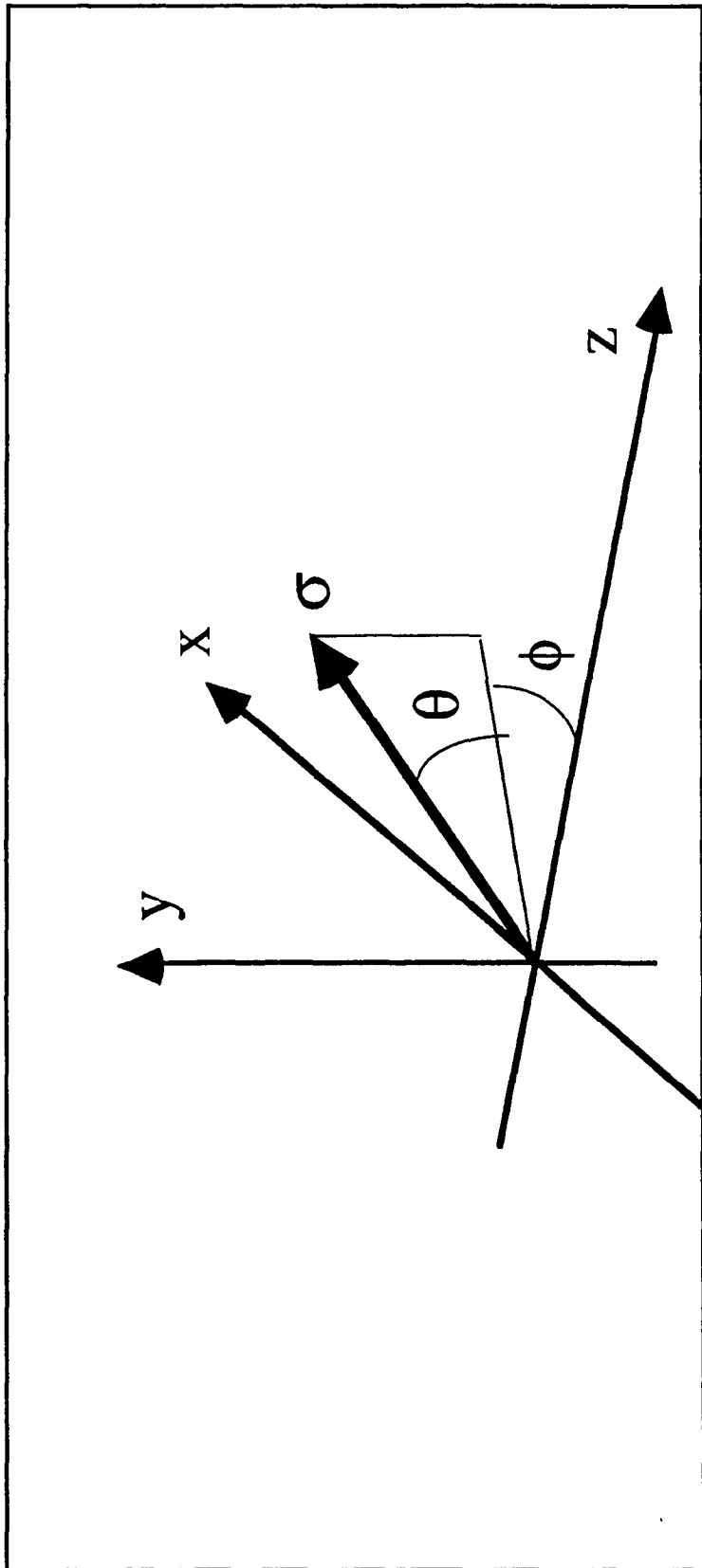


This axis is then perpendicular to the vector  $\delta\mathbf{s} = \mathbf{s}_f - \mathbf{s}_0$ . If we repeat the same argument for a different spin orientation  $\mathbf{s}^A$ , we obtain the result that the axis of precession must be also perpendicular to a new defined vector  $\delta\mathbf{s}^A$ . The axis of precession  $\boldsymbol{\sigma}$  is therefore perpendicular both to  $\delta\mathbf{s}$  and to  $\delta\mathbf{s}^A$

$$\boldsymbol{\sigma} = \delta\mathbf{s} \times \delta\mathbf{s}^A$$

and the angles are

$$\left\{ \begin{array}{l} \tan \phi = \frac{\sigma_x}{\sigma_z} \\ \tan \theta = \frac{\sigma_y}{\sqrt{\sigma_x^2 + \sigma_z^2}} \end{array} \right.$$



## Magnetic Field

A snake or spin rotator is composed by sequence of magnets: transverse or helical dipoles. Each magnet has a body field and an in- and out-edge field.

In a transverse dipole, we represent the body field as a constant, and the edge with a reciprocal cosh function. This is a para axial representation, where we assume that the transverse field is only a high order function of  $x$  and  $y$ . The transverse field components are

$$\text{Transverse dipole: } B^{(body)} = B_0 \quad B^{(edge)} = B_0 / \cosh(|z^{(e)}/g|)$$

where  $z^{(e)}$  is the distance from the magnet hard edge, and  $g$  the magnet half gap.

In a helical dipole, body and edge transverse field components are

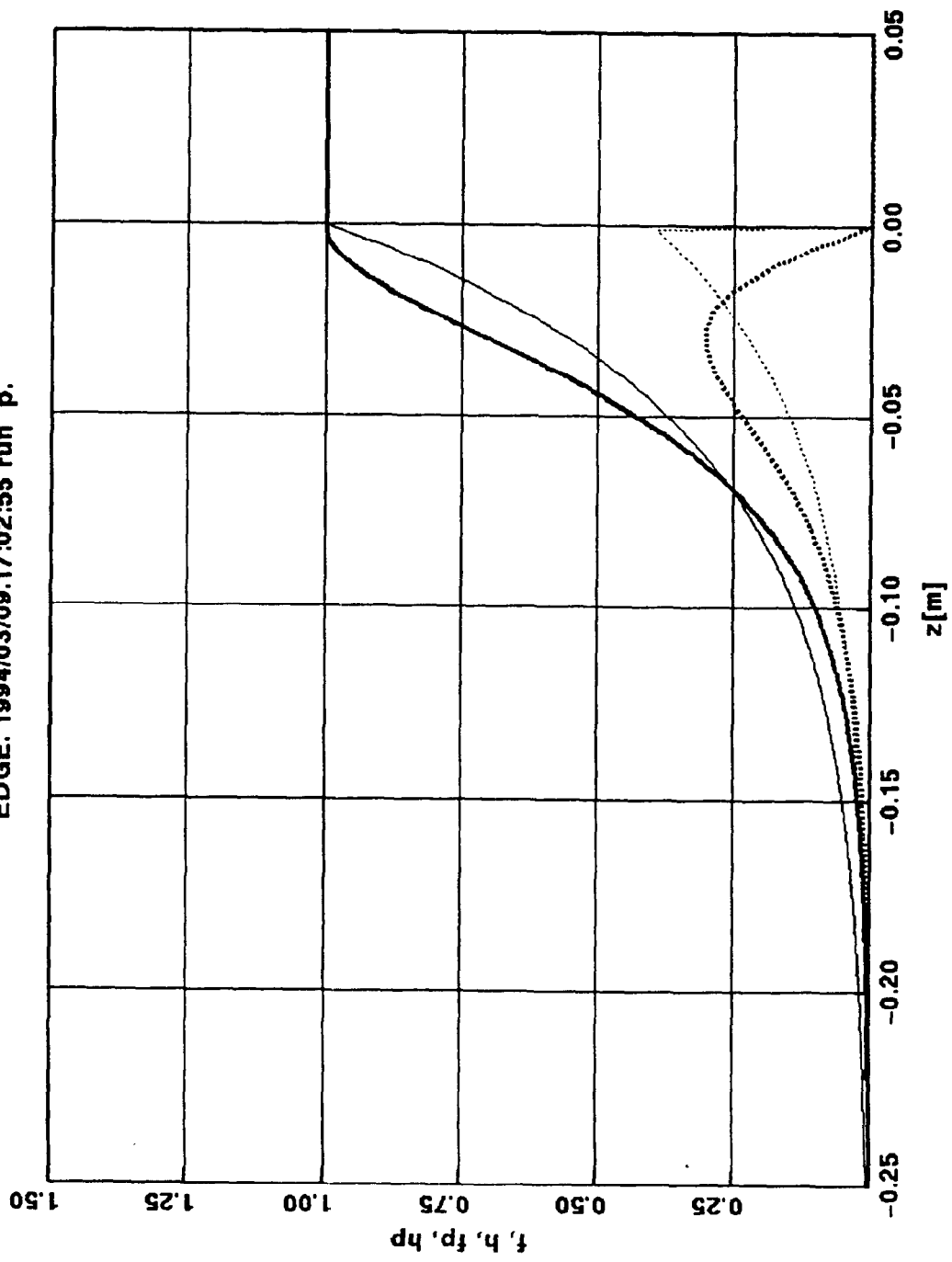
$$\text{Helical dipole: } B^{(body)} = B_0 \frac{\sin}{\cos} \left( \int dz / \lambda(z) + \varphi \right) \quad B^{(edge)} = B_0 \frac{\sin}{\cos} \varphi / \cosh(|z^{(e)}/g|)$$

The longitudinal field component, close to the axis, to first order is obtained from the

$$\nabla \times \mathbf{B} = 0$$

$$\text{i.e: } B_z = \frac{B_0}{\lambda_0} \left[ x \frac{\partial B_x}{\partial z} + y \frac{\partial B_y}{\partial z} \right]$$

EDGE. 1994/03/09.17:02:55 run p.



SNIG

nter run no, page no 700 2

ontinue [y/n]? y

btune = 1.00000000 1.00000000

z	x [mm]	xp[mrad]	y [mm]	yp[mrad]	sx	sy	sz	phi	theta	
0.000	0.0000000	1.1730000	0.0000000	0.0000000	0.0000000	1.0000000	0.0000000	35.000	0.000	1.000000000
1.420	-4.4986511	0.2040149	-7.8775336	-13.1057840	0.1431529	0.8010776	0.5811900	105.056	-5.046	1.000000000
2.781	0.6165773	-0.7414224	-15.7538414	-0.0011066	0.2826962	0.9588167	0.0274489	179.984	-33.658	1.000000000
4.141	16.4313871	1.2005439	6.2932157	36.8530108	0.7784326	-0.4047940	-0.4797755	45.969	8.254	1.000000000
5.501	4.0408946	3.2701085	28.2725958	-0.0052606	0.2847853	-0.1065188	-0.9526548	-167.728	38.186	1.000000000
6.860	-8.4564855	0.2524860	6.8429871	-35.5386494	0.6701273	0.4528967	-0.5880596	128.462	58.433	1.000000000
8.221	4.7284990	-2.7522233	-14.5706573	-0.0010039	0.3721433	-0.9210695	-0.1146309	131.716	10.444	1.000000000
9.580	7.0970839	-1.9509651	-6.6096793	13.2801370	0.2114090	-0.8616508	0.4613720	136.128	-5.582	1.000000000
11.000	-0.6247813	-1.1080772	1.3395393	0.0004403	0.0474040	-0.9871912	-0.1523367	136.084	4.105	1.000000000

psi = 9.180305756425062 or 170.8196942435749

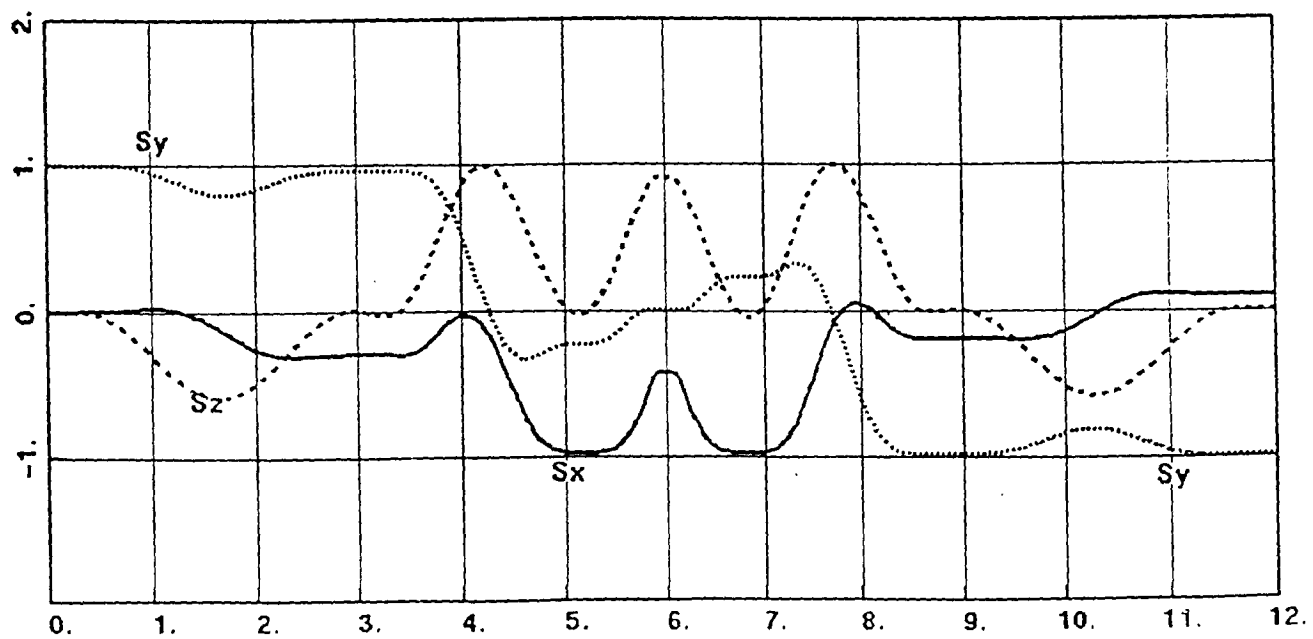
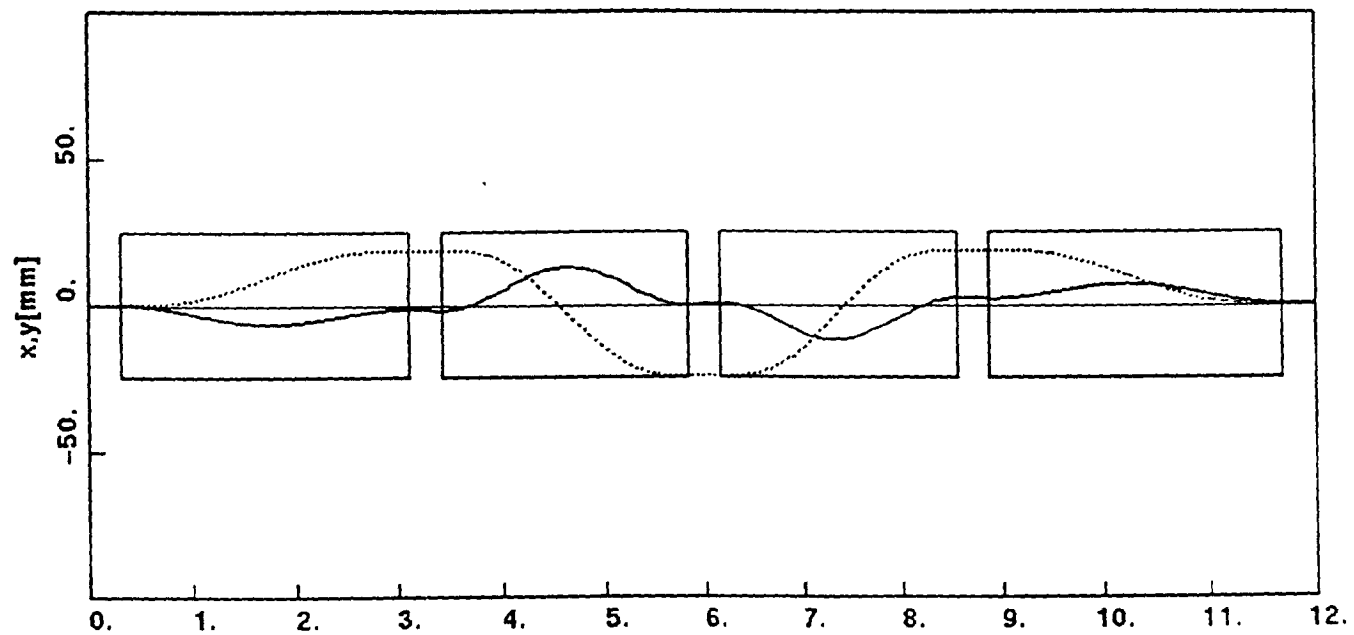
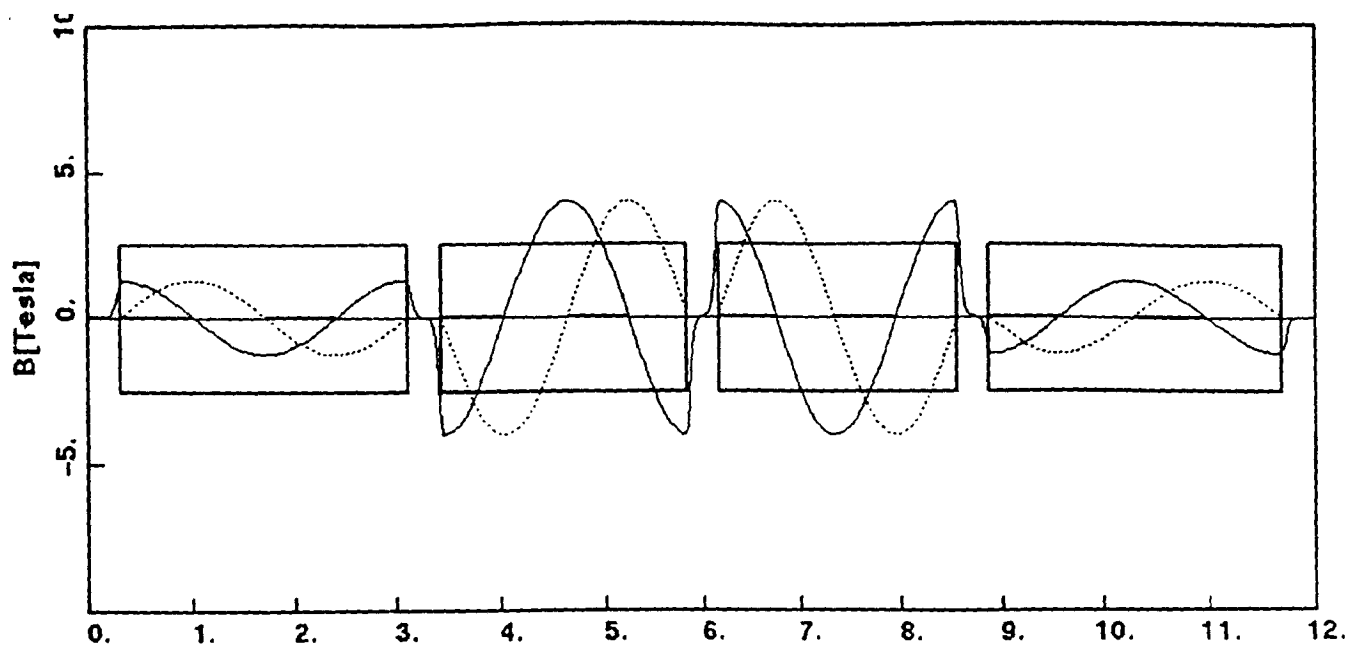
theta = 4.104944370826322 phi = 136.0836722784004

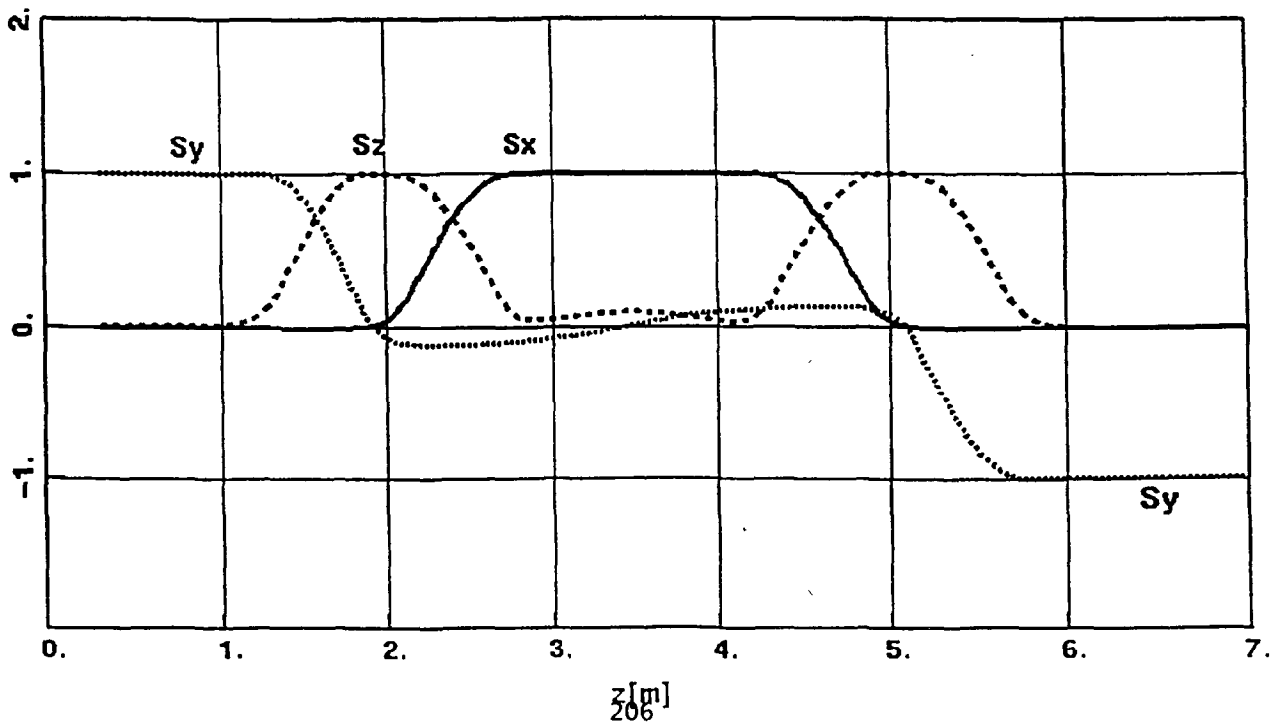
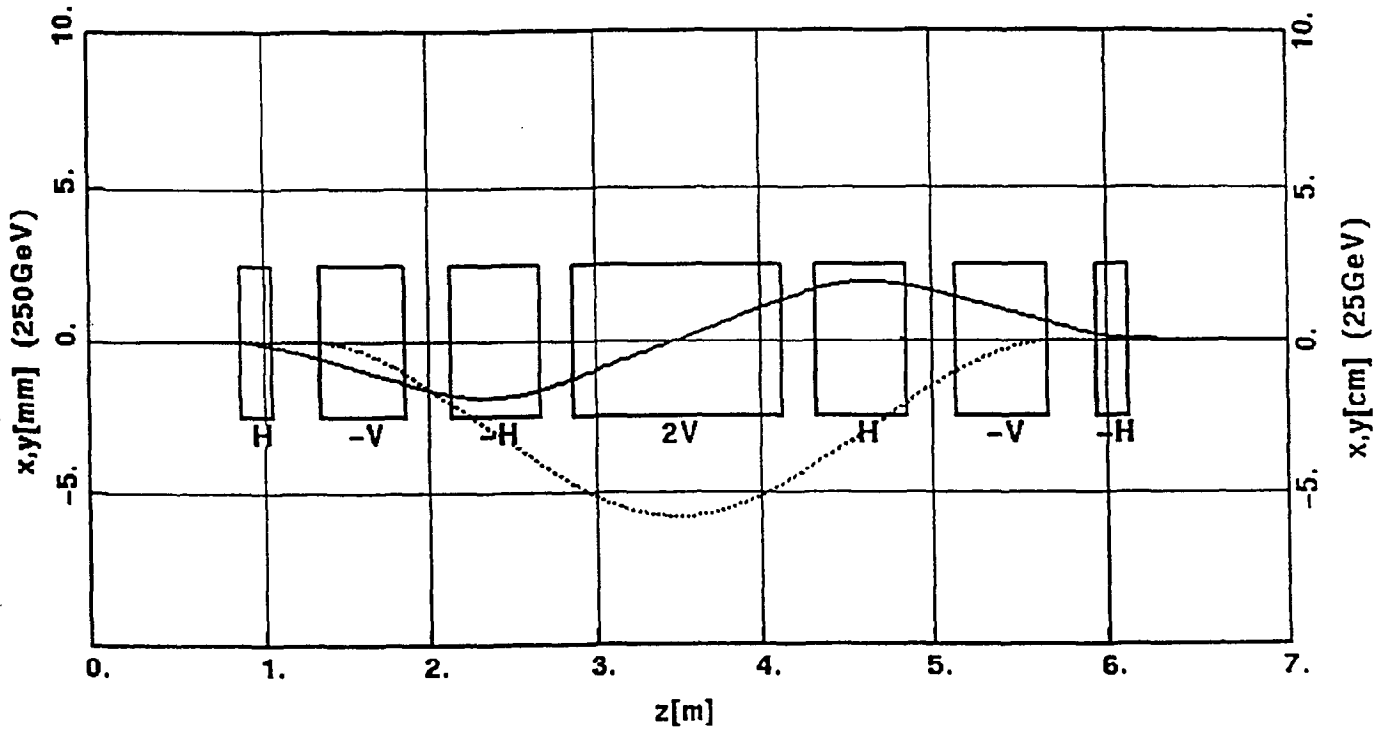
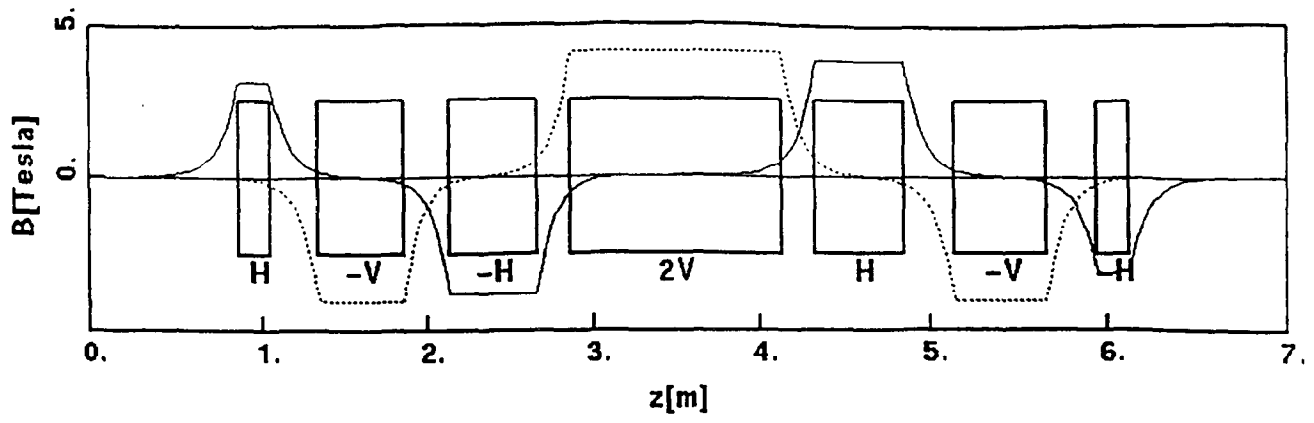
4 dipoles

half-gap[mm] = 50.000

	center[m]	length[m]	angle[deg]	helix[deg]	field[T]	field integrals [T-m]		
1	1.42000	2.40000	0.00000	-360.00	1.45800	2.22792	2.38074	0.05108
2	4.14000	2.40000	180.00000	-360.00	4.00000	6.11526	6.53588	0.35870
3	6.86000	2.40000	0.00000	-360.00	4.00000	6.11337	6.53479	0.34550
4	9.58000	2.40000	180.00000	-360.00	1.45800	2.22804	2.38074	0.04953

Field integrals (x,y,z) [T-m] = 16.6845642 17.8127556 0.8046529  
 Traj Lengthening [mm] = 1.7886492





standard\_input

enter run no, page no 4H 401

continue [y/n]? y

btune = 1.00000000 1.00000000

z	x [mm]	xp[mrad]	y [mm]	yp[mrad]	sx	sy	sz	phi	theta
0.000	0.0000000	0.0000000	0.0000000	0.0000000	0.0000000	1.0000000	0.0000000	35.000	0.000
3.281	-1.7582144	9.6466311	24.2450455	4.7086129	-0.8137487	0.5810979	0.0117588	-179.387	-0.534
ihlf = 11 at z= 3.560001562499889: force integration!									
6.000	-0.9578981	-0.1509676	10.6453288	-0.0005310	-0.9472601	0.2923422	-0.1312797	-172.510	19.718
8.720	-0.8248315	1.6006738	-3.3334773	0.7377118	-0.9958996	-0.0417663	0.0802466	-166.631	8.422
12.000	-0.7868801	0.0952840	0.4315327	-0.0005731	-0.9998586	-0.0155142	0.0064863	-167.710	11.494

psi = 89.11111538439651 or 90.88888461560349

theta = 11.49411068162717 phi = -167.7095363210670

4 dipoles

half-gap[mm] = 4.000

	center[m]	length[m]	angle[deg]	helix[deg]	field[T]	field integrals [T-m]		
1	2.58000	1.96000	0.00000	360.00	3.41000	4.25489	4.28318	0.09114
2	4.86000	1.96000	180.00000	360.00	1.94000	2.42068	2.43694	0.07504
3	7.14000	1.96000	180.00000	360.00	1.94000	2.42068	2.43694	0.02873
4	9.42000	1.96000	180.00000	-360.00	0.53000	0.66132	0.66576	0.00193

Field integrals (x,y,z) [T-m] = 9.7575793 9.8227801 0.1866442  
 Traj Lengthening [mm] = 0.5200829

## standard\_input

enter run no, page no 3H YZ

continue [y/n]? y

btune = 1.33000000

z	x [mm]	xp[mrad]	y [mm]	yp[mrad]	sx	sy	sz	phi	theta
0.000	0.0000000	0.0000000	0.0000000	0.0000000	0.0000000	1.0000000	0.0000000	35.000	0.000
3.101	5.7759610	-0.0000020	0.0739971	0.0528269	-0.0424452	0.9990704	-0.0075309	169.913	-1.183
4.501	-15.9107837	-36.1112599	-13.8849586	-0.1260379	-0.6177343	0.5010153	-0.6061254	178.473	49.943

1hlf = 11 at z= 5.700001464843313: force integration!

5.900	-37.5538083	0.0006571	-0.3584726	-0.3615173	-0.6496804	-0.5117466	0.5603390	40.793	-0.009
9.000	0.0002671	0.0012516	-0.8754896	-0.0063952	-0.0817333	-0.1359936	0.9873325	-165.854	-39.529

psi = 82.18391978422778 or 97.81608021577222

theta = -39.52937995609591 phi = -165.8543635620809

3 dipoles

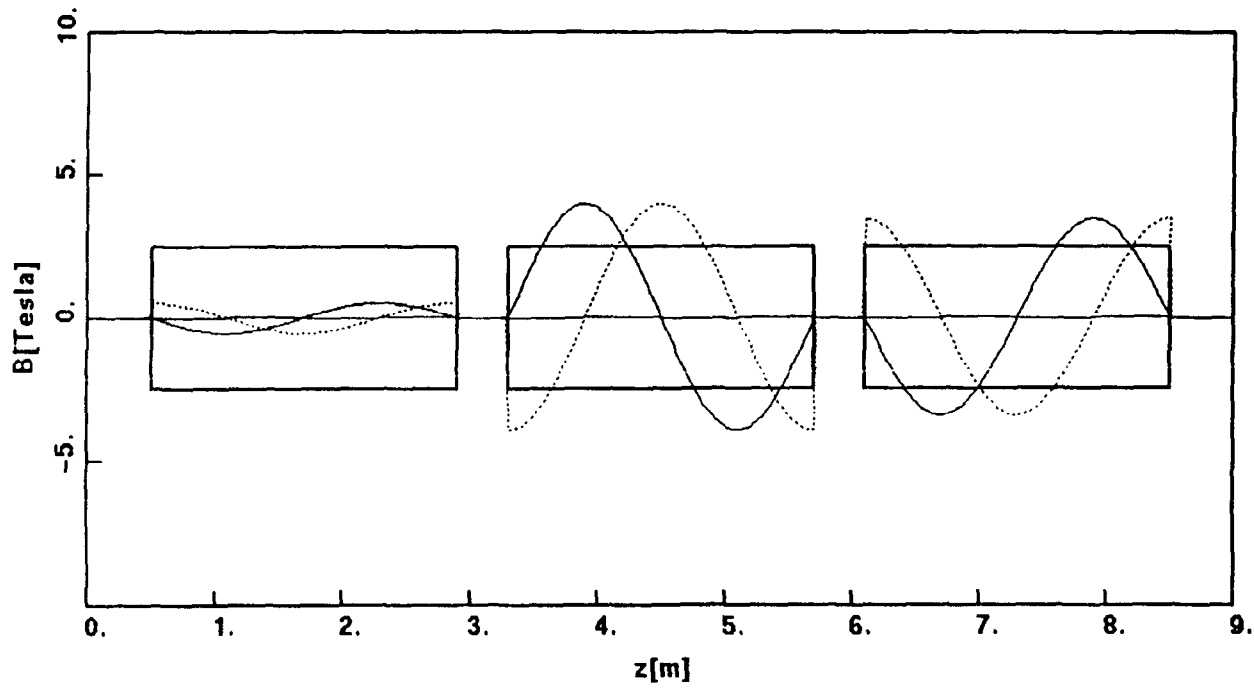
half-gap[mm] = 4.000

	center[m]	length[m]	angle[deg]	helix[deg]	field[T]	field integrals [T-m]		
1	1.70000	2.40000	90.00000	360.00	0.53200	0.81738	0.81284	0.00354
2	4.50000	2.40000	90.00000	360.00	-3.99000	6.13028	6.09626	0.19716
3	7.30000	2.40000	90.00000	360.00	3.45800	5.31240	5.28343	0.14009

Field integrals (x,y,z) [T-m] = 12.2598492 12.1925301 0.3197267

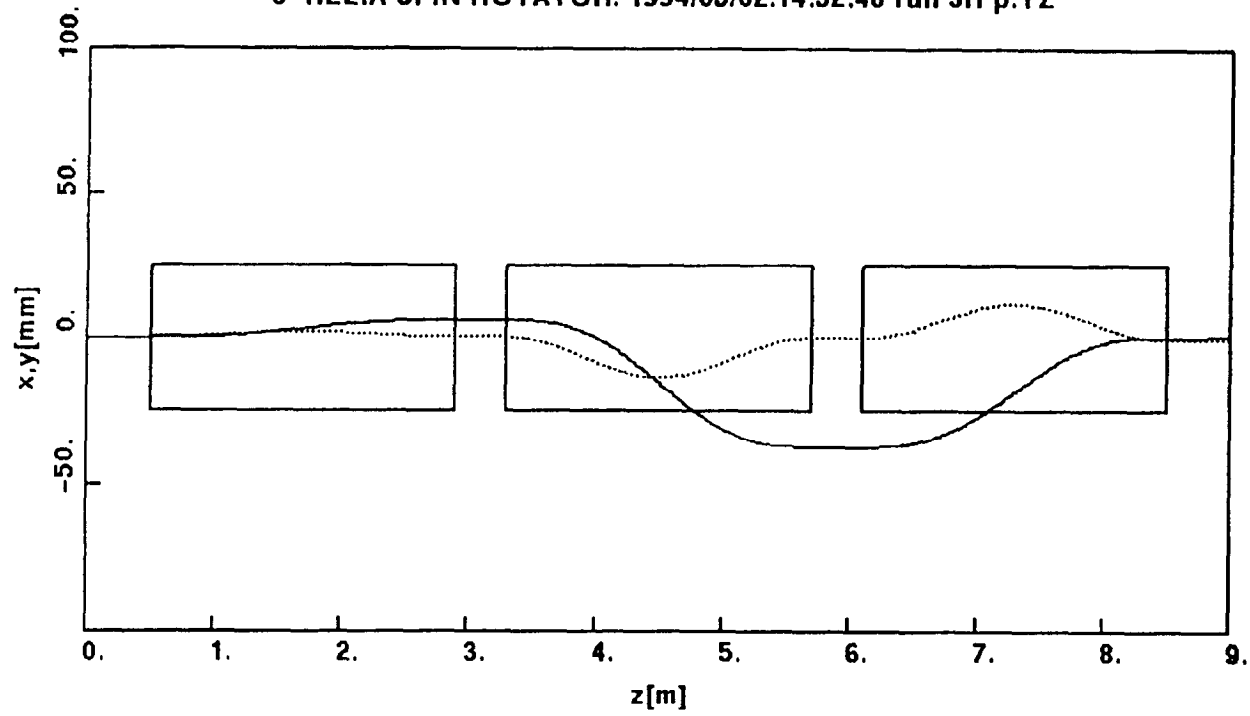
Traj Lengthening [mm] = 1.3832471

3-HELIX SPIN ROTATOR. 1994/05/02.14:54:14 run 3H p.YZ

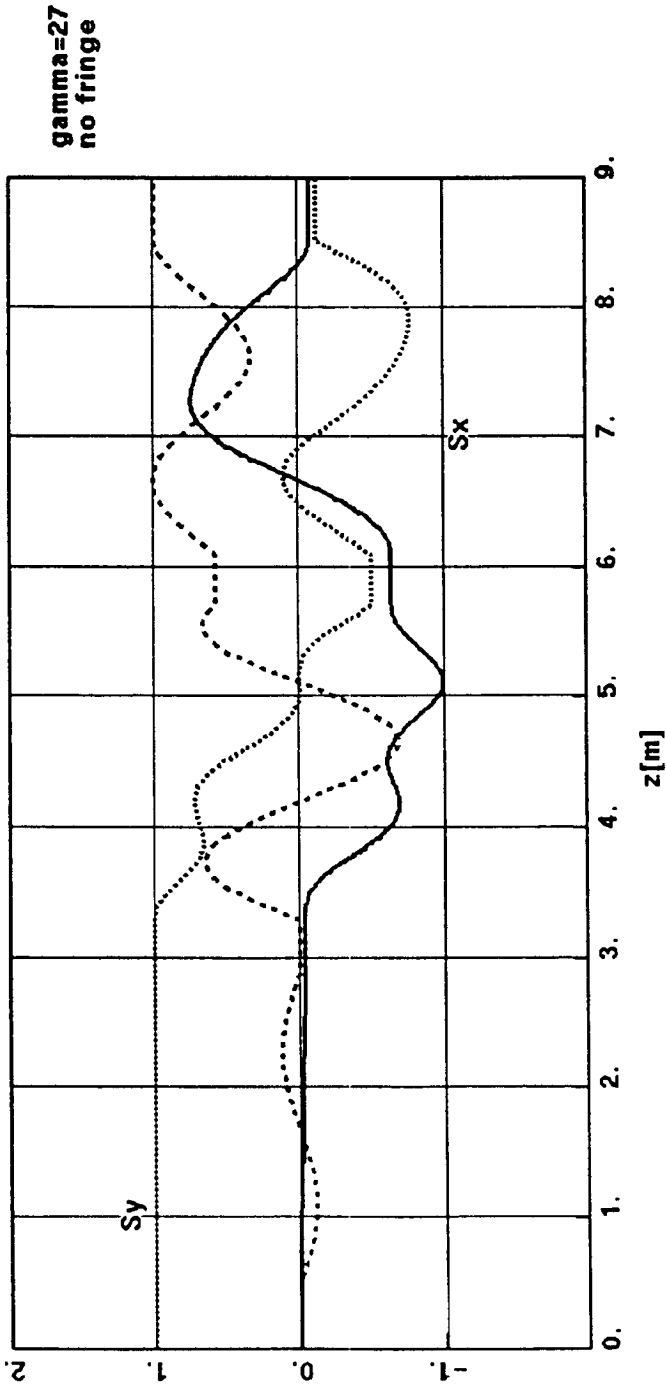


$\gamma=27$   
 $B=0.532/3.99/3.458$  [T]  
no fringe

3-HELIX SPIN ROTATOR. 1994/05/02.14:52:46 run 3H p.YZ



3-HELIX SPIN ROTATOR. 1994/05/02.14:49:32 run 3H p.YZ





**S. Tepikian**

**Brookhaven National Laboratory**

**Upton, NY 11973-5000**

**Snake Resonances**

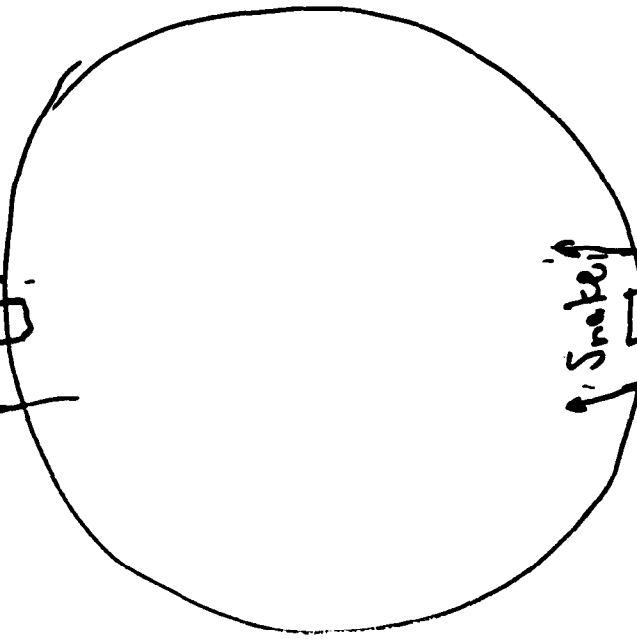
# Snake Resonances

Resonances:  $MG = 2$

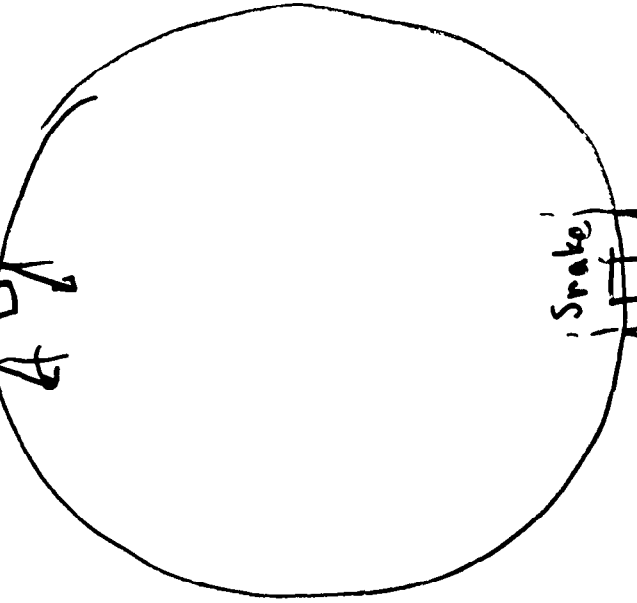
Imperfection

First Revolution

↑ error field



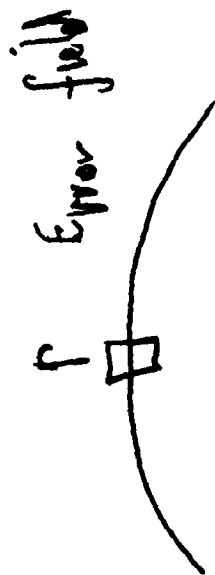
Second Revolution  
↑ error field



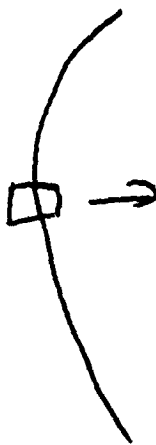
# Snake Resonances

Snake Resonance

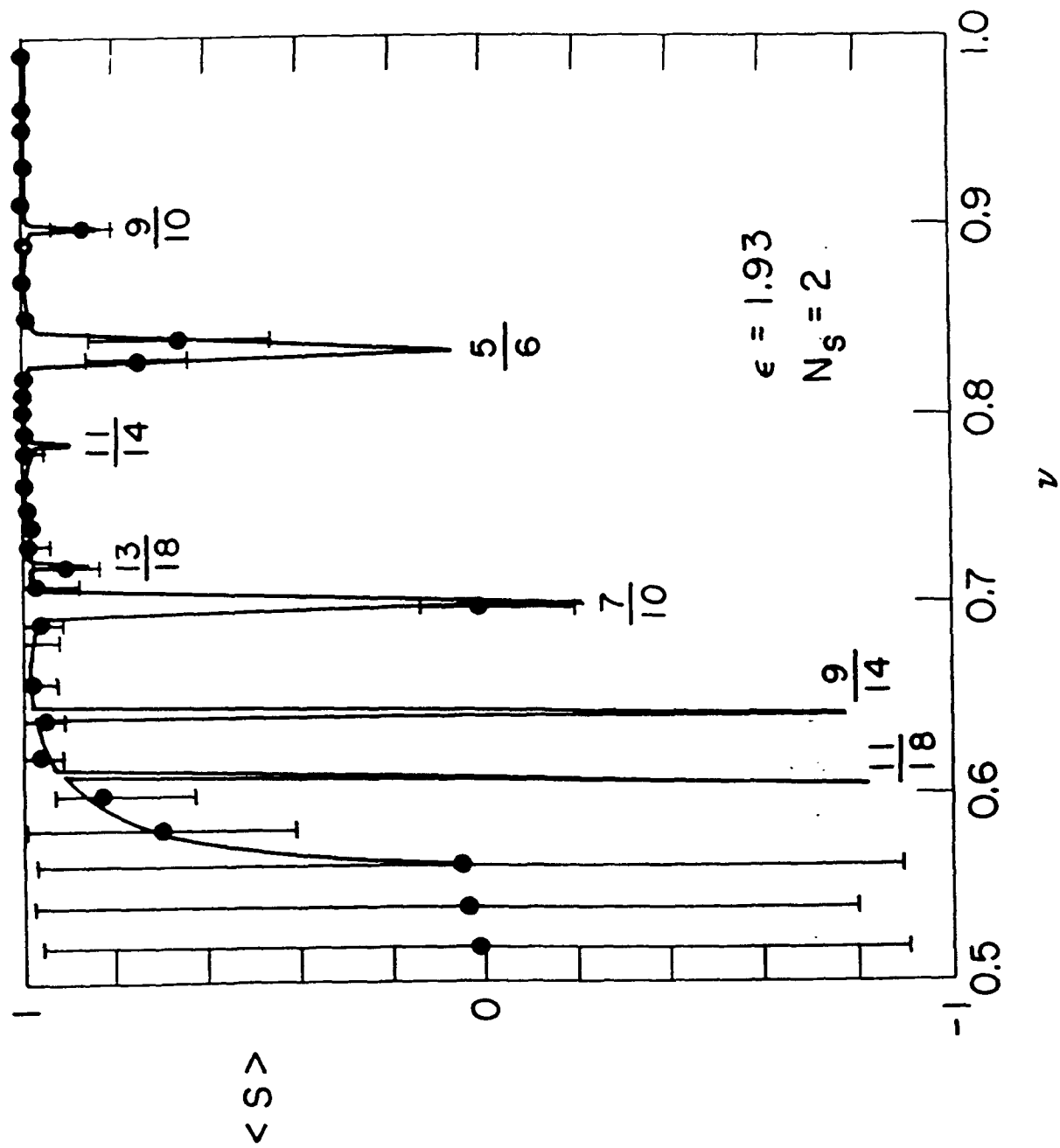
First Revolution



Second Revolution



Error Accumulate Rather than Cancell.



## Snake Resonances

Higher order Snake Resonance requires more revolutions to observe.

$$\text{integer} = p \frac{2}{N_s} (v_s \pm mK)$$

$p \rightarrow$  order of Snake resonance

$m \rightarrow 1, 2, \dots, 2p-1$

Model:  $N_s$  Siberian Snakes

$$\text{Precession axis} = \pm \frac{\pi}{2N_s}$$

## Snake Resonances

- 1) Theory assumes single Resonance
- 2) May be model dependant.

Solution:

Needs Spin tracking

# Tracking Programs

Snake  
(Jean Buon)

Smile  
(Satish Manu)

Teuspoon  
(Satish Manu, R. Palmer)

Cosy + Spin  
(M Barz)

## Tracking Programs

Snake:

[1] Tracks Vertical dimension only,

[2] Quadruples  $\rightarrow$   $2 \times 2$  matrix

Used to test ideas and gain understanding of Snakes.

## Tracking Programs

Smile:

- [1] Thin lens tracking of orbit with spin.
- [2] Uses radiative correction for polarized electron machines.

# Tracking Programs

Teaspoon = Teapot + Spin

[1] Thin lens tracking code.

[2] R.F. Acceleration

[3] Teapot is the standard Simulation Program of RHIC

Cosy + Spin

[1] DA Package

# Tracking Programs

Candidates for RHIC:

Teaspoon

Cosy + Spin

No Helical Magnet

Needs translation from Database

Needs:

Helical Snake, Fixed field



**R. A. Phelps**

University of Michigan

Ann Arbor, Michigan 48109

**Spin Flipping a Stored Polarized Proton Beam in the  
Presence of Siberian Snakes**

# Spin Flipping a Stored Polarized Proton Beam in the Presence of Siberian Snakes

Richard A. Phelps  
Randall Laboratory of Physics  
University of Michigan  
Ann Arbor, Michigan 48109

## A. Introduction

When scattering asymmetry experiments are performed in the Tevatron or in RHIC with a stored polarized beam it will be necessary to reverse the beam polarization quite often to reduce systematic errors in the experiment. “Spin flipping” a stored polarized proton beam is a relatively new technology; I discuss the requirements for spin flipping a stored polarized proton beam in a high energy storage ring with Siberian Snakes present.

This paper is organized as follows. I first give a brief introduction to spin dynamics for protons in a storage ring, including a description of induced rf depolarizing resonances. Next it is shown how an rf resonance can be used to spin flip a stored polarized beam. Then data is presented which proves this technique works in principal. I then describe a complication for spin flipping in a storage ring with snakes present, and how to modify the spin flipping hardware to avoid this complication. A description of a device which could be used to flip the polarization of a proton beam in a storage ring possessing an even number of snakes is then presented.

## B. Spin motion in storage rings

As a proton passes through the magnetic fields of a storage ring, at each point its spin will precess around a direction parallel to the magnetic field vector at the point. Because of this precession, as a proton traverses the ring back to the same point, it’s spin will have rotated with respect to it’s initial direction. The direction around which the spin has rotated is called the stable spin direction (SSD) at the point. This stable spin direction can be different from point to point. The angle of precession for a single turn around the ring, which will be the same from point to point, is  $2\pi\nu_{sp}$ , where  $\nu_{sp}$  is called the spin tune. For a ring with no substantial horizontal fields, for most energies the stable spin direction will be everywhere vertical and the spin tune is given by

$$\nu_{sp} = G\gamma, \tag{1}$$

where  $G = 1.792846$  is the anomalous magnetic moment of the proton, and  $\gamma = E/m$ . A full Siberian Snake fixes the spin tune at 1/2 independent of the energy; the stable spin direction in a ring with an even number of snakes as proposed for the Tevatron and for RHIC will also be everywhere vertical.

If there are regions where a horizontal magnetic field exists, the proton’s spin will precess around a horizontal direction in this region. In general these small horizontal precession “kick” will be uncorrelated with the spin motion. However, if the kicks become correlated with the spin motion, the polarization of the beam will quickly be destroyed. In this case, it is said that a depolarizing resonance condition exists. If  $f_{nv}$  is the frequency

at which the protons experience these horizontal magnetic fields, and  $f_c$  is the circulation frequency of the protons, then the condition for correlation of the horizontal precession kicks with the spin motion is

$$f_{nv} = f_c \times (k \pm \nu_{sp}). \quad (2)$$

If one introduces a horizontal rf magnetic field with frequency  $f_{rf} = f_{nv}$  into the storage ring, by varying the frequency and measuring the polarization, one can use equation 2 to measure the spin tune of the beam. This technique of spin tune measurement was successfully tested at the Indiana University Cyclotron Facility (IUCF) several years ago by our University of Michigan group. An rf solenoid of about 0.002 T-m was used to depolarize the horizontally polarized 104.1 MeV (kinetic energy) beam with a single full snake present. The rf resonance frequency was approximately predicted using equation 2 with  $\nu_{sp} \approx 1/2$ . Polarized protons were injected into the ring with the rf off; the rf magnet was then turned on at a specific frequency and the polarization was measured with the rf on. Runs were taken with frequencies around the predicted position of the depolarizing resonance. Figure 2 shows the radial beam polarization vs this rf frequency. There are two depolarization “dips” because the spin tune is not exactly 1/2. If  $\Delta$  is the “detune” away from 1/2, that is  $\nu_{sp} = 1/2 - \Delta$ , then these resonances are at  $f_{res}^{\pm} = f_c \times (3/2 \pm \Delta)$ . The dips are expected to converge to one dip at  $1.5f_c$  for a perfect snake. The half width half minimum<sup>(2)</sup>  $\delta$  of each dip is proportional to the induced magnetic field strength.

### C. Spin flipping with an rf magnetic field

An rf magnetic field can also be used to reverse the polarization direction of a stored, polarized proton beam. I will now assume that the stable spin direction is everywhere vertical and the spin tune is not 1/2. Figure 1 shows the stable spin direction in a frame rotating with a frequency  $f_{rf}$  when a horizontal rf field of frequency  $f_{rf}$  is applied. The angle  $\alpha$  of the stable spin direction off the vertical is given by

$$\cos(\alpha) = \frac{f_{rf} - f_{res}}{\sqrt{(f_{rf} - f_{res})^2 + \delta^2}}, \quad (3)$$

where  $f_{res}$  is the resonance frequency, and  $\delta$  is the rf resonance width. It should be noted that equation 3 holds only when the spin tune is a sufficient distance from 1/2. The complication when  $\nu_{sp} = 1/2$  will be discussed later. From equation 3, one sees that if the applied rf is turned on at a frequency which is many widths away from the resonance,  $\alpha = 0^\circ$ . If the rf frequency is then ramped through the resonance value and turned off when  $f_{rf}$  is many widths to the other side of the resonance, the stable spin direction will rotate from the vertical, through the horizontal direction, then to the opposite vertical direction. If this rf ramp is very slow, so that the protons see very tiny changes in the stable spin direction from turn to turn, then the spin will simply follow the stable spin direction and be reversed.

This “adiabatic passage” technique has been demonstrated for the case of a stored polarized beam without a snake. Figure 3 shows data taken at IUCF with a vertically polarized proton beam. Polarized protons were injected with the rf off, then the rf was turned on 1.75 kHz below the resonance frequency and ramped linearly to 1.75 kHz above

the resonance frequency; the polarization was measured after the ramp. The plot is the vertical polarization after the rf ramp vs the rf ramp time. All the points had the same rf magnetic field strength. As can be seen from the data, spin flipping is more efficient for slower ramp times. The curve is a fit to the data of a modified version of the Froissart-Stora formula<sup>(1)</sup> for the polarization,  $P_f$ , after passage through an rf depolarizing resonance:

$$P_f = P_i \times [2\exp\left(-\frac{(\pi\delta)^2}{df_{rf}/dt}\right) - 1]. \quad (4)$$

The curve is a fit in the parameters  $P_i$ , the initial polarization, and  $\delta$ .  $df_{rf}/dt$  is the rf ramp rate. The value obtained for  $\delta$  is in good agreement with the value obtained from the spin tune measurement as described above.

An rf field used for spin flipping should be orthogonal to the stable spin direction at the rf magnet location to optimize the spin-field coupling. This stable spin direction is vertical in a storage ring with an even number of snakes, hence the rf field direction should have longitudinal and/or radial components. Since the spin precession for a given field strength of a longitudinal field is inversely proportional to the momentum, and for a radial field is momentum independent at high energy, to get a large enough horizontal rf field to flip at hundreds of GeV one would use a radial rf dipole.

The data from figure 3 was taken without a snake. The adiabatic passage technique has not been tested in the presence of a Siberian Snake when the spin tune is very close to 1/2. There is an added complication to the spin flipping mechanism<sup>(3)</sup> when the spin tune is close to 1/2, which can be seen by the following argument. When the spin tune is exactly 1/2 the resonance frequency is  $(n + 1/2)f_c$ . Assuming one has a single rf magnet, when the magnet is set to the resonance frequency, some particles will see no field at all each time they pass through the magnet, since the field reverses sign each time a particular particle goes through, and some particles will be at the 0 of the sine wave. Hence ramping through the resonance frequency will not flip the spin of these particles.

The picture of the stable spin direction given in figure 1 is derived assuming that the rf field generates a single isolated depolarizing resonance. Figure 4 shows how the field generated by a radial dipole can be decomposed into two counter rotating fields in the horizontal plane rotating with frequency  $f_{rf}$ . When the resonance frequency is approached, for most values of the spin tune, the field rotating in one direction, say  $\mathbf{B}_+$ , causes the resonance, while  $\mathbf{B}_-$  is uncorrelated with the spin motion and can be ignored. In figure 2, one of the resonances is caused by  $\mathbf{B}_+$  and the other is caused by  $\mathbf{B}_-$ . Then equation 3 for the angle of the stable spin direction off the vertical is correct. When the spin tune gets close to 1/2, both rotating fields are correlated with the spin precession, and hence there are two “overlapping” resonances present; this would correspond to having 2 closely spaced dips in figure 2. These overlapping resonances are expected to spoil the spin flip mechanism. To correct this problem, one must eliminate the field  $\mathbf{B}_-$ .

$\mathbf{B}_-$  is eliminated by installing two rf magnets with the correct positions and relative phase for cancellation. This cancellation is made almost trivially if the snakes flip the radial and longitudinal spin components (180° spin rotation about a horizontal direction which is directed 45° between the radial and longitudinal directions). These “hybrid” snakes (neither type I or type II) are proposed for the Tevatron<sup>(4)</sup>, and will be the only

case considered here. An rf dipole at the entrance of one of the snakes has a field

$$\mathbf{B}_u(t) = B_o \cos(2\pi f_{rf} t) \hat{\mathbf{r}}, \quad (5a)$$

where  $\hat{\mathbf{r}}$  is a unit vector in the radial direction and  $f_{rf}$  is the applied frequency. Because of the snake, this field is physically equivalent to a field at the exit with  $\hat{\mathbf{r}}$  in equation 5a replaced by  $\hat{\mathbf{l}}$ , the unit longitudinal vector (this is not exactly true, since we still get the precession one expects from a transverse field, but it is around the longitudinal direction). Place a second rf dipole just downstream of the snake, with a field of the same magnitude, phase advanced by  $\pi/2$  and time advanced by  $d/c$  with respect to  $\mathbf{B}_u(t)$ , where  $d$  is the distance between the rf dipoles and  $c$  is the speed of light. That is, the downstream field should be

$$\mathbf{B}_d(t) = B_o \sin(2\pi f_{rf} [t - d/c]) \hat{\mathbf{r}}. \quad (5b)$$

The total effect of these 2 fields and the snake will be equivalent to a field at the exit of the snake

$$\mathbf{B}_{\text{eff}}(t) = B_o \times [\cos(2\pi f_{rf} t) \hat{\mathbf{l}} + \sin(2\pi f_{rf} t) \hat{\mathbf{r}}] = \mathbf{B}_+(t). \quad (6)$$

The field  $\mathbf{B}_-$  has been canceled, and the field  $\mathbf{B}_+$  has doubled in strength. Then ramping the frequency through the resonance will flip the spin.

#### D. Positioning of rf magnets

If space for rf magnets is tight, it is not necessary to place the rf dipole magnets in the same straight section as the snake. For the cancellation of the field  $\mathbf{B}_-$ , it is necessary that the total spin precession between the 2 rf dipoles have the effect of flipping the radial and longitudinal components of the spin. Let  $\mathbf{S}$  be the spin precession matrix of the snake, and let  $\mathbf{D}$  be the spin precession matrix for the dipoles just before and just after the snake (these horizontal bends are assumed to give equal spin precessions around the vertical direction). It is easy to show that the combination  $\mathbf{DSD}$  also flips the radial and longitudinal spin components if  $\mathbf{S}$  alone does, regardless of the particle energy. Hence these radial rf dipoles can be placed in the straight sections just before and just after the section the snake is in, as long as the field integrals of these sets of horizontal bends are equal.

#### E. Orbit correction

Each of the rf dipoles will cause a vertical kick of the beam. This will cause emittance blowup unless these kicks can be corrected. If each magnet is replaced by 2 magnets separated by  $180^\circ$  in vertical betatron phase, the kick from the second magnet can correct the kick from the first. The requirements for correction are that (a.) the rf excitation of the first magnet is time delayed with respect to the second by  $d/c$ , where  $d$  is the distance between the magnets, and (b.) if  $\beta_1$  is the vertical beta function at the first magnet and  $\theta_1$  its orbit kick, and  $\beta_2$  and  $\theta_2$  are for the second magnet, then

$$\sqrt{\beta_1} \theta_1 = \sqrt{\beta_2} \theta_2. \quad (7)$$

We must check that  $\mathbf{B}_-$  is still cancelled. This is no problem if the arrangement is made symmetrical upstream and downstream of the snake. Then the 2 magnets closest to the

snake are separated from the snake by the same number of horizontal bends, hence the  $\mathbf{B}_-$  field they generate is cancelled; the same can be said for the 2 outer rf dipoles, even though they are each separated from the snake by a different number of vertical bends than the inner rf dipoles. The arrangement is shown in figure 5. Bending dipole 2 should have the same horizontal bend as dipole 3, and dipole 1 the same as 4. If all rf magnets are equal length, these radial rf fields should be

$$\begin{aligned}
B_1(t) &= B_1 \cos(2\pi f_{rf} t), \\
B_2(t) &= B_2 \cos(2\pi f_{rf} [t - d/c]), \\
B_3(t) &= B_2 \sin(2\pi f_{rf} [t - d/c - d'/c]), \\
B_4(t) &= B_1 \sin(2\pi f_{rf} [t - 2d/c - d'/c]).
\end{aligned}
\tag{8}$$

$B_2/B_1 = \theta_2/\theta_1 = \sqrt{\beta_1/\beta_2}$  as in equation 7. If  $\beta_3$  and  $\beta_4$  are the vertical beta functions at rf dipole 3 and 4 respectively, one should also arrange that  $\beta_1/\beta_2 = \beta_4/\beta_3$  for proper orbit correction and resonance cancellation.

It should be noted that since there will be at least one horizontal bend between rf dipoles 1 and 2 (horizontal bend= $\phi$ ), and also between rf dipoles 3 and 4, the spin will have precessed by an amount  $G\gamma\phi$  between each pair of rf magnets, so the rf spin precession kick will not add up in phase unless  $G\gamma\phi = 2\pi n$  for some integer  $n$ . This will weaken the resonance strength by a factor  $\sqrt{B_1^2 + B_2^2 + 2B_1B_2\cos(G\gamma\phi)}/(B_1 + B_2) \leq 1$ . This is no problem as long as the energy or the number of dipoles between each pair of rf magnets is chosen judiciously, and the rf ramp rate is increased to take this lower resonance strength into account.

## F. Magnet requirements

To get an idea of the rf field required, I will consider spin flipping 900 GeV protons in the Tevatron when  $\nu_{sp} \approx 1/2$ . The parameters to be fixed are the resonance width  $\delta$  and the rf ramp rate  $df_{rf}/dt$ . For protons of momentum  $p$ , the resonance width is given by:

$$\delta[H z] = \frac{f_c[H z]}{4\pi} \frac{(1 + G\gamma)}{3.33p[GeV/c]} \int B dl [T \cdot m] \approx \frac{f_c}{22} \int B dl,
\tag{9}$$

where  $\int B dl$  is the total integrated field amplitude over all 4 rf magnets. From equation 4, we see that the ratio of final to initial polarization goes like  $2\exp(-\kappa) - 1$ , where

$$\kappa \approx \frac{f_c^2 (\int B dl)^2}{50 \Delta f_{rf} / \Delta t}.
\tag{10}$$

Here  $\Delta f_{rf}$  is the rf ramp interval, and  $\Delta t$  is the ramp time.

Conservatively choosing  $\kappa \approx 10$ , then  $P_f/P_i = -0.9999$ . The ‘‘half life’’ of the spin, or the number of times one can spin flip before the polarization is half gone, will be about 7000. The goal then is to choose  $\int B dl$  large enough to achieve spin flip in a reasonable time  $\Delta t$ .

For 900 GeV protons,  $f_c \approx 48$  kHz. To avoid turning on the rf too close to resonance, one should choose  $\Delta f_{rf} \gg \delta$ , say for example  $\Delta f_{rf} = 20 \times \delta$ . There is great flexibility in

choosing the parameters  $\int Bdl$ ,  $\Delta f_{rf}$  and  $\Delta t$ . If the system is also to be used to measure the spin tune, then  $\delta$ , the half-width of the rf resonance curve dip, should be at least 75 Hz so the rf resonance is easy to find; then  $\Delta f_{rf} = 1.5$  kHz and by equation 9,  $\int Bdl = 0.034 T \cdot m$ . Since  $\nu_{sp} \approx 1/2$ , then  $f_{res} \approx f_c/2 \approx 24$  kHz. To make  $\kappa = 10$  with  $\int Bdl = 0.034 T \cdot m$ , by equation 10 the rf ramp time should be  $\Delta t \approx 280$  msec for a spatially uniform rf magnetic fields. Due to nonuniformities in these fields, one might increase the ramp time slightly.

### G. Conclusions

A scheme has been presented for an rf dipole device which will flip the spin of a stored polarized proton beam in a high energy storage ring which uses an even number of Siberian Snakes to preserve polarization during acceleration. This method utilizes a particular "hybrid" snake's property of switching the radial and vertical components of the spin as the particle passes through it. This hybrid snake has been considered for both the Tevatron and RHIC. The scheme requires 4 simple rf radial field dipoles located symmetrically around one of the snakes. The device self corrects its orbit kick to the extent that one can estimate the vertical beta function in the storage ring. The conditions for placement of the rf dipoles are flexible enough so that this solution, though not unique, should be considered for use in high energy polarized proton storage rings.

This research was supported by grants from the U.S. Department of Energy and the U.S. National Science Foundation.

### References

- (1) M. Froissart and R. Stora, Nucl. Instr. and Methods, **7**, 297 (1960).
- (2) V. A. Anferov et al., Phys. Rev. A **46**, R7383 (1992).
- (3) Yu. Shatunov, presentation at the SPIN93 meeting in Protvino, Russia, 1993.
- (4) Progress Report: Acceleration of Polarized Protons to 1 TeV in the Fermilab Tevatron, University of Michigan Report, August 1994 (unpublished).

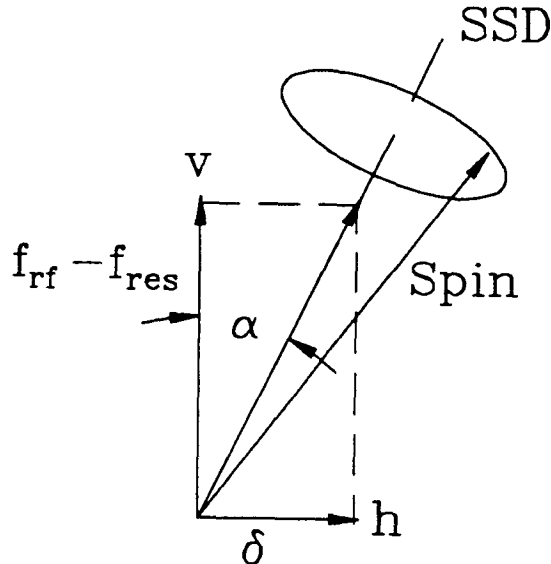


Figure 1. The tilt of the stable spin direction (SSD) in the presence of an rf field.  $\delta$  is the rf resonance width.

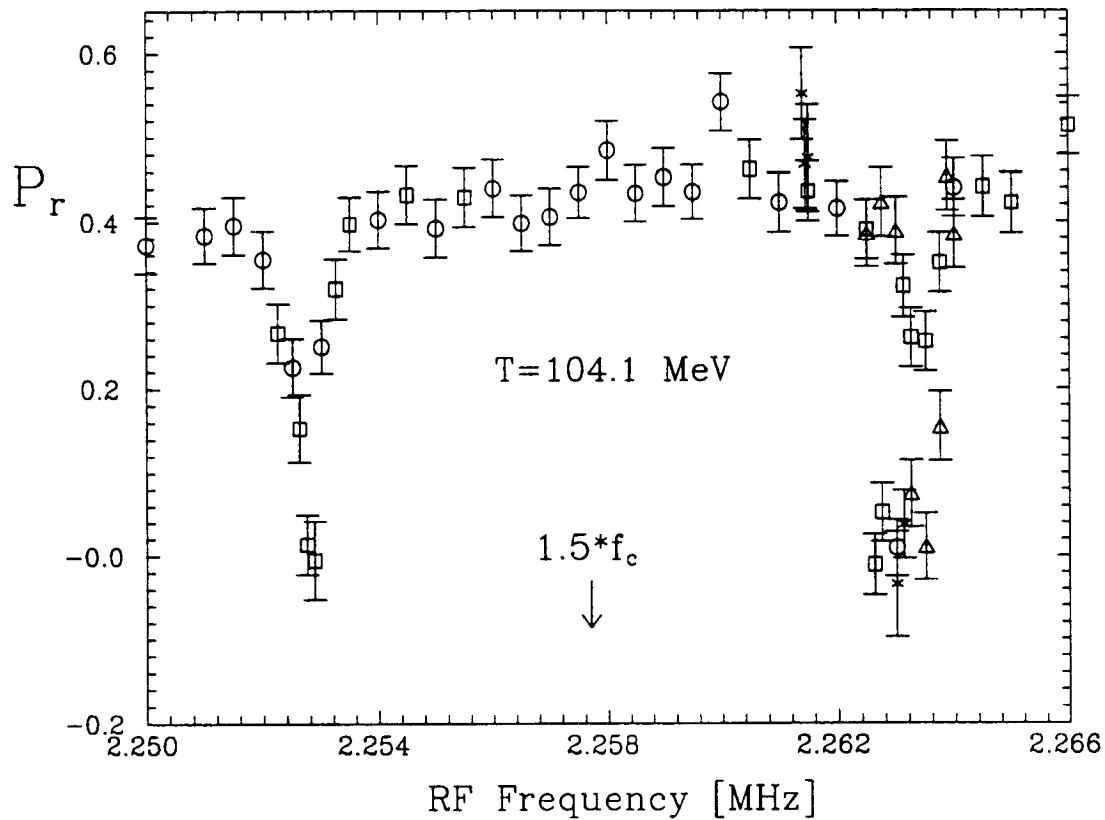


Figure 2. rf induced resonances in the presence of a Siberian Snake. The 2 dips centered around  $1.5f_c$  should merge to one dip when the spin tune is exactly  $1/2$ .

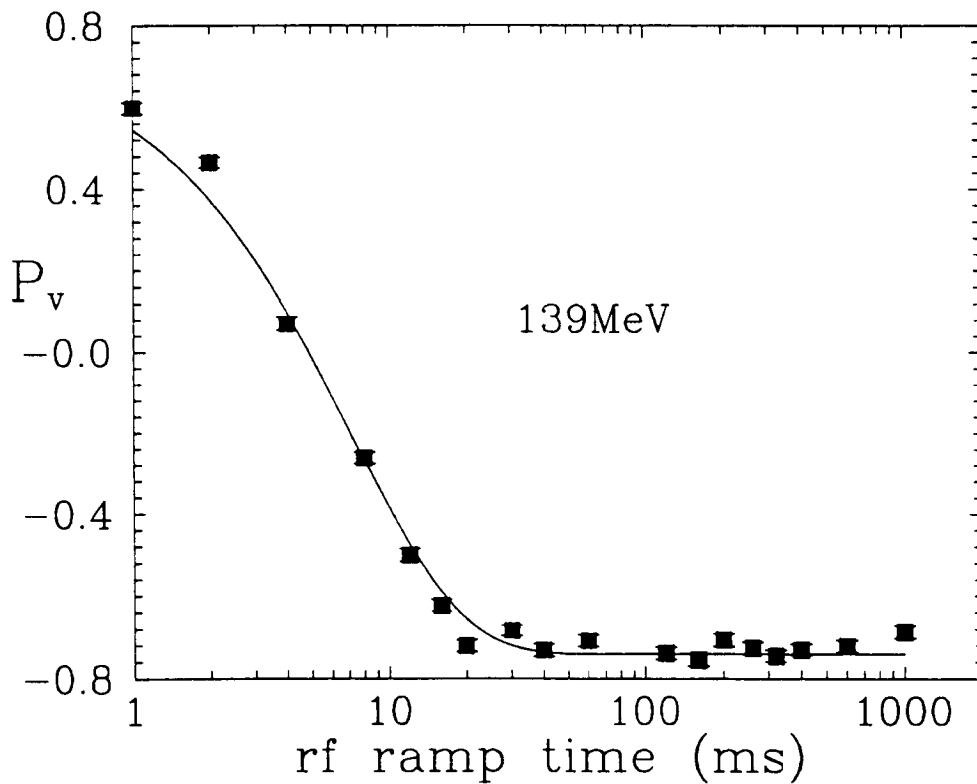


Figure 3. Spin flip data taken at IUCF with a single rf solenoid magnet and no Siberian Snake.

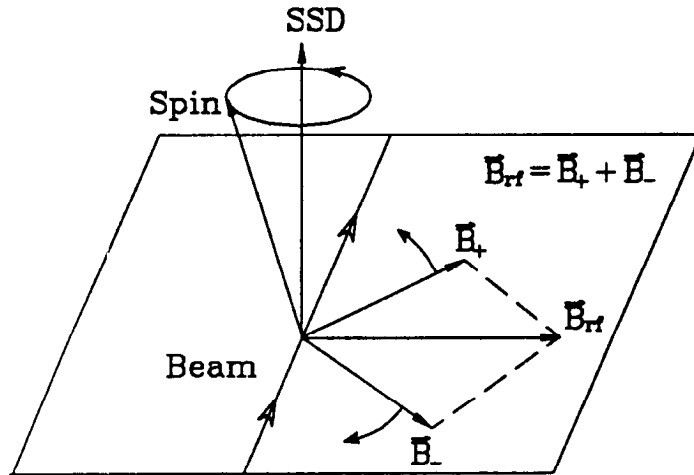


Figure 4. Decomposition of a radial rf dipole field into 2 counter rotating fields. If the spin tune is away from 1/2, near the resonance frequency  $B_+$  becomes correlated with the spin motion while  $B_-$  does not. When the spin tune is close to 1/2, both are correlated with the spin motion.

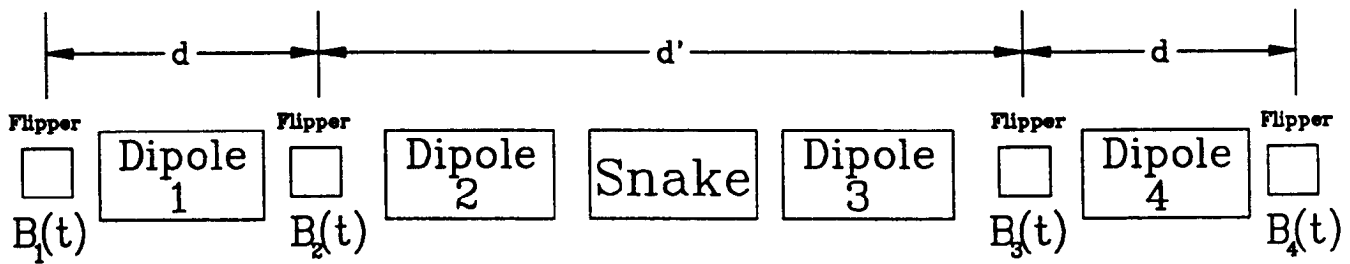


Figure 5. The full spin flip configuration.



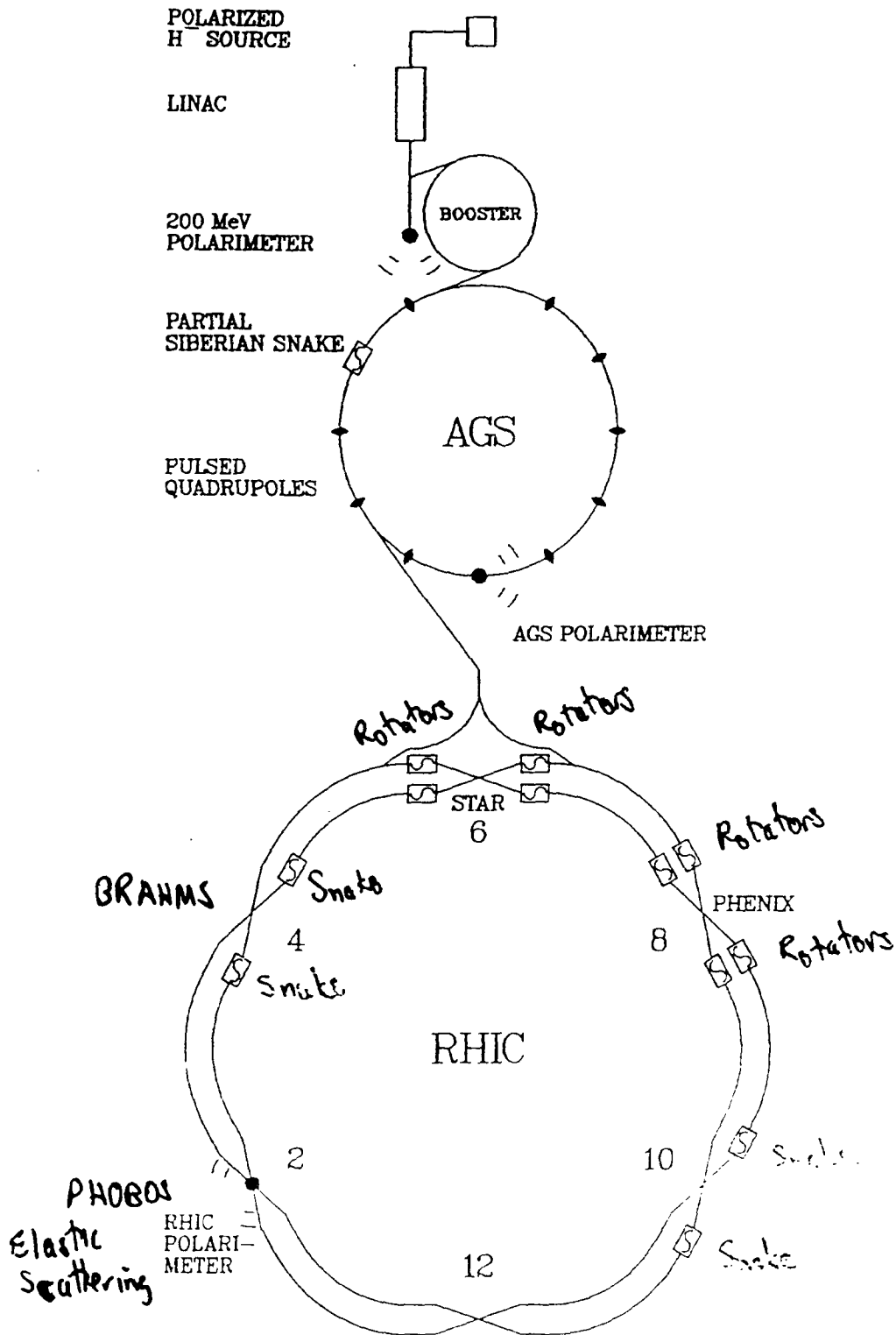
**S. Tepikian**

**Brookhaven National Laboratory**

**Upton, NY 11973-5000**

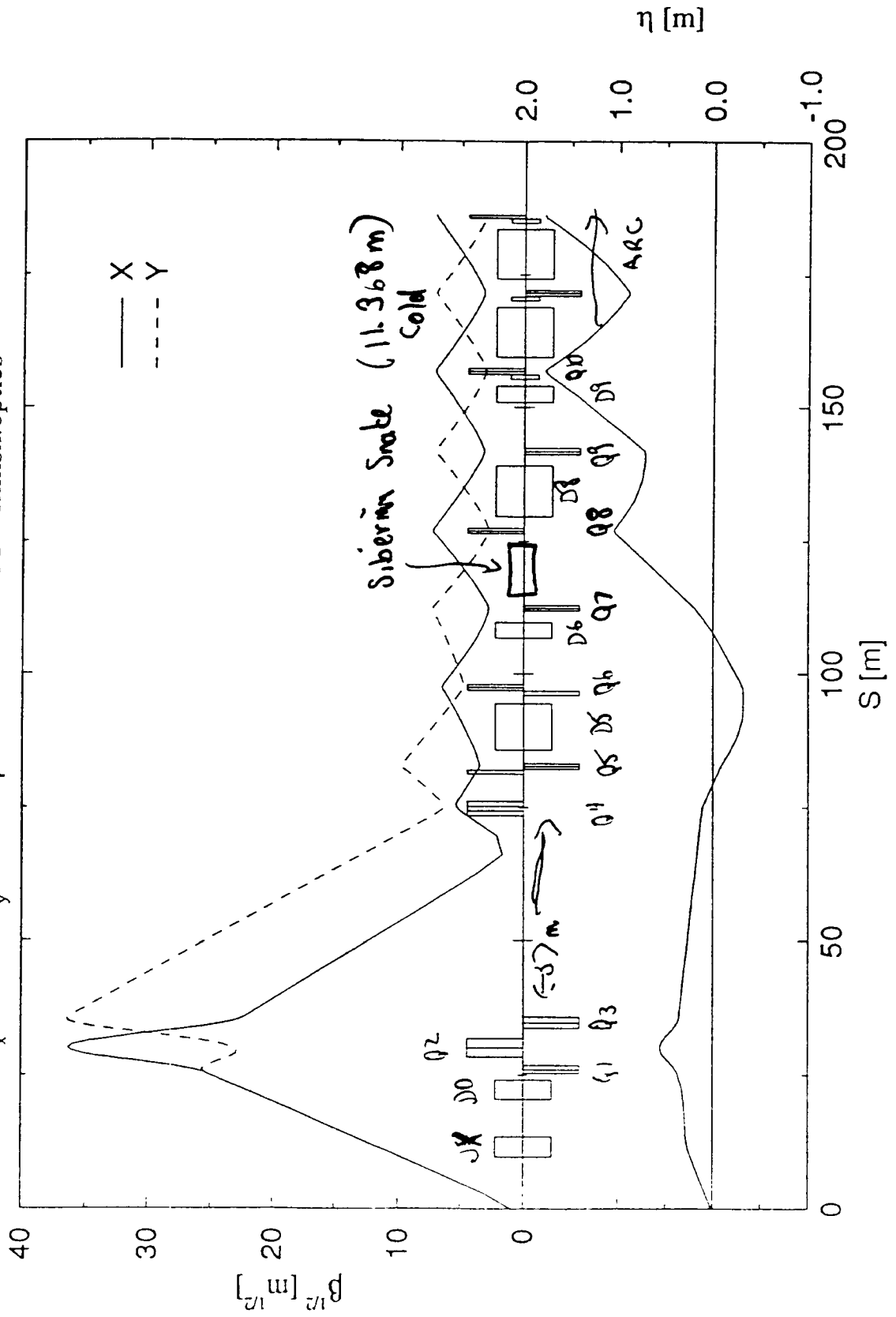
**Polarized Proton Collisions at Brookhaven**

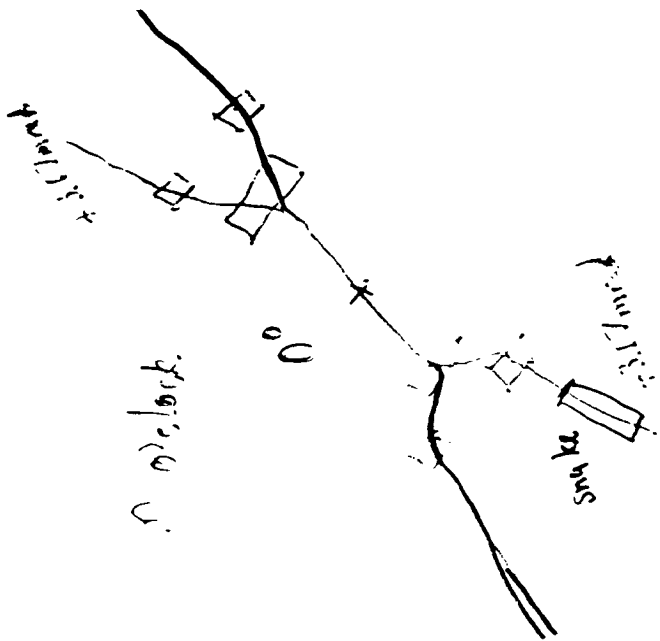
# POLARIZED PROTON COLLISIONS AT BROOKHAVEN



# RHIC Insertion Functions

$v_x = 28.19$   $v_y = 29.18$   $\beta^* = 1.00456$  FILE = rhinsh.optics





$$\Delta\theta = 180^\circ - 7.35 \text{ mrad}$$



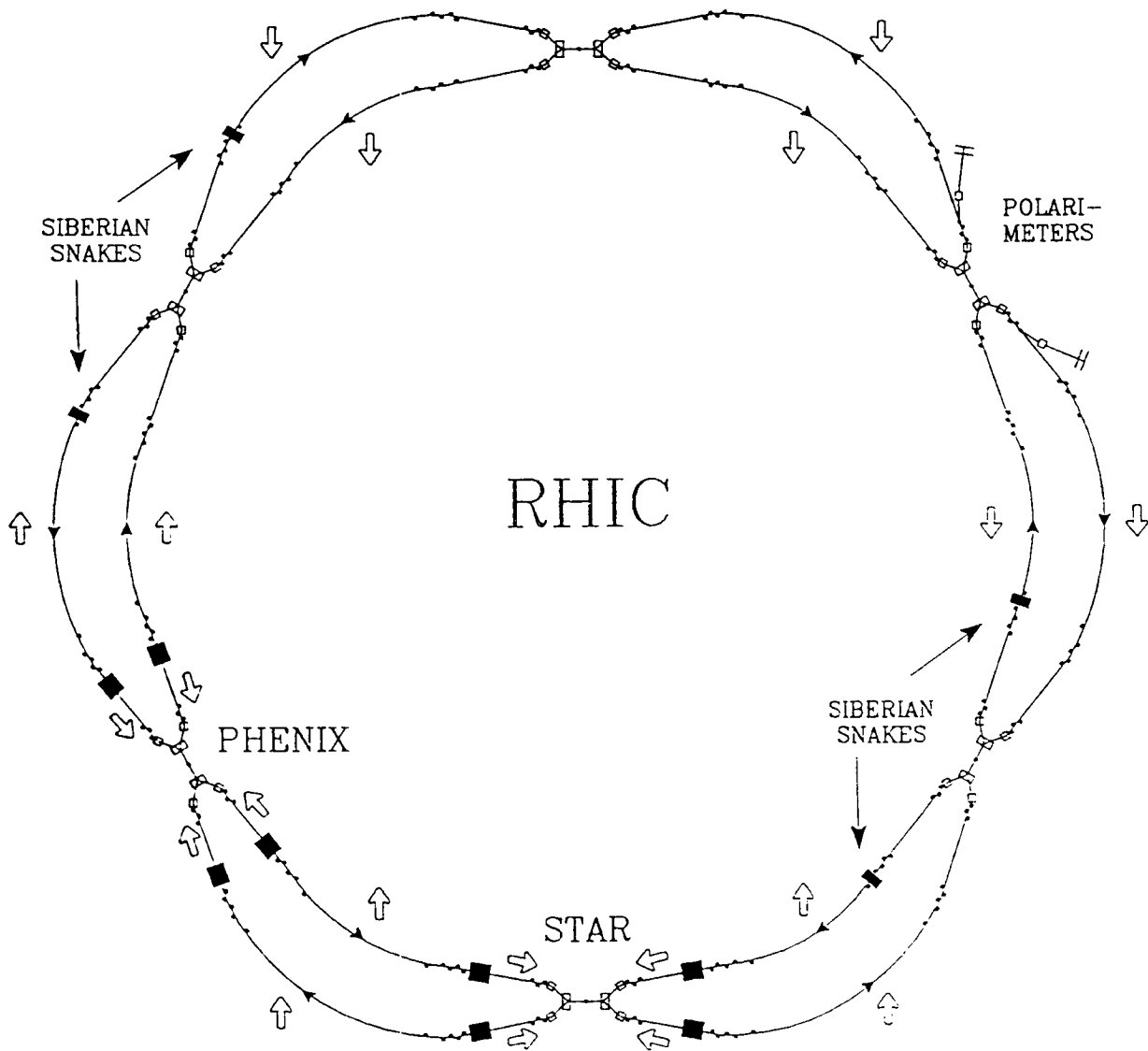


Figure 2





